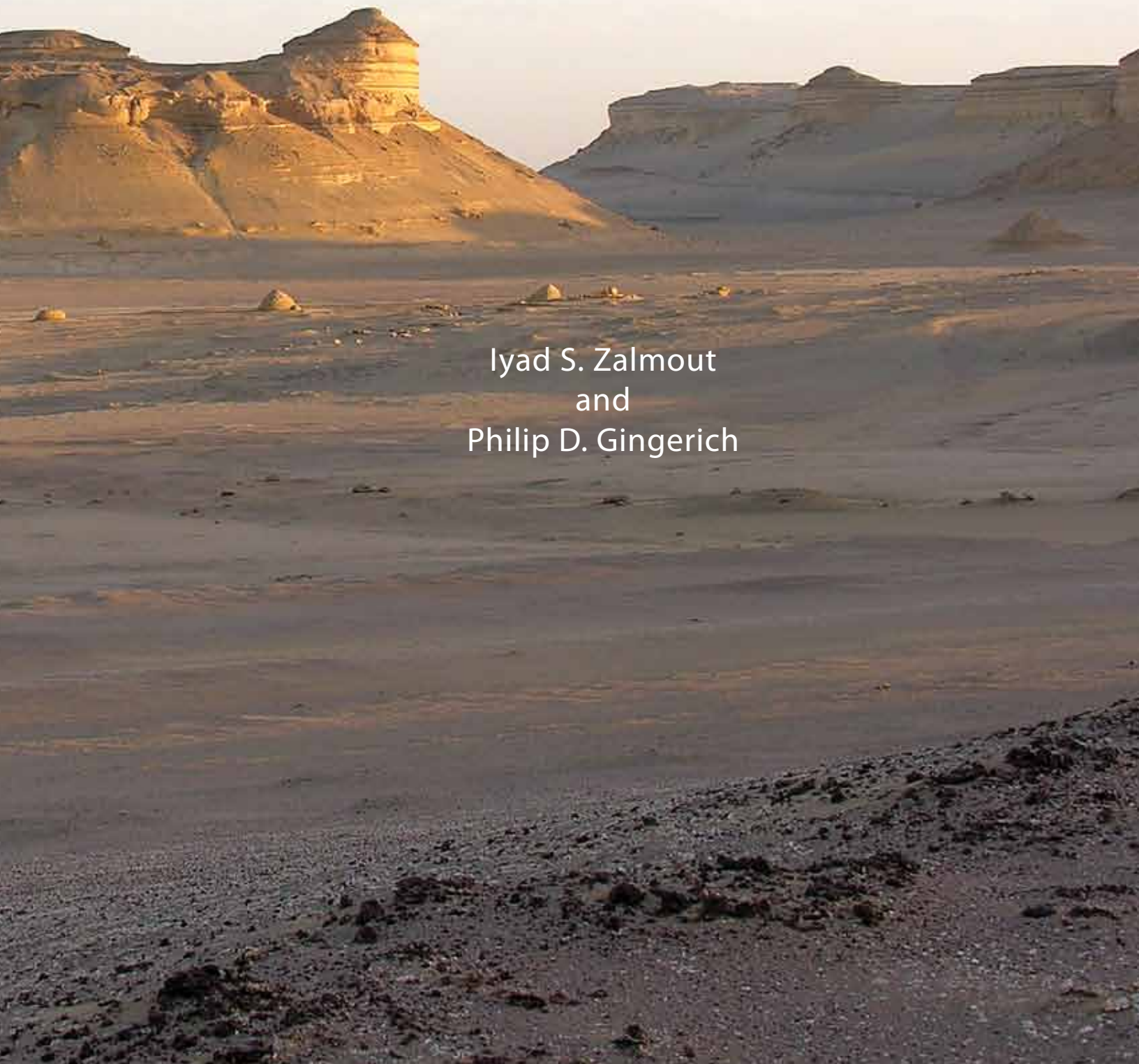


**LATE EOCENE SEA COWS (MAMMALIA, SIRENIA)
FROM WADI AL HITAN IN THE
WESTERN DESERT OF FAYUM, EGYPT**

Iyad S. Zalmout
and
Philip D. Gingerich



**LATE EOCENE SEA COWS (MAMMALIA, SIRENIA)
FROM WADI AL HITAN IN THE
WESTERN DESERT OF FAYUM, EGYPT**

PAPERS ON PALEONTOLOGY — RECENT NUMBERS

26. The Clarkforkian Land-Mammal Age and Mammalian Faunal Composition across the Paleocene-Eocene Boundary by *Kenneth D. Rose* (1981)
27. The Evolutionary History of Microsypoidea (Mammalia, ?Primates) and the Relationship between Plesiadapiformes and Primates by *Gregg F. Gunnell* (1989)
28. New Earliest Wasatchian Mammalian Fauna from the Eocene of Northwestern Wyoming: Composition and Diversity in a Rarely Sampled High-Floodplain Assemblage by *Philip D. Gingerich* (1989)
29. Evolution of Paleocene and Eocene Phenacodontidae (Mammalia, Condylarthra) by *J. G. M. Thewissen* (1990)
30. Marine Mammals (Cetacea and Sirenia) from the Eocene of Gebel Mokattam and Fayum, Egypt: Stratigraphy, Age, and Paleoenvironments by *Philip D. Gingerich* (1992)
31. Terrestrial Mesonychia to Aquatic Cetacea: Transformation of the Basicranium and Evolution of Hearing in Whales by *Zhexi Luo and Philip D. Gingerich* (1999)
32. Fishes of the Mio-Pliocene Ringold Formation, Washington: Pliocene Capture of the Snake River by the Columbia River by *Gerald R. Smith, Neil Morgan, and Eric Gustafson* (2000)
33. Paleocene-Eocene Stratigraphy and Biotic Change in the Bighorn and Clarks Fork Basins, Wyoming by *Philip D. Gingerich (ed.) and others* (2001)
34. Form, Function, and Anatomy of *Dorudon atrox* (Mammalia, Cetacea): An Archaeocete from the Middle to Late Eocene of Egypt by *Mark D. Uhen* (2003)
35. The Tiffanian Land-Mammal Age (Middle and Late Paleocene) in the Northern Bighorn Basin, Wyoming by *Ross Secord* (2008)
36. Earliest Eocene Mammalian Fauna from the Paleocene-Eocene Thermal Maximum at Sand Creek Divide, Southern Bighorn Basin, Wyoming by *Kenneth D. Rose, Amy E. Chew, Rachel H. Dunn, Mary J. Kraus, Henry C. Fricke, and Shawn P. Zack* (2012)
37. Late Eocene Sea Cows (Mammalia, Sirenia) from Wadi Al Hitán in the Western Desert of Fayum, Egypt by *Iyad S. Zalmout and Philip D. Gingerich* (2012)

LATE EOCENE SEA COWS (MAMMALIA, SIRENIA)
FROM WADI AL HITAN IN THE
WESTERN DESERT OF FAYUM, EGYPT



Frontispiece: Central 'qalah' or 'citadel' in Wadi Al Hitan in late afternoon light. The citadel is Birket Qarun Formation sandstone capped by Qsar El Sagha Formation shell beds. The type skull and partial skeleton of *Protosiren smithae* were found weathering out of the base of the sandstone capping the isolated hillock in the left foreground.

**LATE EOCENE SEA COWS (MAMMALIA, SIRENIA)
FROM WADI AL HITAN IN THE
WESTERN DESERT OF FAYUM, EGYPT**

Iyad S. Zalmout

*Department of Earth and Environmental Sciences
and Museum of Paleontology
University of Michigan
Ann Arbor, Michigan 48109-1079*

*Present address: KSU Mammals Research Chair
Department of Zoology, College of Science
King Saud University, P.O. Box 2455
Riyadh 11451, Saudi Arabia
izalmout@ksu.edu.sa*

Philip D. Gingerich

*Department of Earth and Environmental Sciences
and Museum of Paleontology
University of Michigan
Ann Arbor, Michigan 48109-1079
gingeric@umich.edu*

UNIVERSITY OF MICHIGAN
PAPERS ON PALEONTOLOGY NO. 37

2012

Papers on Paleontology No. 37

Museum of Paleontology
The University of Michigan
Ann Arbor, Michigan 48109-1079

Daniel C. Fisher, Director

Philip D. Gingerich, Editor

ISSN 0148-3838
Published December 17, 2012

TABLE OF CONTENTS

Frontispiece.....	iv	III. New Eocene Sirenia from the Priabonian of Wadi Al Hitan	37
Title Page.....	v	Systematic Paleontology	37
Table of Contents.....	vii	IV. Comparisons and Relationships of Wadi Al Hitan <i>Eotheroides</i>	95
List of Figures.....	viii	Discussion.....	102
List of Tables.....	xi	Conclusions.....	106
Abstract.....	xiii	V. Quantitative Comparison of Skeletal Elements in Eocene Sirenia from Egypt	109
I. Introduction	1	Cranial Measurements.....	109
Sirenian Evolution.....	1	Mandibular Measurements.....	109
Sirenia of Egypt (Cairo and Fayum)	2	Vertebral Measurements.....	109
Objectives.....	6	Rib Measurements.....	113
Methods.....	9	Forelimb Measurements.....	114
Institutional Abbreviations.....	11	Hind Limb Measurements.....	115
Anatomical Abbreviations.....	14	VI. Sexual Dimorphism in Eocene Sirenia	133
Acknowledgments.....	21	Dimorphism in Eocene Sirenia.....	134
II. Geology and Stratigraphy	23	Discussion and Conclusions.....	138
Geology of the Fayum Basin and Surrounding Areas.....	23	VII. Paleobiology of Wadi Al Hitan Sirenia	143
Stratigraphy of Sirenian-Bearing Formations in Cairo and Wadi Al Hitan.....	23	Paleoenvironment.....	143
Stratigraphic Levels Yielding Sirenia in Wadi Al Hitan.....	35	Paleoecology.....	145
		Secondary Adaptation to Life in the Sea.....	145
		Locomotion.....	148
		Feeding Behavior.....	149
		Discussion and Conclusions.....	150
		VIII. Literature Cited	153

LIST OF FIGURES

<i>Figure</i>	<i>Page</i>
1. Phylogeny of the order Sirenia.....	2
2. Geographic distribution of Eocene sirenians.....	3
3. Political map of Egypt and surrounding countries...	4
4. Geological map of the Fayum Basin in the Western Desert of Egypt.....	5
5. Late Eocene sirenian fossils in Wadi Al Hitán plotted in geological context.....	9
6. Distribution of sirenian fossils in Wadi El Rayan....	10
7. Distribution of sirenian fossils in and north of Birket Qarun (Lake Moeris).....	11
8. Key to measurements of cranial elements used in this study.....	12
9. Key to measurements of mandibular elements used in this study.....	13
10. Key to measurements of vertebrae used in this study	14
11. Key to measurements of ribs used in this study.....	14
12. Key to measurements of scapulae used in this study	14
13. Key to measurements of humeri used in this study..	15
14. Key to measurements of ulnae used in this study....	16
15. Key to measurements of radii used in this study.....	17
16. Key to measurements of pelvic bones used in this study.....	18
17. Key to measurements of femora used in this study..	19
18. Key to measurements of tibiae and fibulae used in this study.....	20
19. Key to measurements of sternebrae used in this study	21
20. Correlation of stratigraphic units of the Cairo and Fayum areas	24
21. Legend for the stratigraphic sections illustrated in this study	25
22. Stratigraphic section of Lutetian-Bartonian strata in Wadi El Rayan.....	26
23. Stratigraphic section of Minqar El Hut near Three Sisters in Wadi Al Hitán	28
24. Stratigraphic section at Wadi Al Hitán locality WH-230.....	31
25. Stratigraphic section of the Qasr El Sagha Formation near Garet El Esh	32
26. Stratigraphic section of the uppermost Qasr El Sagha Formation in Wadi Efreet	33
27. Stratigraphic section of the Qasr El Sagha Formation near Dir Abu Lifa	34
28. Excavation of <i>Eotheroides sandersi</i> (UM 97514) at locality WH-110	36
29. Holotype cranium and mandible of <i>Eotheroides clavigerum</i> (CGM 60551).....	39
30. Holotype cranium of <i>Eotheroides clavigerum</i> (CGM 60551).....	41
31. Holotype cranium of <i>Eotheroides clavigerum</i> (CGM 60551).....	42
32. Toothless right maxilla of <i>Eotheroides clavigerum</i> (UM 97524)	43
33. Holotype cervical, thoracic, sacral, and caudal vertebrae of <i>Eotheroides clavigerum</i> (CGM 60551)	44
34. Holotype cervical, thoracic, sacral, and caudal vertebrae of <i>Eotheroides clavigerum</i> (CGM 60551)	45
35. Holotype cervical, thoracic, sacral, and caudal vertebrae of <i>Eotheroides clavigerum</i> (CGM 60551)	46
36. Holotype left and right ribs of <i>Eotheroides clavigerum</i> (CGM 60551)	48
37. Holotype forelimb elements of <i>Eotheroides clavigerum</i> (CGM 60551)	49
38. Holotype right metapodials of <i>Eotheroides clavigerum</i> (CGM 60551)	50
39. Holotype innominate pelvic bones of <i>Eotheroides clavigerum</i> (CGM 60551)	52
40. Holotype cranial elements of <i>Eotheroides sandersi</i> (CGM 42181)	62
41. Cranium of <i>Eotheroides sandersi</i> (UM 111558)	63
42. Cranium of <i>Eotheroides sandersi</i> (UM 111558)	64
43. Skull roof of <i>Eotheroides sandersi</i> (UM 94809)	65
44. Anatomy of the ear region of <i>Eotheroides sandersi</i> (UM 111558)	69

LIST OF FIGURES (cont.)

Figure	Page
45. Mandible of <i>Eotheroides sandersi</i> (UM 100138).....	70
46. Holotype cervical, thoracic, and caudal vertebrae of <i>Eotheroides sandersi</i> (CGM 42181)	72
47. Cervical, thoracic, lumbar, and caudal vertebrae of <i>Eotheroides sandersi</i> (UM 111558)	73
48. Cervical, thoracic, lumbar, and caudal vertebrae of <i>Eotheroides sandersi</i> (UM 111558).....	74
49. Cervical, thoracic, lumbar, and caudal vertebrae of <i>Eotheroides sandersi</i> (UM 111558).....	75
50. Thoracic vertebrae of <i>Eotheroides sandersi</i> (UM 97514)	76
51. Thoracic vertebrae of <i>Eotheroides sandersi</i> (UM 97514)	77
52. Lumbar, sacral, and caudal vertebrae of <i>Eotheroides sandersi</i> (UM 97514)	79
53. Thoracic, lumbar, sacral, and caudal vertebrae of <i>Eotheroides sandersi</i> (UM 97514)	79
54. Holotype ribs of <i>Eotheroides sandersi</i> (CGM 42181) compared to those of <i>Eotheroides aegyptiacum</i> (SMNS 43949)	81
55. Left and right ribs of <i>Eotheroides sandersi</i> (UM 111558).....	82
56. Left and right posterior ribs of <i>Eotheroides sandersi</i> (UM 97514).....	83
57. Xiphisternum of <i>Eotheroides sandersi</i> (UM 111558)	84
58. Holotype scapular and humeral elements of <i>Eotheroides sandersi</i> (UM 97514).....	85
59. Forelimb elements of <i>Eotheroides sandersi</i> (UM 111558)	86
60. Left ulna of a juvenile <i>Eotheroides sandersi</i> (UM 97515)	88
61. Left metapodials and carpal (?) of <i>Eotheroides sandersi</i> (UM 111558)	89
62. Holotype innominate pelvic bones and femora of <i>Eotheroides sandersi</i> (CGM 42181)	90
63. Sacrum and left and right innominates of <i>Eotheroides sandersi</i> (UM 97514)	92
64. Femora of <i>Eotheroides sandersi</i> compared to that of <i>Eosiren</i> sp.	93
65. Femora, tibiae, and fibulae of <i>Protosiren</i> from Egypt and Pakistan	93
66. Upper left cheek teeth of Paleogene sirenians from Cairo and Fayum	96
67. Mandible of a late Eocene dugongid collected from Wadi Al Hitan (YPM 24851)	97
68. Mandible of late Eocene <i>Eotheroides</i> sp. from North Carolina (USNM 214596).....	98
69. Holotype mandible of late Eocene <i>Protosiren smithae</i> (CGM 42292; cast UM 94810).....	99
70. Mandible of late Eocene <i>Eosiren stromeri</i> from the Qasr El Sagha Formation (UM 100137).....	101
71. Vertebrae of late Eocene <i>Eosiren libyca</i> (UM 101226) from the Qasr El Sagha Formation.....	101
72. Vertebrae of late Eocene <i>Protosiren smithae</i> (UM 101224) from the Birket Qarun Formation	102
73. Vertebrae of late Eocene <i>Eosiren libyca</i> (UM 101226) from the Qasr El Sagha Formation.....	103
74. Vertebrae of late Eocene <i>Protosiren smithae</i> (UM 101224) from the Birket Qarun Formation.....	104
75. Ribs of late Eocene <i>Eosiren libyca</i> (UM 101226) from the Qasr El Sagha Formation.....	105
76. Ribs of late Eocene <i>Protosiren smithae</i> (UM 101224) from the Birket Qarun Formation	105
77. Comparison of innominates of African Paleogene sirenians.....	106
78. Sternal elements of <i>Protosiren</i> , <i>Eotheroides</i> , and <i>Eosiren</i> from Fayum.....	107
79. Pattern profiles of cranial measurements for five species of <i>Protosiren</i> , <i>Eotheroides</i> , and <i>Eosiren</i>	110
80. Pattern profiles of mandibular measurements for four species of <i>Protosiren</i> , <i>Eotheroides</i> , and <i>Eosiren</i>	111
81. Pattern profiles of vertebral centrum length in Sirenia	115
82. Pattern profiles of maximum vertebral breadth in Sirenia.....	118
83. Pattern profiles of vertebral centrum width-to-length shape relationships in Sirenia.....	121

LIST OF FIGURES (cont.)

<i>Figure</i>	<i>Page</i>
84. Pattern profiles of rib midshaft cross-sectional area in <i>Sirenia</i>	124
85. Pattern profiles of scapula measurements for three species of <i>Protosiren</i> and <i>Eotheroides</i>	125
86. Pattern profiles of humerus measurements for three species of <i>Protosiren</i> and <i>Eotheroides</i>	126
87. Pattern profiles of ulna measurements for four species of <i>Protosiren</i> and <i>Eotheroides</i>	127
88. Pattern profiles of innominate measurements for four species of <i>Protosiren</i> , <i>Eotheroides</i> , and <i>Eosiren</i>	128
89. Pattern profiles of femur measurements for four species of <i>Protosiren</i> , <i>Eotheroides</i> , and <i>Eosiren</i>	130
90. Pattern profiles of tibia measurements for <i>Protosiren smithae</i> and <i>Pezosiren portelli</i>	131
91. Innominates of possible female (SMNS 43976) and male (CGM 42292) <i>Protosiren</i>	135
92. Innominates of possible female <i>Protosiren sattaensis</i> (GSP-UM 3001 and 3197)	136
93. Innominate of a possible female <i>Eotheroides clavigerum</i> (holotype CGM 60051)	137
94. Innominates of possible male (UM 97514) and female (CGM 42181) <i>Eotheroides sandersi</i>	138
95. Innominates of possible male (UM 101226 and CGM 29774) and female (UM 101228) <i>Eosiren libyca</i>	139
96. Sexual dimorphism in the pelvic bones of Eocene sirenians <i>Protosiren</i> , <i>Eotheroides</i> , and <i>Eosiren</i> ...	140
97. Sexual dimorphism in the pelvic bones of Eocene sirenians.....	141
98. Paleogeography and paleobathymetry of northern Egypt in the late Bartonian-Priabonian	144
99. True-scale computed cross-section of Wadi Al-Hitan stratigraphy projected from three-dimensional GPS mapping of bed traces.....	144
100. Priabonian age fossil plant remains found with marine mammal skeletons in the Birket Qarun and Qasr El Sagha formations of Fayum	146
101. Comparison of size and shape for upper molars of <i>Protosiren</i> , <i>Eotheroides</i> , and <i>Eosiren</i>	150

LIST OF TABLES

Table	Page
1. Global record of Eocene sirenians.....	6
2. Eocene and Oligocene sirenians in the Fayum Basin.....	8
3. Measurements of the holotype skull of <i>Eotheroides clavigerum</i> sp. nov.....	40
4. Measurements of the holotype mandible of <i>Eotheroides clavigerum</i> sp. nov.....	47
5. Measurements of the holotype upper and lower teeth of <i>Eotheroides clavigerum</i> sp. nov.....	51
6. Measurements of upper cheek teeth of <i>Eotheroides aegyptiacum</i>	51
7. Measurements of lower teeth in USNM 214596 from the Eocene of North Carolina.....	51
8. Measurements of the holotype vertebrae of <i>Eotheroides clavigerum</i> sp. nov.	53
9. Measurements of the holotype ribs of <i>Eotheroides clavigerum</i> sp. nov.	56
10. Measurements of the holotype scapula of <i>Eotheroides clavigerum</i> sp. nov. and other Eocene sirenians	57
11. Measurements of the holotype humerus of <i>Eotheroides clavigerum</i> sp. nov. and other Eocene sirenians	58
12. Measurements of the holotype ulna of <i>Eotheroides clavigerum</i> sp. nov. and other Eocene sirenians..	59
13. Measurements of the holotype radius of <i>Eotheroides clavigerum</i> sp. nov. and other Eocene sirenians	59
14. Measurements of the holotype metacarpals and phalanx of <i>Eotheroides clavigerum</i> sp. nov.....	59
15. Measurements of the holotype innominate of <i>Eotheroides clavigerum</i> sp. nov. and other Eocene sirenians	60
16. Measurements of the holotype cranium of <i>Eotheroides sandersi</i> sp. nov. and other Eocene sirenians	66
17. Measurements of the maxillary teeth of <i>Eotheroides sandersi</i> sp. nov.	69
18. Measurements of the vertebrae of <i>Eotheroides sandersi</i> sp. nov., UM 111558	71
19. Measurements of the vertebrae of <i>Eotheroides sandersi</i> sp. nov., UM 97514	78
20. Measurements of the holotype ribs of <i>Eotheroides sandersi</i> sp. nov.	80
21. Measurements of the ribs of <i>Eotheroides sandersi</i> sp. nov., UM 111558	80
22. Measurements of the ribs of <i>Eotheroides sandersi</i> sp. nov., UM 97514.....	83
23. Measurements of the holotype scapula of <i>Eotheroides sandersi</i> sp. nov. and another Eocene sirenian	84
24. Measurements of the holotype humerus of <i>Eotheroides sandersi</i> sp. nov. and another Eocene sirenian	87
25. Measurements of the holotype ulna of <i>Eotheroides sandersi</i> sp. nov. and other Eocene sirenians.....	87
26. Measurements of the metacarpals of <i>Eotheroides sandersi</i> sp. nov.	89
27. Measurements of the holotype innominate of <i>Eotheroides sandersi</i> sp. nov. and other Eocene sirenians	91
28. Measurements of the holotype femur of <i>Eotheroides sandersi</i> sp. nov. and other Eocene sirenians	91
29. Measurements of crania of Eocene sirenians known to date	112
30. Measurements of mandibles of Eocene sirenians known to date	114
31. Measurements of sirenian vertebral centrum length..	116
32. Measurements of sirenian vertebral maximum breadth	119
33. Centrum dimensions and shape quotients for sirenian vertebrae studied here	122
34. Cross-sectional area of sirenian rib midshafts	124
35. Scapular dimensions of Eocene sirenians from Egypt	125

LIST OF TABLES (cont.)

<i>Table</i>	<i>Page</i>		
36. Humerus dimensions of Eocene sirenians from Egypt	126	41. Tibia and fibula dimensions of Eocene sirenians from Egypt and Jamaica	134
37. Ulna dimensions of Eocene sirenians from Egypt...	127	42. Measurements of upper molar teeth in Eocene sirenians	151
38. Pelvic dimensions of Eocene sirenians from Egypt.	129	43. Upper molar length and width ratios in Eocene sirenians	151
39. Femur dimensions of Eocene sirenians from Egypt and Jamaica	130	44. Total area of upper cheek teeth in Eocene sirenians from Egypt.....	151
40. Ischium dimensions of Eocene sirenians from Egypt and Pakistan	131		

ABSTRACT

The Eocene sea cows *Protosiren*, *Eotheroides*, and *Eosiren* have been known for more than a century from skulls and jaws found at Gebel Mokattam near Cairo and Birket Qarun near Fayum in Egypt. *Protosiren* and *Eotheroides* are known from Gebel Mokattam (Lutetian, middle Eocene), and *Eosiren* is known from north of Birket Qarun (middle Priabonian, late Eocene). In recent years we have collected exceptionally complete skeletons of *Protosiren* and *Eotheroides* of intermediate early Priabonian age in Wadi Al Hitán in the Western Desert west of Fayum. The Wadi Al Hitán *Protosiren* (Protosirenidae) is *Protosiren smithae* Domning and Gingerich, 1994, a probable descendant of Gebel Mokattam *Protosiren fraasi* Abel, 1907. Wadi Al Hitán *Eotheroides* (Dugongidae) is represented by two species, *Eotheroides clavigerum*, sp. nov., and *Eotheroides sandersi*, sp. nov. Both are probable descendents of Gebel Mokattam *Eotheroides aegyptiacum* (Owen, 1875).

Eotheroides clavigerum and *Eotheroides sandersi* are each represented by skulls, lower jaws, and exceptionally complete postcranial skeletons with pectoral limbs and pelvic girdles. Wadi Al Hitán *Eotheroides* were medium to large dugongs, ranging in length from 1.5 to 2.5 m; bones of the skull are robust and dense; the rostrum is deflected and bears diminutive to medium tusks; the trunk is widest between the ninth and eleventh thoracic vertebrae; the end of the tail is flat, indicating the presence of a fluke; the pelvis is greatly reduced, with a shallow acetabulum but an expanded club-like ilium; and the femur is short and slender. *Eotheroides clavigerum* and *Eotheroides sandersi* share the following derived characteristics of *Eotheroides*: there is a prominent falx cerebri and bony tentorium in the roof of the braincase; the nasals are long with a long contact along the midline; the palate is broad and long, with the posterior border positioned behind the tooth row; and anterior ribs are pachyosteosclerotic. Pelves and slender femora are retained, but there cannot have been any substantial lower leg or foot.

Protosiren, *Eotheroides*, and *Eosiren* all exhibit secondary sexual dimorphism of the bony pelvis. As in modern dugongs, males of the Eocene species have a distal ischium about twice as thick as the ischial ramus, while females have a distal ischium and ischial ramus of approximately equal thickness.

Coexistence of *Protosiren smithae*, *Eotheroides clavigerum*, and *Eotheroides sandersi* in the same biotope reflects both the taxonomic diversity and morphological disparity of sirenians in early Priabonian Tethys, and observed morphological differences between the species reflect dietary and environmental specialization and niche partitioning. All are assumed to have fed on sea grass. Sea grass preserved as leaf impressions is direct evidence of the shallowness of Tethyan shelf waters where Eocene sirenians are found in Wadi Al Hitán and elsewhere.

Protosiren had larger tusks, lacked rib pachyostosis, and had ribs articulating via a cartilaginous connection to the thoracic vertebrae. Larger tusks suggest feeding on rhizomes, and the unique rib articulations suggest breathing and buoyancy different from other sirenians. If the ribcage was collapsible, this may have enabled *Protosiren* to feed in deeper water, and retention of functional hind limbs may have enabled *Protosiren* to move while submerged feeding on the seabed.

Eotheroides and *Eosiren* differ from *Protosiren* in having osteosclerotic and pachyostotic ribs packed closely together, ribs with more restrictive synovial articulations, and much more reduced hind limbs. The rib cage was probably more rigid, with pachyosteosclerosis balancing pneumatic buoyancy. *Eotheroides* and *Eosiren* may have fed in shallower water than *Protosiren*, where it was easier to come to the surface to breath. Their reduced hind limbs precluded moving on the seabed as postulated for *Protosiren*.

I

INTRODUCTION

Sirenia or sea cows, represented by living dugongs and manatees, are relatively large herbivorous marine mammals that are fully aquatic, have fore limbs modified as flippers, and lack external hind limbs. Sirenians make their first appearance in the fossil record in the early middle Eocene. The earliest representatives were not fully aquatic but amphibious or semiaquatic, and they retained well developed fore- and hind limbs like terrestrial mammals (Domning, 2001b).

Sirenia are interesting from an evolutionary point of view because they represent one of two replicated experiments involving land mammals that became fully aquatic. Sirenians parallel whales in crossing the boundary between terrestrial and aquatic adaptive zones. Sirenia are herbivorous and most closely related to Proboscidea today (Gill, 1870; Schlosser, 1923; Simpson, 1945; McKenna, 1975, Shoshani, 1986), while Cetacea are piscivorous and planktivorous and most closely related to Artiodactyla (Gingerich et al., 2001). Both groups made the transition from land to sea independently in the early and middle Eocene, and fossils described here show that sirenians were marine and fully aquatic by the late Eocene.

Most sirenians living today inhabit tropical near-shore marine habitats, but there are exceptions. Manatees are restricted to fresh and brackish water of rivers, deltas, and keys, but in contrast the recently-extinct 10-meter long Steller's sea cow, a dugongid, lived in fully marine habitats at higher latitudes (Steller, 1751). Sea cows today eat sea grass, which is dependent on light for energy and thus restricted to relatively clear, shallow water. This was seemingly true for most sirenians throughout their evolutionary history, and sirenians are thus important paleoenvironmental indicators.

The following introductory paragraphs provide an overview of sirenian evolution, the history of study of fossil sirenians in Egypt, new sirenian specimens from Egypt described here, methods used to study these, and objectives of this study. Following chapters will consider the geology and stratigraphy of sirenian-bearing deposits in Egypt, description of the new specimens, and a consideration of their sexual dimorphism, paleoenvironments, paleoecology, and paleobiology.

SIRENIAN EVOLUTION

Sirenia have a dense fossil record, and much is known about their evolution in the middle and late Cenozoic (Fig. 1). The earlier record is less well known. The oldest sirenian represented

by substantial parts of a skeleton is *Pezosiren portelli* from the early middle Eocene of Jamaica (Domning 2001b). This is classified in the family Prorastomidae, and is more primitive than all other sirenians in retaining a longer neck, a fused sacrum, and well developed fore- and hind limbs capable of supporting the animal's weight on land.

Extant sirenians are fully aquatic with morphological and hydrostatic characteristics reflecting secondary adaptation to an aquatic habitat. Morphological and skeletal characteristics of interest include: an overall fusiform body shape, thick and almost hairless skin, and large mobile lips. Sirenians have short necks (short cervicals), forelimbs modified as flippers, hind limbs reduced to internal vestiges, and a tail that is modified into a horizontal caudal fluke for propulsion by dorsoventral undulation of the spine.

Like whales, the earliest sirenians show a gradual transition from more terrestrial ancestors with well developed pelvic bones and hind limbs attached to a multi-centrum sacrum (Abel, 1907; Domning and Gingerich, 1994; Domning, 2001b); while the derived forms of these have the pelvic girdle reduced to a vestigial state isolated in soft tissue.

Sirenia, which are a sister taxon to Proboscidea and Hyracoidea (McKenna, 1975: 42), made its first appearance in the middle Eocene and reached its highest diversity during the Miocene (Fig. 1; Domning, 1994 and 1996). The oldest sirenians come from the early middle Eocene of Jamaica (Table 1; Fig. 2): *Prorastomus sirenoides* (Owen, 1855) and the quadrupedal *Pezosiren portelli* of Domning (2001b). However, evidence from the oldest sister taxa in the Eocene of the Old World, and new fossil material from the middle Eocene of Senegal, may support the idea of a Tethyan origin (Domning et al., 1982; Wells and Gingerich, 1983; Rose et al., 2006; Hautier et al., 2012).

According to Domning (1994), there are over 42 species of living and fossil sirenians belonging to 24 genera included in 4 families: Prorastomidae (early middle Eocene of Jamaica); Protosirenidae (middle and late Eocene of Egypt and Pakistan); Dugongidae (Eocene to Recent); and Trichechidae (Miocene to Recent). Four species of the genera *Dugong* and *Trichechus* are living today, and are distributed on the northern margins of southern continents and the Gulf of Mexico.

The global distribution of Eocene sirenians shows that Old World Tethys and the eastern and southeastern coasts of the United States are the most common places where sirenian fossils are found (Fig. 2).

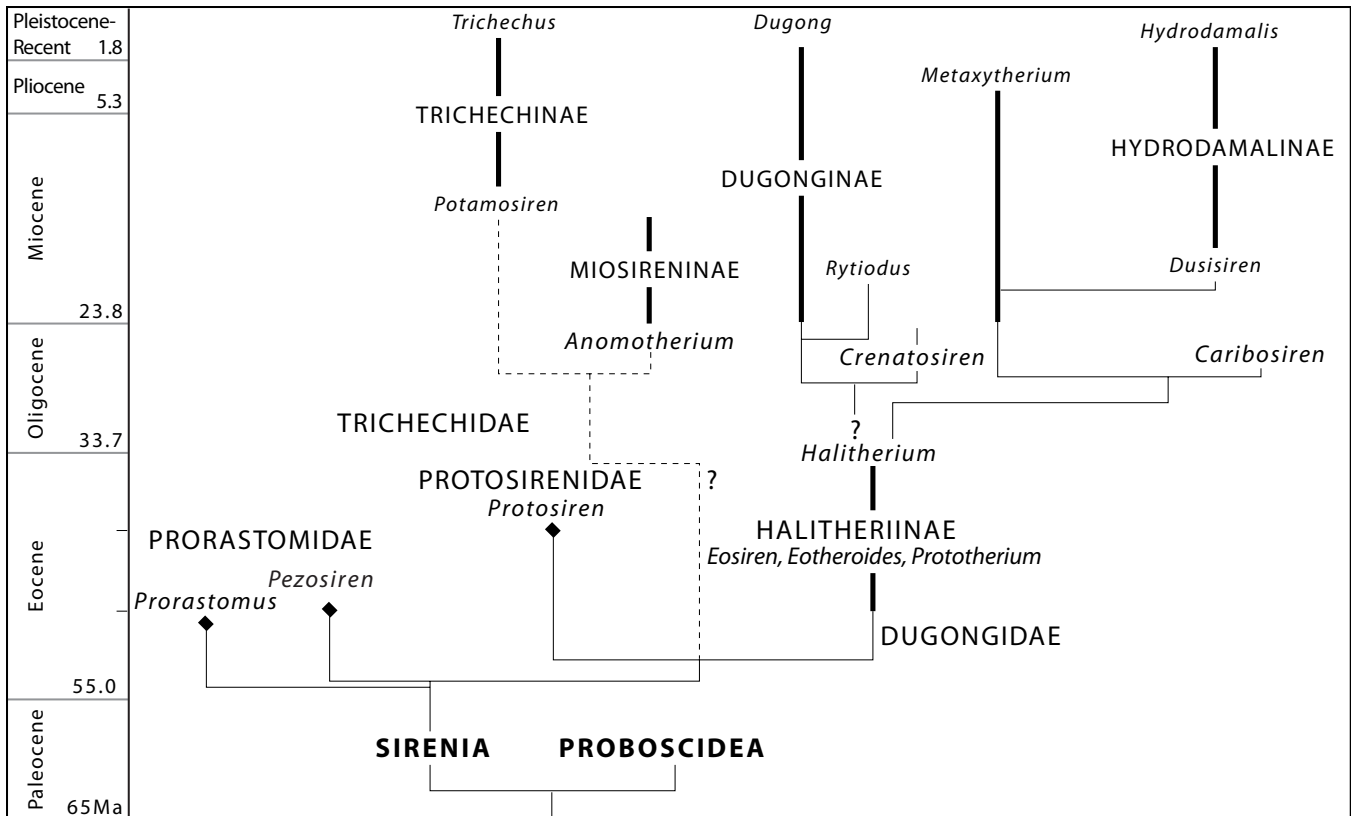


FIGURE 1 — Phylogeny of the order Sirenia. Known stratigraphic ranges are indicated by bold lines; dashed lines indicate uncertain phylogenetic relationships and sirenian family ranges. Black diamonds represent extinct families with very short stratigraphic ranges (modified from Gheerbrant et al., 2005; Domning et al., 2010).

SIRENIA OF EGYPT (CAIRO AND FAYUM)

Sirenians were the first fossil vertebrates to be reported from Paleogene rocks of Africa and the first marine mammal fossils to be discovered in Egypt, based on a collection of vertebrae and rib fragments that were initially identified and illustrated as pinniped material (de Blainville, 1840: 43 and 51). De Blainville's interpretation of the specimens he studied as marine mammals was correct, but the specimens were not pinnipeds. In a note four years later, de Blainville corrected himself (1844:119-120) and concluded that the specimens were rather the first fossil sirenians from Africa. De Blainville was not specific about the locality where the fossils were collected, however he hinted that they came from chalk beds on the left side of the River Nile in Lower Egypt. These chalk beds are probably the Lutetian nummulitic limestone, building stone of the great pyramids, near the historic city of Giza, on the west bank of the Nile opposite Cairo (Fig. 3).

Later Richard Owen (1875) described '*Eotherium*' (now *Eotheroides*) *aegyptiacum* from the upper part of the Lower Building Stone Member of the Gebel Mokattam Formation of middle Lutetian age (Strougo et al., 1982). From the same level, which is also the level of *Protocetus atavus* of Fraas (1904), Abel (1904)

wrote about a new taxon of sirenian that he published as a *nomen nudum* with no illustration or diagnosis. Abel's 'new taxon' was later published as *Protosiren fraasi* Abel (1907). Filhol (1878) erected *Manatus coulombi* from the Mokattam, which was later synonymized with *Protosiren fraasi* (Abel, 1907). Sickenberg (1934) revised the fossil sirenians from Egypt and the Mediterranean region and added *Eosiren abeli* (replacement of *Eotherium aegyptiacum* of Abel, 1912) to the Mokattam sirenians, on the basis of very limited elements including a skull that was destroyed in World War II. *Eotherium majus* of Zdansky (1938) is the last sirenian to be named from the Mokattam Formation near Cairo. This taxon was based in a single upper molar. The specimen is now lost. It was never catalogued, and the locality in Zdansky's publication is confusing. Gingerich (1992) concluded that the sirenians from the Lutetian of the Mokattam Limestone belong to two taxa: *Eotheroides aegyptiacum* and *Protosiren fraasi* (Table 1 and Table 2).

Southwest of Cairo and west of the Nile valley, the Fayum Basin has drawn great paleontological and geological attention for its fossil vertebrates from the Birket Qarun, Qasr El Sagha, and Gebel Qatrani formations (Fig. 4). The Fayum fossils have been studied for more than a century (Andrews, 1902a; Beadnell and Andrews, 1904; Andrews, 1906). These unique deposits

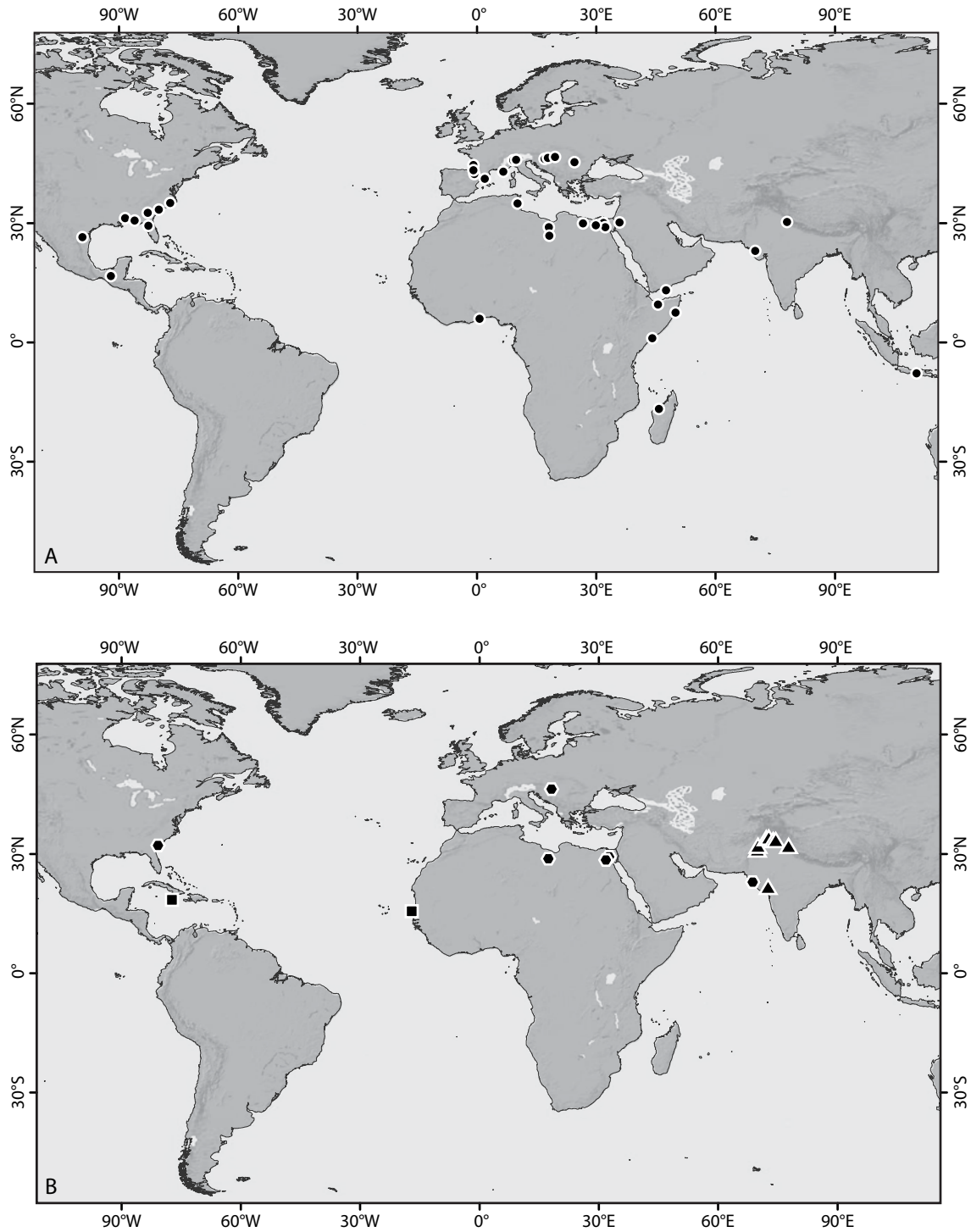


FIGURE 2 — Spatial distribution of Eocene sirenians and their potential ancestors compiled from authors listed in Table 1. A: Distribution of Eocene Dugongidae (circles). B: Distribution of Anthracobunidae (triangles), Prorastomidae (squares), Protosirenidae (hexagons). Ypresian and early Lutetian anthracobunid records from India and Pakistan are after Wells and Gingerich (1983) and Rose et al. (2006).

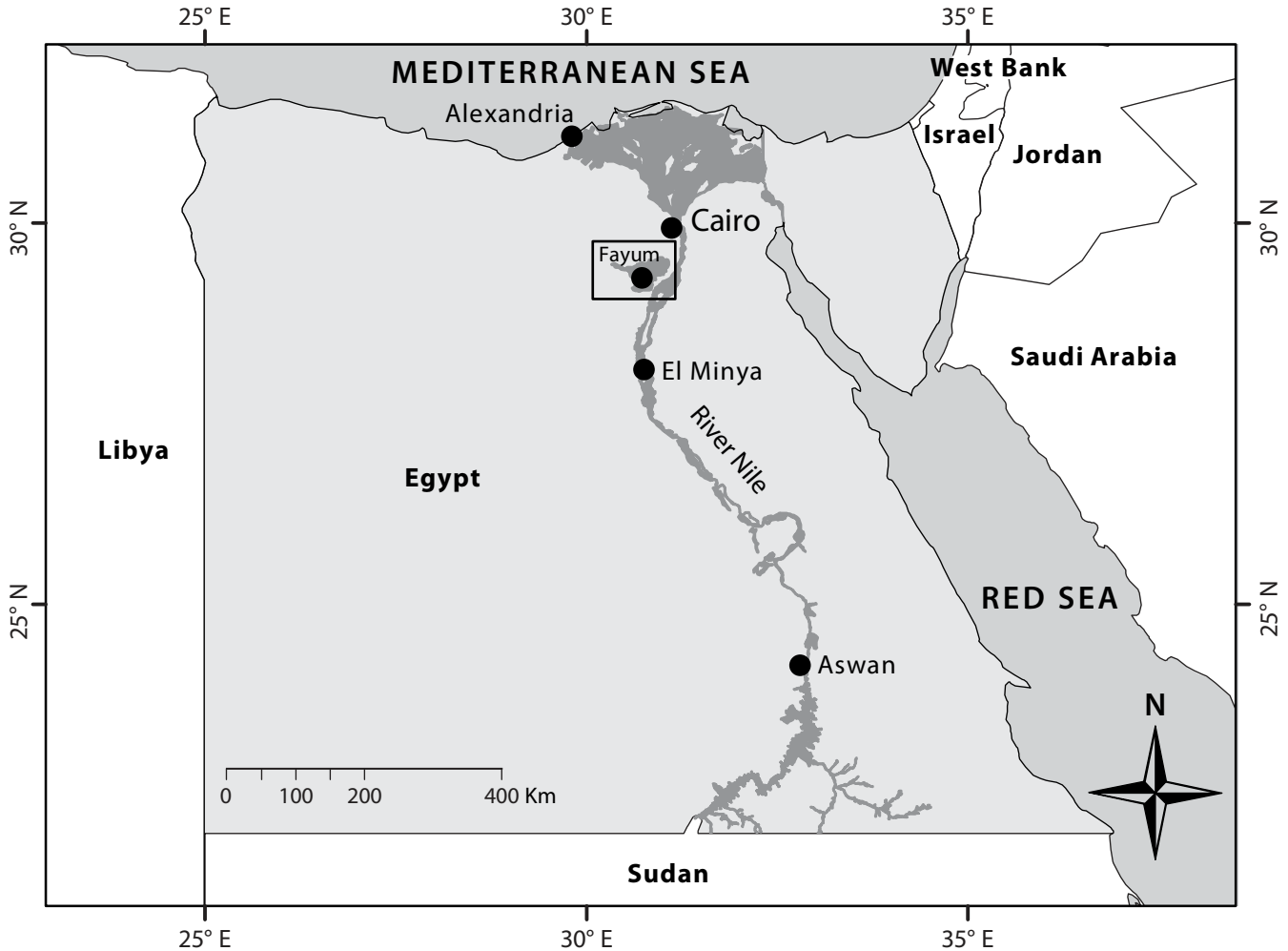


FIGURE 3 — Political map of Egypt and the surrounding countries of northeastern Africa. The Fayum Basin is bounded by the rectangle southwest of Cairo.

have produced many North African near-shore vertebrate specimens.

During the middle and late Eocene (40-33.9 Ma) and lower Oligocene (33.9-28.4 Ma) the Fayum area provided suitable environments for both shallow marine and terrestrial vertebrate faunas; these faunas are now preserved in thick sedimentary packages that are extensively exposed in wide valleys and benches in the Fayum Basin. The faunas are parts of prehistoric biotopes that included terrestrial mammals (Proboscidea, Primates, Carnivora), marine mammals (archaeocetes and sirenians), birds, reptiles (chelonians, crocodylians, and snakes), and fishes (see Simons and Rasmussen, 1990). Invertebrate fossils such as benthic and planktonic foraminiferans are very common, and floral remains, such as tropical trees and mangrove-like plants, also have been recorded from the Eocene beds of the Fayum Basin (Wing and Tiffney, 1982; Bown and Kraus, 1988; Wing et al., 1995).

Marine mammals from these beds have special interest because they provide detailed information about the early evolutionary history of both Cetacea and Sirenia. In Fayum, Andrews (1902b, 1906) described *Eosiren libyca* from the Qasr El Sagha Formation. *E. libyca* is represented by a number of skulls and partial skeletons (Sickenberg, 1934). Siegfried (1967) described a femur and pelvis, and some lumbar and caudal vertebrae of *E. libyca* from the Qasr El Sagha Formation near lake Birket Qarun, and noticed that the femur is substantially different from that of the Oligocene *Halitherium schinzii*. He concluded that the hind limbs of *Eosiren* were functionless, but possibly retained some minor muscle movement. From the same beds of the Qasr El Sagha Formation and from an area near the west side of the ancient town of Dimeh (north of Birket Qarun), *Eosiren stromeri* was described by Sickenberg (1934: 131). Reinhart (1959) described a partial sirenian cranium and called it *Eotheroides*. Domning et al. (1982: 55) reported a sirenian mandible from

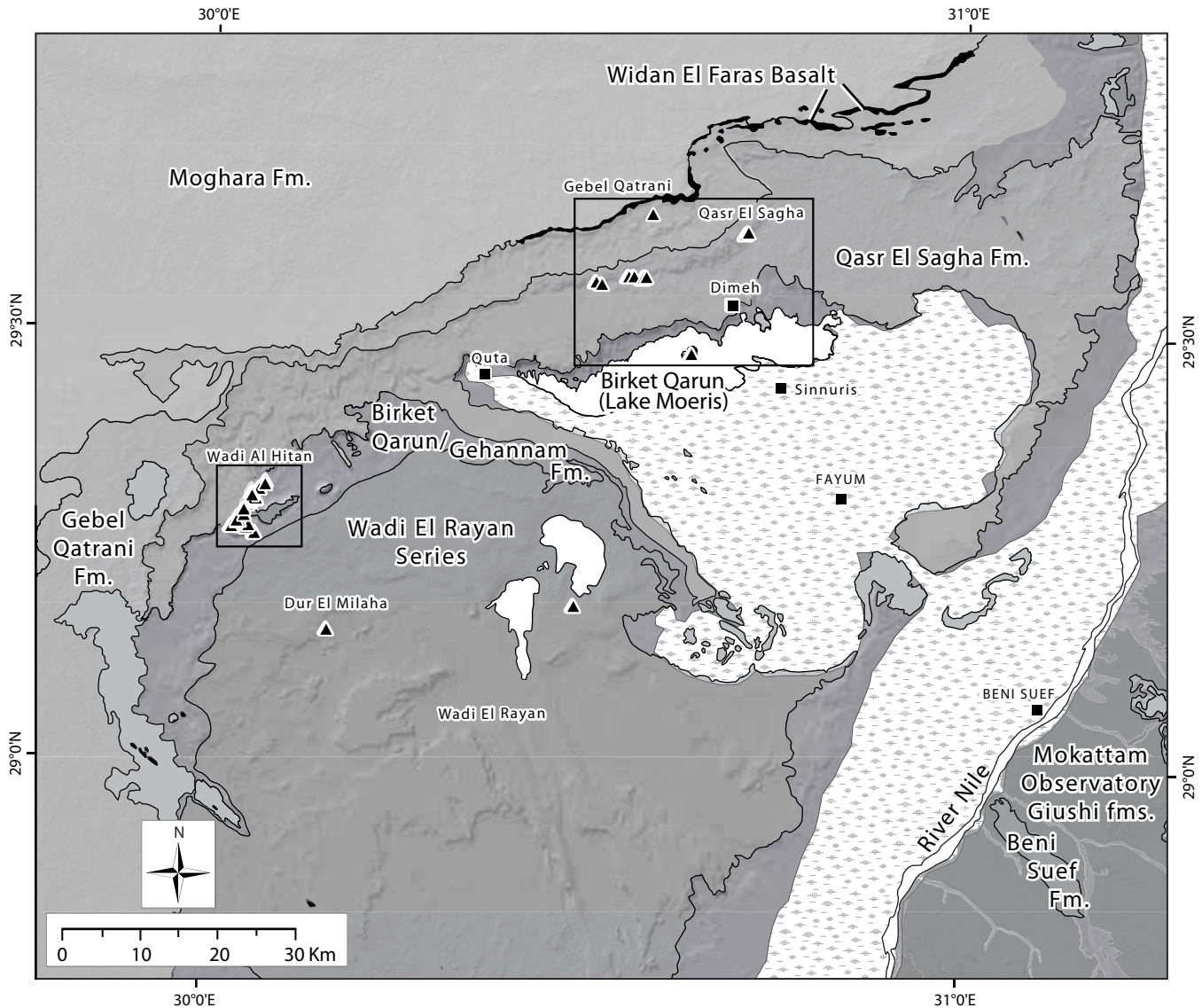


FIGURE 4 — Geological map of the Fayum Basin in the Western Desert of Egypt, west of the Nile Valley, showing Paleogene stratigraphic units that produced marine mammals and other marine and terrestrial vertebrates. Geological units and their boundaries are extracted and modified from the Conoco Oil Company 1:500,000 geological map series, including sheets for Alexandria, Baharia, Beni Suef, and Cairo. The Wadi El Rayan Series, the Gehannam, Birket Qarun, Qasr El Sagha, and Gebel Qatrani formations, and the Widan El Faras Basalt of Beadnell (1905) were revised by Bown and Krause (1988), Gingerich (1992), and recent field mapping in Fayum. Black triangles show the distribution of sirenian fossils known from the study area (listed in Table 2). The two larger rectangles north and southwest of Birket Qarun represent the main fossil fields with abundant marine mammal skeletons.

beds below the Qasr El Sagha Formation. Domning and Gingerich (1994) described *Protosiren smithae* from Wadi Al Hitan ('Zeuglodon Valley' or Valley of Whales) based on a very good skull associated with a vertebral column and pectoral and pelvic girdles. Oligocene beds of the Gebel Qatrani Formation above the Qasr El Sagha Formation produced a more derived taxon named *Eosiren imenti* (Domning et al., 1994).

New fossil sirenians described here include virtually complete skeletons from Wadi Al Hitan (Table 2) collected from the

western side of the Fayum depression and from escarpments above the north shore of Birket Qarun (Lake Moeris). These fossils provide detailed information about the evolution and systematics of Eocene sirenians in Egypt because they include cranial and postcranial elements found in association. Most of the sirenian fossils described from the Mokattam Hills near Cairo (Owen, 1875, Andrews, 1902b; Abel, 1907; Sickenberg, 1934) were found as isolated elements or partial skeletons (skulls with no postcrania, isolated vertebrae, rib cages with no cranial or

TABLE 1 — The global record of Eocene sirenians. Localities are plotted on the world map in Figure 2. Data are based on Domning et al. (1982, 2010), the Paleobiology Data Base (paleodb.org), and new material at the University of Michigan. The table is organized stratigraphically, with the oldest sirenians at the bottom and youngest at the top.

Taxon	Family	Country	Age	Reference
<i>Sirenia</i> indet.	Dugongidae	Libya	Priabonian-Rupelian	Savage, 1977
<i>Eotheroides sandersi</i>	Dugongidae	Egypt	Priabonian	This study
<i>Eotheroides clavigerum</i>	Dugongidae	Egypt	Priabonian	This study
“ <i>Eotheroides</i> , <i>Halitherium</i> ”?	Dugongidae	Romania	Priabonian	Sickenberg, 1934
<i>Eotheroides</i> sp.	Dugongidae	France	Priabonian	Freudenthal, 1970; Savage, 1977
<i>Eotheroides</i> sp.	Dugongidae	Jordan	Priabonian	Zalmout et al. 2003b
<i>Eotheroides</i> sp.	Dugongidae	Egypt	Priabonian	Vliet and Abu el Khair, 2010
<i>Eotheroides</i> sp.	Dugongidae	Egypt	Priabonian	Zalmout et al., 2012
<i>Indosiren javaensis</i>	Dugongidae	Java	Priabonian	von Koenigswald, 1952
<i>Prototherium veronense</i>	Dugongidae	Italy	Priabonian	de Zigno, 1875
<i>Prototherium intermedium</i>	Dugongidae	Italy	Priabonian	Bizzotto, 1983, 2005
<i>Paralitherium tarkanyense</i>	Dugongidae	Hungary	Priabonian	Kordos, 1977
<i>Halitherium taulannense</i>	Dugongidae	France	Priabonian	Sagne, 2001
<i>Eosiren libyca</i>	Dugongidae	Egypt	Priabonian	Andrews, 1902b
<i>Sirenia</i> indet.	Dugongidae	Mexico	Priabonian	Müllerried, 1932
<i>Sirenia</i> indet.	Dugongidae	USA	Priabonian (Jacksonian)	Domning et al., 1982
<i>Sirenia</i> indet.	Dugongidae	USA	Priabonian (Jacksonian)	Flower and Garson, 1884
<i>Protosiren smithae</i>	Protosirenidae	Egypt	Bartonian-Priabonian	Domning and Gingerich, 1994
<i>Protosiren sattaensis</i>	Protosirenidae	Pakistan	Bartonian	Gingerich et al., 1995
<i>Protosiren fraasi</i>	Protosirenidae	Egypt	Bartonian	Filhol, 1878; Abel, 1907
<i>Protosiren</i> indet.	Protosirenidae	USA	Bartonian	Beatty and Geisler, 2010
<i>Eotheroides</i> sp.	Dugongidae	USA	Bartonian	Domning et al., 1982
<i>Prototherium montserratense</i>	Dugongidae	Spain	Bartonian	Pilleri et al., 1989
<i>Prototherium solei</i>	Dugongidae	Spain	Bartonian	Pilleri et al., 1989
<i>Eosiren</i> sp.	Dugongidae	India	Bartonian	Bajpai et al., 2006
<i>Eosiren stromeri</i>	Dugongidae	Egypt	Bartonian	Sickenberg, 1934
<i>Sirenia</i> indet.	Dugongidae	Qatar	Bartonian	This study
<i>Eotheroides</i> sp.	Dugongidae	USA	Bartonian (Claibornian)	Domning et al., 1982
<i>Sirenia</i> indet.	Dugongidae	USA	Bartonian (Claibornian)	Domning et al., 1982
<i>Sirenia</i> indet.	Dugongidae	USA	Bartonian (Claibornian)	Arata and Jackson, 1965
<i>Sirenia</i> indet.	Dugongidae	USA	Bartonian (Claibornian)	Siler, 1964
<i>Sirenia</i> indet.	Dugongidae	USA	Bartonian (Claibornian)	Domning et al., 1982
<i>Sirenia</i> indet.	Dugongidae	USA	Bartonian (Claibornian)	Reinhart, 1976
<i>Sirenia</i> indet.	Dugongidae	USA	Bartonian (Claibornian)	Vernon, 1951, Reinhart, 1976
<i>Sirenia</i> indet.	Dugongidae	USA	Bartonian (Claibornian)	Domning et al., 1982
<i>Sirenia</i> indet.	Dugongidae	USA	Bartonian (Claibornian)	Domning et al., 1982
<i>Sirenia</i> indet.	Dugongidae	USA	Bartonian (Claibornian)	Domning et al., 1982
<i>Sirenia</i> indet.	Dugongidae	USA	Bartonian (Claibornian)	Domning et al., 1982
<i>Sirenia</i> indet.	Dugongidae	USA	Bartonian (Claibornian)	Domning et al., 1982

pectoral elements), which made it difficult to develop a clear understanding of the overall morphology of these animals.

Table 2 summarizes the fossil sirenian material from Wadi Al Hitan and the surrounding areas. Some specimens have been published already, but the rest are either new or represent new material of previously known taxa that add more detailed information. Locations and stratigraphic units for all studied specimens are plotted in Figures 5, 6, and 7.

Published reports on Fayum paleontology discuss the structure, systematics, habitats, and secondary adaptation of *Sirenia* to life in water (Andrews, 1906; Abel, 1907; Sickenberg, 1934; Siegfried, 1967; Gingerich, 1992; Domning and Gingerich,

1994; Domning et al., 1994). However, previous authors writing about Egyptian sirenians rarely included any discussion or interpretation of postcranial elements and their paleobiological value, either because little was known about postcranial skeletons, or because postcranial elements were overlooked or underestimated.

OBJECTIVES

The three sirenian genera *Eotheroides*, *Eosiren*, and *Protosiren*, known from the Eocene of Fayum, are reviewed and

TABLE 1 — (continued).

Taxon	Family	Country	Age	Reference
Sirenia indet.	Dugongidae	USA	Bartonian (Claibornian)	Sanders, 1974
Sirenia indet.	Dugongidae	USA	Bartonian (Claibornian)	Domning et al., 1982
Sirenia indet.	Dugongidae	USA	Bartonian (Claibornian)	Domning et al., 1982
Sirenia indet.	Dugongidae	USA	Bartonian (Claibornian)	Domning et al., 1982
Sirenia indet.	Dugongidae	USA	Bartonian (Claibornian)	Domning et al., 1982
Sirenia indet.	Dugongidae	USA	Bartonian (Claibornian)	Emmons, 1858
Sirenia indet.	Dugongidae	Egypt	Bartonian?	Gingerich et al., 2007
<i>Eotheroides lambdrano</i>	Dugongidae	Madagascar	Middle Eocene	Samonds et al., 2009
Sirenia indet.	Dugongidae	Madagascar	Middle Eocene	Samonds et al., 2007
Sirenia indet.	Dugongidae	Spain	Lower Bartonian	Astibia et al., 2005
<i>Halitherium</i> sp.	Dugongidae	Spain	Lutetian-Bartonian	Bataller, J. R., 1956
<i>Protosiren</i> sp.	Protosirenidae	Egypt	Lutetian	This study
<i>Eotheroides aegyptiacum</i>	Dugongidae	Egypt	Lutetian	Owen, 1875; Zdansky, 1938
<i>Eosiren abeli</i>	Dugongidae	Egypt	Lutetian	Sickenberg, 1934
<i>Protosiren</i> sp.	Protosirenidae	Egypt	Lutetian?	Blainville, 1840, 1844
<i>Protosiren minima</i>	Protosirenidae	France	Lutetian	Sickenberg, 1943; Richard, 1946
<i>Protosiren</i> cf. <i>fraasi</i>	Protosirenidae	Hungary	Lutetian	Kordos, 1978
<i>Sirenavus hungaricus</i>	Dugongidae	Hungary	Lutetian	Kretzoi, 1941
<i>Anisosiren pannonica</i>	Dugongidae	Hungary	Lutetian	Kordos, 1979
<i>Eotheroides</i> sp.	Dugongidae	Hungary	Lutetian ?	Kordos, 1980, 2002
<i>Protosiren fraasi</i>	Protosirenidae	India	Lutetian	Sahni and Mishra, 1975
<i>Protosiren</i> sp.	Protosirenidae	India	Lutetian	Bajpai et al., 2006
<i>Eotheroides babiae</i>	Dugongidae	India	Lutetian	Bajpai et al., 2006
<i>Indosiren koenigswaldi</i>	Dugongidae	India	Lutetian	Sahni and Mishra, 1975
<i>Ashokia antiqua</i>	Protosirenidae	India	Lutetian	Bajpai et al., 2009
Sirenia indet.	Dugongidae	Jordan	Lutetian	Zalmout et al. 2003b
<i>Libysiren sickenbergi</i>	Protosirenidae	Libya	Lutetian	Heal, 1973
<i>Eotheroides</i> sp.	Dugongidae	Libya	Lutetian	Heal, 1973
<i>Protosiren eothene</i>	Protosirenidae	Pakistan	Lutetian	Zalmout et al., 2003a
Sirenia indet.	Dugongidae	Somalia	Lutetian	Savage, 1969
Sirenia indet.	Dugongidae	Somalia	Lutetian	Savage, 1969
Sirenia indet.	Dugongidae	Somalia	Lutetian	Savage, 1969
Sirenia indet.	Dugongidae	Togo	Lutetian	Gingerich et al., 1992
Sirenia indet.	Dugongidae	Tunisia	Lutetian	Batik and Fejfar, 1990
Sirenia indet.	Dugongidae	Yemen	Lutetian	As-Saruri et al., 1999
Prorastomidae indet.	Prorastomidae	Senegal	Lutetian	Hautier et al., 2012
<i>Pezosiren portelli</i>	Prorastomidae	Jamaica	Lutetian	Domning, 2001b
<i>Prorastomus sirenoides</i>	Prorastomidae	Jamaica	Lutetian	Owen, 1855
Sirenia indet.	Dugongidae	Hungary	Ypresian?	Kretzoi, 1953

compared to one another in terms of anatomy and adaptation to water based on new cranial and skeletal specimens. Bartonian and Priabonian sirenians from the Fayum Basin are compared to those known from the Lutetian nummulitic limestone at Gebel Mokattam near Cairo.

This work addresses questions concerning the Eocene Sirenia and their environments at Wadi Al Hitan in the Fayum Basin. Questions to be addressed include the following:

How many sirenian species lived in Wadi Al Hitan? What were the reasons behind such diversity? Was high diversity primarily due to biological factors, physical factors, or both?

What were the environments inhabited by sirenians in Wadi

Al Hitan? Can differences in environment be detected and associated with morphological differences characteristic of different sirenian genera?

What were the locomotive behaviors in these marine mammals? How can these be studied, constrained, and explained?

How much difference is there between marine vertebrate communities in different geological formations and locations in Fayum? How similar are Eocene Tethys Sea communities in Wadi Al Hitan to those in Asia, Europe, and North America?

What was the destiny of Bartonian and Priabonian sirenians in Wadi Al Hitan, and how do they differ from later Rupelian sirenians in the same basin (the fauna of the Gebel Qatrani Formation)?

TABLE 2 — Eocene and Oligocene sirenian specimens of known locality in the Fayum Basin. The oldest specimen, UM 101229, was collected from the top of the Midawara Formation (Lutetian), and the youngest, CGM 40210, came from the Rupelian Gebel Qatrani Formation. Abbreviations for localities: *DUQ*, Duke University Quarry in the Gebel Qatrani Formation; *GelEsh*, Garet El Esh; *QS*, Qasr El Sagha; *WR*, Wadi El Rayan; *WH*, Wadi Al Hitan.

Specimen	Taxon	Family	Locality	Longitude	Latitude	Age
CGM 40210	<i>Eosiren imenti</i>	Dugongidae	DUQ-O	30.57570	29.64346	Rupelian
CGM 42179	<i>Eosiren libyca</i>	Dugongidae	QS-5	30.70044	29.62192	Priabonian
CGM 42180	<i>Eosiren libyca</i>	Dugongidae	QS-9	30.54544	29.57050	Priabonian
CGM 42181	<i>Eotheroides sandersi</i>	Dugongidae	WH-230	30.06849	29.32138	Priabonian
CGM 42189	<i>Eotheroides</i> indet	Dugongidae	QS-8	30.55245	29.57063	Priabonian
CGM 42287	<i>Eotheroides clavigerum</i>	Dugongidae	WH-190	30.05552	29.26340	Priabonian
CGM 42292	<i>Protosiren smithae</i>	Protosirenidae	WH-54	30.04581	29.29639	Priabonian
CGM 42298	<i>Eotheroides clavigerum</i>	Dugongidae	WH-101	30.04472	29.26962	Priabonian
CGM 60551	<i>Eotheroides clavigerum</i>	Dugongidae	WH-219	30.05147	29.30901	Priabonian
CGM 60582	<i>Protosiren</i> indet	Protosirenidae	WR05-01	30.48042	29.18617	Bartonian
UM 83903	<i>Eotheroides clavigerum</i>	Dugongidae	WH-207	30.05684	29.30225	Priabonian
UM 94806	<i>Eotheroides clavigerum</i>	Dugongidae	WH-33	29.28212	30.03437	Priabonian
UM 94809	<i>Eotheroides sandersi</i>	Dugongidae	WH-79	30.02493	29.27087	Priabonian
UM 97514	<i>Eotheroides sandersi</i>	Dugongidae	WH-110	30.03139	29.27626	Priabonian
UM 97515	<i>Eotheroides sandersi</i>	Dugongidae	WH-117	30.03531	29.27690	Priabonian
UM 97520	<i>Eotheroides clavigerum</i>	Dugongidae	WH-128	30.03170	29.27729	Priabonian
UM 97523	<i>Protosiren smithae</i>	Protosirenidae	WH-144	30.05695	29.30296	Priabonian
UM 97524	<i>Eotheroides clavigerum</i>	Dugongidae	WH-145	30.05664	29.30362	Priabonian
UM 97539	<i>Eosiren libyca</i>	Dugongidae	GelEsh-1	30.56436	29.56816	Priabonian
UM 97540	<i>Eosiren libyca</i>	Dugongidae	GelEsh-1	30.56436	29.56816	Priabonian
UM 97549	<i>Eosiren libyca</i>	Dugongidae	GelEsh-1	30.56436	29.56816	Priabonian
UM 97556	<i>Eosiren libyca</i>	Dugongidae	GelEsh-1	30.56436	29.56816	Priabonian
UM 97568	<i>Eosiren libyca</i>	Dugongidae	GelEsh-1	30.56436	29.56816	Priabonian
UM 100137	<i>Eosiren stromeri</i>	Dugongidae	GelEsh-4	30.56503	29.56934	Priabonian
UM 100138	<i>Eotheroides sandersi</i>	Dugongidae	WH-180	30.04124	29.28403	Priabonian
UM 100184	<i>Eotheroides clavigerum</i>	Dugongidae	WH-200	30.06089	29.31468	Priabonian
UM 100191	<i>Eosiren stromeri</i>	Dugongidae	GelEsh-9	30.56856	29.57004	Priabonian
UM 100192	<i>Eosiren stromeri</i>	Dugongidae	GelEsh-10	30.56857	29.57004	Priabonian
UM 101220	<i>Eotheroides clavigerum</i>	Dugongidae	WH-220	30.05200	29.30940	Priabonian
UM 101224	<i>Protosiren smithae</i>	Protosirenidae	WH-227	30.06853	29.32028	Priabonian
UM 101226	<i>Eosiren libyca</i>	Dugongidae	QS-3	30.50982	29.56094	Priabonian
UM 101228	<i>Eosiren libyca</i>	Dugongidae	QS-6	30.70333	29.62390	Priabonian
UM 101229	<i>Protosiren smithae</i>	Protosirenidae	WH-224	30.15395	29.15310	Lutetian
UM 111558	<i>Eotheroides sandersi</i>	Dugongidae	WH-174	30.04108	29.29035	Priabonian
Field	<i>Eotheroides</i> indet	Dugongidae	QS-2	30.50217	29.56340	Priabonian
Field	<i>Eotheroides</i> indet	Dugongidae	WH-34	30.03386	29.28175	Priabonian
Field	<i>Eotheroides</i> indet	Dugongidae	WH-124	30.04743	29.27235	Priabonian
Field	<i>Eotheroides</i> indet	Dugongidae	WH-130	30.03498	29.27845	Priabonian
Field	<i>Eotheroides sandersi</i>	Dugongidae	WH-231	30.06913	29.32319	Priabonian

In the following chapters we provide a geological and stratigraphic overview of the main Eocene fossil beds yielding Sirenia in the Fayum Basin (Chapter II); systematic descriptions and identifications of new fossil Sirenia from the Fayum Basin (Chapter III); comparisons of Wadi Al Hitan *Eotheroides* (Chapter IV); quantitative comparison of skeletal elements (Chapter

V); a discussion of sexual dimorphism in Eocene Sirenia (Chapter VI); and information about the paleoenvironments and paleoecology of beds yielding Sirenia in the Fayum Basin, with a discussion of secondary adaptation to water, swimming capabilities, and feeding behavior of Eocene Sirenia (Chapter VII).

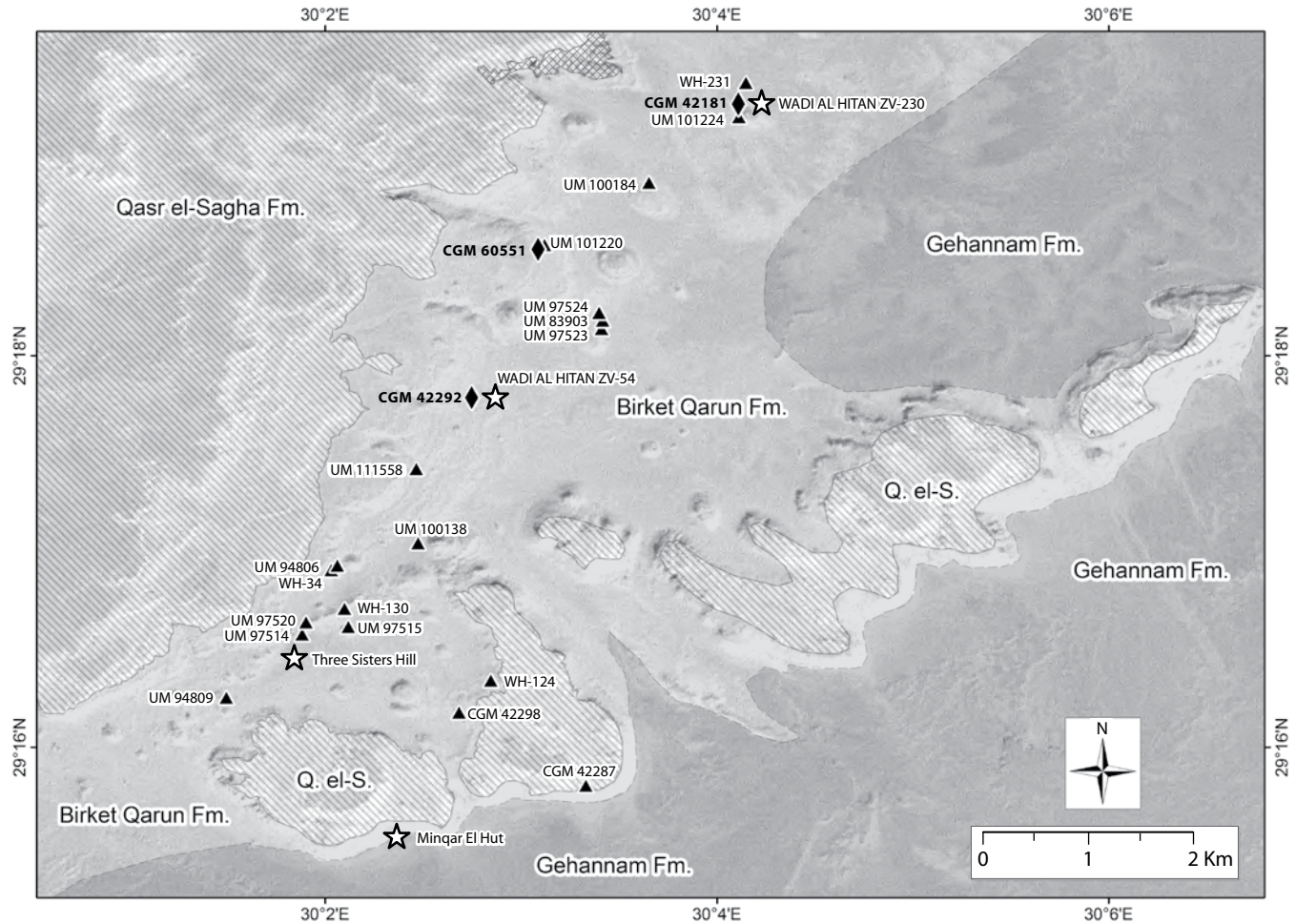


FIGURE 5 — Late Eocene sirenian fossils in Wadi Al Hitan in the western Fayum Basin plotted in geological context. Most specimens come from the Birket Qarun Formation (lower Priabonian). Diamonds represent type specimens of the order Sirenia known from Wadi Al Hitan; triangles represent all other sirenian fossils in Wadi Al Hitan. Stars mark the locations of stratigraphic columns described later in this work.

METHODS

Specimens described here were obtained during field research in Wadi Al Hitan between 1983 and 1993. Field work included prospecting for fossils, field identification, mapping and registration of specimens on site, surface collecting and excavation, plaster jacketing, geological mapping, and stratigraphic section measuring. A GPS unit was first available for mapping fossils in 1993. Localities of specimens collected earlier were revisited in order to place each in geological and stratigraphic context, and to record GPS coordinates. Digital satellite imagery was used in the field to trace local stratigraphic units and to find new fossil localities.

Many of the Eocene fossil vertebrates found in Egypt, sirenians included, are exceptionally well preserved. However, recovery of their full scientific value requires extensive laboratory preparation by trained experts working to remove them from

their sedimentary matrix and glue the fossils with hardener that will preserve them. Once cleaned, fossils were compared, measured, and identified, and then landmarks and characteristics that provide the raw material for this research were recorded.

Sirenian remains were hardened in the field using polyvinyl acetate (PVA) dissolved in acetone. Broken pieces were glued in the field or later in the laboratory using Duco, Uhu, epoxy, or PaleoBond. Sirenian skeletons that were excavated and removed from the field in plaster jackets were prepared carefully using aircsribes under magnification.

Examination of Eocene sirenians here included two major tasks. The first was identification of all sirenian skeletal elements and assignment to systematic position based on primitive and derived characteristics published by Domning (1994, 1996). The second task was measurement of the variable dimensions of cranial (Figs. 8, 9) and postcranial elements (Figs. 10-19) to quantify the morphological variation.

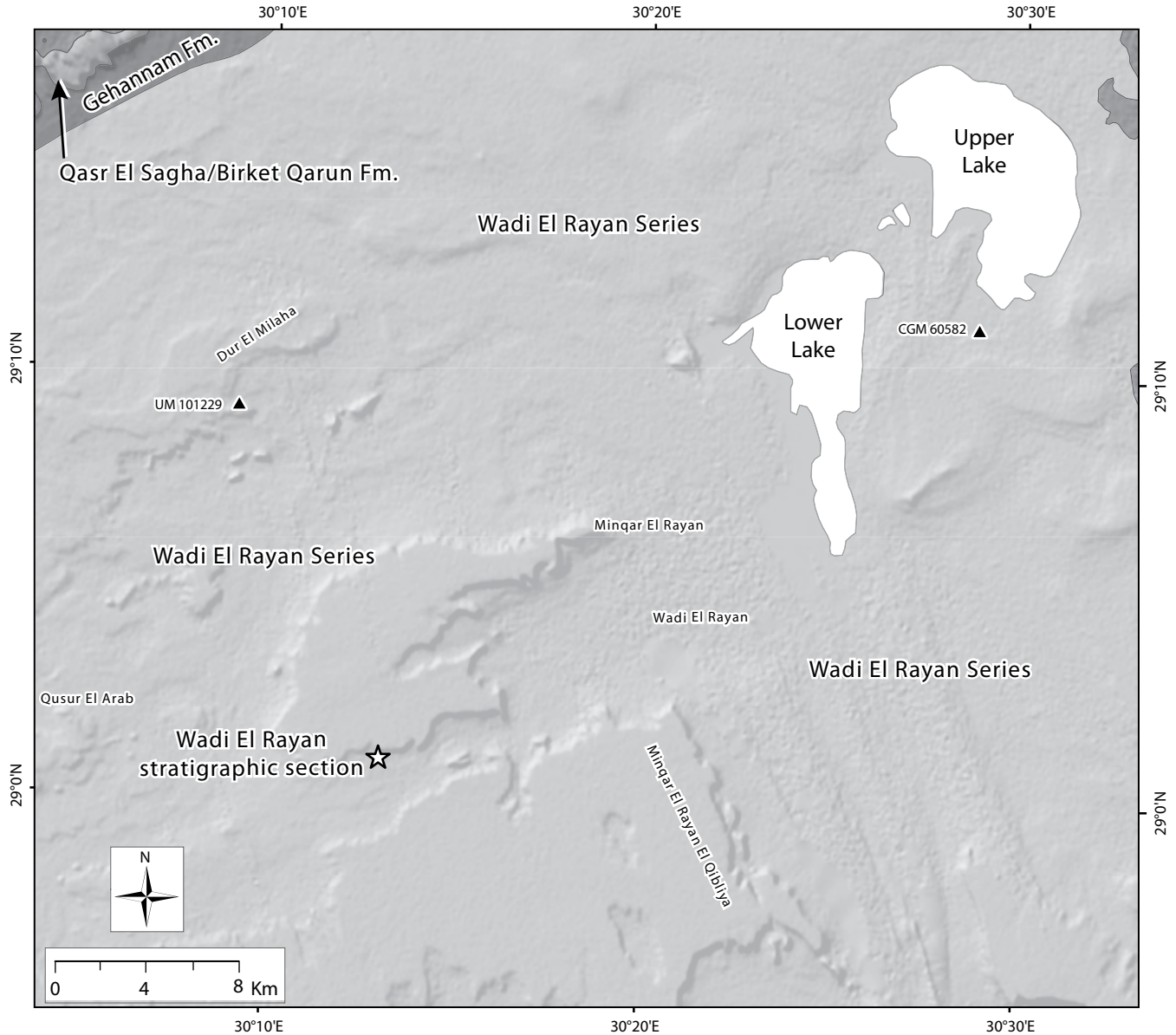


FIGURE 6 — Distribution of sirenian fossils in Wadi El Rayan, east and southeast of Wadi Al Hitan. Strata exposed here belong to the Wadi El Rayan series of Lutetian and Bartonian age. Triangles represent sirenian fossils found in the Wadi El Rayan area. UM 101229 was collected from the top of the Midawara Formation, and CGM 60582 was collected from the El Gharaq Formation.

Postcranial elements with significantly variable attributes include vertebrae, where variations in centrum length and height are interesting, and pectoral and pelvic elements where lengths differ between taxa. Measurements of these characteristics were used to show variation among the different groups of the Eocene sirenians of Egypt. Pectoral and pelvic girdle elements were measured in detail for comparative purposes.

A Mitutoyo digital calipers was used to measure linear dimensions. Circumferences, arc lengths, and perimeters were all measured using a measuring tape. Most measurements of cranial and postcranial elements follow Domning (1978a) and Furusawa (1988).

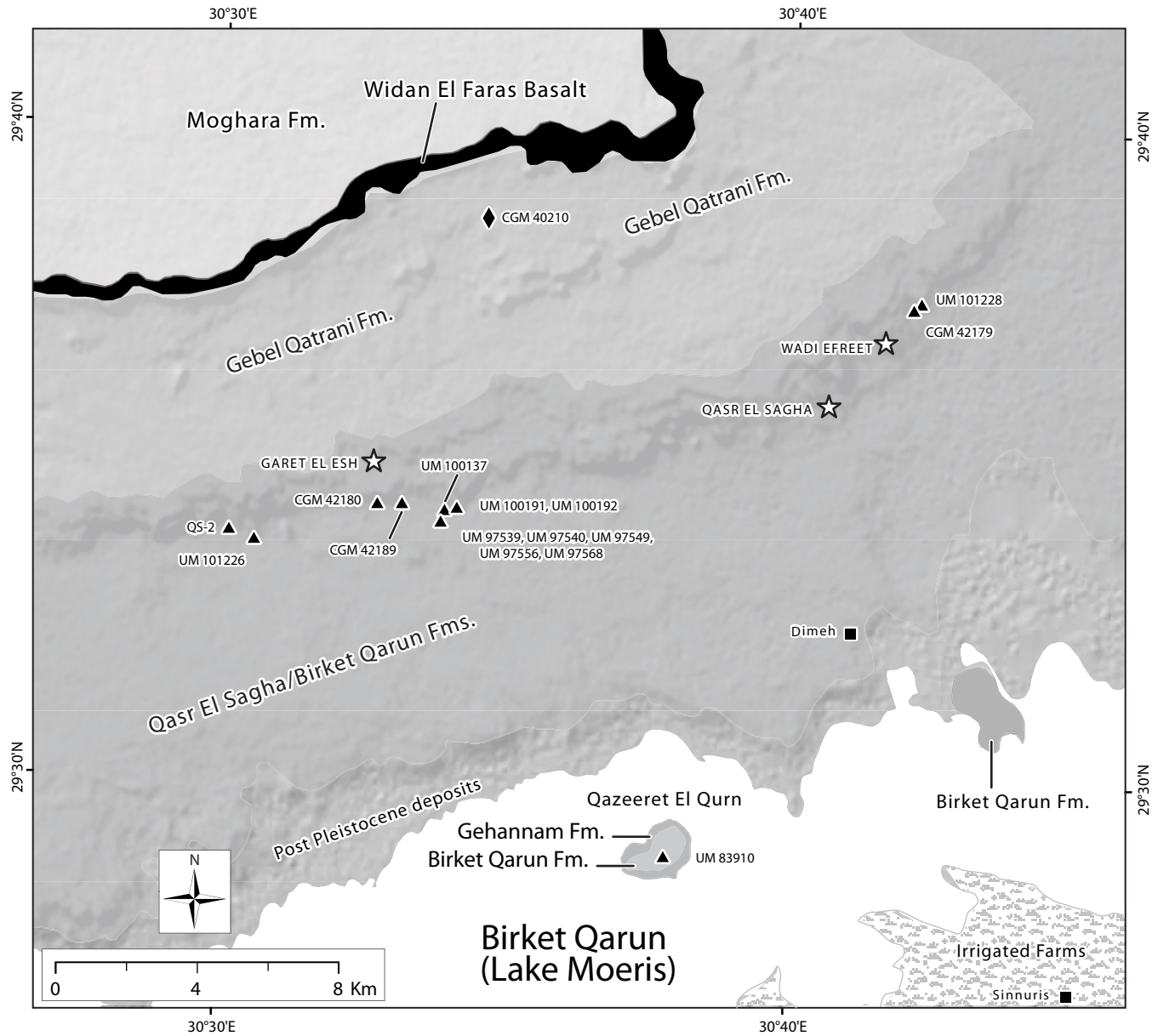


FIGURE 7 — Distribution of sirenian fossils in and north of Birket Qarun (Lake Moeris). The oldest rocks exposed here are located on the lower part of Geziret El Qarn and belong to the early Priabonian Gehannam Formation. Most sirenian fossils in this area come from the later Priabonian Qasr El Sagha Formation. The type specimen of *Eosiren imenti* (CGM 40210) was found in Rupelian Oligocene beds of the Gebel Qatrani Formation. UM 83910 is an isolated candal vertebra of *Protosiren* sp.

INSTITUTIONAL ABBREVIATIONS

- | | |
|--|--|
| <p>BMNH — British Museum of Natural History (NHML=Natural History Museum), London, England</p> <p>CGM — Cairo Geological Museum (Egyptian Geological Museum), Cairo, Egypt</p> | <p>MTM — Magyar Természettudományi Múzeum (Hungarian Natural History Museum), Budapest, Hungary</p> <p>MÁFI — Magyar Állami Földtani Intézet (Geological Institute of Hungary), Budapest, Hungary</p> <p>NSM-PV — National Science Museum-Vertebrate Paleontology collection, Tokyo, Japan</p> |
|--|--|

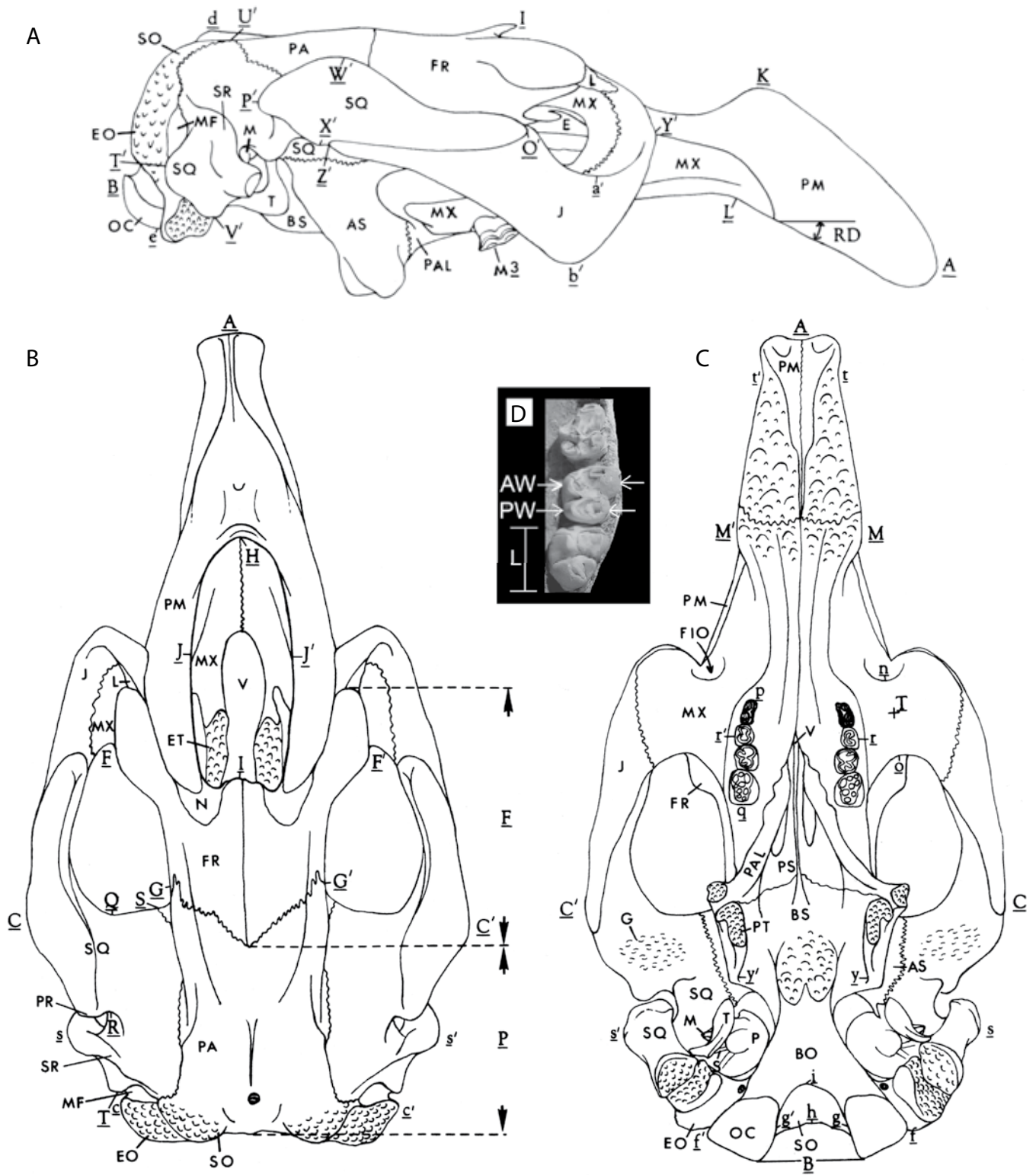


FIGURE 8 — Key to measurements of cranial elements used in this study, based on Domning (1978a). A, B, and C, are lateral, dorsal, and palatal views of *Dusiares jordanii*. D is an occlusal view of a *Protosiren fraasi* maxilla.

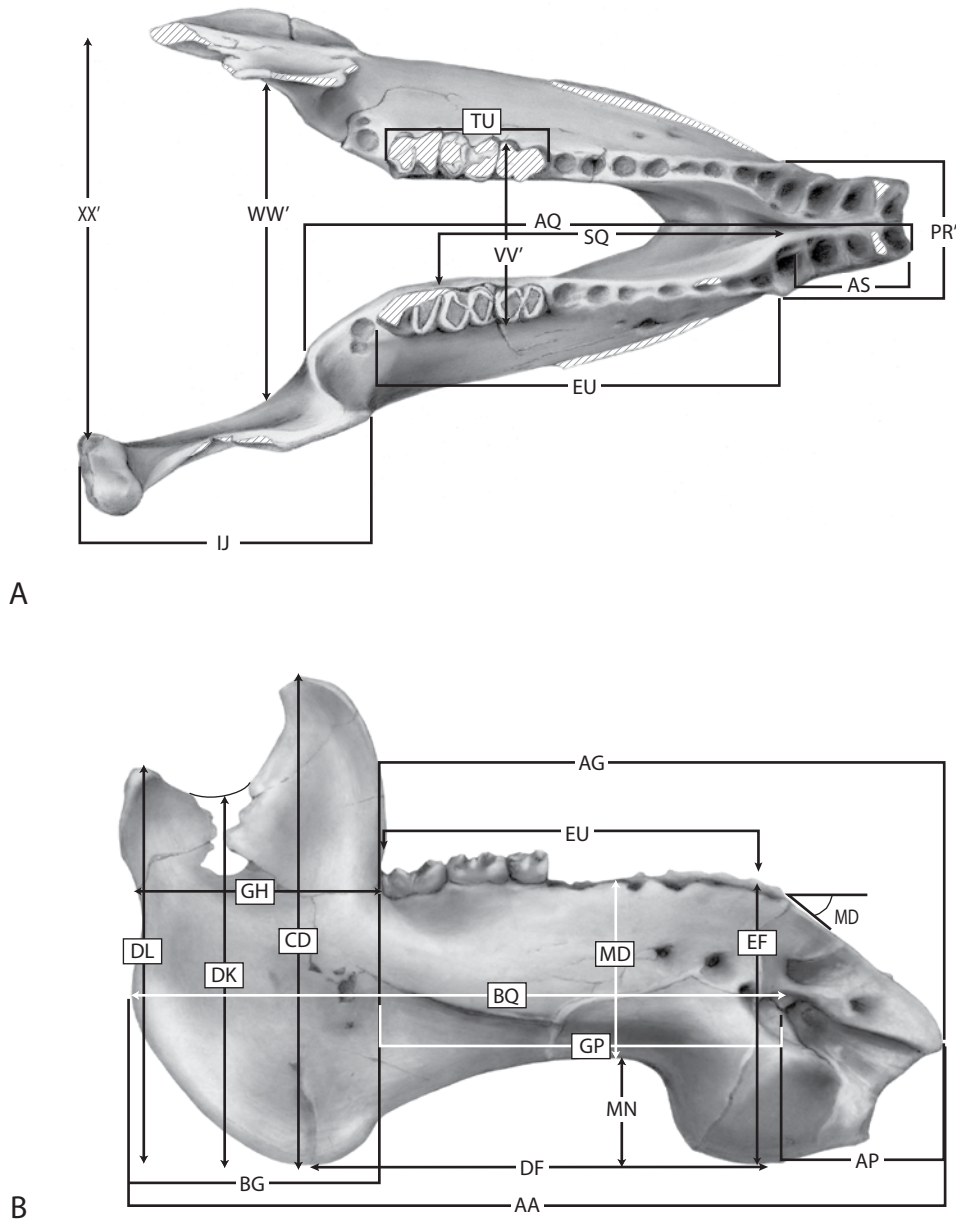


FIGURE 9 — Key to measurements of mandibular elements used in this study, based on Domning (1978a). A, B, are dorsal and lateral views of the *Eotheroides clavigerum* type specimen (CGM 60551).

- SMNS — Staatliches Museum für Naturkunde, Stuttgart, Germany
- UM — Museum of Paleontology, University of Michigan, Ann Arbor (USA)
- UMMZ — Museum of Zoology, University of Michigan, Ann Arbor (USA)
- USNM — Former United States National Museum collections deposited in the National Museum of Natural History, Smithsonian Institution, Washington D.C. (USA)

- YPM — Peabody Museum of Natural History, Yale University, Yale (USA)

In addition, DUQ-O is used for a specimen from Duke University Quarry 'O' in the Gebel Qatrani Formation. WH is used for Wadi Al Hitan World Heritage Site or 'Valley of Whales' specimens in the Cairo Geological Museum (Egypt); for specimens in the Museum of Paleontology, University of Michigan, Ann Arbor (USA); and for specimens remaining in the field.

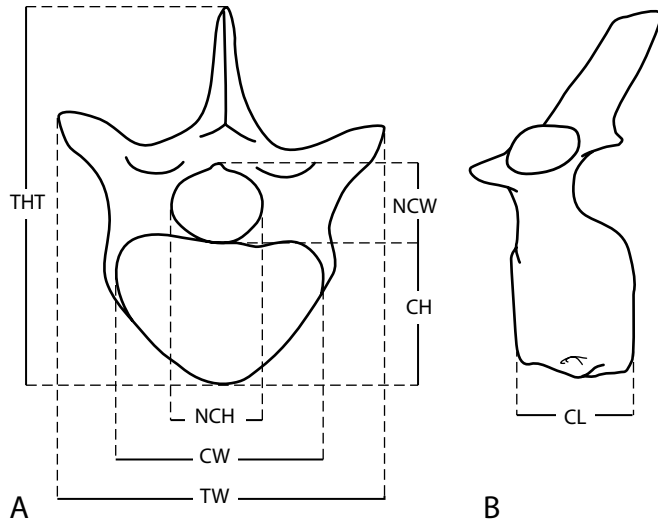


FIGURE 10 — Key to measurements of vertebrae used in this study. A and B are cranial and lateral views of the thoracic vertebra of a dugongid sea cow.

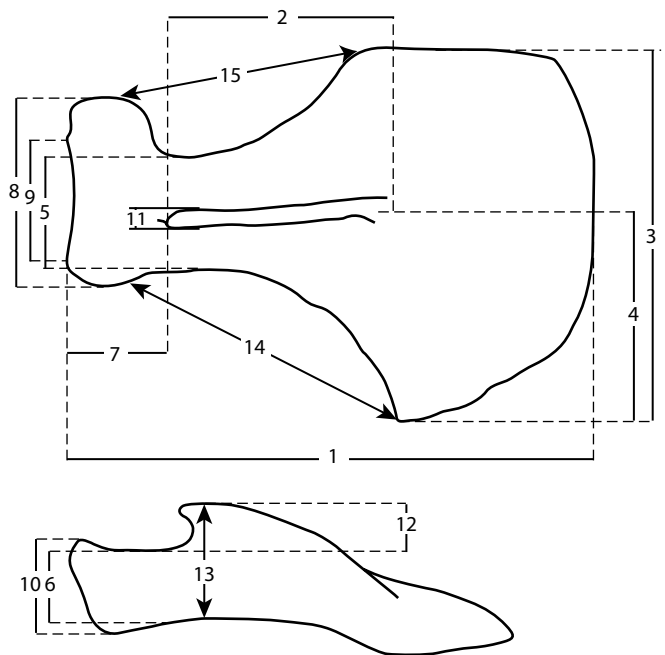


FIGURE 12 — Key to measurements of scapulae used in this study, based on Furusawa (1988). A and B are lateral and posterior views of the left scapula of a dugongid.

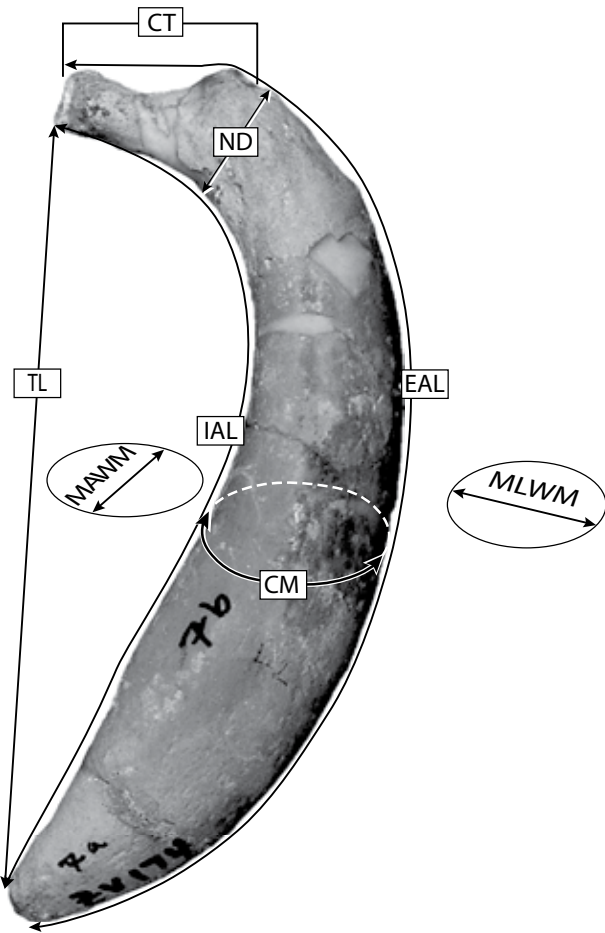


FIGURE 11 — Key to measurements of ribs used in this study. The anterior rib of *Eotheroides sandersi* (UM 111558) shown here is pachyosteosclerotic (with bone thickened and dense).

ANATOMICAL ABBREVIATIONS

- AC alisphenoid canal (foramen in *Eotheroides* and *Eosiren*)
- act. n. acetabular notch
- act. acetabulum
- ANG. P. angular process
- ant. anterior
- APF anterior palatine foramen
- AS alisphenoid
- BO basioccipital
- BS basisphenoid
- C¹ upper canine or alveolus
- c₁ lower canine or alveolus
- C1, C2, C3. cervical vertebrae
- Ca caudal vertebra
- CF condyloid foramen
- COND. P. processus condylus
- COR. CAN. coronoid canal
- COR. P. coronoid process
- cre. cranial epiphysis of centrum
- CT temporal crest
- dor. il. sp. dorso iliac spine
- dp alv. alveolar of lower deciduous premolar
- dP¹ etc. deciduous upper premolar
- dP₁ etc. deciduous lower premolar
- E ethmoid

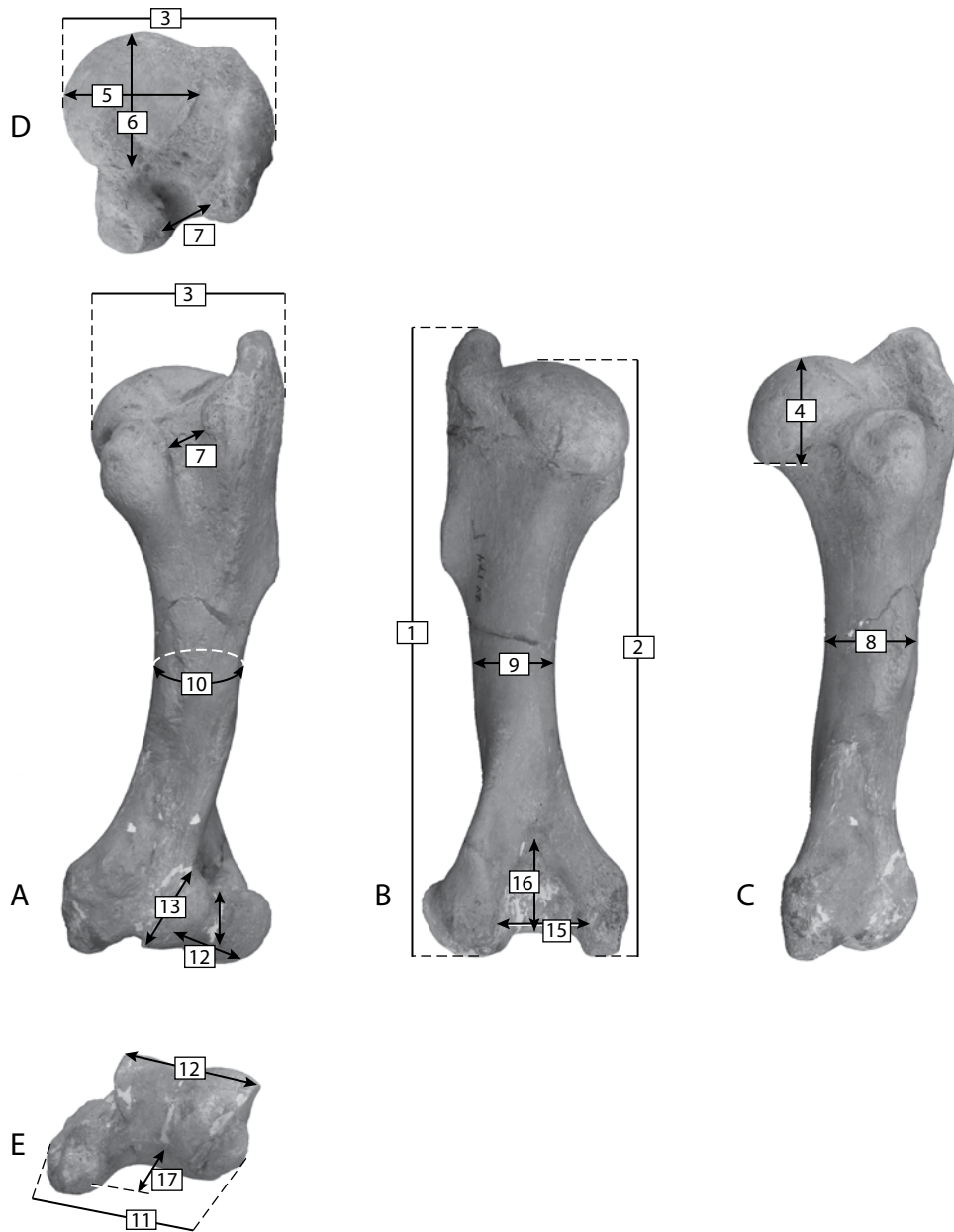


FIGURE 13 — Key to measurements of humeri used in this study. A-E are anterior, posterior, medial, proximal, and distal views E of a left humerus of *Eotheroides sandersi* (UM 111558).

ENR external nares (mesorostral fossa)
EO exoccipital
Fb. fibula
FIO foramen infraorbital
FM foramen magnum
Fm. femur
FOV foramen ovalis
FPT fossa pterygoidea
FR frontal

FRT foramen rotundum
G glenoid articulation
HOR. RAM. horizontal ramus
I¹ etc. upper incisor or alveolus
I₁ etc. lower incisor or alveolus
IC incus
il. shft. iliac shaft
il. ilium
INP interparietal groove

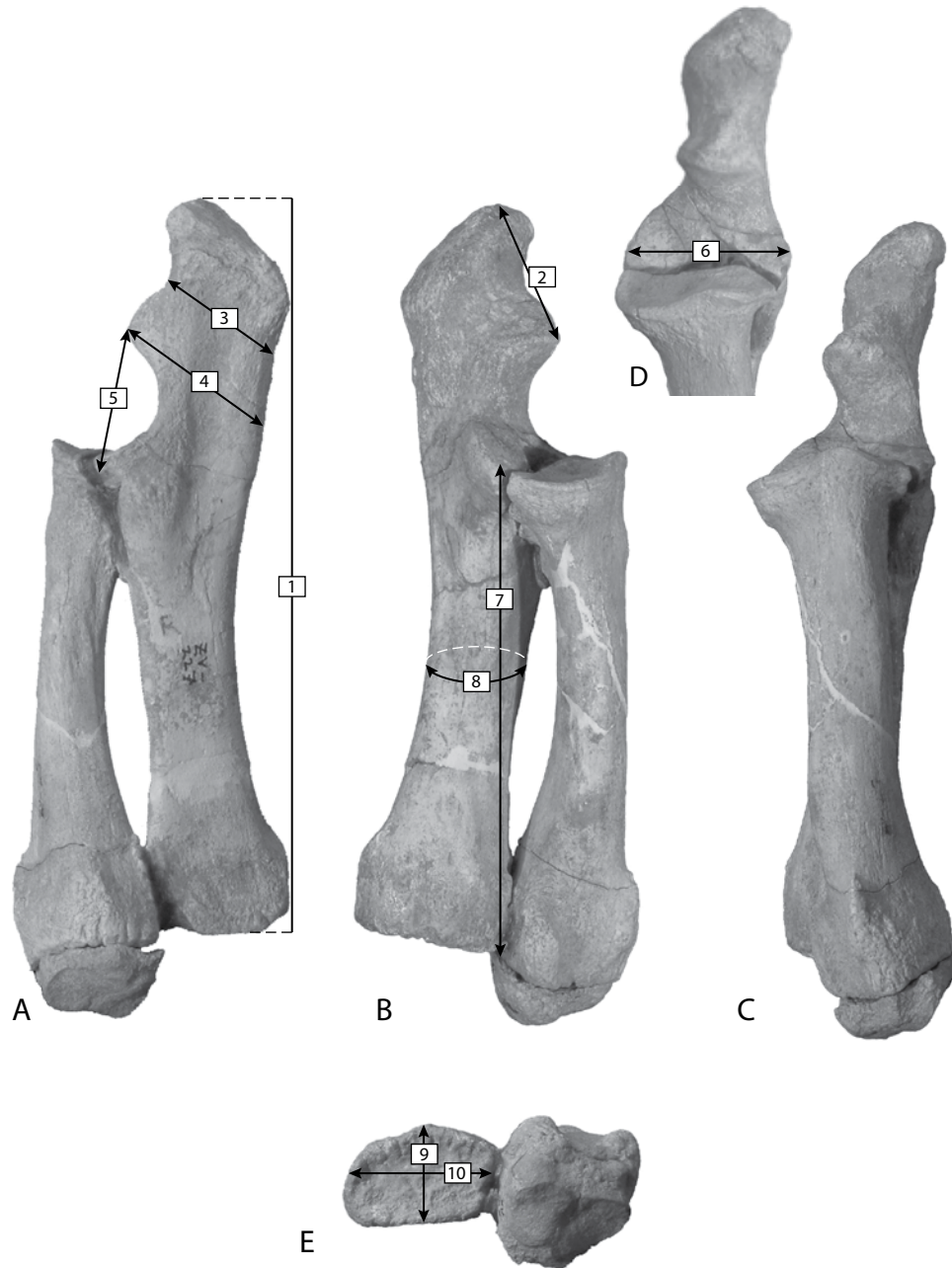


FIGURE 14 — Key to measurements of ulnae used in this study. A-E are medial, lateral, anterior, proximal, and distal views a right ulna and radius of *Protosiren smithae* (UM 101224).

INR internal nares
isc. shft. ischiac shaft
isc. tub. ischiac tuberosity
isc. ischium
J jugal
L1, L2, L3. left ribs
LAC lacrimal
Lr lumbar vertebra

M¹ etc. upper molar or alveolus
M₁ etc. lower molar or alveolus
MAL malleus
MAL. M. manubrium mallei
MAND. FOS. mandibular fossa
MAND. RAM. mandibular ramus
ME mesethmoid
MENT. FOR. mental foramen

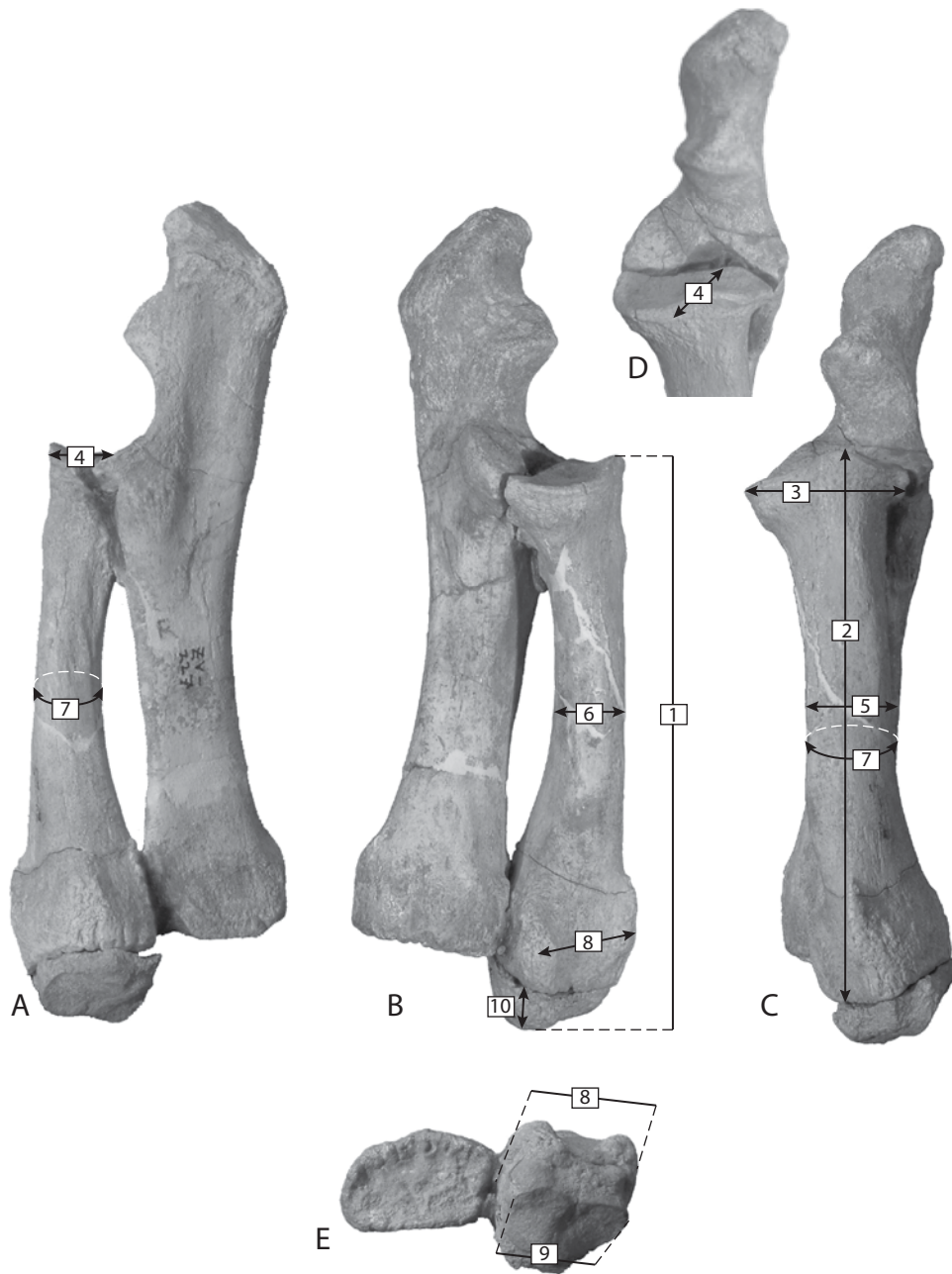


FIGURE 15 — Key to measurements of radii used in this study. A-E are medial, lateral, anterior, proximal, and distal views of a right ulna and radius of *Protosiren smithae* (UM 101224).

MENT. PROT. mental protuberance
Met. metacarpals
MF mastoid foramen
MSF mastoid foramen
MX maxilla
N Nasal
n. c. neural canal
n. sp. neural spine

obt. f. obturator foramen
OCC occipital condyle
OF optic foramen
OVF oval foramen
P. MAS. pars mastoidea (=pars petrosa, pars labyrinthica, also pars fonticulus or 'PFT')
P.TEM. pars temporalis (=tegmen tympani)
P¹ etc upper premolar or alveolus

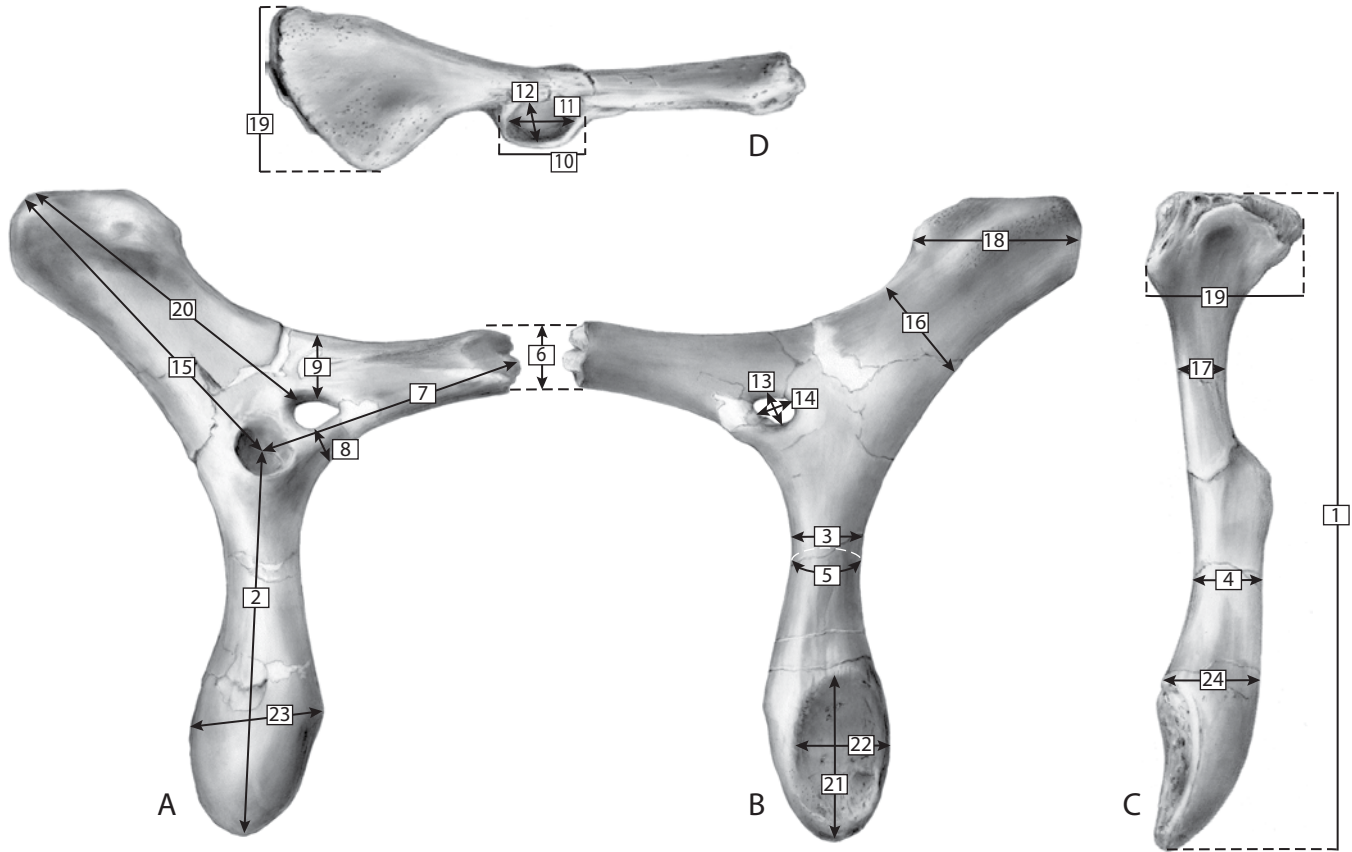


FIGURE 16 — Key to measurements of pelvic bones used in this study. A-D are lateral, medial, dorsal, and posterior views of a left innominate of *Eotheroides sandersi* (UM 97514).

P₁ etc.	lower premolar or alveolus	pub. ram. post.	posterior pubic ramus
PA	parietal	pub. symph.	pubic symphysis
PAL	palatine	R1, R2, R3	right ribs
PAR. O. P.	paroccipital processes	RCD	rectus semispinalis dorsalis
PF	processus folianus	S	sacral vertebra
PFT	pars fonticulus	sac. il. artic.	sacroiliac articulation surface
PGF	postglenoid fossa	sac. il.	sacral pleurapophyses
PLG	perlymphatic glenoid	SF	sulcus facialis
PM	premaxilla	SO	supraoccipital
POP	post occipital process	SOP	supraorbital process
POST. T. P	post-tympanic process	SQ	squamosal
post.	posterior	SSC	semispinalis capitata
PR	periotic	ST	sulcus tympanicus
pr. zph.	prezygapophysis	T	tympanic (=tympanic ring)
PRTM	promontorium	t. pr.	transverse process
PS	presphenoid	Tb.	tibia
ps.	pubis	TF	temporal fossa
PT	pterygoid	Th	thoracic
PTP	pterygoid process	TH	tympanohyale
pub. cleft.	pubic cleft	V	vomer
pub. ram. ant.	anterior pubic ramus	ZP	zygomatic process of the jugal

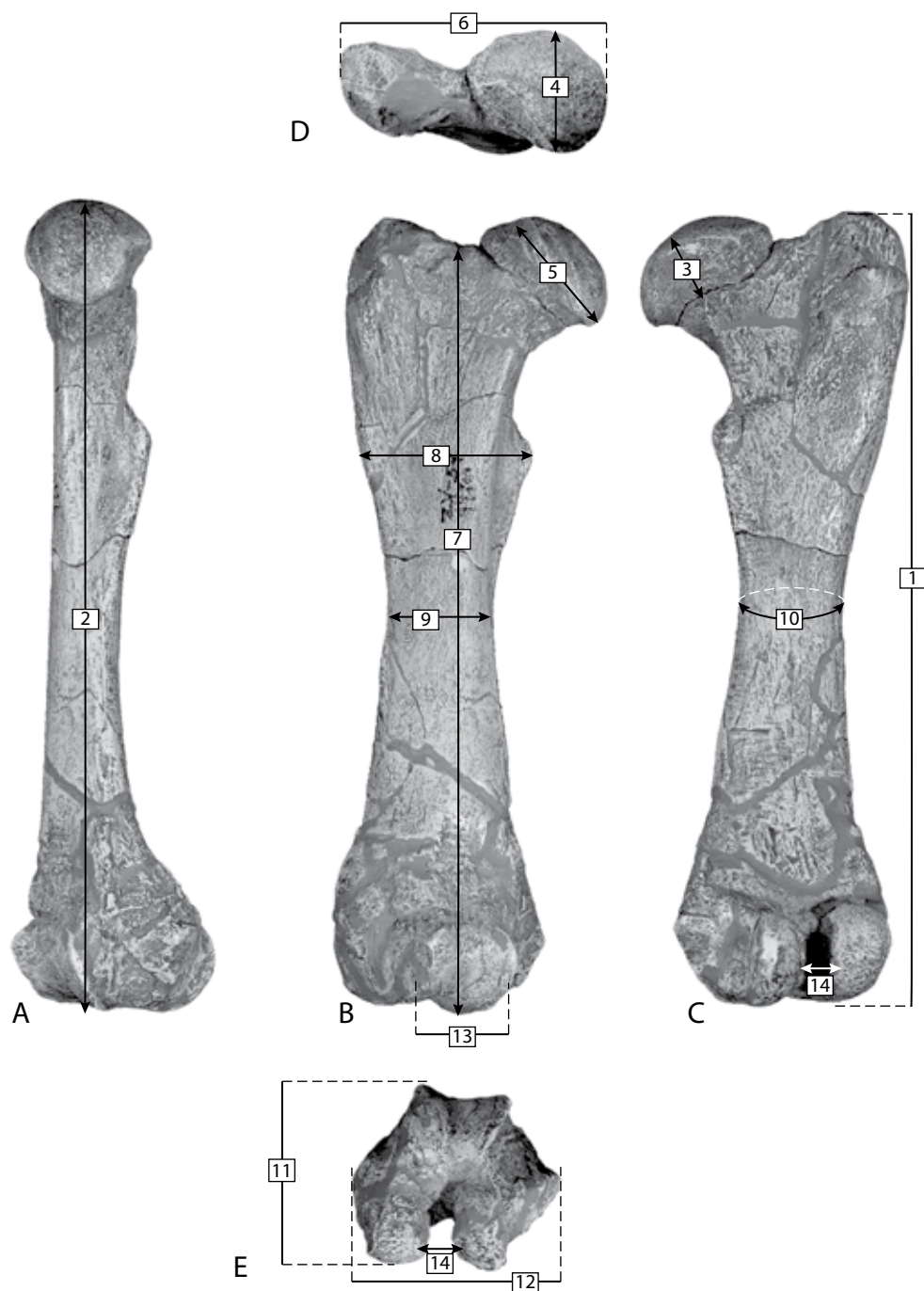


FIGURE 17 — Key to measurements of femora used in this study. A-E are medial, anterior, posterior, proximal, and distal views of a right femur of *Protosiren smithae* (CGM 42292).

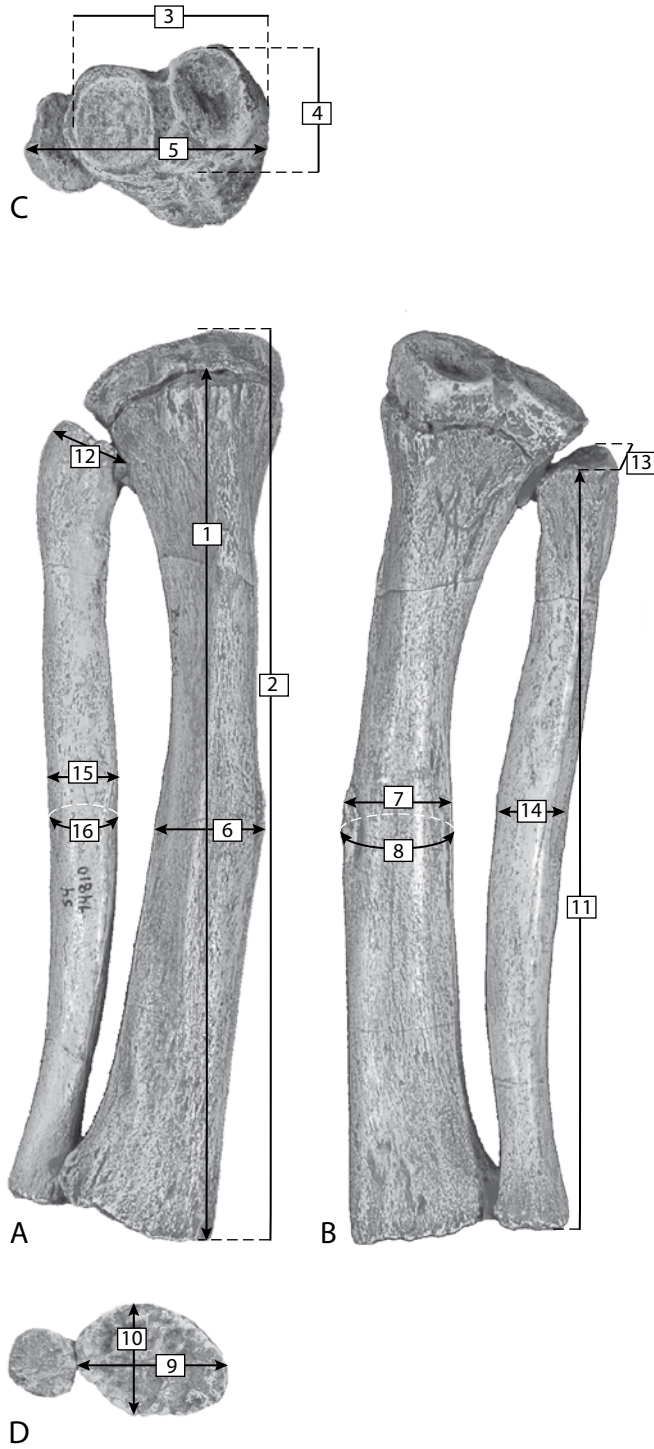


FIGURE 18 — Key to measurements of tibiae and fibulae used in this study. A-D are anterior, posterior, proximal, and distal views of a right tibia and fibula of *Protosiren smithae* (CGM 42292).

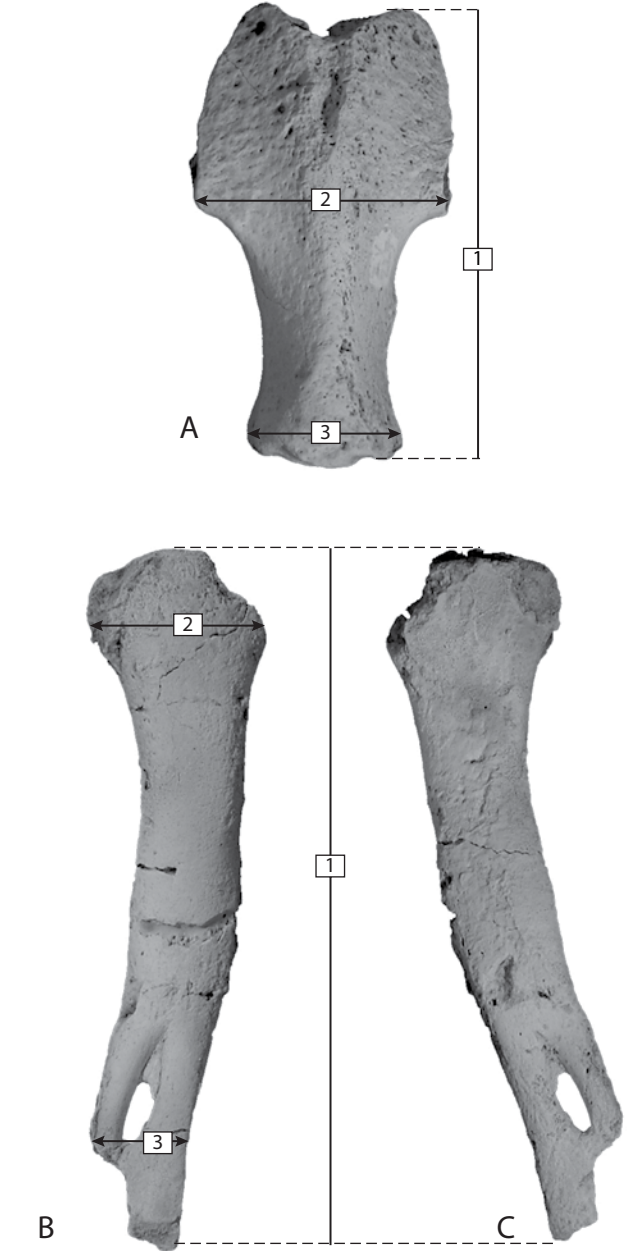


FIGURE 19 — Key for measurements of sternebrae used in this study. A, manubrium of *Protosiren smithae* (CGM 101224) in ventral view; B and C, xiphisternum of *Eotheroides sandersi* (UM 111558) in ventral and dorsal views. Measurement '1' is anterior-posterior length; measurement '2' is anterior breadth; and measurement '3' is posterior breadth.

ACKNOWLEDGMENTS

We thank Daniel C. Fisher for many conversations, insightful guidance, and helpful suggestions; Philip Myers for his experience in studying mammalian evolution and taxonomy; William J. Sanders, whose interest and substantial contribution to this work are much appreciated; and Gregg F. Gunnell for his many helpful comments and assistance with identification and management of specimens. The manuscript for this study was first submitted as a Ph.D. dissertation by Iyad Zalmout, and all named here were members of the dissertation committee.

This research could not be achieved without Egyptian Government collaborations, specifically the Egyptian Mineral Resources Agency (EMRA, including the Geological Survey of Egypt), the Egyptian Geological Museum in Cairo (CGM), and the Egyptian Environmental Affairs Agency (EEAA). Special thanks are due to Drs. Mustafa Fouda, Mohammad Sameh Antar, Mohammed Talaat El-Hennawy; Messrs. Ahmed Awad, Mohammad Al Hakeem, Ehab El-Sady, Medhat Al Said, Afifi Hassan Abdelghafar, and Gebbeli Abuelkair; and the late Messrs. Yusri Attia and Magdi Zakaria Soliman.

We thank field crew members who participated in expeditions to Wadi Al Hitan during the time when fossil sirenians were being collected and studied for the dissertation: Elwyn L. Simons, B. Holly Smith, Thomas M. Bown, Alex van Nievelt,

M. Hilal, A. A. Abdul Latif, William J. Sanders, Ali Barakat, William C. Clyde, Amin Strougo, Jeffrey A. Wilson, Shannon Peters, Carole Gee, Martin Sander, David J. Ward, and Chris King. Jacques LeBlanc of Qatar Petroleum, Doha, brought sirenian remains from Qatar to our attention.

We are especially grateful to Dr. Daryl P. Domning of Howard University and the National Museum of Natural History for his guidance, valued discussions, and access to Eocene Sirenia from Jamaica and other comparative material at the Smithsonian Institution. Dr. Carole Gee helped with identification of plant remains. Drs. David Bohaska, James Mead, and Charles Potter provided access to comparative collections of extinct and extant sirenians at the National Museum of Natural History, Smithsonian Institution. William J. Sanders, Joseph R. Groenke, and John Graf did exceptional work to prepare, mold, and cast the sirenian material studied here. We thank Museum of Paleontology illustrator Bonnie J. Miljour for many of the illustrations included here. Timothy P. Utter and Karl E. Longstreth from the Map Library of the University of Michigan were very helpful and supportive during this research.

Research in Egypt was funded by grants from the National Geographic Society (CRE 7226-04 and Waitt 1035-09) and from the U. S. National Science Foundation (EAR-0517773, OISE-0513544, and EAR-0920972). This research would not have been possible without facilities and infrastructure provided by the University of Michigan Museum of Paleontology.

II

GEOLOGY AND STRATIGRAPHY

The distribution of Eocene deposits yielding sirenian fossils in Egypt was to a great extent controlled by the tectonic history of the African continent. Major rifting events during the Late Jurassic and Early Cretaceous along the North African–Arabian margin of Tethys caused a series of pull-apart basins to form in northern Egypt and Sinai. This system, the Syrian Arc system of Krenkel (1924), extended as far north as western and central Jordan and most of Syria. Continuous movement of the Afro-Arabian plate to the northeast imposed severe compressional forces through the Late Cretaceous and middle to late Eocene, which gave final shape to this system and its basins (Guiraud and Bosworth, 1999; Guiraud et al., 2001; Guiraud et al., 2005).

Two aspects are of interest here: first, the geology of the Fayum and surrounding areas, and second, the stratigraphy of the sirenian-bearing formations in northern Egypt.

GEOLOGY OF THE FAYUM BASIN AND SURROUNDING AREAS

The Fayum or Fayum Basin (also referred to as the Fayum-Gindi Basin) is a 120 km wide graben filled with 2 km of Eocene sediments (Salem, 1976). These lie unconformably on top of Upper Cretaceous strata. The basin is bounded by two major highlands: El Kattaniya-Abu Rosh in the north, and Nashfa to the south of Wadi El Rayan. The latter forms the southern edge of the Syrian Arc system.

Within this graben, the Fayum Basin represents a classic model of marine progradation, with a carbonate shelf facies occupying the lower and lower middle parts of the Eocene, and siliciclastic estuarine, lagoonal, and deltaic facies predominating in the upper middle and upper Eocene (Kostandi, 1959; Salem, 1976).

Northern Egypt, including the Fayum Basin, was a broad stable marine platform during the middle and late Eocene, following Syrian Arc rifting and compression, but preceding Red Sea rifting. The platform subsided passively, with little or no tectonic influence, and preserved a good record of shallow marine strata.

STRATIGRAPHY OF SIRENIAN-BEARING FORMATIONS IN CAIRO AND WADI AL HITAN

Gebel Mokattam (Mokattam Hills) near Cairo is important paleontologically because it is made up of Eocene sediments

that produced informative marine mammal fossils that span the middle and late Eocene (Fig. 20). It produced the first sirenian, the type specimen of *Eotheroides aegyptiacum* (Owen, 1875), primitive whales such as *Protocetus atavus* and *Eocetus schweinfurthi* Frass (1904), and later another sirenian taxon known as *Protosiren fraasi* Abel (1907). These marine mammals are at least 8 million years older than the marine mammal assemblages of Wadi Al Hitan in the Fayum Basin. Gebel Mokattam is also famous for its nummulitic limestone, which is also known as the Building Limestone in reference to the stone quarries from which the Pyramids of Giza were built.

Strougo (1986) and Said (1990: 459) divided the rocks of Gebel Mokattam into three formations, the lowermost is the Mokattam Formation, which is made of nummulitic limestone and produced all the Mokattamian marine mammals. This is followed by the Giushi Formation which is mostly a limestone coquina of *Operculina* bivalves. At the top is the Maadi Formation which is mostly fine sandstones and silty marl. The Mokattam Formation and the Giushi Formation at Gebel Mokattam are Lutetian and Bartonian (middle Eocene) in age, and were deposited in offshore marine shelf and shallow-shelf environments. The Maadi Formation at Gebel Mokattam is Bartonian and Priabonian (middle and late Eocene) in age, and was deposited in nearshore and lagoonal environments. According to Schweinfurth (1883) and later Strougo (1985a, b), Gebel Mokattam has a thickness between 220 and 300 meters, depending on which side of the hill the section was measured. Southwest of Cairo, in the Fayum Basin, the Eocene sedimentary cover is almost twice as thick as deposits in Cairo, and more siliciclastic as well. Vertebrate fossils here are abundant and more complete.

Our understanding of the Eocene stratigraphy in Fayum is mostly based on Beadnell's (1901, 1905) and Blanckenhorn's (1903) studies of stratigraphic levels and rock units at Wadi El Rayan (the type locality for the Wadi El Rayan series) in the southwestern part of Fayum Basin. Division and nomenclature of strata exposed in the Fayum Basin, starting from older formations of the Lutetian-Bartonian Wadi El Rayan series, heading north and northwest to the top of the Oligocene Gebel Qatrani terrestrial deposits, were reexamined after reading many paleontological and geological descriptions and interpretations (Beadnell, 1901, 1905; Iskander, 1943; Said, 1990; Gingerich, 1992).

According to Beadnell (1901, 1905), the lower-most four formations of the Wadi El Rayan series (Figs. 20, 21, 22) are Lutetian and Bartonian in age, and exposed in the Wadi El Rayan

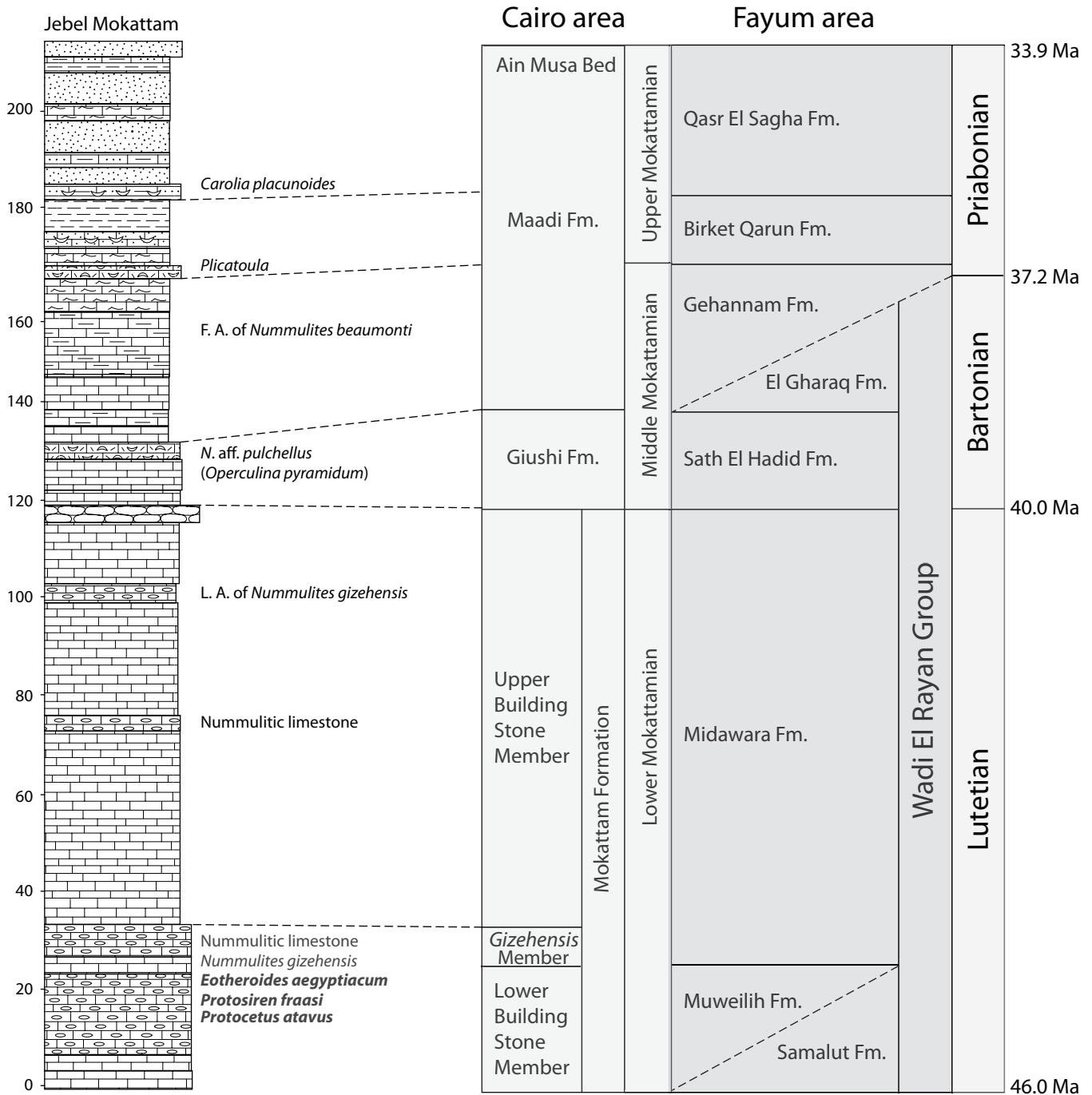


FIGURE 20 — Correlation of stratigraphic units of the Cairo and Fayum areas (following Schweinfurth, 1883; Said, 1990; Strougo and Haggag, 1984; Strougo 1985a,b; Gingerich, 1992; and Strougo, 1992). The stratigraphic section of Jebel Mokattam near Cairo (on the left) is about 220 meters thick, which is only one-third the total stratigraphic thickness of equivalent Eocene strata in Fayum. Most Fayum marine mammals were found and excavated from Bartonian and Priabonian age strata of the Gehannam, Birket Qarun, and Qasr El Sagha formations. ‘F. A.’ and ‘L. A.’ here refer to first and last appearances of index fossils.



FIGURE 21 — Legend for the stratigraphic sections illustrated in this study (Figs. 22-27).

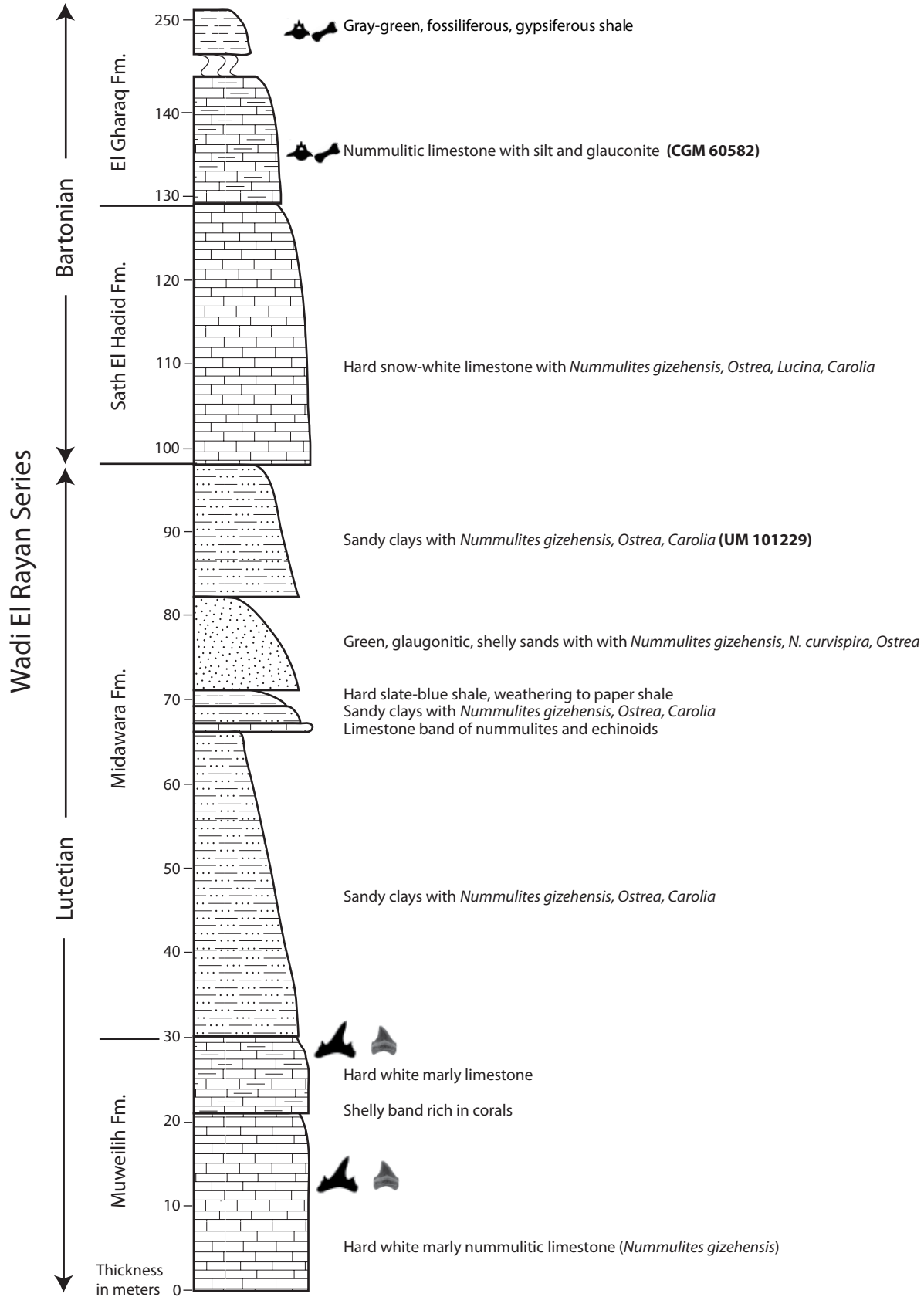
valley floor and its mesas and escarpments. These were mapped by Beadnell (1905) and Iskander (1943, 1:100,000) as the Wadi El Rayan Series. The entire section includes (from the bottom):

A. *Muweilih Formation* (Figs. 20-22)

This is the lowest formation exposed in the area, named Muweilih because it forms the floor of the Muweilih Oasis (the Salt Oasis). The Muweilih formation represents bed number 6 in the Minqar El Rayan section of Beadnell 1905. It is made of shallow marine, gray to dark colored, nummulitic, shaley, sandy, hard limestones. The exposed thickness of the formation is 36.5 m.

B. *Midawara Formation* (Figs. 20, 22)

Iskander (1943) indicated that there is no physical interruption in the transition between the Muweilih and Midawara formations. The Midawara Formation is mostly thick brown and light brown shales, sandy shales, sandy limestones, and glauconitic sand. The maximum thickness of this formation may reach 127 meters at Gebel El Mishgega (Latitude 29° 12' N, Longitude 30° 21' E; see Iskander, 1943: 12). Sirenian and whale remains were recorded in the upper one third of this formation in the bioturbated glauconitic sands near Dur El Milaha east of Qusor El Arab.



C. Sath El Hadid Formation (Figs. 20, 22)

'Iron surface' in Arabic, it is a nummulite limestone bank with large and small *Nummulites*. The Sath El Hadid Formation is 25 meters thick, overlies the Midawara Formation, and caps many mesas in the Wadi El Rayan area. The base of the Sath El Hadid formation is recognized as the contact between the snow-white Sath El Hadid limestone and the brown sandy limestone of the Midawara Formation. The upper contact with the El Gharag Formation can be recognized by the first appearance of brown and light brown shales above the snow-white nummulitic limestone. The top of the Sath El Hadid Formation is also distinctive in having secondary flint concretions.

D. El Gharaq Formation (Figs. 20, 22)

The measured sections of Beadnell (1905) and Iskander (1943) show this to be the thickest formation of the Wadi El Rayan Series, reaching 124 m at Ilw El Bireig in the southeastern part of Wadi El Rayan. The El Gharaq Formation is nummulitic limestone and siltstone, with glauconite and shale at the top. This formation conformably overlies the Sath El Hadid Formation, the top of which is marked by the last appearance of white-snow limestone. The top of the El Gharaq Formation itself is defined by the abrupt loss of large and small nummulites, and by an increase in the glauconitic concentrations that mark the base of the Gehannam Formation. According to Boukhary et al. (2003), the age of the El Gharaq Formation is Biarritzian (i.e., late middle Eocene or Bartonian), based on the nummulitic scale of Schaub (1981). The top of the formation is exposed at the base of the northern and eastern foothills of Gareh Gehannam. Teeth of sharks and rays were collected from the formation; marine mammals are fragmentary and rare.

E. Gehannam Formation (Figs. 20, 23, 24)

Beadnell (1905) and Iskander (1943) called the Gehannam Formation the 'Ravine Beds' because its sediments are often exposed in ravines and small valleys. Said (1962, 1990) called the beds the Gehannam Formation as they are well exposed at Gareh Gehannam. Ismail and Abdel-Kereem (1971a,b) divided the Gehannam Formation into two members, a lower part equal to the Ravine Beds was designated as the Gehannam Marl Member, with an upper part that they called the Gehannam Shale Member. However because the beds are exposed very well at Gareh Gehannam, with a defined base and top, the name Gehannam Formation is used here rather than Ravine Beds. The Gehannam Formation has a variable thickness and may reach 35 meters near the Gareh Gehannam plateau. The base of the formation is marked by thick deposits of glauconitic sandstone and marls that lack large benthic forams but are rich in fish scales, shark and ray teeth, and marine mammal skeletons. Marl and

glauconite deposits of the Gehannam Formation are replaced at the higher stratigraphic levels by gypseous fine sands and brown shale capped with pale sandstone of the Birket Qarun Formation. East of Gareh Gehannam and just west of lake Birket Qarun, near the village of Guta, the Gehannam Formation is represented by limestone and marly limestone facies (Strougo, 1992). This area also produced many skeletons of marine mammals.

In Wadi Al Hitani the middle and top parts of the Gehannam Formation are exposed and form the base of the valley in many areas. Beadnell (1905, p. 38) provided an ambiguous boundary between the 'Ravine Beds' (now Gehannam Formation) and his overlying Birket Qarun Series (now Birket Qarun Formation). Beadnell represented this diagrammatically by a dashed line, and placed this more or less in the middle of a homogeneous 24-meter-thick sandstone unit. Gingerich (1992) placed the boundary between the two formations at the bioturbated Camp White Layer. We now follow Strougo (2008, p. 90) in placing the Gehannam-Birket Qarun formational boundary at the top of the fine-grained calcareous sandstone that is ledge-forming in the vicinity of Gareh Gehannam, at the base of Minqar el Hut, and elsewhere in Wadi Al Hitani. Strougo called this the '*Schizaster vicinalis* Sandstone' and equated it with the "yellow-white marls and marly limestone" at the base of Beadnell's bed 14 and the "hard light yellow shelly limestone, in part marly, in part sandy" at the top of Beadnell's bed 15 (Beadnell, 1905, p. 39). The *Schizaster vicinalis* Sandstone seemingly merges with the Camp White Layer offshore to the north in Wadi Al Hitani, but it lies well below the Camp White Layer and is not equivalent in the central part of the valley.

Gingerich (1992) proposed a shallow open shelf environment for the Gehannam Formation. Abdou and Abdel-Kireem (1975), Strougo and Haggag (1984), Haggag (1995, 1990), assigned a Bartonian-Priabonian age to this formation based on its foraminiferal content. The Gehannam Formation is early Priabonian following the sea level interpretation and correlation of Gingerich et al. (2012).

F. Birket Qarun Formation (Figs. 20, 23, 24)

The Birket Qarun Formation is very well exposed along the northern cliffs of Lake Qarun and to the west in Wadi Al Hitani. Its thickness ranges between 20 and 85 meters. It includes clays, shales, thick fine-grained sandstones, ferruginous bioclasts, and calcareous grits. The Birket Qarun Formation is thick and well exposed in Wadi Al Hitani. It shows an alternation of two major lithologies: (1) greenish, gypseous shales with minor silts; and (2) very fine, mature sandstones with bases thoroughly bioturbated by *Ophiomorpha* and *Thalassinoides*. Gingerich (1992) interpreted the Birket Qarun Formation as a series of barrier bar deposits trapping clay and silts in small lagoons. However, information from recently studied sections covering a larger area of the Birket Qarun Formation exposure in Wadi Al Hitani shows that this formation is thicker than was previously thought, with complex architecture that we now interpret to reflect deposition in heterogeneous shallow shelf and shoreface settings (Peters et al., 2009, 2010; Abdel-Fattah et al., 2010). The fossil marine mammals and other vertebrates of the Birket Qarun Formation were collected from many levels.

FIGURE 22 — Stratigraphic section of Lutetian-Bartonian strata of the Wadi El Rayan Series in Wadi El Rayan, including: Muweilih, Midawara, Sath El Hadid, and El Gharaq formations and fossiliferous intervals. Section follows Beadnell (1905) and Iskander (1943).

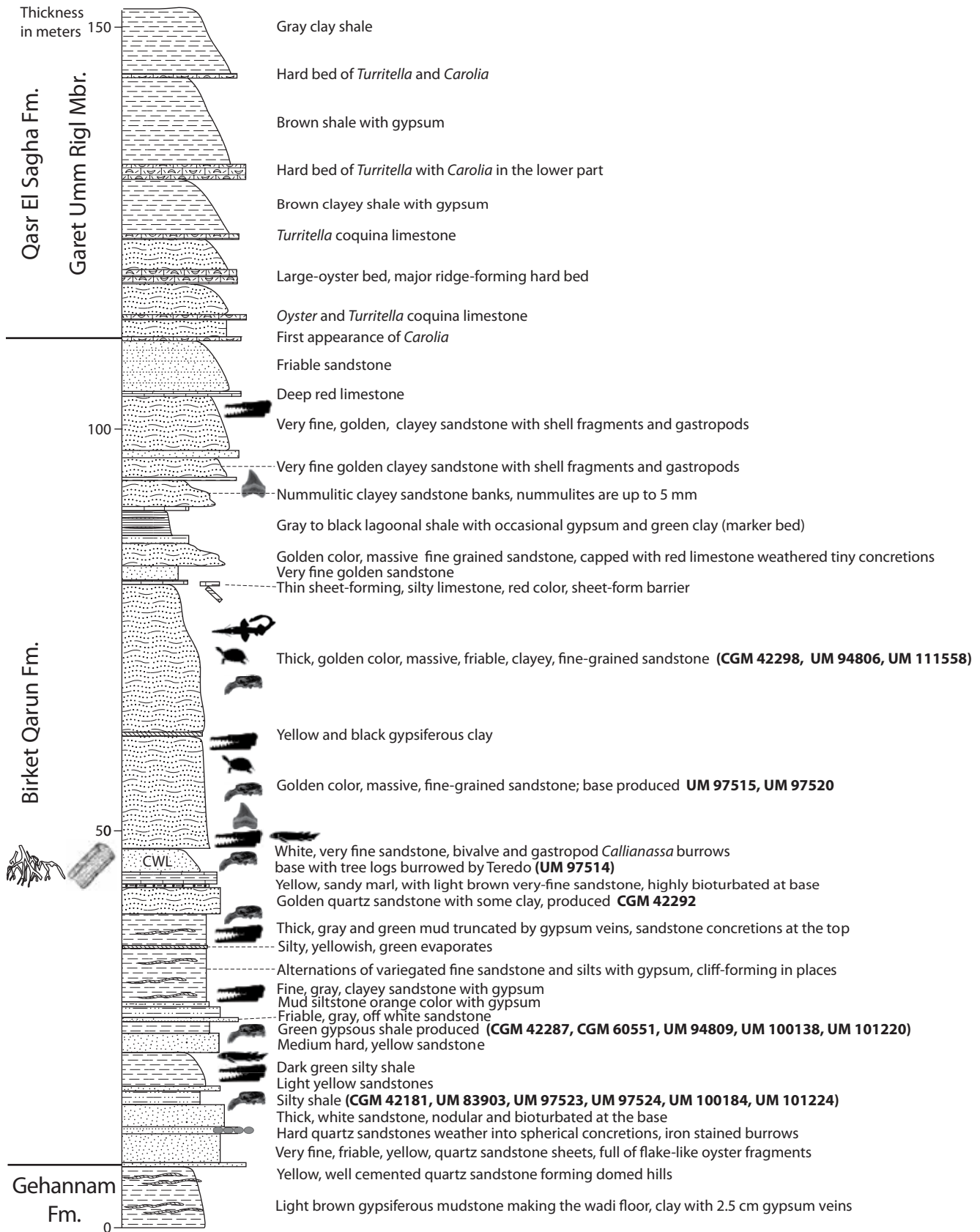


FIGURE 23 — Caption of facing page.

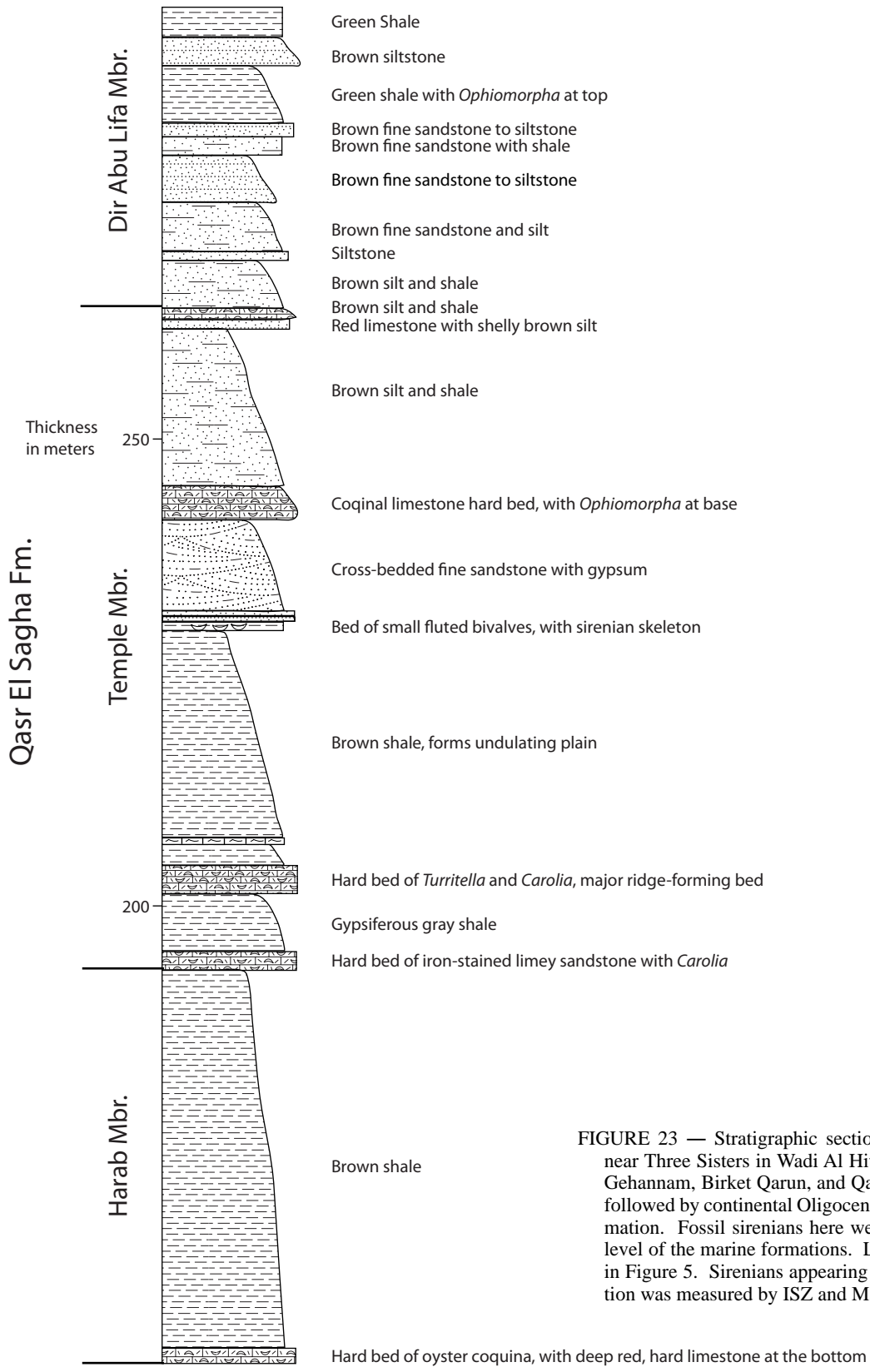


FIGURE 23 — Stratigraphic section of Minqar El-Hut extending near Three Sisters in Wadi Al Hitan showing the Priabonian-age Gehannam, Birket Qarun, and Qasr El Sagha marine formations, followed by continental Oligocene beds of the Gebel Qatrani Formation. Fossil sirenians here were collected from almost every level of the marine formations. Location of the section is shown in Figure 5. Sirenians appearing here are listed in Table 2. Section was measured by ISZ and MSA.

FIGURE 23 — (continued).

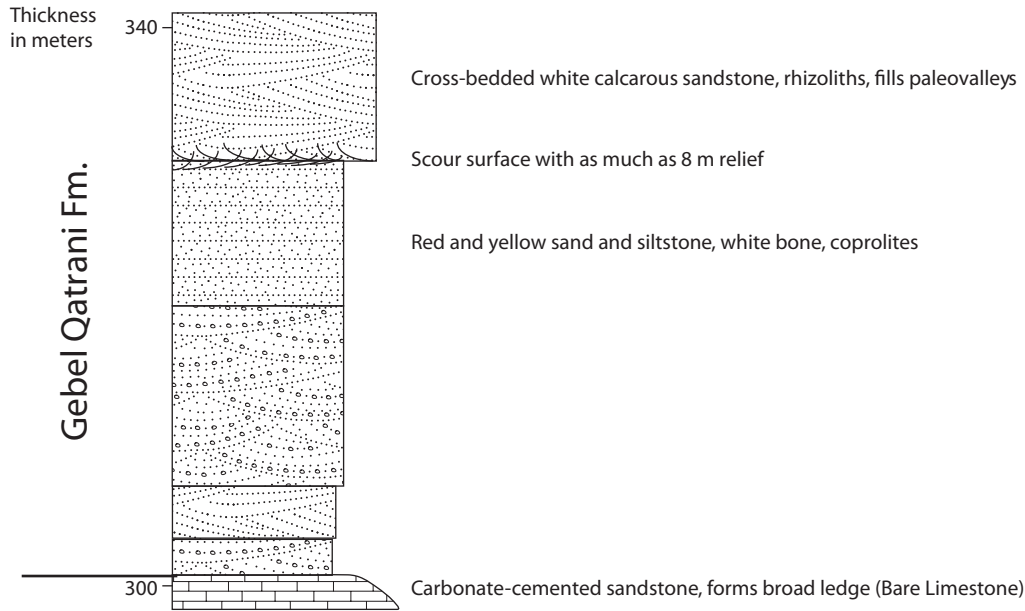


FIGURE 23 — (continued).

According to Strougo (pers. comm., April 2007), the marine mammal-bearing beds from the top of the Gehannam Formation and the lower third of the Birket Qarun Formation at Wadi Al Hitan are early Priabonian in age based on the overlapping of the calcareous nannoplankton zone NP18 and planktonic foraminifera zone P15 (*Globigerinatheka semiinvoluta*). The Gehannam and Birket Qarun formations are early Priabonian following the sea level interpretation and correlation of Gingerich et al. (2012).

G. Qasr El Sagha Formation (Figs. 20, 25, 26, 27)

The last and thickest Eocene formation in Fayum is the Qasr El Sagha Formation, which may exceed 180 meters in total thickness. It overlies the Birket Qarun Formation conformably in most places, but there are major incised valleys filled with re-worked sediment in places. The base of the Qasr El Sagha Formation is defined by the first appearance of paper-thin *Carolia placunoides* bivalves, while the top is marked by a disconformity with the varicolored fluviomarine and terrestrial sandstones of the Gebel Qatrani Formation. According to Vondra (1974) and Bown and Kraus (1988), the Qasr El Sagha Formation was deposited in a retreating shallow sea that received sediment from an exposed hinterland. They interpreted the influx of terrigenous material as being exceptionally high during the latest Eocene, when large rivers seem to have discharged into the sea, forming submarine deltas.

One of the best classic deltas deposited by latest Eocene rivers is exposed to the north of the Qasr El Sagha Temple (Temple locality). The deltaic and interdeltic sediments of the upper Eocene are well exposed in Fayum north of Birket Qarun. Vondra (1974) listed four major facies present in the Qasr El

Sagha Formation: (1) the *lowermost arenaceous bioclastic facies* made up of bioturbated (mainly by the crustacean *Callianassa*) glauconitic and fossiliferous calcareous sandstone; (2) the *gypsiferous and carbonaceous laminated claystone and siltstone facies*, which seems to have been deposited in back-bar open and restricted lagoons; (3) the *interbedded claystone, siltstone and quartz sandstone facies*, which is a fining upward cycle of very fine to fine-grained white quartz sandstone, pale yellowish brown and dark grey siltstone and claystone; and (4) the *quartz sandstone facies* which seems to represent distributary channel deposits. Each unit of facies 3 constitutes a foreset of large-scale planar cross-stratification deposits. Vondra interpreted this facies as having been deposited in a rapidly prograding delta front environment in quiet shallow brackish marine waters.

In Wadi Al Hitan the Qasr El Sagha Formation is divided into four members. From bottom to top these are: (1) Umm Rigl Member; (2) Harab Member; (3) Temple Member, and (4) Dir Abu Lifa Member. The lowest two members were added to the Fayum stratigraphic system by Gingerich (1992), as recognized north of Birket Qarun and in Wadi Al Hitan, while the top two were named and described by Bown and Kraus (1988). According to Gingerich (1992), the Umm Rigl Member consists of an alternation of Vondra's arenaceous bioclastic carbonate facies (hard beds) and Vondra's gypsiferous and carbonaceous laminated claystone and siltstone facies, similar to the alternation found in the Temple Member (but separated by the intervening Harab Member). The overlying Harab Member is a deeper central lagoon, and is made of a barren interval of brown shale that today forms a broad featureless plain.

The Temple Member of Bown and Kraus (1988), is dominated by two of Vondra's (1974) Qasr El Sagha facies: the arenaceous

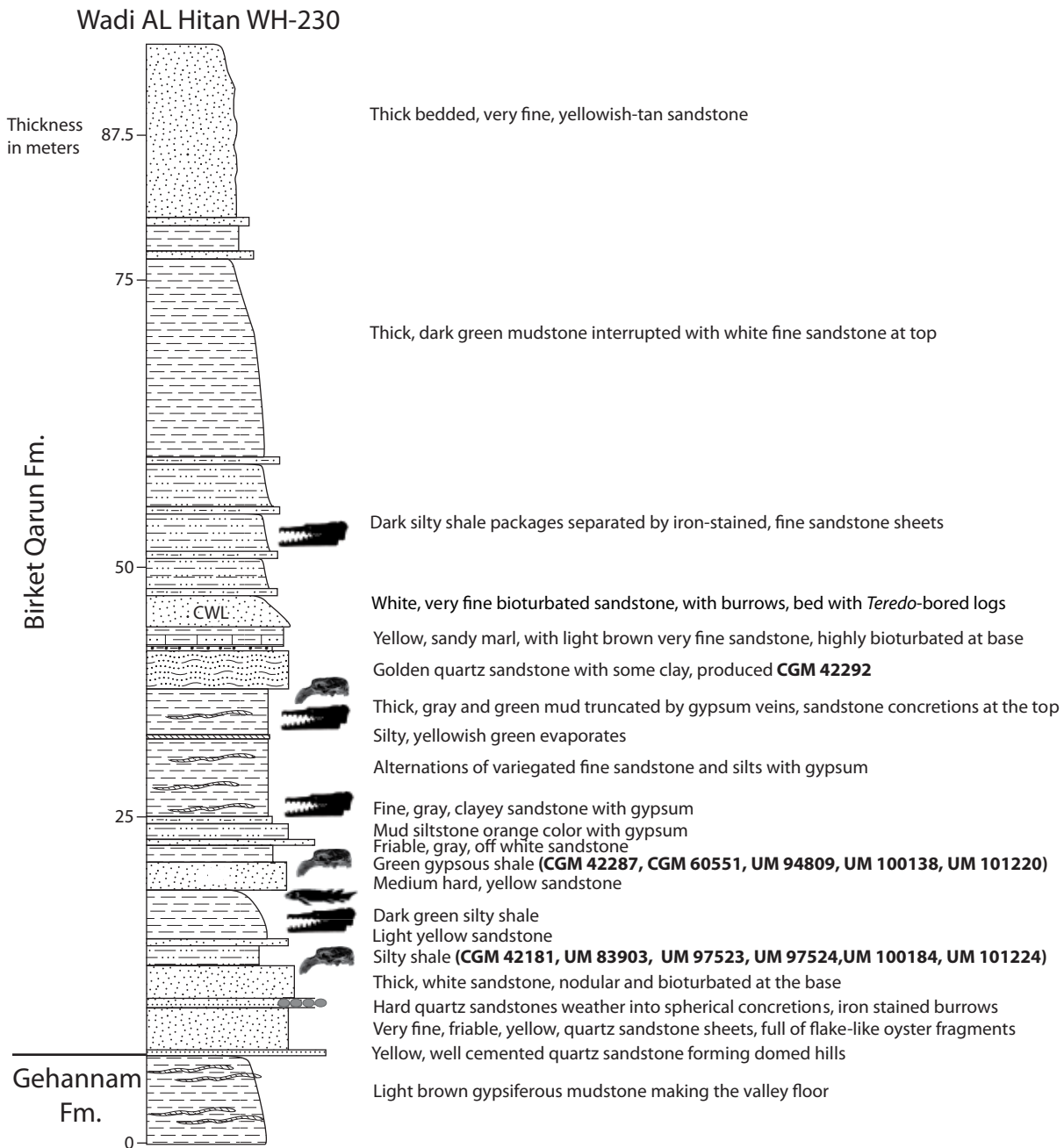


FIGURE 24 — Stratigraphic section at Wadi Al Hitan locality WH-230 showing the Priabonian age Gehannam and Birket Qarun formations. Location of the section is shown in Figure 5. Sirenians appearing here are listed in Table 2. Section was measured by ISZ and MSA.

bioclastic carbonate facies (facies 1), and the gypsiferous and carbonaceous laminated claystone and siltstone facies (facies 2). The Dir Abu Lifa Member of the Qasr El Sagha Formation, is cross-bedded sandstone, that appears to be composed of Vondra's facies 3, the inter-bedded claystone, siltstone, and quartz sandstone facies (delta front), and facies 4, the quartz sandstone facies (delta distributary facies).

H. Gebel Qatrani Formation (Fig. 23)

The Rupelian Gebel El Qatrani Formation overlies the Priabonian Qasr El Sagha Formation disconformably. Beadnell (1905), Vondra (1974), Bown et al. (1982), and Bown and Kraus (1988), studied this formation intensively and found that it includes 110 to 340 m of fluvial sandstone, siltstones and claystones, and very minor carbonate lenses and carbonaceous shale. The lower third is a complex of large-scale trough cross-

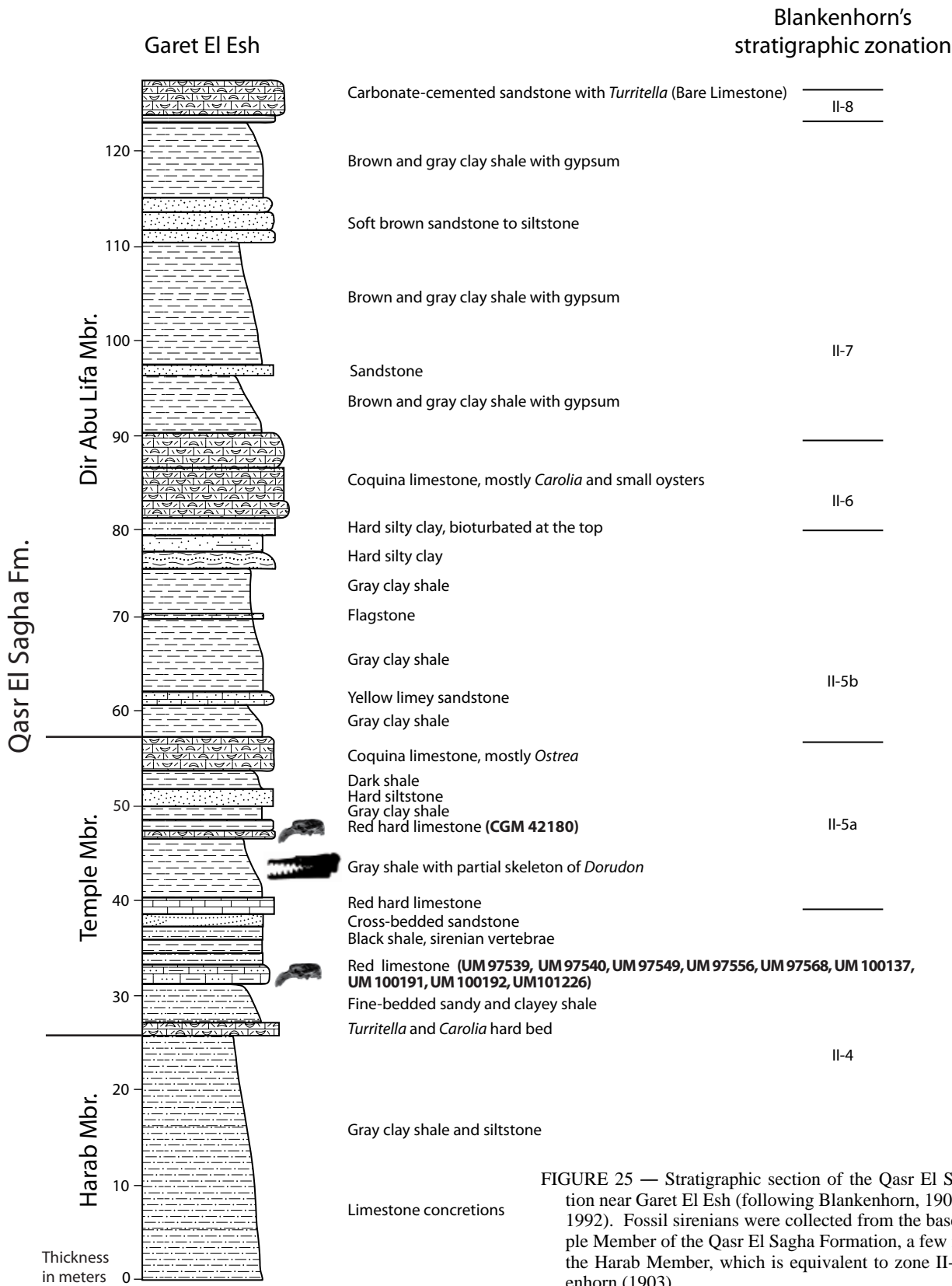


FIGURE 25 — Stratigraphic section of the Qasr El Sagha Formation near Garet El Esh (following Blankenhorn, 1903; Gingerich, 1992). Fossil sirenians were collected from the base of the Temple Member of the Qasr El Sagha Formation, a few meters above the Harab Member, which is equivalent to zone II-4 of Blankenhorn (1903).

Wadi Efreet (2 km NNE Qasr El Sagha)

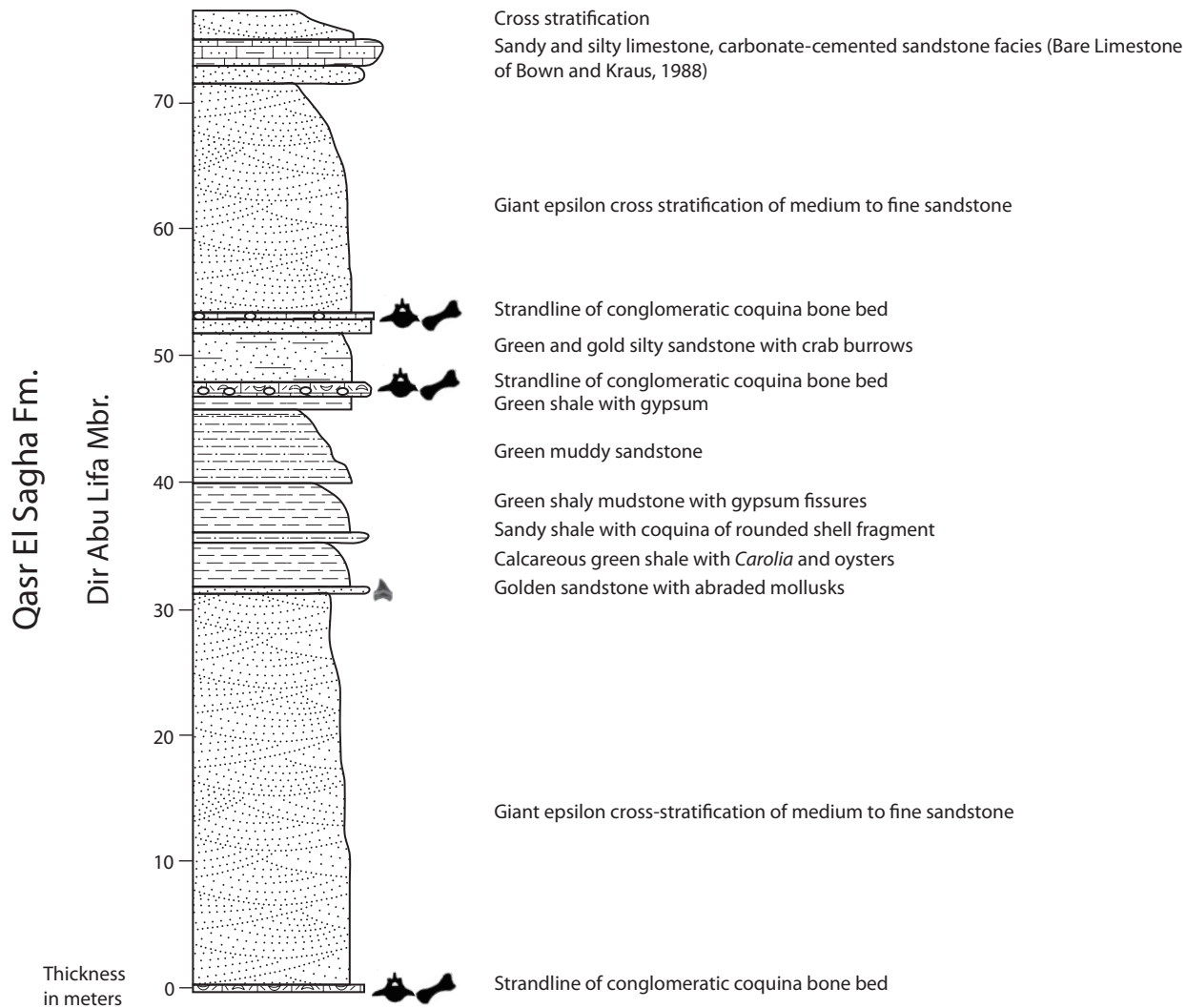


FIGURE 26 — Stratigraphic section of the uppermost Qasr El Sagha Formation in Wadi Efreet (Valley of the Ghost, 2 km NNE of Qasr El Sagha temple; section from Bown and Kraus, 1988). Note the deltaic giant cross-stratification of the Dir Abu Lifa Member. Vertebrate fossils were collected from lag beds at the base of incised valley fill deposits and are disarticulated.

stratified channel lag and point bar sands, indicating deposition in a loosely sinuous, low gradient, medium velocity stream. The upper part of the formation is point bar, flood plain splay, and channel fill deposits, pointing to an overloaded and more tightly meandering stream.

The point bar deposits are very fossiliferous in the lower as well as in the upper parts of the formation, containing abundant silicified tree logs and fossil vertebrates. Nearly all the sandstones show diagenetic alteration reflecting ancient pedogenesis. Part of the lower part of this formation was deposited in a near-shore setting as indicated by the presence of shark teeth, ray mouth parts, brackish-water molluscs, and abundant mangrove

rhizoliths. Among the diverse fossil vertebrates from Gebel Qatrani, the following are abundant: crocodylians, turtles, browsing artiodactyls and hyracoids, arboreal quadrupedal anthropoid primates, hyaenodontid creodonts, and phiomyid rodents (Andrews, 1906; Simons, 1968; Simons and Gingerich, 1974; El Khashab, 1974; Simons and Rasmussen, 1990; Gagnon, 1997). Ichnofossils and rhizoliths are abundant, well preserved and diverse in form (Bown, 1982). The ichnofauna contains traces of probable annelid, insect, crustacean, and vertebrate origin. These include fossil nest structures and gallery systems of subterranean termites. Rhizoliths associated with the ichnofauna document a variety of small wetland plants, coastal mangroves,

Dir Abu Lifa (3.5 km NNE Qasr El Sagha Temple)

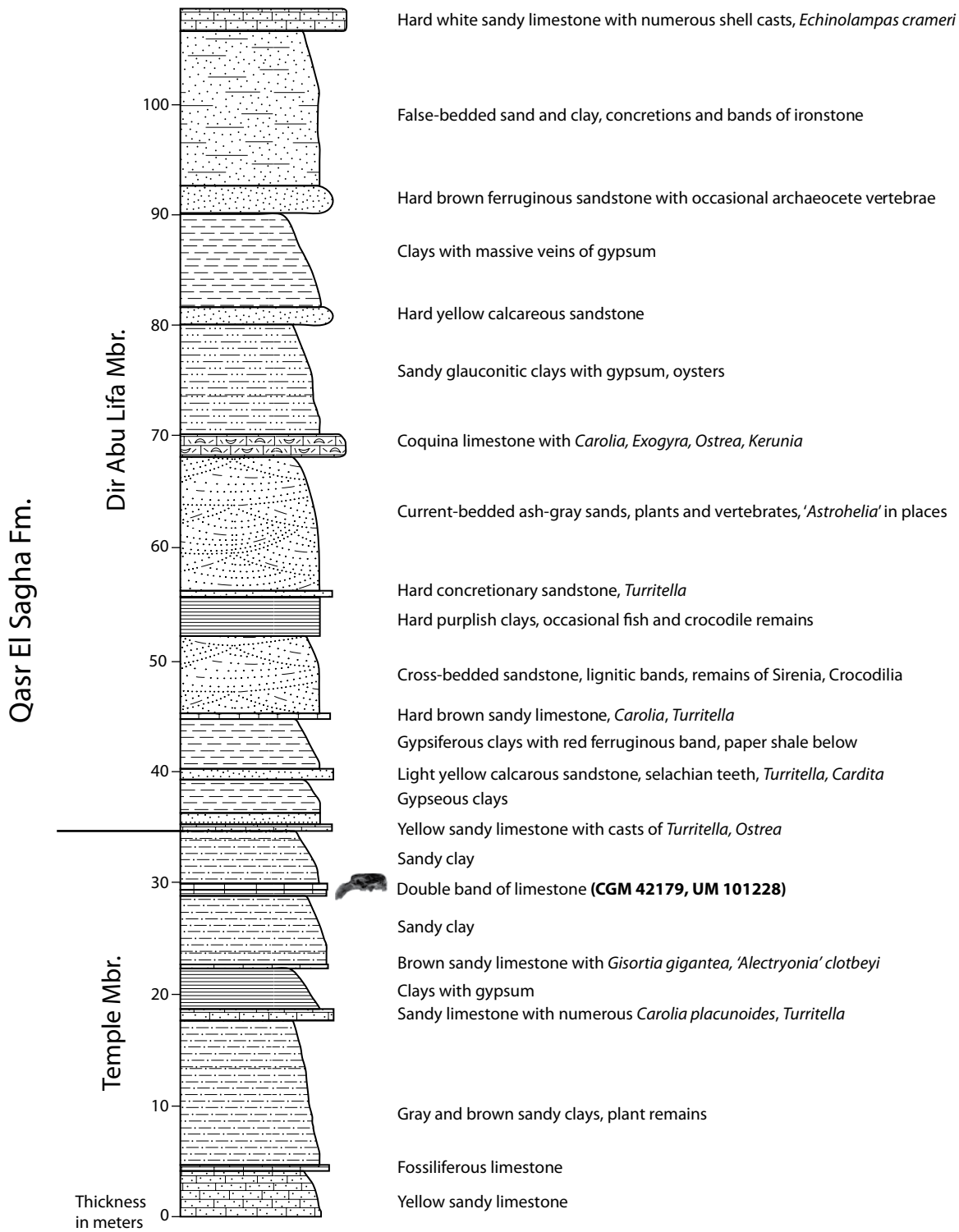


FIGURE 27 — Stratigraphic section of the Qasr El Sagha Formation near Dir Abu Lifa fossil localities (Gingerich, 1992). Fossil sirenians were collected from the thin hematite-stained band of limestone some 20 meters below the cross-bedded sandstone.

and large trees. Kortland (1980) believed that the Gebel Qatrani flora indicates a drier (Sahelian) climate. It differs from that of Qasr El Sagha in containing no identified leaves and in having only two fruit species (of a waterlily and a palm relative).

I. *Widan El Faras Basalt* (Figs. 4, 7)

The Gebel Qatrani Formation is unconformably overlain by the Widan El Faras Basalt (Bowen and Vondra, 1974), the lower part of which is dated at 31 ± 1 m.y. (Fleagle et al., 1986a,b). The basalt occurs in three sheets. The lower and upper sheets are amygdaloidal, vesicular and intensely altered, whereas the middle sheet is massive, compact, and fresh. Layering is noted in the upper sheet. The three sheets are similar petrologically and are of tholeiitic nature (Heikal et al., 1983).

STRATIGRAPHIC LEVELS YIELDING SIRENIA IN WADI AL HITAN

Two representative stratigraphic sections were measured at Wadi Al Hitan in order to append the collected fossils to their stratotypes. The first section (Fig. 23) was measured to cover the areas of Minqar El-Hut, the old University of Michigan 1983-1993 camp at Wadi Al Hitan, and the Three Sisters hill (see location of section in Fig. 5); this section is referred to as the Minqar El-Hut and Three Sisters section. The second section (see location of section in Fig. 5) was measured in the eastern part of Wadi Al Hitan to cover the exposed lithologies around localities WH-230, northeast of WH-54 where the type specimen of a Wadi Al Hitan sirenian was found. This section is referred to as the Wadi Al Hitan WH-230 section.

Other sections included in this study were redrawn and slightly modified from Beadnell (1905), Iskander (1943), Bown and Kraus (1988), and Gingerich (1992) in order to allocate fossils to stratigraphic levels.

Minqar El-Hut and Three Sisters section: The Minqar El-Hut and Three Sisters stratigraphic section (Fig. 23) includes the top part of the Gehannam Formation, which is marked by a thick layer of brown shale with gypsum. This is followed by a white marly bed of sandstone with many skeletons of *Basilosaurus*; the marly bed is well exposed at the bottom of the southern cliffs of Minqar El-Hut. This is followed by two white fine-sandstone beds that fine upward into another thin layer of marly sandstone that marks the top of the Gehannam Formation.

The top marl of the Gehannam Formation is overlain by a series of white, very fine, highly bioturbated sandstones that extend for several kilometers in this area. The Camp White Layer (CWL) is a prominent marker bed that varies in thickness from 30 cm to 7m. It may be synchronous or may be replaced by different facies in other areas of Wadi Al Hitan. The CWL in most cases preserves infilled *Callianassa* burrows. These tubes have a typical J shape, and are mostly filled with fine sand or nummulites. The base of the CWL contains fossil tree trunks that were riddled with *Teredo* shipworm tubes later replaced by celestite. The top of the CWL preserved many whale and sirenian fossils intact, but many of these suffered severe sandblasting when exposed by erosion.

The CWL is topped by 14 to 30 meters of thick, massive, cliff-forming, golden-colored, very fine, friable sandstone that produced many whale and sirenian skeletons. This bed starts at the base with white sandstone that is extremely rich in selachian teeth, turtles, and crocodilian remains. The middle part of the sandstone has a black sulphurous gypseous clay.

The thick sandstone is followed by a 30-60 cm thick, hematite-stained, sheet-forming limey siltstone, this is followed by 2.5 meters of gold and white-colored friable sandstones with a hard bioturbated base similar to the CWL lithology. This is then overlain in turn by a 3-meter-thick massive fine-grained sandstone that gets very fine at the top. The top of the sandstone is clayey, preceding an episode of slow deposition in a restricted environment. This episode is represented by a locally deposited gray-to-black clay bed ranging in thickness from 20 cm to 5 meters, with a maximum thickness at Qaret Gehannam (about 10 km NE of Wadi Al Hitan), the clay is overlain by a thick bed of nummulitic, gold-colored sandstone.

The fine sandstones interrupted with minor clays and shale beds continue in the overlying 15 meters to the top of the Birket Qarun Formation, with minor change in the biological content. The transition into the Qasr El Sagha Formation is marked by a 40 cm thick carbonate-rich sandstone with *Carolia* shells weathering out on flat benches. The rest of the section includes the entire 190 meters of Qasr El Sagha Formation capped by the Bare Limestone and the Gebel Qatrani Formation already described by Gingerich (1992).

Wadi Al Hitan WH-230 section: The second section is Wadi Al Hitan WH-230 (Fig. 24), located about 9 km northeast of the Minqar El-Hut and Three Sisters section (Fig. 5). The base of the section is located 150 meters east of locality WH-230 (type locality of *Eotheroides sandersi*, CGM 42181).

The top the Gehannam Formation, with gypsum and silty brown clays, makes the floor of the valley. The clays are followed by a 40 cm thick yellow calcareous sandstone topped by a 4 m thick friable pale white sandstone; this sandstone is then followed by a 1 meter thick white to gray bioturbated sandstone with its top weathering into sandstone concretions. This bed is the base of the section illustrated in Gingerich (1992: 43; fig. 35).

Just above the white calcareous sandstone is a 2 meter thick unit of very friable silty shale. This bed has produced many marine mammal skeletons, including the type specimen of *Eotheroides sandersi* (CGM 42181). Higher in the section is a yellow and gold-colored sandstone that may be equivalent to the CWL marker bed of the Birket Qarun Formation.

Higher still is an 11-meter thick, massive bed of gypsiferous clay and shale marked by a thin yellow sulphurous layer in the middle. This thick mudstone bed is traceable and mappable for several kilometers in Wadi Al Hitan. This clayey shale is overlain by a 5-meter thick fine, golden-colored sandstone; the base of this sandstone produced the type specimen of *Protosiren smithae* (CGM 42292 at locality WH-54). This sandstone is followed by a 2-meter thick, yellow colored, very fine-grained marly sandstone. This marly sandstone grades into another calcareous, fine, white sandstone 4 meters thick that has J-shaped burrows like those in the CWL marker bed.



The burrowed sandstone is followed by an alternation of thick, dark-colored silty shale packages that are separated by thin layers of iron-stained, bioturbated, fossiliferous sheet sandstones; this is followed by a thick, dark green mudstone interrupted by fine sandstone at the top. Finally, a thick-bedded, very fine, yellow colored sandstone caps the shale.

All fossil sirenians from Wadi Al Hitan were collected from fine sandstone and silty facies. Most of the fossils are either skeletons or partial skeletons found in articulation and/or association (Fig. 28). Preservation and articulation patterns in Wadi Al Hitan were mostly governed by physical rather than biological factors (bioturbation, scavenging or predatory behavior). The Birket Qarun and most of Qasr El Sagha Formation were deposited in a quiet and restricted environment, close to the shoreface, and at the same time near a source of siliciclastic sediments. Repetitions of thick fine sandstone, shale, and clay, and their lateral variations shifting from one facies to another in a shallowing upward sequence, as in Wadi Al Hitan, are diagnostic of a lagoonal or estuarine environment. Lutetian and Bartonian carbonate rocks of the Wadi El Rayan Series were mostly nummulitic, with slightly siliciclastic and glauconitic components deposited in a deeper environment than those of the Birket Qarun and Qasr El Sagha formations.

FIGURE 28 — Excavation of *Eotheroides sandersi* (UM 97514) at locality WH-110. The matrix here is poorly consolidated sandstone just above the Camp White Layer (flat surface in background). These sandstones were deposited in a shoreface environment with limited wave action. William J. Sanders is shown wrapping a sirenian skeleton (photo by PDG).

III

NEW EOCENE SIRENIA FROM THE PRIABONIAN OF WADI AL HITAN

Two new species of *Eotheroides* are described here. Both were collected from the lower part of the Birket Qarun Formation in Wadi Al Hitan. The Birket Qarun Formation here is early Priabonian, early late Eocene, in age.

SYSTEMATIC PALEONTOLOGY

Class MAMMALIA Linnaeus, 1758
Order SIRENIA Illiger, 1881
Family DUGONGIDAE Gray, 1821
Subfamily HALITHERIINAE (Carus, 1868) Abel, 1913

EOTHEROIDES Palmer, 1899

Eotheroides clavigerum, sp. nov.

Figures 29-39

Holotype.— CGM 60551 (Figs. 29-31 and 33-39) is the skeleton of a dentally-mature adult sirenian. It includes a skull with left and right M^{1-3} , both dentaries with left M_{1-3} and right dP_5 to M_3 , most cervical and thoracic vertebrae, one sacral, and three caudals (C1-3, C5, C7; Th1-13, Th17-18, S1, Ca2, Ca16, and Ca19), a virtually complete ribcage, left scapula and humerus, left radius and ulna fused, several metacarpals, a phalanx, and both innominates.

Type locality.— University of Michigan field locality WH-219 in Wadi Al Hitan (Figs. 1-5), some 75 km west of the city of Fayum, and 140 SW of the city of Cairo. UTM grid coordinates for the holotype in zone 36N are 213606 m E and 3245831 m N.

The type specimen of *Eotheroides clavigerum* was excavated from the base of the Birket Qarun Formation of Beadnell (1905), a few meters above the top of the Gehannam Formation (Fig. 24). This level was included in the Gehannam Formation by Gingerich (1992), however recent stratigraphic revision of the Birket Qarun and Gehannam formations by Strougo (in preparation; pers. comm., 2007) assigns the thick brown shale with gypsum of Wadi Al Hitan to the base of the Birket Qarun Formation.

Age and distribution.— The marine mammal-bearing beds from the lower third of the Birket Qarun Formation are early Priabonian in age, based on overlap of calcareous nannoplankton zone NP18 and planktonic foraminifera zone P15 (*Globigerinatheka seminvoluta*). *Eotheroides clavigerum* sp. nov. is only known from the lower and middle parts of the Birket Qarun Formation (Fig. 24) in Wadi Al Hitan.

Diagnosis.— *Eotheroides clavigerum* (Figs. 29-39) differs from *Eotheroides aegyptiacum* (Owen, 1875; Abel, 1912) and *E. sandersi* (Figs. 40-64) in having convex-upward and strongly arched nasals along the midline that are higher than the parietals; lacrimal is directed anteroposteriorly and barely exposed laterally; lacrimal foramen is closed. *E. clavigerum* also differs from *Eotheroides sandersi* in having a robust, rugose-edged atlas with knoblike transverse processes directed upward; first rib swollen with tapered end, and middle ribs are pachyosteosclerotic (i.e., extensively swollen and thickened in bone; following Domning and de Buffrénil, 1991). Moreover, *E. clavigerum* has a short, club-like ilium; flat, broad, and thin ischium; small obturator foramen; short, gracile cleft on a medially-pointed pubic bone on both sides, lacking any real public symphysis. Dental formula is 2.1.5.3/3.1.5.3; I^1 is enlarged into a tusk; narrow and deep posterior palate; anterior palatal gutter across both upper second premolars (P^2) is narrow and deep. Mandibles run straight along the symphyseal axis. Differs from *Eotheroides lambondrano* in being larger. *Eotheroides lambondrano* is smaller than all other *Eotheroides* specimens known (Samonds et al., 2009).

Etymology.— *Clavigerum*, Latin, club-like, in reference to the swollen proximal end of the ilium (Fig. 39).

Referred specimens.— CGM 42287, lumbar vertebrae from locality WH-190 (UTM grid coordinates in zone 36N: 213872 m E and 3240765 m N); Priabonian, lower part of Birket Qarun Formation.

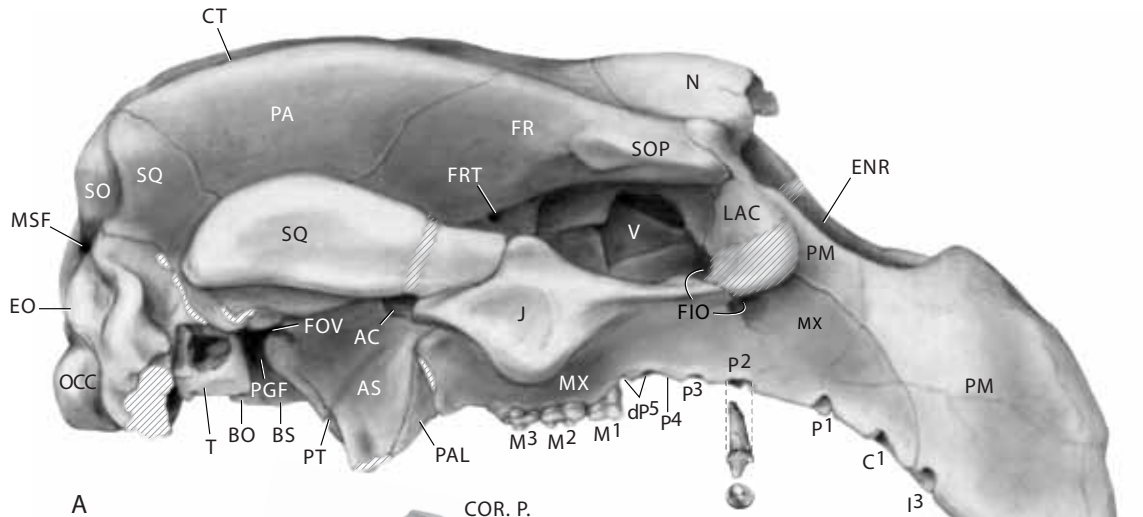
CGM 42298, right squamosal and right M^3 from locality WH-101 (UTM grid coordinates in zone 36N: 212840 m E and 3241481 m N); Priabonian, lower part of Birket Qarun Formation.

UM 83903, five caudal vertebrae from locality WH-207 (UTM grid coordinates in zone 36N: 214109 m E and 3245069 m N); Priabonian, lower part of Birket Qarun Formation.

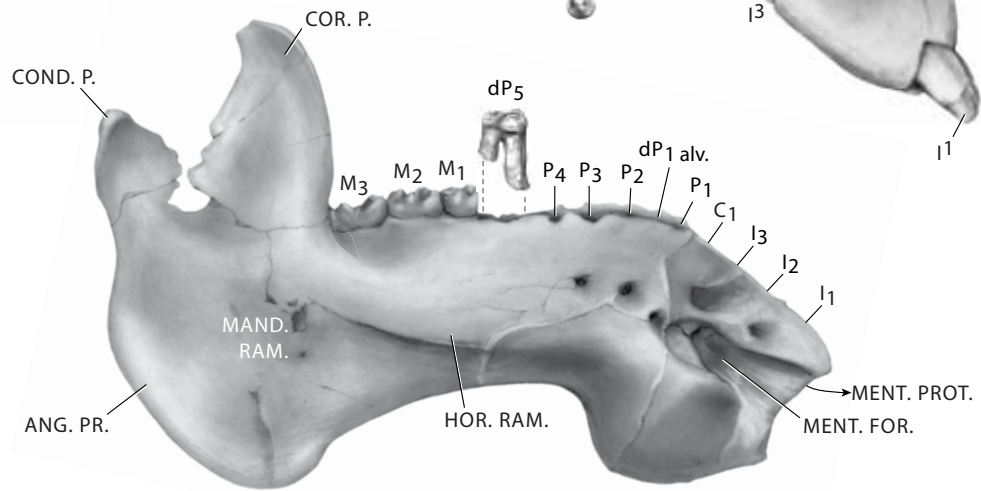
UM 94806 (Fig. 32), includes a left premaxilla, and right scapula and humerus from locality WH-33 (UTM grid coordinates in zone 36N: 211669 m E and 3243892 m N); Priabonian, lower part of Birket Qarun Formation.

UM 97520, fragments of isolated left scapula from locality WH-128 (UTM grid coordinates in zone 36N: 212595 m E and 3242363 m N); Priabonian, lower part of Birket Qarun Formation.

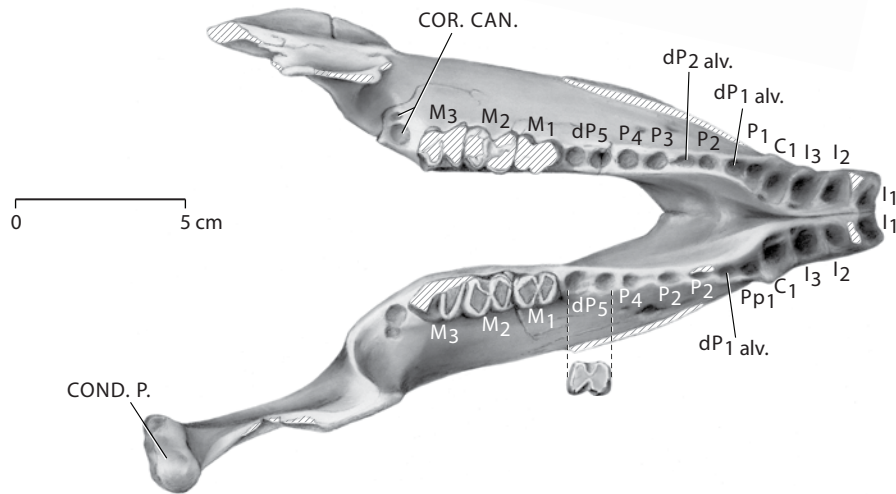
UM 97524, right maxilla (Fig. 32) and skull roof from locality WH-145 (UTM grid coordinates in zone 36N: 214093 m E and 3245221 m N); Priabonian, lower part of Birket Qarun Formation.



A



B



C

UM 100184, partial skull roof includes the sutured area of the frontals and parietals from locality WH-200 (UTM grid coordinates in zone 36N: 214537 m E and 3246438 m N); Priabonian, lower part of Birket Qarun Formation.

UM 101220, fragments of rostrum and vertebrae (atlas and some thoracics) from locality WH-220 (UTM grid coordinates in zone 36N: 213658 m E and 3245870 m N); Priabonian, lower part of Birket Qarun Formation.

Associated fauna.— In addition to *Eotheroides clavigerum*, the same beds produced *Eotheroides sandersi* sp. nov., described later in this chapter. *Protosiren smithae* was described from nearby localities above the interval that produced *Eotheroides clavigerum*. Following Gingerich (1992), the Birket Qarun Formation also contains the archaeocete whales *Basilosaurus isis* and *Dorudon atrox* (Cetacea); with rare *Moeritherium* (Proboscidea); occasional *Crocodylus* and *Paratomistoma* (Crocodylia); cf. *Podocnemis* sp., cf. *Stereogenys* sp., and cf. *Dermochelys* sp. (Chelonia); *Pterospheenus schweinfurthi* (Squamata); *Fajumia* sp., cf. *Arius* sp., *Cylindracanthus* sp., *Xiphorhynchus aegyptiacus* (Osteichthyes); and abundant teeth of sharks and rays (Neoselachii).

Cranium

Premaxilla.— Both premaxillae are well preserved in CGM 60551 (Figs. 29-31). UM 94806 includes an isolated left premaxillary blade (Fig. 32) that is missing its anterior and posterior borders. The premaxillary length from the anterior tip of the symphyseal process to the posterior end of the nasal process where it overlaps with the nasal and the frontal is 192 mm in CGM 60551. At the tip of the rostrum is a pair of enlarged alveoli for upper incisor tusks that measure 19 × 15 mm in diameter. Tusk alveoli do not rise higher than the lower third of the premaxillary symphysis. Deflection of the masticating surface of the rostrum is 43° from the occlusal plane (Table 3). The premaxillary symphysis in all specimens is enlarged relative to the cranium, with the ratio of symphyseal length to total length of the skull being about 3:1 (Table 3). Left and right premaxillary symphyses meet along a gently convex dorsal border. The rostrum has a weak dorsal keel that is very pronounced at its anterior end and is broadened posteriorly into a strongly convex summit emerging in a flattened peak at the rear of the symphyseal suture.

The nasal processes of the premaxillae are curved in dorsal and lateral views. These have a length of 92 mm in CGM 60551,

while they are incomplete in UM 94806. The nasal processes of the premaxillae have a suboval cross-section that is 14 mm in diameter in CGM 60551, with no sign of dorsoventral flattening (Figs. 29-31). The most posterior extensions of the premaxillary processes are angular and little-expanded mediolaterally. These are slightly flattened dorsoventrally, but not to the degree seen in *Protosiren*, where they overlap the nasal and frontal bones. As in more advanced dugongs, the mesorostral fossa opens dorsally, has an oval outline anteriorly, and is truncated by the nasals posteriorly, indicating an advance stage of adaptation to an aquatic environment. The rostral end of the premaxillary canal in *E. clavigerum* enters the premaxilla and maxilla, and penetrates the medial wall of the infraorbital foramina, indicating that veins and nerves enter into the infraorbital canal.

The isolated partial left premaxilla of UM 94806 was somewhat more than 76 mm long, with a straight dorsal border. The rostrum apparently formed a thin dorsal keel anteriorly, which broadened posteriorly into a strongly convex summit, ending in a sharp peak at the rear of the symphyseal suture (more or less similar to that in CGM 60551). The thin anterior part of the bone is pierced by a large premaxillary canal, but no incisor alveoli are preserved and there is no indication that the first incisor was enlarged. The nasal process is preserved for a distance of 40 mm behind the symphysis, at which point it has a suboval cross-section that is 7 mm in diameter, showing no sign of dorsoventral flattening. The mesorostral fossa appears to have been broadly semicircular in outline when viewed anteriorly.

Nasal.— Nasal bones are elongated anteroposteriorly (Figs. 29-31). They are exposed dorsally, forming oval wings that reach a length of 65 mm; are symmetrical and maintain a 30-mm long contact along their median borders; and are stout and highly arched upward, rising higher than both frontals and parietals. The lobes or wings are cleft by the frontals posteriorly. The nasals are set into a socket in the anteromedial margin of the frontals; they are exposed dorsally and measure 65 mm along their long axis (anteroposteriorly). The maximum breadth of both nasals is equal to their anteroposterior length. Anterolaterally the nasals bear a concavity for the nasal processes of the premaxillae. The lateral sides of the nasals, covered by the frontals, are 23 mm apart medially. These form the side walls of the upper part of the nasal cavity, which is roofed anteriorly by the arching dorsomedial flanges of the nasals. The ventrolateral side of each nasal is massive and fused to the ethmoid.

FIGURE 29 — (page 38). Holotype skull and mandibles of *Eotheroides clavigerum* (CGM 60551) from the Priabonian age Birket Qarun Formation of Wadi Al Hitan. A, lateral view of the cranium; the zygomatic process of the jugal was removed temporarily to expose the alisphenoid opening. B and C, lateral and occlusal views of the lower dentaries, which are tightly fused together. Abbreviations: AC, alisphenoid canal (foramen in *Eotheroides*); ANG. P., angular process; AS, alisphenoid; BO, basioccipital; BS, basisphenoid; COND. P., processus condylus; COR. CAN., coronoid canal; COR. P., coronoid process; CT, temporal crest; C_l, lower canine; C^l, upper canine; dP, deciduous premolar; dP alv., alveolar of deciduous premolar; ENR, external nares (mesorostral fossa); EO, exoccipital; FIO, foramen infraorbital; FOV, foramen ovalis; FPT, fossa pterygoidea; FR, frontal; FRT, foramen rotundum; G, glenoid articulation; HOR. RAM., horizontal ramus; I_l etc., lower incisor; I^l etc., upper incisor; J, jugal; LAC, lacrimal; M_l etc., lower molar or alveoli; M^l etc., upper molar or alveoli; MAL, Malleus; MAND. RAM., mandibular ramus; MENT. FOR., mental foramen; MENT. PROT., mental protuberance; MF, mastoid foramen; MX, maxilla; N, Nasal; OCC, occipital condyle; OF, optic foramen; OVF, oval foramen; P_l etc., lower premolar alveoli; P^l etc., upper premolar alveoli; PA, parietal; PAL, palatine; PM, premaxilla; PT, pterygoid; PTP, pterygoid process; POP, post occipital process; SO, supraoccipital; SOP, supraorbital process; SQ, squamosal; T, tympanic; V, vomer; ZP, zygomatic process of the jugal.

TABLE 3 — Measurements of cranial elements of the holotype skull of *Eotheroides clavigerum* sp. nov., CGM 60551 from the Priabonian of the Birket Qarun Formation, compared to cranial measurements of *Eotheroides sandersi* sp. nov., UM 111558 from the Priabonian of the Birket Qarun Formation, and *Eotheroides aegyptiacum* of Sickenberg (1934), SMNS St. III from the Eocene Mokattam Hills. Cranial measurements are after Domning (1978a). Measurements are in mm.

Abbr.	Measurement	<i>Eotheroide clavigerum</i> CGM 60551	<i>Eotheroides sandersi</i> UM 111558	<i>Eotheroides aegyptiacum</i> SMNS St. III
AB	Condylobasal length	335	309	—
ab	Height of jugal below orbit	37	37	—
AH	Length of premaxillary symphysis	112	97	—
BI	Rear of occipital condyles to the anterior end of interfrontal suture	182	194	180
CC'	Zygomatic breadth	187	142	—
cc'	Breadth across exoccipitals	104	95	72
de	Top of supraoccipital to ventral sides of occipital condyles	103	92	79
F	Length of frontals, level of tips of supraorbital processes of frontoparietal suture	126	120	85
FF'	Breadth across supraorbital processes	107	82	89
ff'	Breadth across occipital condyles	73	65	54
GG'	Breadth of cranium at frontoparietal suture	44	50	49
gg'	Width of foramen magnum	32	32	26
HI	Length of mesorostral fossa	78	69	—
hi	Height of foramen magnum	25	25	26
JJ'	Width of mesorostral fossa	39	37	—
KL	Maximum height of rostrum	65	56	—
MM'	Posterior breadth of rostral masticating surface	43	42	—
no	Anteroposterior length of zygomatic-orbital bridge of maxilla	65	53	52
OP	Length of zygomatic process of squamosal	98	88	—
OT	Anterior tip of zygomatic process to rear edge of squamosal below mastoid foramen (length of the squamosal)	120	117	—
P	Length of parietals, frontoparietal suture to rear of external occipital protuberance	62	56	78
Pq	Length of the alveoli tooth row (dP ⁵ -M ³)	54	44	42
QR	Anteroposterior length of zygomatic process of squamosal	47	35	34
rr'	Maximum width between labial edges of left and right alveoli across M ¹	70	59	57
ST	Length of cranial portion of squamosal	78	57	—
ss'	Breadth across sigmoid ridges of squamosals	147	126	106
T	Dorsoventral thickness of zygomatic-orbital bridge	18	12	15
tt'	Anterior breadth of rostral masticating surface	28	25	—
UV	Height of posterior part of cranial portion of squamosal	92	77	72
WX	Dorsoventral breadth of zygomatic process	38	34	—
yy'	Maximum width between pterygoid processes	38	41	29
YZ	Length of jugal	177	133	—
LFr	Length of frontals in midline	123	88	57
Hso	Height of supraoccipital	53	50	41
Wso	Width of supraoccipital	69	68	55
HIF	Height of infraorbital foramen	27	30	20
WIF	Width of infraorbital foramen	19	20	11
RD	Deflection of masticating surface of rostrum from occlusal plane (degrees)	43	49	—

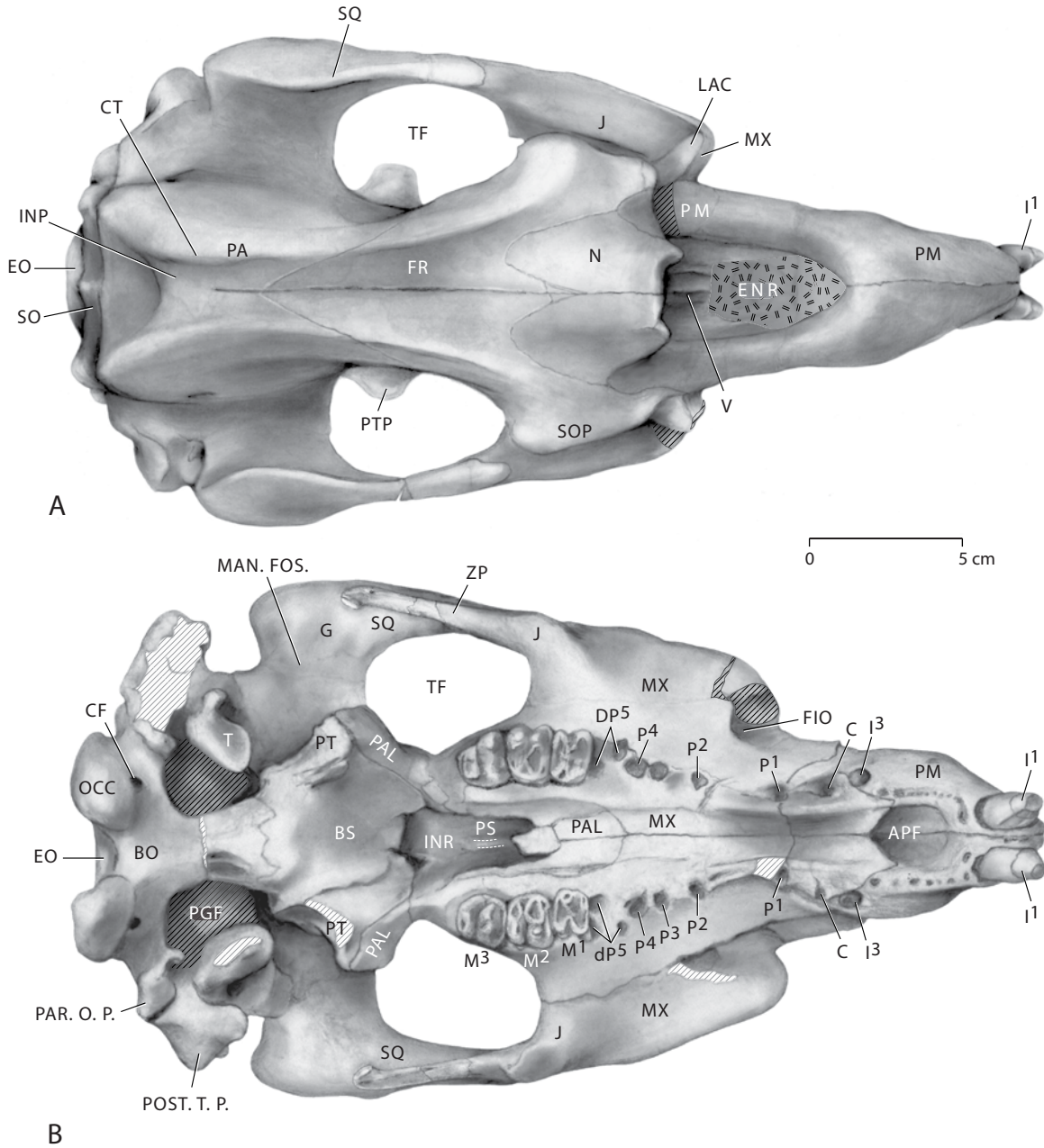


FIGURE 30 — Holotype cranium of *Eotheroides clavigerum* (CGM 60551) from the Priabonian age Birket Qarun Formation of Wadi Al Hitan. A, Dorsal view. B, Ventral view. The skull is tilted more caudally in B to expose greater detail in the ventral view of the rostrum. Abbreviations: *APF*, anterior palatine foramen; *AS*, alisphenoid; *BO*, basioccipital; *BS*, basisphenoid; *C¹*, upper canine; *CF*, condyloid foramen; *CT*, temporal crest; condyloid foramen; *dP*, deciduous premolar of maxilla; *dp alv.*, alveolar of deciduous premolar; *E*, ethmoid; *ENR*, external nares (mesorostral fossa); *EO*, exoccipital; *FR*, foramen rotundum; *FIO*, foramen infraorbital; *FM*, foramen magnum; *FPT*, fossa pterygoidea; *F*, frontal; *G*, glenoid articulation; *I¹* etc., first upper incisor; *INR*, internal nares; *INP*, interparietal groove; *J*, jugal; *LAC*, lacrimal; *M¹* etc., first upper molar or alveoli; *MAL*, Malleus; *MAND. FOS.*, mandibular fossa; *ME*, Mesethmoid; *MF*, mastoid foramen; *MX*, maxilla; *N*, Nasal; *OCC*, occipital condyle; *P¹* etc., first upper premolar alveoli; *PA*, parietal; *PAL*, palatine; *PAR. O. P.*, paroccipital processes; *PGF*, postglenoid fossa; *PM*, premaxilla; *POST. T. P.*, posttympenic process; *PR*, periotic; *PT*, pterygoid; *PS*, presphenoid; *SO*, supraoccipital; *SOP*, supraorbital process; *SQ*, squamosal; *T*, tympanic; *TF*, temporal fossa; *V*, vomer.

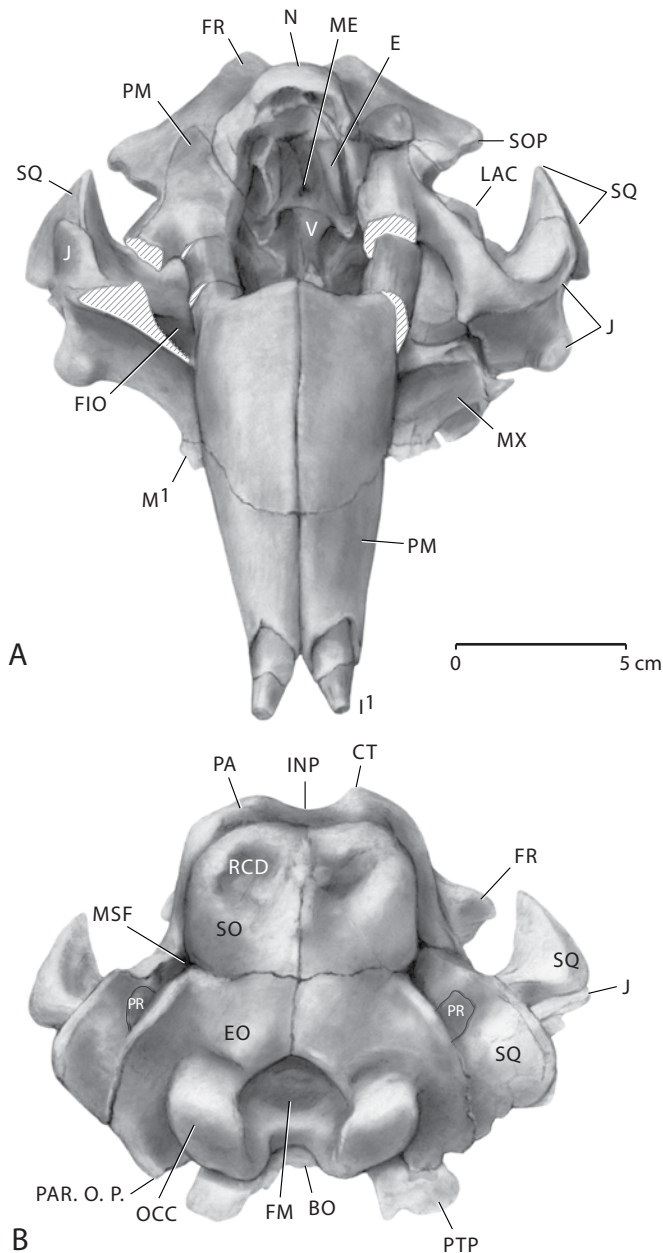


FIGURE 31 — Holotype cranium of *Eotheroides clavigerum* (CGM 60551) from the Priabonian age Birket Qarun Formation of Wadi Al Hitán. A, anterior view. B, posterior view. Abbreviations: *BO*, basioccipital; *CT*, temporal crest; *E*, ethmoid; *ENR*, external nares (mesorostral fossa); *EO*, exoccipital; *FR*, foramen rotundum; *FIO*, foramen infraorbital; *FM*, foramen magnum; *J*, jugal; *LAC*, lacrimal; *M¹* etc., first upper molar or alveoli; *ME*, mesethmoid; *MSF*, mastoid foramen; *MX*, maxilla; *N*, nasal; *OCC*, occipital condyle; *P¹* etc., first upper premolar alveoli; *PA*, parietal; *PAL*, palatine; *PAR. O. P.*, paroccipital processes; *PGF*, postglenoid fossa; *PM*, premaxilla; *PR*, periotic; *SO*, supraoccipital; *SOP*, supraorbital process; *SQ*, squamosal; *V*, vomer.

Ethmoid region.— The nasal arch is long, providing a large surface for attachment of the ethmoid. Ethmoid and mesethmoid are preserved in CGM 60551, extending below the nasals and along the narial passages. Ethmoids (Fig. 31) stand vertically and almost parallel to the medial walls of the nasals; they are 11 mm apart. Turbinals and laminae papyraceae are not preserved.

Vomer.— The vomer is partially preserved in CGM 60551 (Figs. 30, 31). A 9 mm thick sheath runs along most the internal narial passage. It is exposed in the mesorostral fossa, opening as a U-shaped canal and becoming narrow and constricted laterally and posteriorly. It contacts the maxilla and the palatine before embracing the olfactory chamber.

Lacrimal.— The lacrimal is large and irregular, and lacks a lacrimal foramen. It faces posteriorly and slightly laterally, with a distinct prominence laterally (Figs. 29-31). The lacrimal is surrounded by the supraorbital process of the frontal, by the jugal, and by the maxilla.

Frontal.— The frontals form the flat part of the skull roof, just behind the upwardly-arched nasals (Figs. 29-31). The lateral edges of the frontals are sharp and slightly overhanging. The lateral walls of the frontals are constrained and narrow, especially below the frontal-parietal suture. Anterior processes of the frontals on either side of the midline fill a wedge-shaped space between the posterior ends of the nasals, and these slope upward as do the nasals themselves, ending where the nasals meet in the midline. At this extremity the frontals are 7 mm thick where they cover the posterior end of the nasal cavity. The supraorbital process is stout and dense. It is extended anteriorly to embrace the nasal and the tip of the premaxillary processes. The posterolateral corner of the supraorbital process is prominent and distinct, and lies forward of the posterior end of the nasal. No postorbital processes are present. The dorsolateral part of each frontal is marked by a distinct crista temporalis in CGM 60551. The ratio of the maximum breadth across the supraorbital processes to the maximum length of the frontals, reaching the deepest point where the frontal meets the parietal posteriorly, is 0.82.

Parietal.— The parietal is heavy and robust in the holotype and marked by a thick crista temporalis, and a deep and wide interparietal groove (Figs. 29, 30). The lateral edges of the convex temporal crests are closest together just behind the frontoparietal suture, and are separated medially by about 29 mm. The parietal roof is more than 20 mm thick anteriorly along the midline. The squamosal overhangs and slightly indents the temporal crest.

Supraoccipital.— The supraoccipital is very well preserved in CGM 60551 (Figs. 29-31). Very thick and massive, the supraoccipital measures 52 mm along the midline, and its maximum breadth is 70 mm. It has a relatively flat surface, and a pentagonal outline. The nuchal planum is bipartite; lateral to the nuchal planum are a pair of insertions for the rectus capitis dorsalis (Fig. 31); insertions for a capitis semispinalis muscle are not preserved. The anterolateral portion of the supraoccipital is fused with the dorsal process of the squamosal in CGM 60551. The nuchal ridge shows weak rugosity. The parietal-supraoccipital angle is about 105° in CGM 60551 and the posterior surface of the supraoccipital itself is broadly V-shaped.

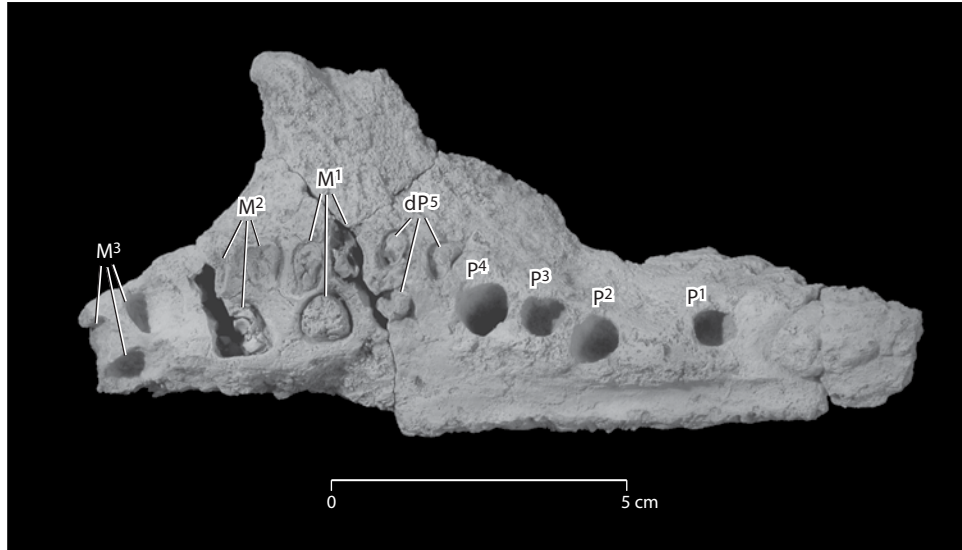


FIGURE 32 — Toothless right maxillary bone of *Eotheroides clavigerum* (UM 97524) bearing alveoli of P¹ through M³. DP⁵ through M³ are triple-rooted, while P¹ through P⁴ are single-rooted.

Exoccipitals.— The exoccipitals are well preserved in CGM 60551 (Fig. 31). They are hexagonal in shape, and connected along a midline suture that measures 21 mm. The ratio of exoccipital maximum height to maximum breadth is 0.59. The supraoccipital-exoccipital suture is almost straight. The mastoid foramen is almost closed. The foramen magnum is dome-like, opening downward, with a width that exceeds its height. Occipital condyles are 15 mm apart. A pair of diminutive hypoglossal foramina (44 mm apart) appear anteroventral to the occipital condyles. Paroccipital processes are very well developed. These are separated by 11 mm from the occipital condyles, and extend ventrally deeper than the occipital condyles themselves. The paroccipital processes have tapered, slightly deflected, and curved ends to accommodate the tympanic along with the squamosal.

Basioccipital.— The basioccipital is completely fused to the exoccipital and basisphenoid in CGM 60551 (Fig. 30); it is 52 mm long (from the base of the foramen magnum to the fusion line with the basisphenoid) and 22 mm wide. The union of the exoccipital and basioccipital produce an anchor-like bone in the posteroventral corner of the skull. The anterior edge is higher than the posterior edge. Ventrolaterally and more anteriorly are the insertions of the longus capitis muscles that are preserved as deep longitudinal grooves separated by a prominent median ridge.

Basisphenoid and presphenoid.— Both bones (Fig. 30) are well preserved and are fused to the surrounding elements (orbitosphenoid, alisphenoid, pterygoid, and palatine); sutures are fused. The basisphenoid is flat ventrally and its posterior end is higher than its anterior end. The presphenoid is projects cranially out of the basisphenoid as it starts narrowing, and its median crest becomes sheath-like and directed anterodorsally before joining the vomer.

Orbitosphenoid.— The orbitosphenoid is partly destroyed by cementation, it is exposed laterally and bounded by the frontal and alisphenoid dorsally, the alisphenoid posterolaterally, alisphenoid, and palatine laterally, and the palatine ventrally. The foramen rotundum is exposed anterolaterally (Fig. 29), and the anteroposterior opening serves as a canal between cranial and pterygoid-palatine fossae. Below the foramen rotundam is the optic foramen, which is partially open.

Alisphenoid.— The alisphenoids are well preserved in CGM 60551 (Fig. 29). They are 75 mm deep dorsoventrally, and are 82 mm apart. The squamosal, parietal, and frontal contact the alisphenoid dorsally and the squamosal dorsolaterally. The alisphenoids are strongly fused with the palatines and the pterygoids, and cover the palatine posterior wing on both sides, while the pterygoid covers its posteromedial wall. The alisphenoid canal is absent. Instead the alisphenoid foramen (14 mm in diameter in CGM 60551) opens posteriorly and directly to the base of the braincase. A pair of concavities occupy the most lateral posterior corners of the basisphenoid above the pterygoid fossa, which might represent the remains of the posterior openings for the alisphenoid canal.

Pterygoid.— The pterygoid is preserved on both sides, along with its processes and grooves (Figs. 29-31). Medial walls of the pterygoid are 45 mm apart as measured in CGM 60551. The pterygoid is fused to the basisphenoid dorsally, the palatine mediolaterally, and the alisphenoid posterolaterally. Lateral and medial edges are pronounced and converge posterodorsally at the posterior corner of the basisphenoid; they gently curve anteriorly, and project backward ventrally. The median edge stands vertically while the lateral edge diverges 20° laterally.

Palatine.— The palatine represents the anteromedial component of the pterygoid processes (Figs. 29, 30). Both palatines are curved anteromedially before rejoining postero-

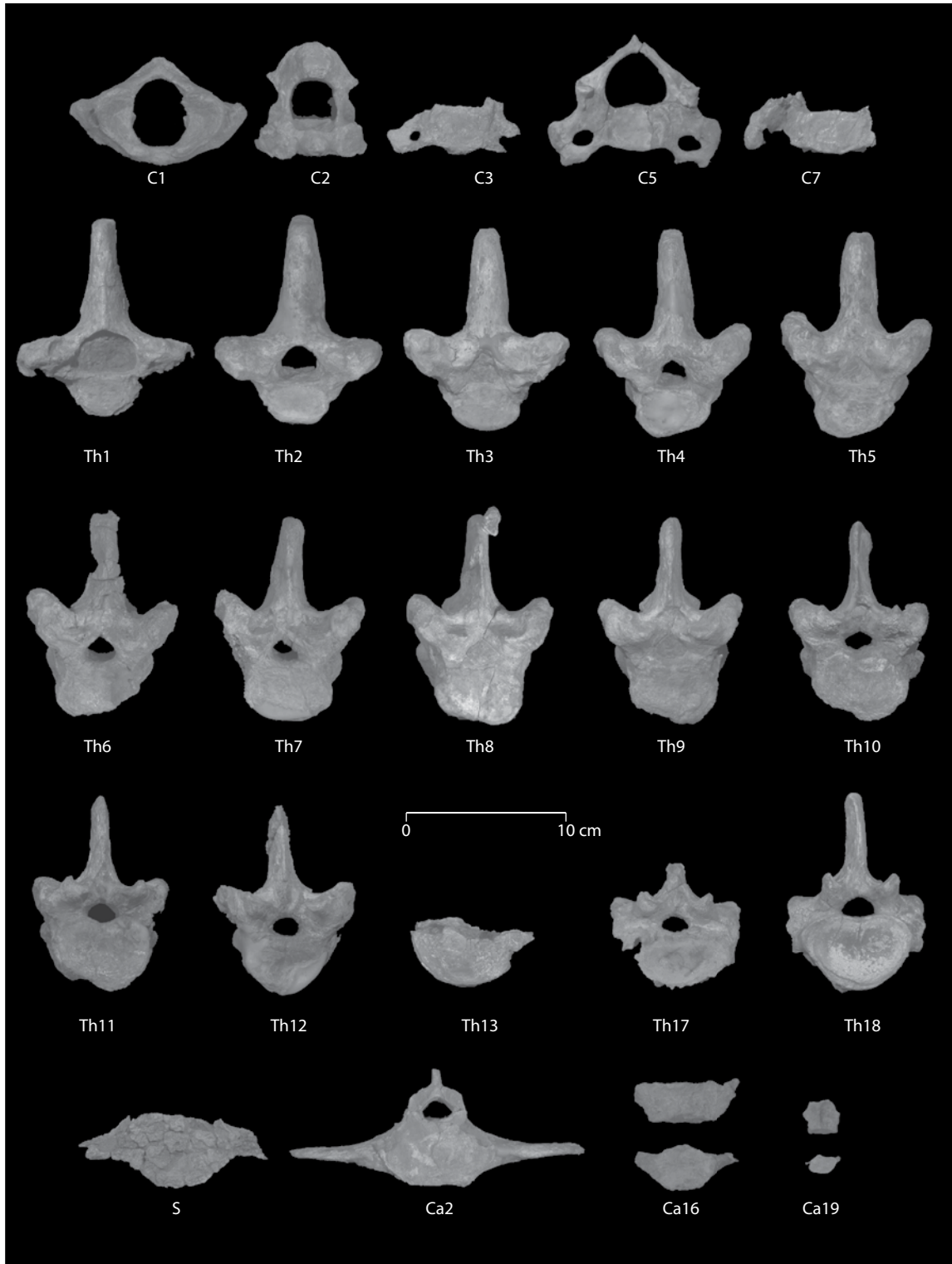


FIGURE 33 — Cervical, thoracic, sacral, and caudal vertebrae of the holotype of *Eotheroides clavigerum* (CGM 60551) from the Priabonian age Birket Qarun Formation of Wadi Al Hitán. Vertebrae are shown in anterior (cranial) view. Abbreviations: *C*, cervical; *Ca*, caudal; *Th*, thoracic; *S*, sacral.

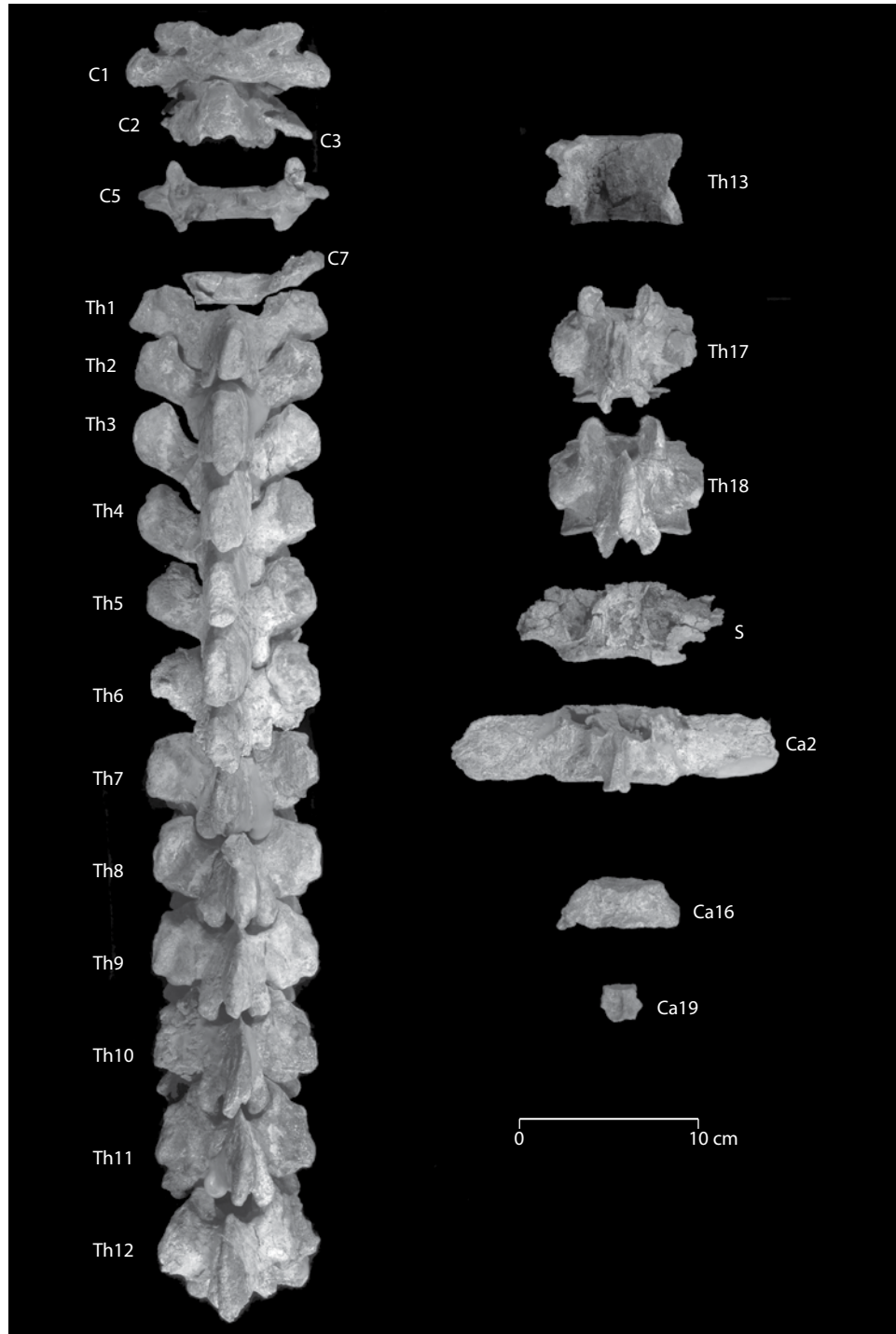


FIGURE 34 — Cervical, thoracic, sacral, and caudal vertebrae of the holotype of *Eotheroides clavigerum* (CGM 60551) from the Priabonian age Birket Qarun Formation of Wadi Al Hitan. Vertebrae are shown in dorsal view, showing their articulation and serial arrangement. Abbreviations: *C*, cervical; *Ca*, caudal; *Th*, thoracic; *S*, sacral.

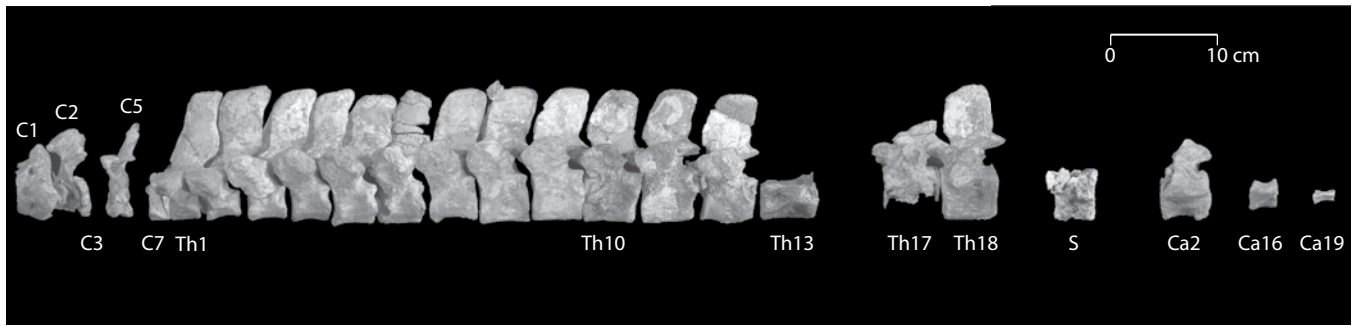


FIGURE 35 — Cervical, thoracic, sacral, and caudal vertebrae of the holotype of *Eotheroides clavigerum* (CGM 60551) from the Priabonian age Birket Qarun Formation of Wadi Al Hitán. Vertebrae are shown in left lateral view, showing their articulation and serial arrangement. Abbreviations: *C*, cervical; *Ca*, caudal; *Th*, thoracic; *S*, sacral.

ventrally along the midline; however the ventral union is not evident in CGM 60551 since most of the palatine is damaged medial to M^3 and M^2 . On the other hand the anterior edge along the ventral midline lies between P^4 and dP^5 . The palatines contact the pterygoid posteromedially and the alisphenoid posterolaterally, and overlap the posterior edge of the maxillae anteriorly and anteroventrally. They also form the posterior wall between the internal nares and the temporal fossa by merging with the presphenoid medially and the orbitosphenoid anterolaterally.

Maxilla.— Maxillae are very well preserved in CGM 60551 (Figs. 29–31). They form a lyre-shaped palate. Molar teeth (M^{1-3}), alveoli for a triple-rooted dP^5 , and single-rooted alveoli for P^4 through C^1 are clear. The maxillary dental battery extends posteriorly about 16 mm behind M^3 in CGM 60551. The orbital bridge (zygomatic bridge), which provides the ventral and mediolateral cover for the infraorbital foramen, is 65 mm long in CGM 60551. The infraorbital foramen is suboval and opens anteriorly, with a width and height of about 21×26 mm in CGM 60551. These are placed about 61 mm from each other across the rostrum. The depth of the zygomatic bridge above the alveolar shelf of M^1 in CGM 60551 is 26 mm. Ventrally, the maxilla is slightly curved and narrow. In lateral profile, it is deflected 30° downward from the horizontal palate at the narrowest point of the rostrum, where the lyriform edges of the palatal ventral gutter are 12 mm wide and 11 mm deep. Furthermore this deflection is anterior to the zygomatic-orbital bridge and exactly at the alveoli for P^1 on both sides. After the anterior constriction and narrowing, the maxillae form a slightly broad shelf before splitting laterally and ending with a large incisive foramen (the anterior palatine foramen). The latter foramen has a heart-like cross-section, lies in a deep concavity where it is formed together by the maxilla and the premaxilla, and opens downward.

UM 97524 includes a virtually complete right maxilla (Fig. 32) with alveoli for P^{1-4} and four three-rooted molariform teeth (dP^5 – M^3). The palatal gutter that would have been about 1.5 cm wide and 0.5 cm deep lay between the toothrows anteriorly. The zygomatic-orbital bridge is about 50 mm long anteroposteriorly, and reaches a thickness of 16 mm near its posterior edge, which

lies at the level of the anterior alveoli of M^2 . The ventral side of the bridge is elevated about 1 cm above the alveolar margin.

Squamosal.— The squamosals make a large portion of the posterolateral sides of the skull, and extend dorsally high enough to indent the temporal crest (Figs. 29–31). The mastoid foramen in CGM 60551 is almost closed. The sigmoidal ridge projects laterally on the posterolateral edge of the squamosal. It appears below the mastoid foramen and extends down to the ventral tip of the post-tympanic process. The sigmoidal ridge is eroded in CGM 60551. The zygomatic process is roughly lozenge-shaped in lateral view, with a nearly straight posterodorsal edge that is very slightly convex laterally. The processus retroversus of the squamosal is slightly developed. The anterior end tapers somewhat without reaching the level of the supraorbital process; the anterodorsal edge is distinctly concave in outline. The zygomatic process in CGM 60551 is 96 mm long and 39 mm wide dorsoventrally; its root is 43 mm long anteroposteriorly. Ventrally, the mandibular fossa, entoglenoid bar, and temporozygomatic suture are all shallow and weakly defined. The spheno-squamosal suture is flat and indented; and the suture with the parietals is interdigitated and rugose posteromedially. The cranial portion of the squamosal, along with the basioccipital, encapsulates the periotic in a semicircular socket that is deep and cylindrical in shape on the cranial portion of the squamosal root.

Jugal.— The jugals are very well preserved on both sides in CGM 60551 (Figs. 29–31). The total length of the jugals is about 177 mm with a maximum dorsoventral height of 44 mm below the postorbital process. The preorbital process is thin and lies against the maxillae. The deepest point, the ventral process of the jugal, is a smooth and curved surface with a rounded tip, mediolaterally compressed, and it lies directly beneath the postorbital process and above the maxillary shelf. The postorbital process has a blunt summit and lies against the anterior tip of the zygomatic process of the squamosal. The zygomatic process is gracile and rounded behind the postorbital process, flattened and thin posteriorly, and curved medially at its posterior tip just in front of the mandibular fossa. The zygomatic process of the jugal is very well preserved; it is directed more laterally than

TABLE 4 — Measurements of the holotype mandible of *Eotheroides clavigerum* sp. nov., CGM 60551, collected from the Priabonian of the Birket Qarun Formation, compared to those of *Protosiren smithae*, CGM 42292, from Birket Qarun Formation; *Eosiren stromeri*, UM 100137, from the Qasr El Sagha Formation; and “*Eotheroides* sp.,” USNM 214596, from the Eocene of North America (Domning et al., 1982). Mandibular measurements are after Domning (1978a). Measurements are in mm.

Abb.	Measurement	<i>Eotheroide clavigerum</i> CGM 60551 (holotype)	<i>Protosiren smithae</i> CGM 42292 (Domning and Gingerich, 1994)	<i>Eosiren stromeri</i> UM 100137	<i>Eotheroides</i> sp. USNM 214596 (Domning et al., 1982)
AA	Total length	216	222	213	181+
AG	Anterior tip to front ascending ramus	150+	154	170	147
AP	Anterior tip to rear of mental foramen	43	70	54	52
AQ	Anterior tip to front of mandibular foramen	132	160	155	—
AS	Length of symphysis	62	65	68	69
BG	Posterior extremity to front of ascending ramus	64	74	—	—
BQ	Posterior extremity to front of mandibular foramen	36	65	50	—
CD	Height of coronoid process	130	154	—	—
DF	Distance between anterior and posterior ventral extremities	120	113	56	—
DK	Height of mandibular notch	106	114	—	—
DL	Height of condyle	119	131	—	—
EF	Height at deflection point of horizontal ramus	69	66	83	55
EU	Deflection point to rear of alveolar row	77	86	105	87
GH	Minimum anteroposterior breadth of ascending ramus	63	63	—	—
GP	Front of ascending ramus to rear of mental foramen	100	76	112	—
IJ	Maximum anteroposterior breadth of dorsal part of ascending ramus	65	76	—	—
MN	Top of ventral curvature of horizontal ramus to line connecting ventral extremities	32	26	37	18
MO	Minimum dorsoventral breadth of horizontal ramus	38	37	46	37
RR'	Maximum breadth of masticating surface	37	51	26	25
SQ	Rear of symphysis to front of mandibular foramen	72	99	88	—
TU	Length of the alveolar row (M ₁₋₃)	44	64	46	46
VV'	Maximum width between labial edges of left and right alveoli across M ₁	56	59	65	40
WW'	Minimum width between angles	89	70	65	—
XX'	Minimum width between condyles	99	100	—	—
MD	Deflection of symphysal surface from occlusal plane (degrees)	50	58	43	37

medially; the posterior end of the jugal is rounded and slightly curved back medially just in front of the glenoid process.

Petrotic.— The petrotympanic bone is damaged on both sides by gypsum, and only the tympanic ring (Figs. 29, 30) is preserved. This is directed and inclined medially, forming an angle less than 45° with the pars mastoidea.

Mandible

Dentary.— CGM 60551 has the best and the only preserved lower jaw in the collected material of this species (Fig. 29). Measurements of the mandible of CGM 60551 are compared to those of other early sirenians in Table 4.

The lower jaw of CGM 60551 preserves almost all of its morphological features on both dentaries (mandibular rami with

coronoid and condylar processes, mandibular corpora, mental and mandibular foramina, symphysis and masticating surfaces, and number of cheek teeth). The total length of the mandible is approximately 210 mm, plus the length of the broken anterior tip of the symphysis. The depth of the mandibular corpus below M₁ is about 48 mm. Dental rows run parallel to each other from M₃ to P₁ where both sides start converging to seal the posterior side of the symphysis. Anterolateral sides of the mandibular corpora are characterized by the presence of a large mental foramen (12 mm in diameter) located just below the canine; 3 or 4 secondary mental foramina decreasing in size posterodorsally are located behind the main mental foramen; in addition to these there are at least two more foramina positioned above the mental

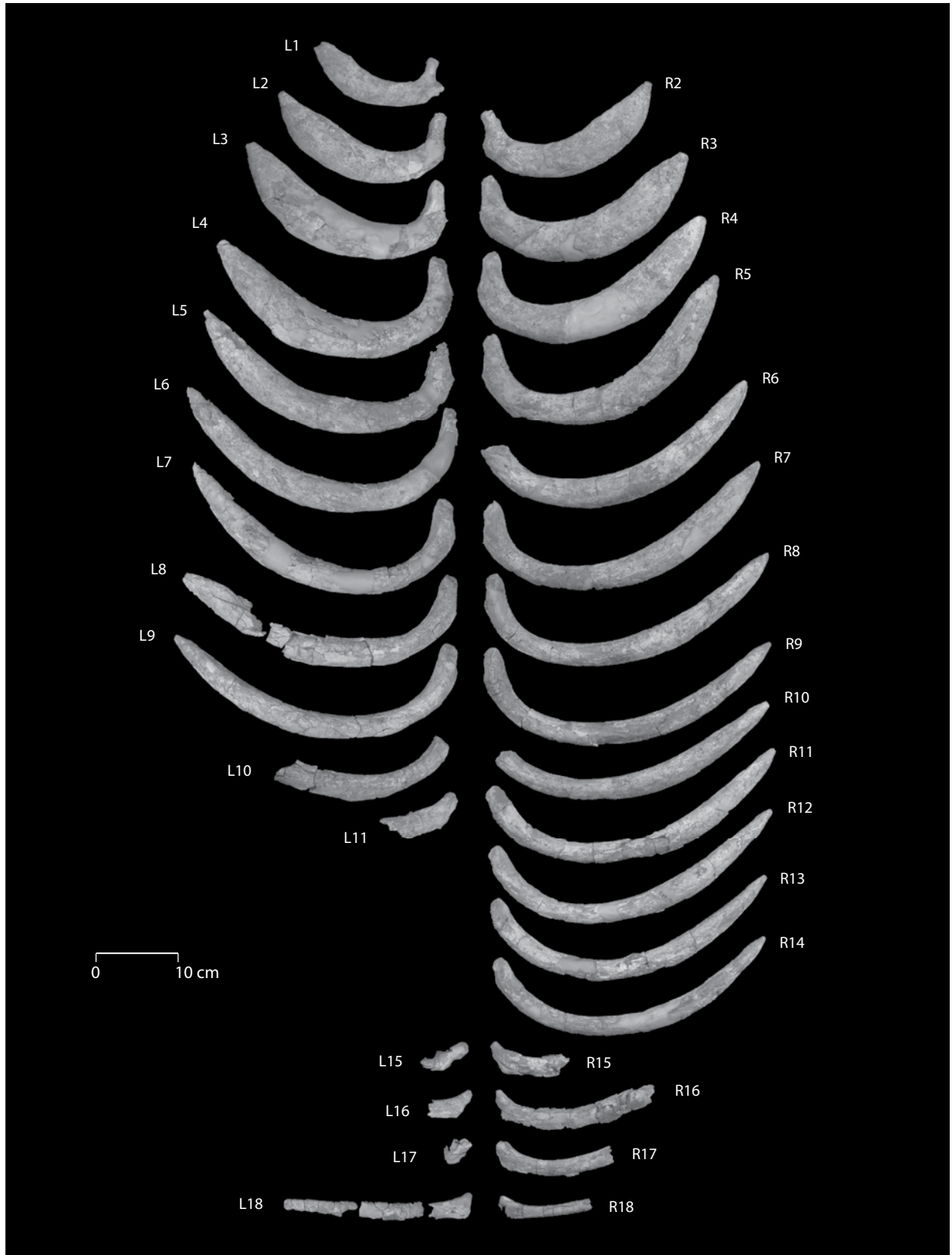




FIGURE 37 — Forelimb elements of the holotype of *Eotheroides clavigerum* (CGM 60551) from the Priabonian age Birket Qarun Formation of Wadi Al Hitan. A, right radius and ulna in medial view (distal epiphyses are missing); B, right humerus in posterior view; C, right scapula in lateral view.

foramen and its downwardly open groove below the alveoli of the masticating surface.

The symphysis is strongly fused, deeply cleft ventrally, deflected about 38 degrees from the mandibular corpus, and

bulbous posteroventrally. It has a length of 62 mm, plus the length of the broken tip of the mandible (protuberantia mentalis = mental protuberance), and is 71 mm high as measured below the posterior edge of I_3 and the base ventrally. The outline of the ascending ramus is perpendicular to the mandibular corpus posteriorly, curved at its posteroventral border, and ascends upward smoothly. The masticating surface of the symphysis consists of a pair of rows with rounded alveoli (sockets) for three incisors, the widest are the most anterior pair. The masticating surface is narrow anteriorly (18 mm wide across I_1) and widens posteriorly (36 mm across I_3) and has a length of 50 mm plus the length of the mental protuberance. The posteromedial portion of the masticating surface is connected to a narrow gutter that is 3 mm wide and 3 mm deep. This short gutter initially emerges as a forward continuation of the labial rims of the symphyseal area as both mandibular corpora start converging medially near the canine alveolus. After this the gutter disappears while a weak

FIGURE 36 — Left and right ribs of the holotype of *Eotheroides clavigerum* (CGM 60551) from the Priabonian age Birket Qarun Formation of Wadi Al Hitan. Ribs are shown in anterior view, and arranged from 1 (top) through 18 (bottom). Identification to position is based on morphology, including the size of both rib body and the proximal articulation of the head and tubercle; fit to thoracic vertebrae; degree of pachyosteosclerosis; and length and straightness of the rib shaft. Left side ribs preserve the upper half of the rib series and the last rib. Right side ribs preserve an almost complete series, missing only the first rib and the distal portions of the posterior ribs. Abbreviations: *L*, left rib; *R*, right rib.

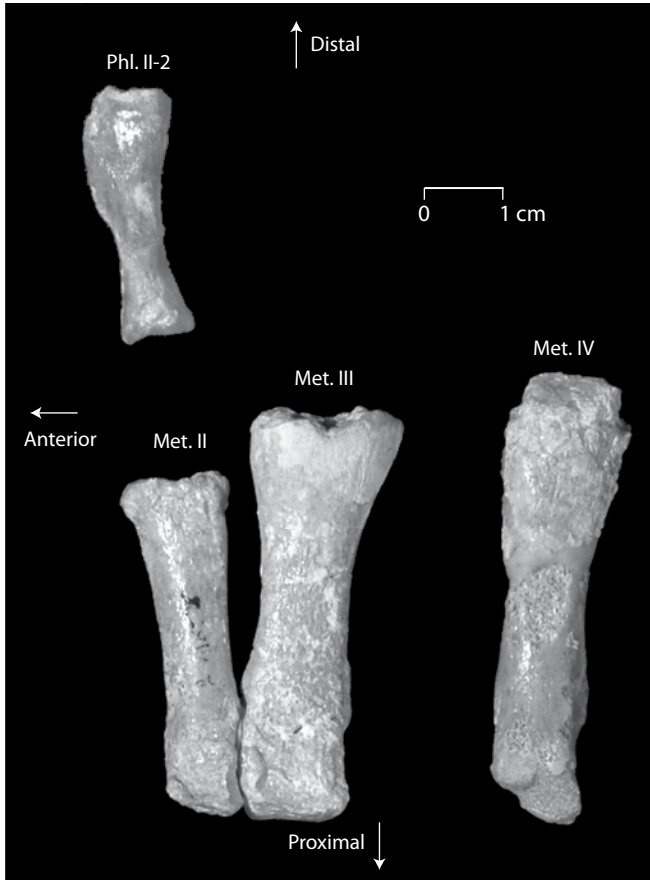


FIGURE 38 — Right metapodials of the holotype of *Eotheroides clavigerum* (CGM 60551) from the Priabonian age Birket Qarun Formation of Wadi Al Hitan, seen in dorsal view. Second and third metacarpals (Met. II and III) fit together as shown here. The fourth metacarpal (Met. IV) is part of the same hand but has a slightly weathered proximal end. Phalanx II-2 is a middle phalanx; it is missing its proximal epiphysis and has a small articular facet on the distal end for phalanx II-3. All are shown in dorsal view.

ridge runs along the rest of the rostrum medially to the broken end of the mental protuberance (Fig. 29).

The long axes of the ascending ramus and mandibular corpus are perfectly perpendicular to each other; the mandibular ramus is 64 mm long anteroposteriorly; it is very thin at the temporalis and zygomatico-mandibular muscle scar attachment. The condylar process is oval in shape, about 23 mm wide and 14 mm long anterodorsally, and extends 117 mm from the base of the angular process. The coronoid process is thin and raised 130 mm from the most ventral point of the angular process to its backwardly curved dorsal peak. The mandibular notch is quite well preserved on the right side of CGM 60551; it is deep and subcircular to crescent-shaped. The internal oblique line connecting the mandibular ramus with the mandibular corpus is robust and stronger than the external line. A prominent shallow trough (coronoid canal) is located just behind M_3 , partly filled

with cancellous bone; in fact the coronoid foramen appears to be exposed in the dental capsule on the medial side of the mandibular ramus behind M_3 and the mandibular foramen. The mandibular foramen opens below the anterior edge of M_3 ; it is 14 mm in diameter at this point and extends posterodorsally in an acute angle to form a flute-like groove. The posteroventral corner of the angular process is rounded with a thick edge. The internal side of the angular process (surface attachment for pterygoidus internus) is flanged and curved medially on both sides.

Dentition

Upper dentition.— The quality of the preserved material and number of specimens allowed for determinations of the formula for the dentition of *Eotheroides clavigerum* (Figs. 29, 30, 66). The dental formula for the upper dentition is 2.1.5.3, and for the lower counterpart is 3.1.5.3. Measurements of upper and lower teeth of *E. clavigerum* are listed in Table 5, with comparative measurements for *E. aegyptiacum* provided in Table 6 and for another dugongid in Table 7.

The upper first incisor is a medium-sized tusk positioned at the anterior tip of the premaxilla of CGM 60551 (Figs. 29-31). The total length of the tusk with its root is 36 mm; the crown is 13 mm long, and the base is between 8 and 10 mm wide. The tusk has an oval cross section. The crown is cone-shaped and its tip is worn, exposing dentine. There is no sign of I^2 or its alveolus; the alveolus at the posterior end of the premaxilla thus was assigned to I^3 . However, I^3 is not preserved, its alveolus is the only alveolus, it lies between the canine and tusk, and it follows the tusk after a 46 mm diastema in CGM 60551.

The upper canines are not preserved, but their alveolae are separated from I^3 by a 13 mm diastema in CGM 60551. Following the canine alveoli, there are 4 pairs of single rooted alveoli marking the loci for P^{1-4} , followed by a three-rooted pair of empty alveoli for dP^5 . The diastemata between the alveoli of C and P^1 , P^1 and P^2 , P^2 and P^3 , P^3 and P^4 , and P^4 and dP^5 , are 13, 25, 7, 3, 2 mm, respectively, in CGM 60551.

Associated with the skull of CGM 60551 is what seems to be a right P^2 (Fig. 29); the tooth has been identified as P^2 because the root fits in the alveolus. The root and the crown are preserved and they measure together about 21.4 mm in total height. The crown is 8.00 mm high, 7.62 mm long and 6.45 mm wide; it consists of a large centrolabial cusp directed lingually, showing slight wear that increases labially; a smaller cusp is lingually associated with the main centrolabial cusp; together, both cusps separate the cingulum into two heels or valleys. To the front of the two cusps a pair of cusplets marks the lingual cingulum; posterior to the main cusp, and more lingually, another pair of cusplets takes a lower position on the postcingulum.

Deciduous dP^5 is missing on all maxillae; the three alveoli (one of them is damaged) that follow M^1 in CGM 60551 are the only marks left from its root. M^{1-3} are preserved in both maxillae of CGM 60551. The cheek teeth are bilophodont, trigon higher than talon, protoloph is larger than metaloph, and there is a gradual increase in tooth size distally. M^1 exposes the most wear facets of all molars, width slightly exceeds length, and labial cusps are deeper and less worn than lingual ones, with the paracone cusp being the highest. Para- and lingual cingulae are

TABLE 5 — Measurements of right upper and lower teeth preserved in *Eotheroides clavigerum* sp. nov., CGM 60551 (holotype), collected from the Birket Qarun Formation. Abbreviations: *AW*, anterior width; *CH*, crown height labially; *L*, length; *PW*, posterior width. Measurements are in mm.

Tooth	L	AW	PW	CH
I ¹	13.09	8.40	—	—
I ²	—	—	—	—
I ³	—	—	—	—
C ¹	—	—	—	—
P ¹	—	—	—	—
P ²	7.62	6.45	6.45	8.00
P ³	—	—	—	—
P ⁴	—	—	—	—
dP ⁵	—	—	—	—
M ¹	12.61	15.57	14.16	6.00
M ²	13.98	17.59	14.60	8.83
M ³	16.53	17.55	12.35	7.89
dP ₅	11.78	9.47	9.47	6.31
M ₁	12.13	10.73	10.73	6.55
M ₂	14.88	12.12	12.12	7.03
M ₃	17.76	12.82	12.82	9.15

TABLE 6 — Measurements of upper right cheek teeth of *Eotheroides aegyptiacum*, SMNS St.XI (XIV), from the Lutetian of the Mokattam Hills near Cairo. Abbreviations: *AW*, anterior width; *L*, length; *PW*, posterior width. Measurements are in mm.

Tooth	L	AW	PW
M ¹	9.80	11.20	9.60
M ²	12.00	12.30	10.70
M ³	12.70	11.90	8.70

TABLE 7 — Measurements of lower teeth preserved in the USNM 214596 dugongid from the Eocene of North Carolina published in Domning et al. (1982). Abbreviations: *AW*, anterior width; *CH*, crown height labially; *L*, length; *PW*, posterior width. Measurements are in mm.

Tooth	L	AW	PW	CH
I ₁	—	—	—	—
I ₂	—	—	—	—
I ₃	—	—	—	—
C	—	—	—	—
P ₁	—	—	—	—
P ₂	—	—	—	—
P ₃	9.69	7.40	7.40	10.0
P ₄	9.89	8.35	8.35	9.60
dP ₅	12.17	9.05	9.80	5.50
M ₁	12.94	10.10	10.60	7.80
M ₂	14.50	11.27	—	9.80
M ₃	18.21	12.10	12.00	9.10

more developed than meta- and labial cingulae. The occlusal surface of M¹ in CGM 60551 has suffered considerable shearing and grinding. M² is more or less square, cusps are higher than those on M¹ and lower than those on M³. The paracone is the highest cusp as on M². Interlophs (intervalleys) are deeper than those on M¹ (Figs. 30, 66). Dentine is less exposed on the lophs than on M¹. The cingulum is weakly developed or almost absent labially, and well developed lingually.

M³ has the best preservation, showing the least wear. It is the largest of all molars in CGM 60551, being 32% larger than M¹ and 15% larger than M². The protoloph is wider and slightly lower than the metaloph, and both are separated lingually and labially by deep valleys; a lingual cingulum blocks these valleys, and no labial cingulum appears on M³ in CGM 60551. The metacone is the highest cusp and the smallest major cusp, and the protocone is the largest. The protoconule is relatively large and positioned equidistant between the protocone and paracone; the three cusps were aligned to form a transverse ridge in early stages before the appearance of wear surfaces. The precingulum is a simple transverse ridge; initially it arises from the most anterolabial corner just at the base of the paracone, extends lingually and reaches its peak just in front of the protocone. Its anterolingual corner bears a single cusp that is mostly obscured by wear in older individuals. The lingual cingulum is marked by up to four small cusps; it extends from the anterolingual base of the hypocone, then gently curves and ascends to join the posterolingual base of the protocone. The postcingulum is a low transverse ridge that is confined posteriorly behind the metaloph, higher at the posterior base of the hypocone, and it is cleft with a wide angle. The valley between the metaloph and the postcingulum in CGM 60551 has an open v-shape and the valley between the metaloph and the postcingulum is open mesiodistally.

The maxilla of UM 97524 (Fig. 32) contains alveoli for four large single-rooted premolars (P¹⁻⁴) and four three-rooted molariform teeth (dP⁵-M³). These alveoli contain roots for dP⁵-M²; M³ was fully erupted as its roots were distinct and separate. The four anterior alveoli are each about 7 mm in diameter; the anteroposterior lengths of each set of alveoli for the molariform teeth are 11, 12, 15, and >15 mm, and their transverse widths are about 14, 15, 17, and >16 mm, respectively. The bone extends for 28 mm anterior to the P¹ alveolus, and only a small part of it is missing where a canine might have been located. The alveoli for P¹ and P² are separated by a 12 mm diastema. The surface of a break passing just behind dP⁵ was excavated in search of an unerupted P⁵, but none was found. The toothrow is distinctly convex laterally from P² to M³. The posterior end of the intermaxillary suture (i.e., the location of the anterior end of the palatine) lies at the level of the posterior dP⁵ alveoli.

Lower dentition.— The lower dental formula of *Eotheroides clavigerum* (CGM 60551 in Fig. 29) is 3.1.5.3. CGM 60551 has dP₅-M₃ preserved on the right side; M₁₋₃ are partially preserved on the left side. In front of dP₅ there are 9 or 10 single alveoli for the roots of I₁-P₄; extra alveoli are remnants of incomplete resorption of the alveoli in deciduous postcanine teeth, which often appeared as small rounded alveoli in front of the permanent alveoli.

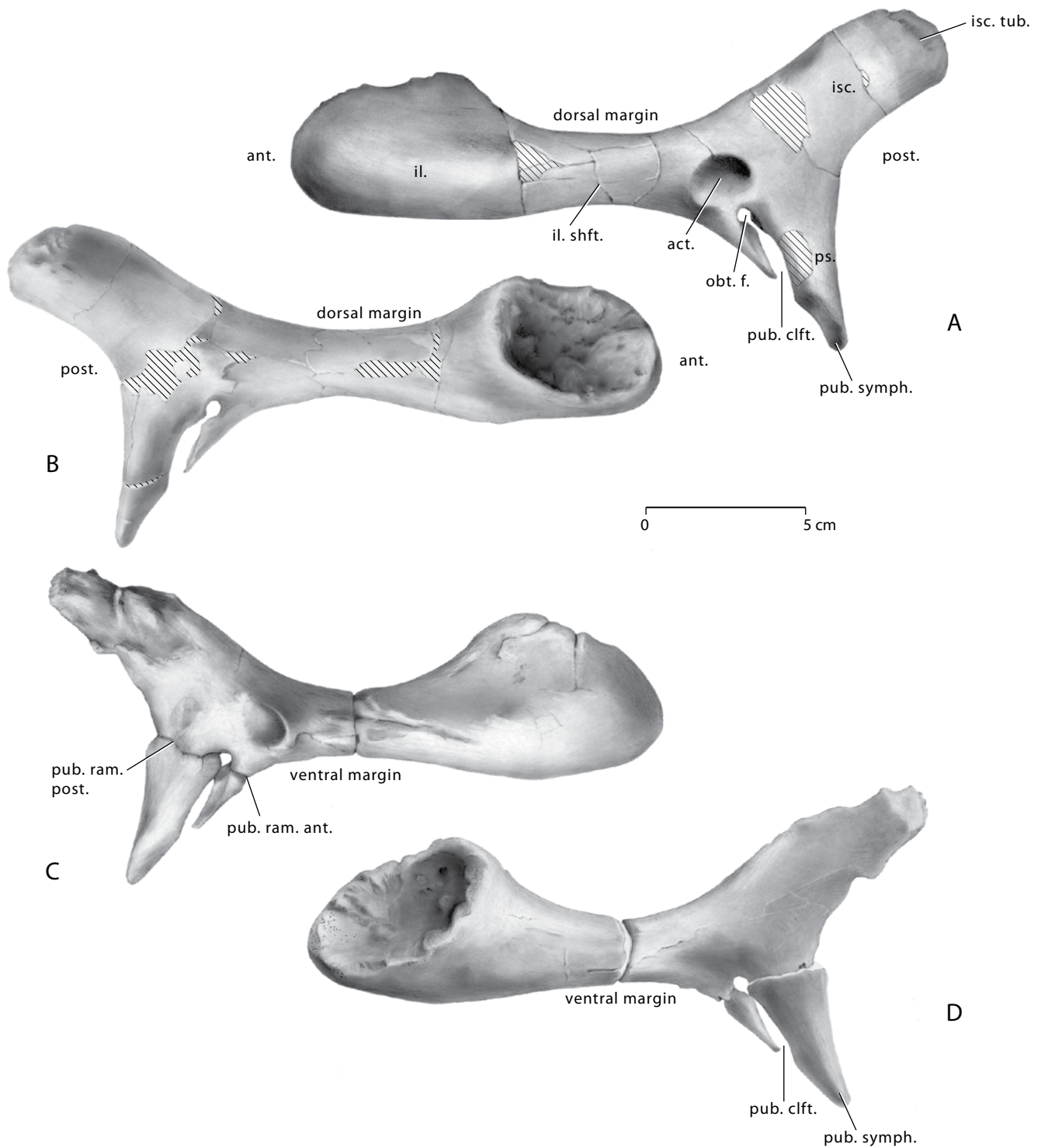


FIGURE 39 — Left and right innominate pelvic bones of the holotype of *Eotheroides clavigerum* (CGM 60551) from the Priabonian age Birket Qarun Formation of Wadi Al Hitán. A-B, left innominate in lateral and medial view. C-D, right innominate in lateral and medial view. Notice the club-like anterior portion of the ilium, the long and cleft pubis, and the reduced acetabulum. Abbreviations: *act.*, acetabulum; *act. n.*, acetabular notch; *dor. il. sp.*, dorso iliac spine; *il.*, ilium; *isc.*, ischium; *isc. tub.*, ischiac tuberosity; *isc. shft.*, ischiac shaft; *obt. f.*, obturator foramen; *ps.*, pubis; *pub. symph.*, pubic symphysis; *pub. clft.*, pubic cleft; *pub. ram. ant.*, anterior pubic ramus; *pub. ram. post.*, posterior pubic ramus; *sac. il. artic.*, sacroiliac articulation surface.

I₁ through P₄ are missing from the lower jaw on both sides; all alveoli are empty and shallow indicating that lower premolars and incisors were replaced and lost before death in CGM 60551. Alveoli for I₁ through C₁ are 16, 11, 10, and 10 mm in anteroposterior length, respectively; and 7, 8, 9, 12 mm in mediolateral width. There is 3-4 mm of medial separation between the left and right canines and incisors. I₁ and I₂ alveoli are separated from each other by an 8 mm diastema; I₃ and C₁ alveoli follow after 6 mm diastemata each. Diastemata between the successive teeth of C₁, P₁, P₂, and P₃ are all equal to 2 mm, respectively. There is a notable diastema between P₃ and P₄, which measures 7 mm on the right side and 4 mm on the left side. P₄ and dP₅ are separated by a 3 mm diastema.

dP₅-M₃ are bilophodont (Fig. 29), double-rooted teeth increasing in size distally, with M₁-M₃ possessing well-developed talonids; occlusal surfaces are strongly worn, with M₁ and dP₅ exhibiting extreme wear. The transverse crest shows a steep lateral wear gradient where the lingual cusps are higher and sharper than the buccal cusps.

dP₅ is the smallest and the highest of all molariform teeth; it is heavily worn; the metalophid (connecting the protoconid and metaconid) is wider and longer than the hypolophid (connecting the hypoconid and entoconid); the crista obliqua is absent, and there are no signs of hypoconulids; a posterior facet on the crown fits against the front wall of M₁.

On M₁ the metalophid is longer and narrower than the hypolophid and both are slightly separated from each other by a crista obliqua that is only 1 mm in length. M₂ is smaller than M₃ and larger than M₁ and dP₅; the metaconid and entoconid are well preserved on M₂, the crista obliqua extends for 3 mm between the metalophid and hypolophid exposing two lakes of dentine; the hypolophid is obscured by wear. M₁ and M₂ have no hypoconulids, instead they have a prominent posterior cingulid or 'distocristid.' M₃ is partially preserved on both sides and is the largest in the series; the hypoconulid is small, low and prominent, consisting of a sharp cusp; the metalophid is larger than the hypolophid; the crista obliqua is broken on both sides; interlophids (intervalleys) are narrow and shallow.

Vertebrae

CGM 60551 (Figs. 33-35; Table 8) preserves the atlas, axis, centrum of the third cervical, the fifth cervical, and the centrum of the last cervical; the thoracic series includes 15 vertebrae arranged serially based on their size and the morphology of their capitular-tubercular facets. The fourteenth through sixteenth thoracic vertebrae are missing as are the lower-most thoracics, so the total number is unknown. The lumbar region is completely missing in the type specimen. What seems to be a sacral vertebra preserves a centrum, and has a broken transverse process bearing a rounded and robust medial crosssection. The tail is represented by a proximal vertebra with articular facets for the chevron bones on the ventral side of the centrum; the transverse processes are broad and extended horizontally. The end of the tail preserves two medially elongated centra, and the most posterior caudal preserved here has distinctively flattened anterior and posterior epiphyses. All vertebrae have their end plates fused to the centra. UM 101220 preserves an atlas that is identical to that

TABLE 8 — Measurements of vertebral elements of *Eotheroides clavigerum* sp. nov., CGM 60551 (holotype), from the Priabonian Birket Qarun Formation. Abbreviations: C, cervical vertebra; Ca, caudal vertebra; CH, centrum height; CL, centrum length; CW, centrum width; NCW, neural canal width; NCH, neural canal height; S, sacral vertebra; Th, thoracic vertebra; THT, total height; TW, total width; V, vertebra. Measurements are in mm.

V	THT	TW	CL	CW	CH	NCW	NCH
C1	68	116	22	—	—	38	41
C2	73	70	44	37	26	26	26
C3	—	—	14	39	31	—	—
C5	84	107	15	29	39	37	32
C7	—	—	18	41	27	33	—
Th1	123	108	28	35	27	42	27
Th2	120	100	31	36	25	31	23
Th3	116	100	35	42	27	21	20
Th4	122	94	38	42	30	21	19
Th5	121	90	40	46	33	23	15
Th6	—	93	42	41	34	—	—
Th7	—	86	47	49	39	20	16
Th8	123	87	45	36	40	21	16
Th9	120	87	45	51	36	20	15
Th10	—	86	47	53	40	20	16
Th11	—	85	47	56	35	—	14
Th12	118	91	41	48	39	17	16
Th13	—	79	49	59	36	19	10
Th14	—	—	—	—	—	—	—
Th15	—	—	—	—	—	—	—
Th16	—	—	—	—	—	—	—
Th17	126	82	50	59	43	21	13
Th18	—	—	48	56	41	—	—
Th19	—	—	—	—	—	—	—
S	—	—	36	67	42	—	—
Ca2	78	182	41	63	38	18	12
Ca16	27	67	24	37	27	—	—
Ca19	12	23	17	18	12	—	—

of CGM 60551, and a posterior caudal vertebra. In addition, UM 83903 contains five caudal vertebrae. The vertebral series in this taxon may include 7 cervicals, 19 thoracics, 4-6 lumbar, 1 sacral, and 22-24 caudal vertebrae.

Cervical vertebrae.— The atlas (Figs. 33-35; Table 8) has a robust, rugose edge, and knoblike transverse processes directed dorsolaterally. The dorsal arch bears a pyramid-like crowning protuberance. The articular facet for the odontoid process is smooth and tilted posteriorly as in *Eotheroides sandersi*, the cranial edge is slightly notched cranially, and its distal edge protrudes caudally for a distance longer than that in *Eotheroides sandersi*. Cranial cotyles are larger and more deeply concave than the caudal sides.

The axis (Figs. 33-35; Table 8) has a neural spine that is robust and swollen, and directed cranially. The neural canal is oval. The centrum has a semicircular outline caudally, bearing a keel on its ventral surface. The transverse processes are short, thin and directed posterolaterally; transverse foramina are unusually large, occupying most of the area of the transverse processes. The cotyles are relatively convex; the projecting odontoid

process is shorter than the centrum, and its ventral surface bears only the keel but no other structures.

C3 (Figs. 33-35; Table 8) lacks its neural arch; the centrum is short, craniocaudally flattened or compressed, and bears a keel ventrally; transverse processes are flanged and directed anteroventrally with their bases flattened horizontally. The transverse foramina are 6-8 mm in diameter.

C5 (Figs. 33-35; Table 8) bears a neural spine that has a pointed summit. The zygapophyseal articular surfaces face ventrally and dorsally. The centrum is marked by a short keel dorsally and it is smooth ventrally. The transverse foramina measure 14 × 12 mm. The transverse processes stand in the same plane as the centrum, however, their ventral sides (below the foramina) form a horizontal ventral lamina. This is prolonged caudally and bears a keel or a ridge on its ventral face. This distinguishes C5 from C6 in *Eotheroides*. C6 is not known for this species, however in *Eotheroides aegyptiacum* (Sickenberg, 1934: pl. 4, fig. 1) the ventral lamina bears a distinct low ridge inclined posteroventrally on its ventromedial surface.

C7 (Figs. 33-35; Table 8) has a centrum bearing the right transverse processes. The centrum is compressed craniocaudally but it is relatively longer than the anterior cervicals (excluding the axis), cranial and caudal outlines are rectangular in shape, the cranial articular surface is more flattened than its caudal counterpart. The dorsal keel is weak and there is no sign of a ventral keel. The transverse processes project anterolaterally; these are robust with ventrolateral knob-like processes. The transverse foramen is open in the form of a deep notch. Demifacets for first ribs are present at the lateroventral end of the caudal articulation surface.

Thoracic vertebrae.— Th1 (Figs. 33-35; Table 8) is the tallest and widest of all thoracics. The neural spine is widest anteroposteriorly just above the neural canal. The anterior edge is slightly sharp at its lower third, blunt dorsally, and flat at the top. The posterior surface is concave anteriorly with a lateral edge forming a thin wall to enclose the anterior edge of the spinous process of the following vertebra. The neural canal is semicircular, enlarged and widened. It is the largest neural canal posterior to C7, and caudally it is subcircular, with width exceeding height. Transverse processes are stout and short, and bear articular facets for rib tuberculi on their ventrolateral corners. Prezygapophyses are 45 mm distant from each other, slightly straight, and shallow; postzygapophyses are partially preserved, flat, and meet along median line forming an angle of 150°. The base of the neural arch (pedicle) is massive and robust on both sides. The centrum is almost twice as long as the last cervical, width is twice the height and length, and caudal and cranial articular surfaces are flattened and fused to the body. The dorsal surface of the centrum is flat cranially and slightly elevated, 2-3 mm, caudally; the ventral surface lacks any pillar or keel; rib capitular articulations form small cups that are deep.

Th2 (Figs. 33-35; Table 8) has a cranially-convex spinous process, with the longest spine (anteroposteriorly) in the vertebral series. The anterior edge is blunt, with an extended dorsal surface longer than that of Th1. The anterior edge curves backward slightly in lateral view. The posterior surface of the neural spine extends around the anterior edge of the spinous process

of Th3. The neural spine is fusiform, convex, and expanded laterally at its base. Prezygapophyses are 35 mm distant from each other and asymmetrical, with the left side deeper and more flattened than the right. The postzygapophyses are more or less flat, and separated from each other by a median groove. The neural canal is narrower than the preceding counterpart (Th1), and larger than that of the following vertebra (Th3). The neural canal has a more or less triangular cross section cranially but it is more rounded caudally. Transverse processes are more rounded and shorter than those of Th1, and the tubercular demifacets for rib articulation are more laterally positioned, larger, and more circular than those of Th1. The centrum is slightly eroded and a bit longer than that on the first thoracic. End plates are firmly fused to the centrum body. The posterior articular surface is wider laterally and shorter dorsoventrally than the cranial face. The ventral surface is gently concave downward but not forming an arch. Capitular articulations for ribs are larger and deeper on the caudal surface.

Th3 and Th4 (Figs. 33-35; Table 8) have massive spinous processes that are directed backward. These are more robust but shorter anteroposteriorly than the neural spine of Th2. Transverse processes are elevated above the dorsal surface of the centrum. These are shorter, rounded, and more massive than those on more anterior vertebrae. Prezygapophyses are close to each other, symmetrical, deep laterally, and elevated medially. Postzygapophyses are slightly tilted from the midline, sloping more ventrolaterally, and notably separated by a groove that is slightly wider than the groove on Th2. The neural canal is smaller and more rounded than those of Th1 and Th2. Epiphyses are firmly fused to the centrum. The anterior surface of the centrum is convex, while the posterior surface is concave.

Th5 and Th6 (Figs. 33-35; Table 8) bear heavy, massive spinous processes. The transverse processes are more elevated, more massive, and more curved dorsally. The neural canal is small, as in Th4. Centra are larger and widen caudally; their dorsal surface lacks any ridges; and epiphyses are fused to the centrum. Ventrally they show slight convexity. A vascular foramen is small and preserved on the right side only.

Th7 through Th9 (Figs. 33-35; Table 8) have their spinous processes shorter, less curved backward, and less robust, with a sharper anterior edge than in preceding thoracics. Cranial epiphyses are flattened, enlarged, and slightly concave; caudal epiphyses are heart-shaped because of a depression on the dorsal surface of the centrum and extension of the rib facet more laterally. The ventral surface of these centra is slightly concave, however at Th8 a ventral torus is developed that is more pronounced.

Th10 through Th12 (Figs. 33-35; Table 8) possess spinous processes that are thinner and shorter anteroposteriorly. The neural canals are smaller and wider than they are high. Anterior and posterior epiphyses are heart shaped. The pre- and postzygapophyses are longer and more curved rather than flat. The postzygapophyses diverge laterally from the midline. Rib demifacets are smaller and shallower, signaling the shift of rib articular facets toward the center of the centrum.

Th13 (Figs. 33-35; Table 8) is partially preserved, but it has both rib capitular and tubercular articular surfaces confluent with the transverse process.

Th17 and Th18 (Figs. 33-35; Table 8) are almost identical. However the spinous process of Th18 is more flattened, larger, and more compressed mediolaterally than that of Th17. It also has sharper anterior and posterior edges. Prezygapophyses protrude more cranially and are closer to each other than those of more anterior vertebrae. In addition, the prezygapophyses have their articular facets inclined dorsomedially about 45°. Capitular and tubercular articular surfaces for ribs are confluent and form one open shallow socket divided equally between the top of the centrum and the base of the neural arch. The centra are heart-shaped in outline and strongly biconcave toward the center. The ventral surface bears a narrow torus directed anteroposteriorly, and lateral to the torus two vascular foramina open laterally. Vertebral epiphyses are strongly fused to the centrum, and both are concave caudally.

There were probably one or two more thoracic vertebrae following Th18, since the capitular and tubercular articular surfaces are not completely closed, nor are they developed into a short transverse process.

Sacral vertebrae.— The sacrum (Figs. 33-35; Table 8) is a single, partially preserved vertebra that is missing its neural arch and transverse processes; the bases of the transverse processes have rounded cross sections on both sides of the centrum. The sacral vertebra is short craniocaudally and has wide epiphyses. It is reduced in height, and its ventral surface is concave, lacking any keel or ridges.

Caudal vertebrae.— The caudal region (Figs. 33-35; Table 8) is represented by three vertebrae. The size and morphology of the largest of these make it a strong candidate for the second (Ca2) or third (Ca3) caudal vertebra. Both transverse processes are straight, horizontal, and flattened; the neural arch and postzygapophyses are very reduced compared to the anterior vertebrae of the trunk. Prezygapophyses are missing. The neural canal is narrow and dorsoventrally compressed caudally. The centrum has a hexagonal outline. Its epiphyses are fused to the centrum and partly eroded, and these are flat cranially and concave caudally. Demifacets for both anterior and posterior chevrons are preserved on the ventral surface.

The remaining two caudals are from the distal end and were assigned to ?Ca16 and ?Ca19. Both are almost certainly positioned in the fluke beyond the peduncle since they have greatly diminished transverse processes and also because they are compressed dorsoventrally, lack neural arches, and lack articulations on their ventral surfaces.

The more anterior caudal vertebra (?Ca16) has very short transverse processes close to the centrum, directed and tapering posteriorly. The centrum has a larger epiphysis anteriorly than posteriorly; and the cranial and caudal ends of the dorsal surface along the midline are slightly elevated. The ventral sides of the transverse processes are truncated by a pair of shallow grooves, one on each side. These grooves probably served as an attachment for the sacrococcygeus ventralis tendons. The extreme distal vertebra (?Ca19) is asymmetrical and very small. It is biconvex anteroposteriorly and dorsoventrally. The dorsal surface bears a fine keel, while there are laterally remains of diminutive transverse processes. Anterior and posterior articular

areas are oval in shape. This is not the last vertebra in the tail since it has a concave caudal epiphysis.

UM 83903 consists of five associated caudal vertebrae, comparable in size to those above. The centra have distinct, sharp, dorsal and ventral midline keels. Thin epiphyses, tightly connected to the centra, are clearly visible. In the two most anterior vertebrae, the ventral sides are nearly flat, and the transverse processes are only slightly elevated above this level.

CGM 42287 is a series of six somewhat eroded vertebrae from the anterior caudal region. The largest, and presumably most anterior of these (probably Ca2), bears on its underside what may be traces of chevron facets on the rear edge only. The ventral side of the centrum is almost flat, with only a very faint median keel. This gives the centrum a distinctly trapezoidal shape in posterior view. The undersides of the transverse processes are in almost the same plane as the centrum, as in the sacral and caudals described for UM 97514. The centrum is 61 mm wide, 40 mm high, and 43 mm thick; the neural canal was about 23 mm wide. The other caudals all exhibit small demifacets for chevrons both anteriorly and posteriorly. The transverse processes are gently inclined downward and backward. The fifth and best-preserved vertebra in the series had an estimated width across the transverse processes of 132 mm; the centrum measures about 56 mm wide, 42 mm high, and 38 mm thick. The neural canal is 16 mm wide.

Chevrons.— A few chevron bones were preserved with caudal vertebrae of CGM 60551. The anterior pairs are long dorsoventrally, short anteroposteriorly, and unfused at their distal end. The angle between the two bones in all chevrons is less than 30°. This is consistent craniocaudally.

Ribs

CGM 60551 has 19 rib pairs (Fig. 36; Table 9), of which 4 or 5 pairs were connected to the sternum. The last rib is extremely reduced and probably was fused to the last thoracic vertebra. All ribs, excluding the 19th, have well developed capitular facets that connect directly to the corresponding articular surface on the centrum.

The first rib (R1) is well preserved from the left side of the ribcage, with considerable pachyosteosclerosis (Fig. 36; Table 9). R1 is missing on the right side. R1 articulates with C7 and Th1. It has a tapered distal end, not a truncated end as in other contemporaneous taxa including *Eotheroides sandersi*. The anterior capitular facet is rounded and is twice the size of the posterior facet. The neck is 20 mm long, cylindrical, and almost straight. The tubercular facet is level with the capitulum, forming a knoblike summit. The angle of downward deflection between the proximal end of the rib and the shaft is about 150°, and this angle has a distinctive flat and circular ligament attachment (the attachment is about 10 mm in diameter). There is considerable variation in thickness and cross-sectional area along the shaft of R1. The proximal end is oval in cross section, the midshaft is more or less triangular in cross section, and swollen laterally with a prominent ridge posteromedially. Just below the midshaft, the anterior edge bears a prominent anterior protuberance; just below this protuberance the distal end begins to flatten and taper toward the broken rugose end.

TABLE 9 — Measurements of left and right ribs of *Eootheroides clavigerum* sp. nov., CGM 60551 (holotype), from the Priabonian age Birket Qarun Formation. Abbreviations: *CM*, circumference around midshaft; *CT*, capitulum to tubercle length; *EAL*, external arc length; *IAL*, internal arc length; *L*, left rib; *MAWM*, maximum anteroposteriorly width of midshaft; *MLWM*, maximum mediolateral width at midshaft; *ND*, neck diameter; *R*, right rib; *TL*, total length. Measurements are in mm.

Rib	TL	EAL	IAL	CT	ND	CM	MLWM	MAWM
L1	158	240	160	45	26	112	37	34
L2	240	—	—	44	32	140	41	38
L3	243	370	275	53	33	154	55	40
L4	270	413	315	54	34	155	54	43
L5	—	—	—	54	35	140	42	46
L6	—	—	—	49	27	133	36	43
L7	315	457	205	52	27	130	35	45
L8	—	—	—	53	26	130	31	46
L9	330	451	385	55	24	118	30	45
L10	—	—	—	55	22	117	30	45
L11	—	—	—	—	19	—	—	—
L15	—	—	—	45	—	—	—	—
L16	—	—	—	37	28	—	—	—
L17	—	—	—	36	—	—	—	—
L18	220	230	225	32	28	65	—	—
R2	206	310	212	45	38	140	47	39
R3	241	365	273	49	38	159	53	43
R4	246	413	311	54	39	153	53	43
R5	284	—	345	58	36	143	45	42
R6	—	—	—	—	31	142	48	46
R7	328	452	381	58	32	133	35	44
R8	328	456	387	54	25	126	33	46
R9	330	452	399	52	23	121	32	46
R10	—	—	—	—	22	120	31	43
R11	335	430	393	52	22	117	30	41
R12	331	435	380	48	21	110	29	38
R13	325	430	370	45	24	108	26	40
R14	315	419	303	49	21	110	27	39
R15	—	—	—	42	21	108	23	36
R16	—	—	—	39	21	105	23	34
R17	—	—	—	36	19	93	21	33
R18	—	—	—	33	23	70	25	25

The second through fourth ribs (R2-R4) are well preserved on both sides, are banana-like in overall morphology (Fig. 36; Table 9), and show extreme pachyosteosclerosis. The second rib R2 is larger than R1, bearing prominent anterior and posterior capitular facets. The neck is almost straight, and more robust than the neck of R1. The tuberculum is very small and weak, followed by a small mediolaterally elongated depression or fossa. The angle is almost the same as that of R1, however the proximal mediolateral surface is broader and inclined dorsally, lowering the tangent of the surface to almost 45° with the mediolateral horizontal surface. The proximal cross section of the shaft is rounded, but this becomes more or less square just above midshaft. The midshaft is almost quadrate to trapezoidal in cross section. The distal third of the rib shows the greatest degree of swelling, with the widest cross section of the whole

rib. The tip of the lower third tapers abruptly to an apical point, forming a cone whose summit is the attachment area for the costal cartilage.

The third and fourth ribs (R3 and R4) are biconvex anteroposteriorly. They have more rounded and more robust heads and shafts than R2. The widest cross section is at midshaft. Capitular facets are rounded and are lower than the tubercular facets. The ventral surface of the head is broader and more straight mediolaterally than those in R1 and R2. The distal end tapers abruptly towards the apical area for the attachment of the costal cartilage.

The fifth and sixth ribs (R5 and R6) have more or less cylindrical shafts, that are rounded and uniform in cross-sectional area along most of the shaft. The distal end tapers gently towards the apical attachment area. The ventral faces of the neck and head are flattened and broad. Iliocostalis thoracic muscle attachment areas are large on both ribs. The end of the distal third of the shaft is compressed mediolaterally.

Ribs seven through fourteen (R7-R14) are compressed mediolaterally (Fig. 38; Table 9). The heads project horizontally and are reduced in length. The proximal end of the shaft has an oval cross section before becoming rounded distally. The lower third of the shaft is swollen. The distal end, which tapers toward the costal attachment region, is flattened and more compressed mediolaterally than those of the preceding ribs.

The posterior third of the ribcage (R15-R17) is partially preserved, represented by heads and/or proximal shafts of ribs (Fig. 36; Table 9). The heads are small, with broad ventral faces. The capitular and tubercular regions are almost confluent and are closer to each other in more posterior ribs. The cross section of the shaft is more or less circular.

Rib R18 is partially preserved on both sides. It is the shortest 'functional rib' at an estimated length of 220 mm. The head is straight and very reduced anteroposteriorly. The shaft is gracile and cylindrical; the distal end tapers very gently toward the apical attachment area and the cross section is oval. It is not clear whether the last thoracic vertebra (Th19), the 'prelumbal,' had a fused rib (Fig. 36; Table 9).

Forelimb

Scapula.— The right scapula of CGM 60551 (Fig. 37; Table 10) is well preserved but missing its acromion process. The scapula of UM 94806 is partially preserved, with a sandblasted and broken cranial and dorsal margin, and a missing acromion process. UM 97520 preserves the proximal part of the scapula, however the acromion and coracoid processes were not fused to the glenoid cavity and are missing.

The scapula of CGM 60551 is sickle-shaped, stout, and marked by a robust spinous process missing the acromion. The total length of the blade is 228 mm, and the maximum breadth of the dorsal portion across the spine is 76 mm. The spine is thick dorsoventrally, bearing rounded edges. At midshaft the spine is thinner but still blunt. The glenoid fossa is deeply concave anteroposteriorly, and shallowly concave transversely. It measures 51, 38, 29 mm in anteroposterior length, mediolateral breadth, and depth, respectively. The coracoid process is broken, but bears a well-defined oval muscle scar on its medial side. When

TABLE 10 — Scapula dimensions of *Eotheroides clavigerum* sp. nov., CGM 60551 (holotype) and UM 94806, from the Birket Qarun Formation, compared to scapulae of *Eotheroides sandersi* sp. nov., UM 111558, and *Protosiren smithae*, UM 101224, found in the same formation. Measurements are in mm.

Key	Measurement	<i>Eotheroides clavigerum</i> CGM 60551 (left scapula)	<i>Eotheroides clavigerum</i> UM 94806 (left scapula)	<i>Eotheroides sandersi</i> UM 111558 (left scapula)	<i>Protosiren smithae</i> UM 101224 (left scapula)
1	Scapular length along the spine	226	218	192	230
2	Spine length	137	118	106	144
3	Scapular breadth	76	—	65	78
4	Infraspinous fossa breadth	51	57	46	60
5	Neck breadth	46	40	34	44
6	Neck height	19	19	15	27
7	Distance from median glenoid cavity to acromion	30	36	29	31
8	Glenoid process breadth	51	52	43	56
9	Glenoid cavity breadth	38	43	34	43
10	Glenoid cavity height	29	30	26	34
11	Breadth of the acromion	—	—	6	11
12	Spine height from dorsal surface	—	—	21	34
13	Spine height from ventral surface	54	48	39	64
14	Distance between anterior tip of glenoid process and anterodorsal edge of blade	142	—	123	153
15	Distance between posterior tip of the glenoid process and first posterior edge of blade	99	—	85	89
16	Circumference of the blade	565	—	475	583

the scapula and humerus are articulated, this muscle scar lines up precisely with the bicapital groove. The supraspinous fossa is broad, with well defined cranial and superior angles. The supraspinous fossa is twice as large as the infraspinous fossa, which is narrow but gets larger toward the vertebral border. The subscapular fossa on the medial side of the blade is slightly concave.

In UM 94806 the maximum length of the blade is 218 mm, the width of the dorsal part of the blade (probably a little short of the actual width) is 65 mm; the width of the dorsal-most part, at the level of the sharp teres major protuberance, is 58 mm. Dorsally, the spine rises to a height (measured from the medial side of the scapula) of 26 mm; more ventrally it is reduced to a height of about 21 mm before rising again to more than 30 mm at the acromion, whose tip is missing. The spine is thickest dorsally (the remnant of a spinous tuber) and elsewhere is very thin, due in part to erosion. Except for a very faint ridge extending for about 2 cm parallel to the midsection of the spine, the infraspinous fossa bears no trace of the 'crista postscapularis' described by Sickenberg (1934: 28) in *Eotheroides aegyptiacum*. The glenoid fossa is similar to that in CGM 60551, but slightly wider transversely. The coracoid process is very small and bears the well-defined oval muscle scar on its medial side. The subscapular fossa is broader than that in CGM 60551.

Humerus.— The humerus of the holotype CGM 60551 (Fig. 37; Table 11) and the right humerus of UM 94806 are almost identical, although the latter is few mm longer. UM 94806 shows better preservation and more anatomical details because

the humerus in CGM 60551 has been partially damaged by gypsum mineralization. In UM 94806 the proximal epiphysis is partly fused to the shaft, but the suture is still conspicuous. The head is irregularly heart-shaped, being notched anteriorly at the top of the bicapital groove. The greater tubercle forms a thin but prominent flange, with a narrow surface for muscle attachment on its summit. The lesser tubercle has an irregular surface and forms the medial edge of a shallow bicapital groove. This groove continues proximally over a low threshold and ends in a shallow cul-de-sac on the bone's proximal surface, bounded posteriorly by the notched border of the head (cf. Sickenberg, 1934: fig. 4b). The deltoid crest, located some 70 mm from the summit of the greater tubercle, is distinct but small and thin in comparison to that of Neogene dugongids. An almost flat, rectangular surface separates it from the bicapital groove. Another 4.5 cm distally a slightly accentuated ridge marks the insertion of pectoralis major. A continuation of this ridge joins the medial edge of the trochlea. On the posterior side, a convex, somewhat spiral ridge (ectocondyloid crest) extends from the midshaft to the ectepicondyle. The parasagittal diameter of the humeral shaft (about 28 mm) greatly exceeds the transverse diameter (18 mm). The entepicondyle is very strong, protruding far posterior as well as distal to the trochlea. The coronoid fossa is distinct; the olecranon fossa is very deep. The axis of the trochlea is inclined about 85° to that of the shaft.

The only humerus of *Eotheroides aegyptiacum* hitherto described was an incomplete juvenile specimen (Sickenberg,

TABLE 11 — Measurements of humeri of *Eotheroides clavigerum* sp. nov., CGM 60551 (holotype) and UM 94806, compared to those of *Eotheroides sandersi* sp. nov., UM 111558 and *Protosiren smithae*, CGM 42292, collected from nearby localities in the Birket Qarun Formation in Wadi Al Hitan. Measurements are in mm.

Key	Measurement	<i>Eotheroides clavigerum</i> CGM 60551 (right humerus)	<i>Eotheroides clavigerum</i> UM 94806 (right humerus)	<i>Eotheroid sandersi</i> UM 111558 (left humerus)	<i>Protosiren smithae</i> CGM 42292 (left humerus)
1	Length (greater tubercle to distal end)	169	179	155	158
2	Length from the head to the distal end	159	164	142	155
3	Proximal end maximum breadth	59	56	51	57
4	Head height	16	18	17	26
5	Head length	42	43	36	45
6	Head width	36	39	31	37
7	Bicipital groove width	13	12	9	18
8	Maximum width of the shaft in the middle	37	29	23	23
9	Minimum width of the shaft in the middle	25	18	19	21
10	Minimum circumference of the shaft	97	76	70	70
11	Distal end maximum breadth	50	39	42	54
12	Trochlea breadth	34	27	31	31
13	Trochlea height	29	19	24	25
14	Trochlea height in the middle	18	11	18	16
15	Olecranial fossa width	18	23	20	21
16	Olecranial fossa height	20	21	28	23
17	Olecranial fossa depth	13	15	8	10

1934: p. 29-30). Apart from its smaller size, it closely resembles the humerus of UM 94806, but it is not clear how reliably these can be distinguished from humeri of *Protosiren fraasi*, which are also inadequately known (Sickenberg, 1934: 93-94). However, UM 94806 is clearly different from the humerus of *Protosiren smithae* described above. While these bones are almost exactly the same size and have the same general appearance and proportions, UM 94806 is distinguished by possession of the cul-de-sac on the proximal end, a more mediolaterally compressed shaft, a prominent ectepicondylar crest, a smaller trochlea, and a much more posteromedially salient and mediolaterally compressed entepicondyle.

Radius and ulna.— The right radius and ulna of CGM 60551 are very well preserved. They are fused together at their proximal and distal ends, leaving a 7-8 mm space between both shafts when seen in lateral view (Fig. 37; Tables 12, 13). The ulna is missing the top of the olecranon, making its end roughened and rugose; both radius and ulna are missing their distal epiphyses. The preserved length of the ulna is 145 mm, and the preserved length of the radius is 120 mm. The ulna and radius of this species are the longest among contemporaneous Fayum sirenians.

The ulna is slightly convex posteriorly. The olecranon is tilted backward 20°, and aligned coaxially with the main axis of the shaft. The olecranon rises 26 mm above the ulnar articular surface, and it is 35 mm long anteroposteriorly across its tuberosity.

Both ulnar (proximal) and radioulnar (distal) articular surfaces for articulation with the humerus are asymmetrical

and separated by a non-articular surface. The ulnar surface is strongly concave anteriorly. The ulnar notch is narrow at its proximal end (16 mm wide), while the radioulnar articulation measures 38 mm mediolaterally, making it the widest region of the shaft. The proximal radioulnar tuberosity, where both bones are fused, is triangular in shape, extends 26 mm distally (as measured medially), and extends 30 mm mediolaterally. Below the articular notch, the ulnar shaft is stout and robust; its medial surface measures 16 × 20 mm for its mediolateral and posterior diameters at the diaphysis, respectively, and 65 mm for circumference. The shaft of the ulna is wide distally, and is slightly projecting at its lowest posteromedial corner. The distal end is rectangular in shape with a rugose surface and an indented outline where the missing epiphysis used to fit.

The radius is slender and gracile; the dorsal surface of the head (the articular surface) is semicircular and divided into two regions, medial (small and shallow), and lateral (enlarged and deep). The neck is as wide as the head and bears the radial tuberosity. The shaft has a uniform ovoid cross section between the head and 15 mm above the distal end. The shaft of the radius is slightly convex posteriorly, and slightly compressed anteroposteriorly. Mediolateral and anteroposterior diameters at midshaft measure 19 and 12 mm, respectively, with a circumference of 55 mm. The groove for extensor tendons faces anteriorly and slightly laterally. It is shallow and the borders of the groove are thin and weak. These are thinner and less prominent than those found in *Protosiren smithae*. The distal epiphysis of the radius is missing, leaving a rugose surface for attachment, with a curved square outline that is more rounded posteromedially.

TABLE 12 — Ulna measurements of the Priabonian *Eotheroides clavigerum*, CGM 60551 (holotype), compared to ulnae of *Eotheroides sandersi*, UM 111558; *Eotheroides aegyptiacum*, SMNS St. XXX, from the Lutetian of the Mokattam Hills (illustrated in Sickenberg, 1934, page 30; pl. 4, Figs. 6 a-b); and *Protosiren smithae*, CGM 42292, from the Birket Qarun Formation. Measurements are in mm.

Key	Measurement	<i>Eotheroides clavigerum</i> CGM 60551 (right ulna)	<i>Eotheroides sandersi</i> UM 111558 (right ulna)	<i>Protosiren smithae</i> CGM 42292 (right ulna)	<i>Eotheroides aegyptiacum</i> SMNS St.XXX (right ulna)
1	Greatest length	146	136	138	—
2	Length of the olecranon	30	21	34	22
3	Smallest depth of olecranon	32	24	24	15
4	Greatest depth at the anconal process	35	26	29	13
5	Height of the trochlear notch	26	22	24	21
6	Breadth across the coronoid process	35	30	23	25
7	Height from the coronoid process to the distal epiphysis	110	98	94	—
8	Circumference of midshaft	61	50	56	—
9	Width of the distal epiphysis	21	16	16	—
10	Length of the distal epiphysis	29	24	28	—

TABLE 13 — Radius measurements of *Eotheroides clavigerum*, CGM 60551 (holotype), compared to those of an incomplete radius of *Eotheroides aegyptiacum*, SMNS St. XXX, from the Lutetian of the Mokattam hills (illustrated in Sickenberg, 1934, page 30; plate 4, Figs. 6 a-b); and *Protosiren smithae*, CGM 42292, from the Birket Qarun Formation. Measurements are in mm.

Key	Measurement	<i>Eotheroides clavigerum</i> CGM 60551 (right radius)	<i>Eotheroides aegyptiacum</i> SMNS St.XXX (right radius)	<i>Protosiren smithae</i> CGM 42292 (right radius)
1	Greatest length	120	—	95
2	Minimum length	112	—	92
3	Breadth of the proximal surface	28	9	26
4	Breadth across the humeral articular surface	24	8	22
5	Maximum width at mid shaft	19	8	21
6	Minimum width at mid shaft	12	6	20
7	Circumference of the mid shaft	55	—	49
8	Greatest breadth of the distal radial end	24	—	24
9	Breadth of the distal articular surface	22	—	23
10	Epiphysis height	—	—	—

Metacarpals and phalanges.— Identifiable hand bones of CGM 60551 (Fig. 38; Table 14) are all from the right side. These include metacarpals I, II, and III, and a proximal phalanx. All metacarpals have their proximal epiphyses fused as is typical for metacarpals, however only metacarpal III retained a solidly co-ossified distal epiphysis. The only phalanx is fairly well preserved, although it is missing its proximal epiphysis.

Metacarpal I is the shortest of all metacarpals in CGM 60551. Its proximal articular surface for articulation with the trapezium is triangular in shape. The shaft has an oval cross section. The shaft is slightly flattened in the dorsal plane while the ventral plane curves inward. The distal articular end, for articulation with the first phalanx, is larger and wider than the proximal end. The articular surface for articulation with metacarpal II is notched along a proximal posterior rugose surface.

Metacarpal II is distinctive in having the largest proximal and distal articular surfaces and the largest cross-sectional area

at midshaft. It may have an equal length to metacarpal III, if the distal epiphysis of metacarpal II had the same length as the distal epiphysis of metacarpal III. The carpal articular surface has a trapezoidal outline. Intermetacarpal facets for articulation with adjacent metacarpals are shallow and curved inward.

Metacarpal III has a slightly complicated proximal end that is compressed anteroposteriorly, and the carpal facet of the proximal articular surface is extended dorsoventrally. The intermetacarpal facets are grooved on both sides. The dorsal surface of the shaft of metacarpal III is flattened, while the ventral surface is slightly keeled. The midshaft is oval in cross section, and the distal epiphysis is wider than the proximal one.

The only preserved phalanx is most probably proximal phalanx I or II. It has an oval proximal end, with a dorsoventral height that exceeds its anteroposterior width. The dorsal plane of the shaft is slightly concave. The distal half of the shaft, including the distal epiphysis, is flattened. There is an elongated

TABLE 14 — Metacarpal and phalanx dimensions of *Eotheroides clavigerum* sp. nov., CGM 60551. Abbreviation: *Met*, metacarpal; *Phl*, phalanx. Measurements are in mm.

Measurement	Right Met I	Right Met II	Right Met III	Right Phl I
Total length	>43	>53	57	33
Proximal width	10	14	12	9
Distal width	13	19	17	11
Proximal height	16	15	15	11
Distal height	8	13	11	6
Midshaft width	9	11	10	7
Midshaft height	6	9	8	5

tuberosity along the distal edge. The distal articular surface is tightly fused to the end of the shaft. The articular facet is smooth and rectangular in shape.

Hind limb

Innomimates.— Both innomimates of CGM 60551 (Fig. 39; Table 15) are well preserved; the left side has better preservation since it was found covered in the original matrix, while the right side is partly sandblasted with an eroded ischium and minor damage in the ilium. The total length for the left side is 215 mm while the right side is 10 mm shorter (Fig. 39; Table 15).

The ilium is short (145 mm on the left side, and 128 on the right side) and massive, with an extreme swelling ('clubbing') on its proximal side, especially seen in lateral (external) view. The medial side of the ilium, where it contacts the auricular processes of the sacral vertebra (sacroiliac joint), is oval in

TABLE 15 — Measurements of left and right innominate of the holotype *Eotheroides clavigerum* sp. nov., CGM 60551 (holotype), compared to innominate measurements of *Eotheroides sandersi*, UM 97514, from the Birket Qarun Formation; *Eosiren libyca*, UM 101226, from the Qasr El Sagha Formation; and *Protosiren smithae*, CGM 42292 (holotype). Measurements are in mm.

Key	Measurement	<i>Eotheroide</i> <i>clavigerum</i> (holotype) CGM 60551 (right pelvis)	<i>Eotheroides</i> <i>sandersi</i> UM 97514 (left pelvis)	<i>Eosiren</i> <i>libyca</i> UM 101226 (right pelvis)	<i>Protosiren</i> <i>smithae</i> CGM 42292 (right pelvis)
1	Total length	205	186	197	250
2	Ilium length (acetabulum to proximal end)	128	107	119	165
3	Ilium dorsoventral diameter at midshaft	22	21	17	27
4	Ilium mediolateral diameter of at midshaft	20	20	18	18
5	Ilium circumference	75	65	49	81
6	Symphysis length	0	18	12	35
7	Pubic line length	74	75	29	56
8	Pubic ramus thickness in front of the obturator foramen	13	12	13	19
9	Pubic ramus thickness behind the obturator foramen	16	21	22	16
10	Acetabulum diameter	18	17	20	24
11	Acetabulum external diameter	21	23	24	30
12	Acetabulum depth	9	10	10	11
13	Obturator foramen length	4	8	5	28
14	Obturator foramen height	5	13	4	22
15	Ischium length from center of the acetabulum to distal end	84	91	105	105
16	Ischial ramus thickness dorsoventral	30	34	32	48
17	Ischial ramus thickness mediolaterally	9	11	12	10
18	Dorsoventral length of the distal end of the ischium	—	52	47	54
19	Mediolateral thickness of the distal end of the ischium	—	16	28	22
20	Distance between the inner posterior edge of the obturator foramen and the ischial tuberosity	82	94	86	73
21	Length of the sacral articulation surface with the sacrum (anteroposterior length of the oval articulation)	58	45	12	26
22	Height of the sacral articulation surface with the sacrum (dorsoventral height of the oval articulation)	46	33	16	14
23	Maximum height of the proximal end of the ilium dorsoventrally	52	33	17	40
24	Maximum width of the proximal end of the ilium mediolaterally	47	28	15	21

shape (52×44 mm as measured on the left side; representing anteroposterior length and dorsoventral height, respectively). It is concave, and is extremely rugose indicating strong attachment with the sacrum via ligaments and cartilage. Distal to the sacroiliac joint, the ilium narrows and becomes rounded. It is 23 mm in diameter at midshaft, and then gets broader again toward the acetabulum.

The acetabulum is rounded, 19 mm in diameter, and 9 mm deep. It is closed anterodorsally and posterodorsally, and is shallow and open ventrally. The acetabular notch is very weak, but still marked by a fine ridge in the lower third of the socket. The ischium is long, broad, and curved medially. It makes an angle of 160° with the long axis of the ilium, and 110° with the pubic bone. The ischium is 88 mm long as measured from the center of the acetabulum. The dorsoventral breadth is 33 mm midway between the acetabulum and the posteriormost edge of its tuberosity. The internal and external sides are smooth, except on its distalmost edge where it is slightly thickened, roughened, and striated. The pubis is short, gracile, and triangular in shape, with a pointed distal end lacking any pubic symphysis. Both pubic bones are cleft on both sides. The clefts intersect the ventral wall of the 5-mm-diameter obturator foramen.

Nothing is yet known of the hind limb distal to the innominates.

***Eotheroides sandersi*, sp. nov.**

Figures 40-64

Holotype.— CGM 42181, Cairo Geological Museum. This specimen is an association of cranial and postcranial elements (Figs. 40, 46, 54, 58, 62; Tables 16, 20, 23, 24, 27), including the skull roof (composed of nasals, frontals, parietals and supraoccipitalis), exoccipitals, sphenoid, parts of the right squamosal, mandibular symphysis, three thoracic vertebrae, five caudals, 16 ribs from the right side (missing the first and second ribs), left second rib, right scapula, left and right humeri, left innominate and right ilium, and both femora (missing epiphyses).

Type locality.— University of Michigan field locality, Wadi Al Hitan WH-230 (Figs. 4, 5; Table 2), some 75 km west of the city of Fayum, and 140 km southwest of Cairo. UTM grid coordinates for the holotype are zone 36N, 215294 m E, and 3247161 m N.

Type and referred specimens were collected from the lower and middle parts of the Birket Qarun Formation of Beadnell 1905 (Figs. 23, 24).

Age and distribution.— The lower part of the Birket Qarun Formation is equivalent to the upper Mokattam series, which is Priabonian in age (Gingerich, 1992). The species is known only from the Birket Qarun Formation of Wadi Al Hitan in the Western Desert of Egypt.

Diagnosis.— Small species of *Eotheroides*; enlarged infraorbital foramen (Fig. 42); slightly concave nasals (Fig. 41); nasals are slender and straight, running at an acute angle to the midline, with the posterior edge curved and rounded; dental formula 2.1.5.3/3.1.5.3.; alveolus for I^1 is for a small tusk; I^3 precedes the upper canine immediately, without a diastema;

posterior edge of palate extends a short distance behind M^3 ; middle part of the palate is broad and shallow; the palate has a shallow and slightly constricted dorsal rostral gutter between left and right P^1 . The atlas has squared transverse processes (Fig. 47) that extend laterally and are directed downward. The first rib is compressed anteroposteriorly in the middle of the shaft, and has a broad distal end (Fig. 55). The innominate has a short, swollen, and club-like ilium (Fig. 62). Innominates bear extremely long and narrow pubic bones (Fig. 63); ischia are robust and project laterally; the obturator foramen is larger than in any other Dugongidae.

Etymology.— Named after Dr. William J. Sanders of the University of Michigan for his contributions to the Cenozoic mammals of Africa, especially Tethytheres. Dr. Sanders prepared and also helped collect many of the sirenian fossils known from the Eocene of Egypt.

Referred specimens.— UM 94809, a skull roof including nasals, frontals, and the parts of the parietals (Fig. 43). Locality WH-79 (Figs. 4, 5; Table 2; UTM grid coordinates within zone 36N: 210909 m E and 3241668 m N), Priabonian, lower part of the Birket Qarun Formation.

UM 97514 (Figs. 50, 51, 53, 56, 63; Tables 19, 21, 27) includes a partial vertebral series (Th4-Th15, Th17, L2-L4, S, Ca1-Ca6, Ca8-Ca10, ?Ca16), the posterior two-thirds of the ribcage, and both innominates. Locality WH-110 (Figs. 4, 5; Table 2; UTM grid coordinates within zone 36N: 211562 m E and 3242250 m N); Priabonian, lower part of Birket Qarun Formation, friable sandstone layer just above the White Camp Layer (Gingerich 1992).

UM 97515, isolated ulna of a juvenile individual (Fig. 60, Table 25). Locality WH-117 (UTM grid coordinates within zone 36N: 214945 m E and 3242312 m N); Priabonian, lower part of Birket Qarun Formation.

UM 100138, partial left and right dentaries (Fig. 45), vertebrae, and ribs. Locality WH-180 (Figs. 4, 5; Table 2; UTM grid coordinates within zone 36N: 212541 m E and 3243088 m N), Priabonian, lower part of the Birket Qarun Formation.

UM 111558 (Figs. 41, 42, 44, 47, 48, 49, 51, 57, 59, 61, 64, 66, 78; Tables 16-19, 22-28) includes a cranium of an adult individual, missing its lower jaw. Preserved teeth with crowns include left and right M^{1-3} , P^{2-3} and C^1 . X-ray images show that all teeth are erupted. Postcranial elements include a partial vertebral series (C1, C5, Th2-Th16, Th18, L1, ?Ca5-Ca7, ?Ca12-Ca13, ?Ca16, and ?Ca19), 13 ribs from the right side (R1-R11 and R13, ?R17) and eight from left side, xiphisternum, left scapula and humerus, right ulna, metacarpal, and left femur missing its epiphyses. Locality WH-174 (Figs. 4, 5; Table 2; UTM grid coordinates within zone 36N: 212541 m E and 3243789 m N); Priabonian, middle part of Birket Qarun Formation, collected from the thick, fine-grained, gold-colored sandstone some seven meters above the White Camp Layer (Gingerich 1992).

Cranium

Premaxillae.— Both premaxillae are well preserved in UM 111558 (Fig. 41). The premaxillary length from the anterior tip of the symphyseal process to the posterior end of the premaxillary arm (nasal process), where it overlaps with the nasal and the

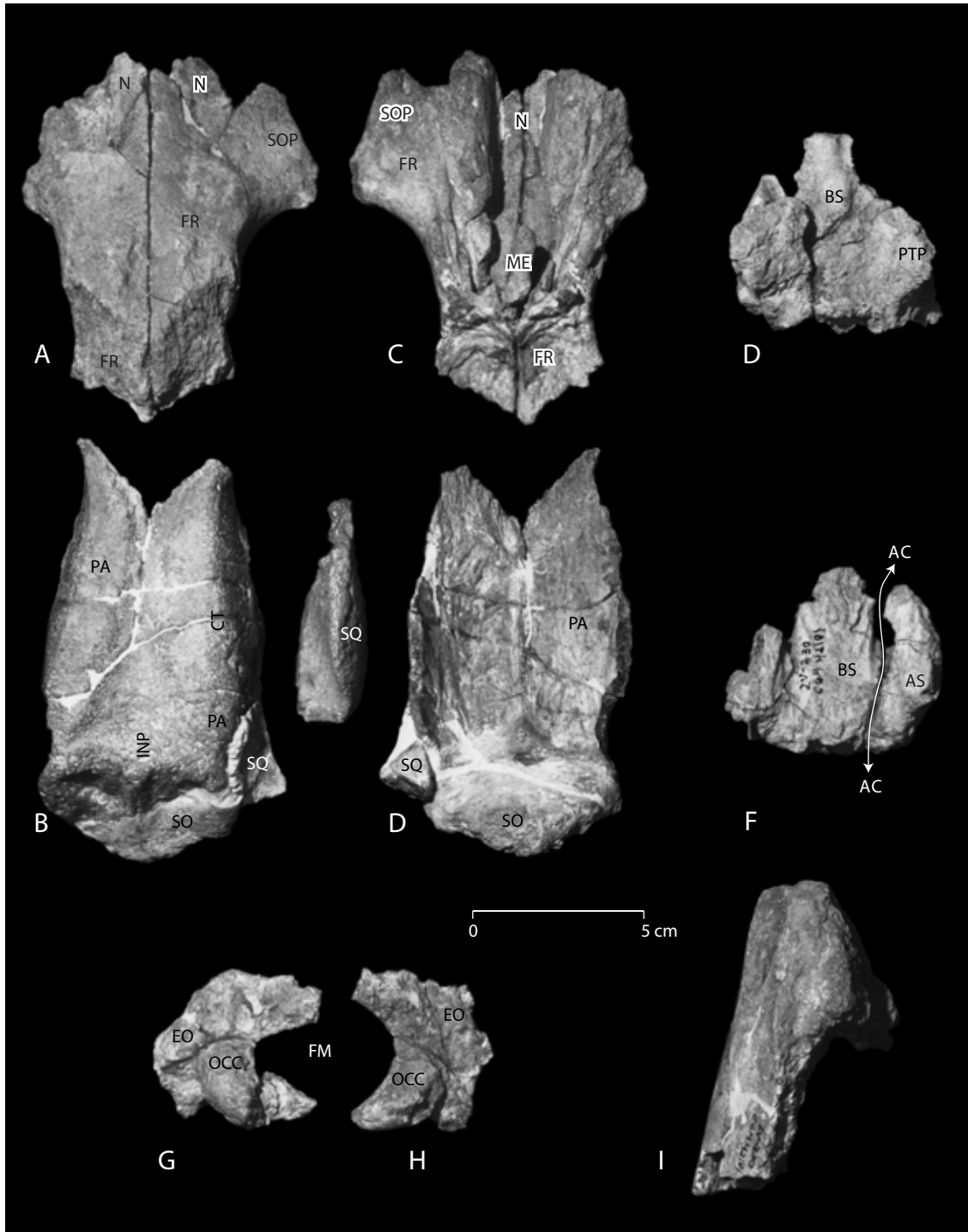


FIGURE 40 — Cranial elements of the holotype of *Eotheroides sandersi* (CGM 42181) from the Priabonian age Birket Qarun Formation of Wadi Al Hitan. A-B, dorsal views of the skull roof including nasal, frontal, parietals, supraoccipital, and portions of the right squamosal. C-D, ventral views of skull roof; note that the parietals and frontals were connected to each other along a deep V-shaped suture. E-F, dorsal and ventral views of the basisphenoid and presphenoid. G, dorsal view of the right squamosal process. H, exoccipitals in posterior view showing the occipital condyles and foramen magnum. I, dorsal view of mandibular symphysis of the lower jaw. Abbreviations: AC, alisphenoid canal (foramen); AS, alisphenoid; BS, basisphenoid; CT, temporal crest; E, ethmoid; EO, exoccipital; FM, foramen magnum; FPT, fossa pterygoidea; FR, frontal; INP, interparietal groove; ME, Mesethmoid; N, Nasal; OCC, occipital condyle; PA, parietal; PR, periotic; PT, pterygoid; PTP, pterygoid process; PS, presphenoid; SO, supraoccipital; SOP, supraorbital process; SQ, squamosal.

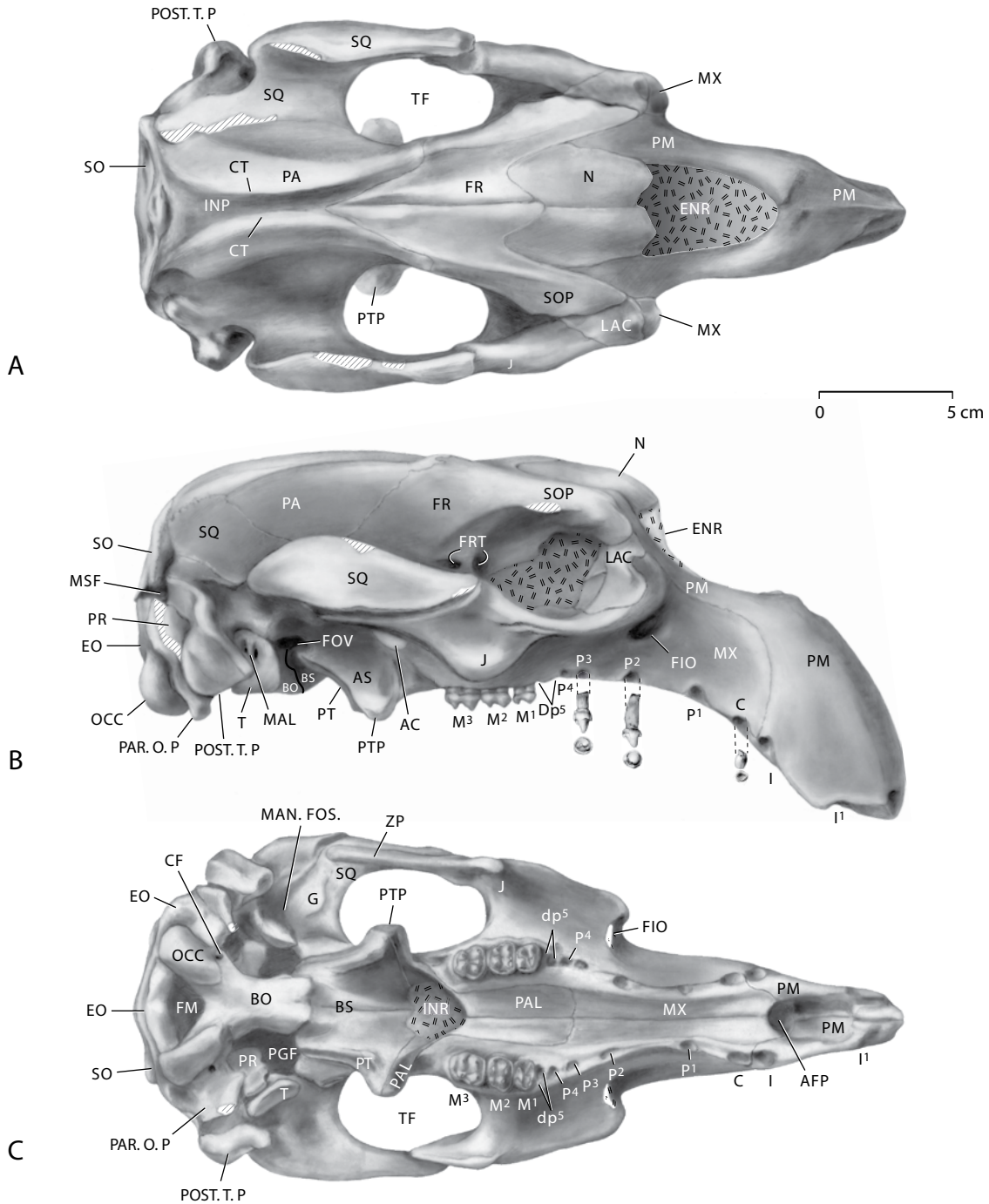


FIGURE 41 — Cranium of *Eotheroides sandersi* (UM 111558) from the Priabonian age Birket Qarun Formation of Wadi Al Hitan. A, dorsal view. B, lateral view. C, ventral view. Abbreviations: AC, alisphenoid canal (foramen); APF, anterior palatine foramen; AS, alisphenoid; BO, basioccipital; BS, basisphenoid; C¹, upper canine; CF, condyloid foramen; CT, temporal crest; dp^{alv.}, alveolar of deciduous premolar; E, ethmoid; ENR, external nares (mesorostral fossa); EO, exoccipital; FRT, foramen rotundum; FIO, foramen infraorbital; FM, foramen magnum; FOV, foramen ovalis; FPT, fossa pterygoidea; FR, frontal; G, glenoid articulation; I¹ etc., first upper incisor; INR, internal nares; INP, interparietal groove; J, jugal; LAC, lacrimal. M¹ etc., first upper molar or alveoli; MAL, Malleus; MAND. FOS., mandibular fossa; ME, Mesethmoid; MSF, mastoid foramen; MX, maxilla; N, Nasal; OCC, occipital condyle; P¹ etc., first upper premolar alveoli; PA, parietal; PAL, palatine; PAR. O. P., paroccipital processes; PGF, postglenoid fossa; PM, premaxilla; POST. T. P., posttympanic process; PR, periotic; PT, pterygoid; PTP, pterygoid process; PS, presphenoid; SO, supraoccipital; SOP, supra-orbital process; SQ, squamosal; T, tympanic; TF, temporal fossa; V, vomer; ZP, zygomatic process of the jugal.

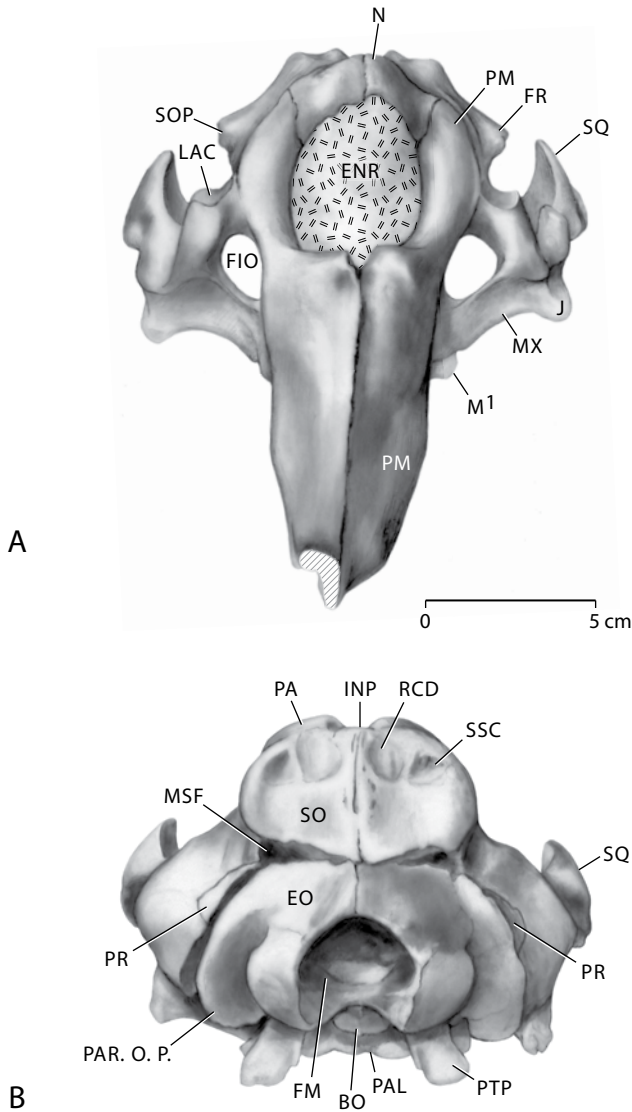


FIGURE 42 — Cranium of *Eotheroides sandersi* (UM 111558) from the Priabonian age Birket Qarun Formation of Wadi Al Hitan. A, anterior view. B, posterior view. Abbreviations: *BO*, basioccipital; *CT*, temporal crest; *ENR*, external nares (mesorostral fossa); *EO*, exoccipital; *FR*, foramen rotundum; *FIO*, foramen infraorbital; *FM*, foramen magnum; *FR*, frontal; *I¹* etc., first upper incisor; *INP*, interparietal groove; *J*, jugal; *LAC*, lacrimal; *M¹* etc., first upper molar or alveoli; *MSF*, mastoid foramen; *MX*, maxilla; *N*, nasal; *OCC*, occipital condyle; *P¹* etc., first upper premolar alveoli; *PA*, parietal; *PAL*, palatine; *PAR. O. P.*, paroccipital processes; *PGF*, postglenoid fossa; *PM*, premaxilla; *PR*, periotic; *RCD*, rectus semispinalis dorsalis; *SO*, supraoccipital; *SOP*, supraorbital process; *SQ*, squamosal; *SSC*, semispinalis capitata.

frontal, is 170 mm. The premaxilla-maxilla lateral contact is steep. At the tip of the rostrum is a pair of small and shallow alveoli that are filled with sand; tusks are absent and appear to have been diminutive based on alveolar diameter. Deflection of the masticating surface of rostrum from the occlusal plane is about 50°. Rostral length to the total length of the skull is about 1:3 (Table 16). The rostrum forms a dorsal keel that is very pronounced anteriorly and broadened posteriorly at the rear of the rostral suture. The nasal processes of the premaxillae (the premaxillary arms behind the rostrum) are relatively concave in lateral profile, with a length of 85 mm. These processes have sub-oval cross-sections, 7 mm in diameter. The posterior ends of the premaxillary processes are angular and pointed, and overlap the nasals and the frontal bones. The mesorostral fossae each have an oval outline anteriorly, truncated by the nasals posteriorly.

Nasals.— Nasals (Figs. 40-43) are slightly concave upward, rising at the level of frontals and parietals. The nasals are long and contact along the midline, with their posterior lobes separated by the frontals.

Dorsally, the nasal is exposed on the skull roof for a distance ranging from 50 mm (in UM 94809) to 59 mm (in UM 111558; Table 16); the ratio of the maximum breadth of both nasals to their anteroposterior axis is 0.83 (Table 16). The nasals form a forwardly-pointing medial projection, on either side of which a V-shaped indentation of the anterior nasal margin intervenes between the midline and the premaxilla. The dorsomedial margin of the nasal is prolonged into a flange to meet its opposite side in a suture that is 29 mm long ventrally (measured in UM 94809), and 40 mm long dorsally. The sutural surface bears posteroventrally-inclined interdigitations.

In the holotype (CGM 42181; Fig. 40), the nasals are broken anteriorly but are large, separated posteriorly by frontal internasal processes about 25 mm long, and form a high arch over the nasal cavity. Between the bodies of the nasals, the nasal cavity is 16 mm wide

Lacrimals.— The lacrimals are relatively large (Figs. 41, 42), slightly exposed laterally with a prominent knob, and lack a lacrimal foramen. The lacrimals are bounded by the supraorbital process of the frontals, premaxillae, maxillae, and jugals.

Frontals.— In CGM 42181 (Fig. 40), the frontal roof is convex, with a median trough on its posterior half that is bordered by a pair of low ridges. The lateral edges of the broadly-convex temporal crests are closest together just behind the frontoparietal suture, and are separated medially by about 10 mm. The frontals form the flat part of the skull roof just behind the concave nasals. The lateral walls of the frontals are narrow especially below the frontal-parietal suture. Medial and anterior processes of the frontals surround and separate the posterodorsal corners of each nasal. At this point, the frontals are at least 7 mm thick (CGM 42181), and cover the posterior part of the nasal cavity.

The ratio of the maximum breadth across the supraorbital processes to the maximum length of the frontals at their longest points (exposed dorsally along the midline), where the frontal meets the parietals posteriorly, is calculated to be 0.86 and 0.70 in CGM 42181 and UM 111558, respectively (Table 16). The supraorbital processes are thin dorsoventrally, and intersect the

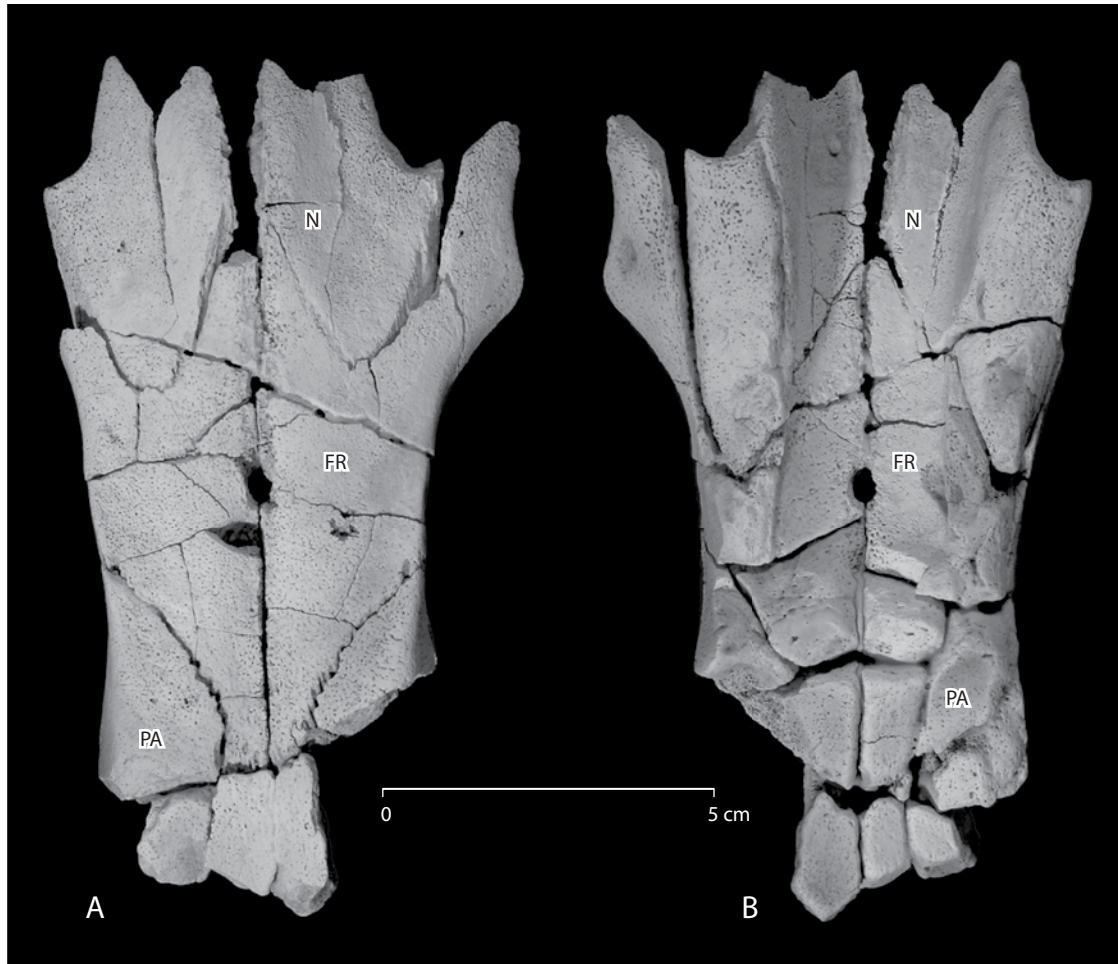


FIGURE 43 — *Eotheroides sandersi* skull roof of (UM 94809) from the Priabonian age Birket Qarun Formation of Wadi Al Hitan. Skull roof is shown in dorsal view A, and ventral view B. Abbreviations: FR, frontal; N, Nasal; PA, parietal.

mid-line at a 30° angle. The crista temporalis is weak on each side of the frontal (Figs. 40-42). The posterior dorsolateral contact between the frontals and parietals is marked by a pair of prominences appearing only in UM 111558 (Fig. 41).

UM 100184 (not illustrated) includes the thick and dense posterior part of the frontals and anterior parts of the parietals of a small sirenian. The frontal portion has a flat roof and is square in cross-section; the parietal is slightly more trapezoidal in cross section due to rounding of the temporal crests. The temporal crests begin at the anterolateral corners of the parietal roof, converge posteriorly, and are separated by a furrow only five mm wide where the bone is broken. The medial edges of the crests are steep and distinct, the lateral surfaces are gently rounded and continuous with the squamosal surface. The parietal roof is 16 mm thick along the midline where it is broken. The width of the roof at the frontoparietal suture is 34 mm. The suture

is V-shaped dorsally and broadly V-shaped on the endocranial surface. The interfrontal suture is 22 mm long endocranially. The bony falx is either broken or eroded along the 10 mm of the preserved frontoparietal suture.

Parietals.— These bones are narrow and elongated dorsally in all specimens (Figs. 40-43). They each have a thick crista temporalis that curves to produce a deep and narrow interparietal groove. The minimum separation between both cristae is 14 mm in UM 111558. The squamosals overhang and slightly indent the temporal crest in all cases, but the squamosals are not exposed dorsally.

The skull roofs of UM 94809 and UM 100184 have only fragments of their parietal portions; these form the usual V-shaped suture with the frontals. The skull roof where this suture intersects is very narrow, especially in UM 100184, and the thickness of the parietal roof in the anterior midline is less

TABLE 16 — Measurements of crania of *Eotheroides sandersi* sp. nov., CGM 42181 (holotype) and UM 111558 collected from the Priabonian of the Birket Qarun Formation, compared to cranial measurements of *Eotheroides aegyptiacum* of Sickenberg (1934), SMNS St. III, from the Lutetian of the Mokattam Hills. Measurements are in mm.

Abbr.	Measurement	<i>Eotheroide sandersi</i> CGM 42181	<i>Eotheroides sandersi</i> UM 111558	<i>Eotheroides aegyptiacum</i> SMNS St. III
AB	Condylobasal length	—	309	—
ab	Height of jugal below orbit	—	37	—
AH	length of premaxillary symphysis	—	97	—
BI	Rear of occipital condyles to the anterior end of interfrontal suture	—	194	180
CC'	Zygomatic breadth	—	142	—
cc'	Breadth across exoccipitals	90	95	72
de	Top of supraoccipital to ventral sides of occipital condyles	—	92	79
F	Length of frontals, level of tips of supraorbital processes of frontoparietal suture	89	120	85
FF'	Breadth across supraorbital processes	92	82	89
ff'	Breadth across occipital condyles	68	65	54
GG'	Breadth of cranium at frontoparietal suture	48	50	49
gg'	Width of foramen magnum	35	32	26
HI	Length of mesorostral fossa	22	69	—
hi	Height of foramen magnum	—	25	26
JJ'	Width of mesorostral fossa	—	37	—
KL	Maximum height of rostrum	—	56	—
MM'	Posterior breadth of rostral masticating surface	—	42	—
no	Anteroposterior length of zygomatic-orbital bridge of maxilla	—	53	52
OP	Length of zygomatic process of squamosal	—	88	—
OT	Anterior tip of zygomatic process to rear edge of squamosal below mastoid foramen	—	117	—
P	Length of parietals, frontoparietal suture to rear of external occipital protuberance	79	56	78
Pq	Length of the alveoli tooth row (Dp5-M3)	—	44	42
QR	Anteroposterior length of zygomatic process of squamosal	—	35	34
rr'	Maximum width between labial edges of left and right alveoli across M ¹	—	59	57
ST	Length of cranial portion of squamosal	—	57	—
ss'	Breadth across sigmoid ridges of squamosals	—	126	106
tt'	Anterior breadth of rostral masticating surface	—	25	—
UV	Height of posterior part of cranial portion of squamosal	—	77	72
WX	Dorsoventral breadth of zygomatic process	33	34	—
yy'	Maximum width between pterygoid processes	—	41	29
YZ	Length of jugal	87+	133	—
LFr	Length of frontals in midline	—	88	57
Hso	Height of supraoccipital	45	50	41
Wso	Width of supraoccipital	48	68	55
HIF	Height of infraorbital foramen	—	30	20
WIF	Width of infraorbital foramen	—	20	11
RD	Deflection of masticating surface of rostrum from occlusal plane (Degrees)	—	49	—

than 15 mm. In CGM 42181 the bony falx, internal occipital protuberance, and tentorium are all prominent.

Supraoccipital.— The supraoccipital of the holotype, CGM 42181 (Fig. 40), is 12 mm thick at the posterior end of midline, 43 mm thick along the midline slope posteriorly, and 57 mm wide. In UM 111558 (Figs. 41-42) the supraoccipital is very well preserved, and is detached from the exoccipital as in the holotype. The supraoccipital of UM 111558 has a relatively flat posterior surface, and a hexagonal outline. The nuchal planum is bipartite, with a weak median ridge that is most prominent

dorsally and fades out ventrally. This ridge separates concavities for rectus capitis dorsalis muscle insertions. Lateral to the rectus capitis dorsalis muscle insertions are sites for insertions of capitis semispinalis, which are smaller and closer to the stout lateral borders of the supraoccipital. The anterolateral portion of the supraoccipital is partly fused with the dorsal processes of the squamosals. The nuchal ridge (a crest in *Protosiren*) is semicircular in shape, curved laterally, and lacks rugosities. The parietal-supraoccipital angle is 120°, and the posterior surface of the supraoccipital itself is broadly V-shaped. The anterior

top of the exoccipital and the posterior end of the parietals bear an emissary foramen, in some cases closed due to fusion, which pierces the external occipital protuberance close to the midline and leads into the transverse sulcus.

Exoccipitals.— The exoccipitals (Figs. 41-42) are well preserved and connected along a 15 mm median suture, so that the foramen magnum is separated from the supraoccipital. The ratio of maximum exoccipital height to maximum breadth is 0.49. The supraoccipital-exoccipital sutures form a V-shaped angle of 130° in UM 111558. The dorsolateral edges of the exoccipitals are thickened and flanged laterally, providing room for the mastoid foramen. The foramen magnum is 24 mm high and 32 mm wide. Occipital condyles are large and kidney-shaped, and greatly separated at their bases in the holotype. Left and right hypoglossal foramina are located anteroventral to the occipital condyles and are 45 mm distant from each other. The paroccipital processes extend more ventrally than the occipital condyles. The paroccipital processes are 8 mm below the base of the occipital condyles, and are 12 mm distant from them ventrally; these processes are very well developed and prominent.

The exoccipitals are badly eroded in CGM 42181 (Fig. 40), but share a common median suture about 10 mm long. The ratio of their maximum height to maximum breadth is 0.49. The supraoccipital-exoccipital suture forms an angle of 132° in CGM 42181.

Basioccipital.— The basioccipital is well preserved and completely detached from the basisphenoid in UM 111558 (Figs. 41-42). It measures 43 mm along its ventral length (from the base of the foramen magnum to the line of fusion with the basisphenoid), and 18 mm across its waisted body. The anterior edge is more elevated than the posterior edge. Longus capitis muscles appear to have been weak and asymmetric.

Basisphenoid and presphenoid.— The basisphenoid and presphenoid are fused together to form a gentle arch similar to that in CGM 60551. The basisphenoid is wide at the pterygoid process (Figs. 40-41). Cranial and posterior contacts of the presphenoid are not defined since the internal nares are covered by cemented sediment.

Orbitosphenoid.— The orbitosphenoid is well preserved, with all foramina open from bottom to top: the alisphenoid opening, optic canal in the middle, and foramen rotundum at top (Fig. 41). The alisphenoid opening (a canal in primitive sirenians, including protosirenids but not *Eotheroides* or *Eosiren*) extends anteroposteriorly for about 30 mm inside the cerebral chamber as a shallow groove, and ends opening into the pterygoid fossa; the anterior opening is connected with a downwardly directed groove for the external pterygoid muscles. The optic foramen is 7 mm in diameter; it enters the orbitosphenoid and passes through to the anterolateral portion of the cerebral chamber. The foramen rotundum is open at the dorsolateral corner of the orbitosphenoid and enters the cerebral chamber medial to the ethmoidal region.

Alisphenoids.— Both alisphenoids are well preserved in UM 111558 (Fig. 41). The alisphenoids are 68 mm high, and 67 mm distant from each other where they join the basisphenoid in *Eotheroides sandersi*. However, they are shorter than the

alisphenoids in *E. clavigerum*. The squamosals, parietals, and frontals contact the alisphenoids dorsally, and the squamosals contact the alisphenoids dorsolaterally. On each side, the alisphenoid is strongly fused with the palatine and the pterygoid, and covers the posterior wing of the palatine while the pterygoid covers its posteromedial surface. An alisphenoid canal is absent as such; instead, the alisphenoid foramen, about 11 mm in diameter in UM 111558, opens posteriorly, coming directly from the base of the braincase.

Pterygoids.— In the holotype, the pterygoids are damaged (Fig. 40); however, UM 111558 preserves pterygoids on both sides, with distinct processes and deeply grooved posterior trochlear surfaces (Figs. 41, 42). The pterygoids are completely fused to the surrounding elements, as in other dugongs.

Palatines.— The palatines are flat in UM 111558 (Fig. 41), narrowest posterior to M³, and slightly wider where they contact the maxilla anteriorly, just 10 mm behind the anterior opening of the infraorbital foramen. The posteroventral edge of each palatine is strongly concave at the posteroventral edge of the internal nares. The posterolateral walls of the palatines extend behind M³ to contact the pterygoid.

Maxillae.— Maxillae are very well preserved in UM 111558 (Figs. 41-42). Molar teeth (M¹⁻³), alveoli for a triple rooted dP⁵, and single-rooted alveoli for P⁴ through C¹ are clear. The atrophied portion of the bone behind M³ is short. The orbital bridge (zygomatic bridge), which provides the ventral and mediolateral cover for the infraorbital foramen, is about 53 mm long in UM 111558. The infraorbital foramen extends ventrally from the vicinity of M² to the posterior edge of the P² alveolus. The infraorbital foramen is sub-oval and opens anteriorly, with width and height of about 20 mm × 21 mm in UM 111558. The depth of the zygomatic bridge above the alveolar shelf of M¹ is about 20 mm in UM 111558. Ventrally, the maxillae and the palatines form a narrow palate with its widest breadth across the anterior edge of M² in UM 111558. The maxilla is smoothly deflected about 30° downward from the horizontal palate at the narrowest point of the rostrum, at the beginning of the ventral gutter across P¹, where the palatal surfaces are closest to each other in UM 111558.

Squamosals.— The dorsal ends of the squamosals (Figs. 40-42) overhang the posterolateral corner of the parietal roof on each side. Its indentations are just 5 mm from the temporal crest. Mastoid foramina open on both posterior surfaces (Figs. 41, 42). The zygomatic process in UM 111558 is 86 mm long and 32 mm wide dorsoventrally; its root is 36 mm long anteroposteriorly. It is roughly lozenge-shaped in lateral view, with a nearly straight posterodorsal edge that is very slightly convex laterally as in CGM 60551. The rear edge of the zygomatic root is notched, with a distinct processus retroversus. This process is well-developed and slightly inflected (Fig. 41). The anterior end tapers somewhat without reaching the level of the posterior end of the supraorbital processes (Fig. 41). The anterodorsal edge is distinctly concave in outline. Ventrally, the mandibular fossa, entoglenoid bar, and temporozygomatic suture are shallow and slightly pronounced (Fig. 41). These are shallower and less pronounced than those in CGM 60551, holotype of *Eotheroides clavigerum*.

The postglenoid process is knoblike and raised 11 mm above the mandibular fossa. There is an arcuate external auditory meatus, 9 mm in anterolateral length and about 8 mm in mediolateral diameter, between the post-tympanic process and the postglenoid process (Fig. 41). The posterior wall of the external auditory meatus, formed by the post-tympanic process, extends deeper ventrally than the anterior surface formed by the posterior edge of the postglenoid process. The post-tympanic process is enlarged and ends with a projecting facet for insertion of the sternomastoid muscle: a primitive feature according to Domning (1994). A sigmoidal ridge is present but weak in UM 111558.

Jugals.— The jugals are complete and 133 mm long in UM 111558 (Figs. 41, 42). The preorbital process of the jugal is thin and applied against the maxillae. It is isolated from the premaxilla. The deepest point of the jugal, the ventral process, has a smooth, curved surface with a rounded, knoblike, mediolaterally-compressed projection, and it lies directly beneath the lower postorbital process and above the maxillary shelf. The postorbital process is a blunt projection that lies against the anterior tip of the zygomatic process of the squamosal. The posterior (zygomatic) process of the jugal is slender and oval in cross-section, complete at its tip in UM 111558. It reaches a little behind the edge of the temporal fossa (Figs. 41, 42).

Periotics.— The petrotympanic bone (Fig. 44) is well preserved in UM 111558, and it is not fused to any of the skull bones (Fig. 44); however, it fits into a socket formed by the posteromedial wall of the squamosal and by the exoccipital. The squamosal covers the lateral and dorsolateral portions of pars mastoideus, leaving the posterolateral corner (processus fonticulus) exposed. The exoccipital covers the periotic posteroventrally and partially posteromedially. The ectotympanic ring is directed anteroposteriorly (Fig. 44); it is dense, flat, and thin ventromedially. The tympanic ring has a length of 22 mm, a maximum height 30 mm, and an internal diameter of 10 mm. The malleus is well preserved; it is small, cone-like, stout, rounded at the narrow base, and pointed at the top. The manubrium mallei appears as a distinct ridge on the malleus that reaches the sulcus tympanicus. The processus folianus (processus folii of the malleus, according to Robineau, 1969) and the incus are pushed medially by the tegmen tympani. The tympanohyale is narrow and short.

The pars temporalis (= tegmen tympani) is lenticular in shape, extending 14 mm below the tegmen tympani and slightly compressed dorsoventrally (Fig. 44). It is perpendicular to the tympanicum ring. The stapes is not preserved in any specimen. The pars mastoidea forms the posterolateral third of the tympanic bone. The pars mastoidea and pars temporalis are solid and dense. They are separated by the perilymphatic conchoidal groove posteromedially, where the perilymphatic duct used to be attached and penetrate both parts laterally through the perilymphatic foramen. The promontorium connects both parts. In cerebral view, both parts are smooth and separated by the sulcus facialis and foramen endolymphaticum.

Mandible

Dentaries.— The dentaries of CGM 42181 are incomplete (Fig. 40); only the front portion of the lower jaw and symphysis

is preserved. The symphysis is synostotic. The height at the deflection point of the mandibular corpus is a little more than 54 mm. Minimum dorsoventral breadth of the mandibular corpus is more than 37 mm; the maximum breadth of the masticating surface is 21 mm. At least one accessory mental foramen is present on the left side, above the principal foramen. Alveoli are obscure. The masticating surface is narrow and incomplete.

UM 100138 (Fig. 45) is a sandblasted and toothless mandible of *E. sandersi*. Both corpora are complete on the right side but considerably damaged on the left, and the ascending rami are missing. The symphysis is fused but marked ventrally throughout its length by a deep, narrow cleft. The symphyseal deflection is between 40° and 50°. The symphyseal masticating surface is badly weathered but relatively narrow. It bore two rows of alveoli that were not separated by any appreciable space. At least three small accessory mental foramina lie posterior to the principal foramen on the right side. The mandibular corpus is slender; its ventral margin is asymmetrical, moderately arched, and sharply downturned at the symphysis. The mandibular foramen is not bridged or divided.

Dentition

Upper dentition.— The dental formula for the upper dentitions is 2.1.5.3 (Figs. 41, 66; Table 17). The anterior tip of the premaxilla of UM 111558 has a pair of broken alveoli for the first incisor (Figs. 41, 42), which was smaller than the tusk in *Eotheroides clavigerum*. The alveolus of I³ is preserved at the posterior end of the premaxilla; and there is no indication of I². However, I³ is separated from I¹ by a 38 mm diastema in UM 111558. In this specimen, the upper canine alveolus is reduced and follows I³ by a diastema of three mm. The only canine known for the species is partially preserved from the left side of UM 111558, and is missing its root. Its crown is very well preserved: it is 4.2 mm long, 3.7 mm wide, and 4.7 mm high, thick and barrel-like showing elliptical wear, with its labial edge higher than its lingual edge.

Following the canine alveolus, there are four pairs of single-rooted alveoli marking the loci for P¹⁻⁴, followed by a triple-rooted pair of alveoli for dP⁵. In UM 111558 the distemata between alveoli for C and P¹, P¹ and P², P² and P³, P³ and P⁴, and P⁴ and dP⁵ are 14, 18, 10, 3, and 2 mm, respectively.

P¹ is missing, leaving an empty alveolus. P² and P³ are complete teeth preserved on the right side of the maxilla of UM 111558. P⁴ is missing from the maxillae, and dP⁵ is missing in all maxillae. P² has a height of 18.8 mm, including the root and the crown together. It consists of a large single labial cusp. Height, length, and width of the crown are 7.0, 6.8, and 6.4 mm, respectively. The central cusp is directed inwardly; the lingual cingulum is deep and crenulated, while the labial cingulum is weak and merging with the labial heel of the central cusp. The root is 11.6 mm high, with roughly a triangular cross-section 4.5 mm in diameter. P³ has a height, length, and width of 7.0, 6.7, and 6.1 mm, respectively. The central labial cusp is directed inwardly as well, associated with a smaller lingual cusp and another posterior cusp that is not part of the cingulum. The cingulum is very well developed lingually, and less pronounced labially. The root has an oval cross-section, and measures between 4.2 and 4.5 mm in diameter.

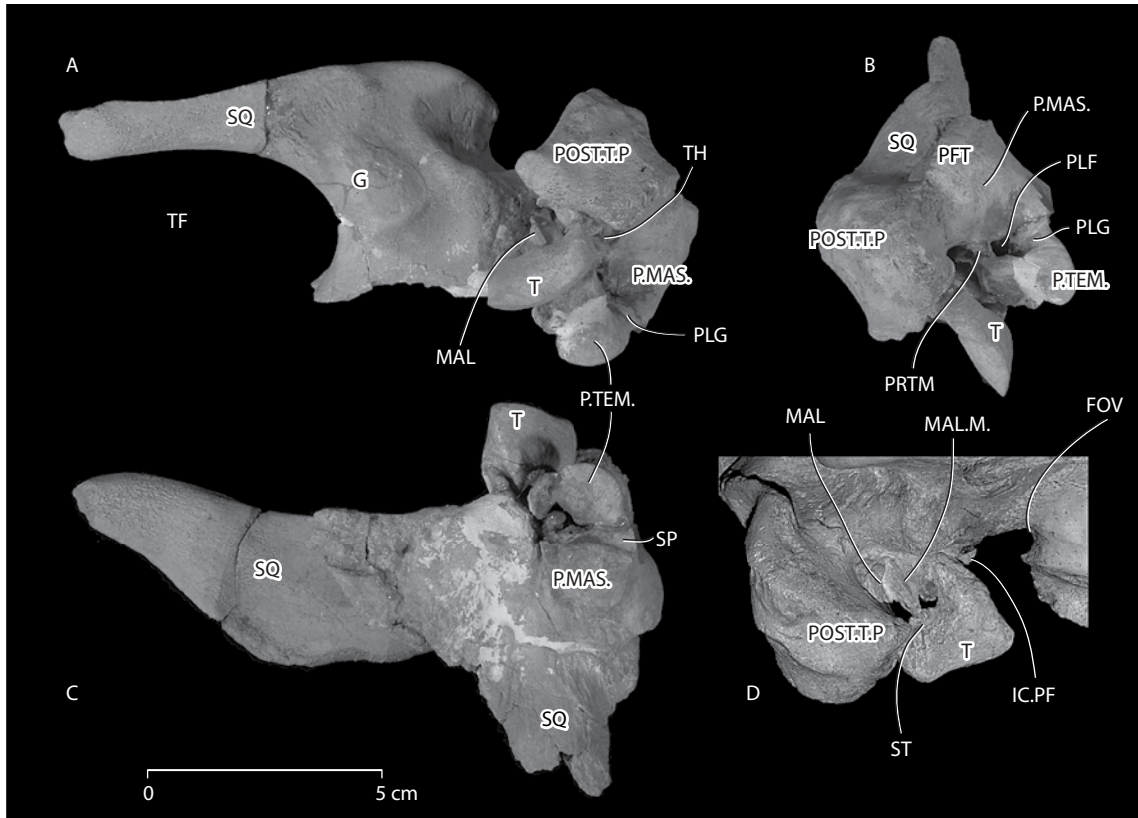


FIGURE 44 — Anatomy of the ear region of *Eotheroides sandersi* (UM 111558) from the Priabonian age Birket Qarun Formation of Wadi Al Hitan. Left squamosal and tympanic elements are shown in A, ventral; B, posterior; and C, cerebral views. Right tympanic region is shown in D, lateral view. The ear region of is divided into three major components: pars mastoidea, pars temporalis, and the tympanic ring. The largest component is the pars mastoidea, which is exposed posteriorly (pars foniculus). Abbreviations: *FOV*, foramen ovalis; *G*, glenoid articulation; *IC*, incus; *MAL*, malleus; *MAL. M.*, manubrium mallei, *PF*, processus folianus; *PFT*, pars foniculus; *PLG*, perlymphatic glenoid; *P. MAS.*, pars mastoidea (=pars petrosa, pars labyrinthica, also pars foniculus “PFT”); *POST.T.P*, post tympanic process; *PRTM*, promontorium, *P.TEM.*, pars temporalis (=tegmen tympani); *SF*, sulcus facialis; *SQ*: squamosal; *ST*, sulcus tympanicus; *T*, tympanic ring; *TH*, tympanohyale; *TF*, temporal fossa.

TABLE 17 — Dental measurements of the maxillary teeth preserved in *Eotheroides sandersi* sp. nov., UM 111558, collected from the Priabonian of the Birket Qarun Formation. Abbreviations: *AW*, anterior width; *CH*, crown height labially; *L*, length; *PW*, posterior width. Measurements are in mm.

Tooth	L	PW	AW	CH
I ¹	—	—	—	—
I ²	—	—	—	—
I ³	—	—	—	—
C ¹	4.20	—	3.70	4.70
p ¹	—	—	—	—
p ²	6.80	—	6.40	7.10
p ³	6.70	—	6.10	7.57
p ⁴	—	—	—	—
dP ⁵	—	—	—	—
M ¹	9.65	10.74	11.28	6.29
M ²	11.06	11.75	13.75	7.17
M ³	14.29	10.51	14.51	8.27

M¹⁻³ are exceptionally preserved on both sides of the maxillae of UM 111558, unlike the condition of the teeth in *Eotheroides clavigerum*. Almost all cusps are preserved, with very minor tooth wear.

M¹ has a well preserved crown, with slight wear on its protoloph. The width of M¹ slightly exceeds its length, and the anterior width exceeds the posterior width. Labial cusps are higher than lingual ones, with the paracone being the highest cusp. Para- and lingual cingula are more developed than meta- and labial cingula.

M² is 28% larger than M¹, and the paracone is the highest cusp. Interlophs are deeper on the labial side, while they are wide and shallow lingually. Dentine is exposed in small transverse lakes on the lophs of the lingual side. Cingula border M² lingually and labially, and the cingulum obliquum is long and very well developed.

M³ is the largest of all molars. It is 18.5% larger than M², and about 41.5% larger than M¹. It shows no wear. Like the teeth



FIGURE 45 — Mandibles of *Eotheroides sandersi* (UM 100138) from the Priabonian age Birket Qarun Formation of Wadi Al Hitán. Mandibles are shown in occlusal A, and lateral view B.

of CGM 60551, the protoloph is wider and slightly lower than the metaloph, and both are separated lingually and labially by deep valleys. However, a lingual cingulum blocks these valleys, while labially a shallow cingulum appears on M³ in UM 111558 (though it is absent in CGM 60551). The precingulum extends labiolingually, covering the anterior front of the protoloph. The lingual cingulum is distinct. The labial cingulum is short, and bears a cleft extending from the anterior base of the metacone to the posterior base of the paracone. The postcingulum is higher lingually than labially; it is shallower than the one in CGM 60551. The valley between the metaloph and the postcingulum is narrow.

Lower dentition.— No tooth crowns are preserved in the mandible of UM 100138 (Fig. 45). The trough behind the M₃ area is sealed with bone, with only a circular outline preserved. A fully erupted M₃ was present, and this had an anteroposteriorly-elongate posterior root. In front of this tooth two roots of M₂ are preserved, as are the two much smaller roots of M₁. Immediately in front of M₁ is a piece of matrix 3 mm in diameter that appears to occupy the anterolabial corner of the M₁ alveolus. Anterior to this is another alveolus 5 mm in diameter, for P₅ or the posterior root of a dP₅. The alveolar row is damaged for the next 25 mm, but this is preceded by a section with four alveoli preserved near where the mandible's dorsal edge is deflected downward. There are only uncertain traces of incisor alveoli in front of this. There was ample room for a dentition with a 3.1.5.3 dental formula.

Vertebrae

The holotype of *Eotheroides sandersi*, CGM 42181 (Fig. 46), preserves two cervicals, three thoracics, and five caudal vertebrae. The more complete individual, UM 111558 (Figs. 47-49; Table 18), contains a well preserved atlas, third cervical, second through sixteenth thoracic series in order, a last thoracic, three middle caudal vertebrae, and four posterior caudal vertebrae.

UM 97514 includes the fourth through sixteenth thoracics (Figs. 50-53; Tables 19), three lumbar (L2-4), a single sacral, caudals Ca1-6, Ca8-10, and one of the most posterior caudals. All of these vertebrae have thin but well-developed epiphyses that are firmly fused to the vertebral bodies. The vertebral bodies are mainly composed of cancellous bone and are connected to dense neural arches and spines. UM 100138 has four mid-thoracic vertebrae. The full vertebral formula for *Eotheroides sandersi* is reconstructed as having been C7, T18-19, L4-5, S1, and Ca 20-22.

Cervical vertebrae.— The atlas of UM 111558 (Figs. 47, 48; Table 18) is smaller in size than that of *Eotheroides clavigerum*, and its transverse processes are more square. They extend laterally and slope posteriorly downward, keeping the vertebral artery passage visible craniocaudally. The first cervical nerve ran transversely behind the top of the anterior condyles, and its passage is visible dorsolaterally. Lateral to that and still behind the condyles, a deep sulcus for the vertebral artery runs down to the transverse foramen. The dorsal arch bears a weakly pointed summit, and on the cranial surface this preserves muscle scars for rectus capitis dorsalis minor. Caudally the summit is gentle and smooth. The ventral surface of the atlas is concave and

smooth, the articular facet for the odontoid process is smooth and tilted posteriorly, the cranial edge is slightly concave cranially, and its distal edge protrudes slightly caudally. The condyles are larger and more deeply concave on the cranial than on the caudal side. The vertebral canal is wide and keyhole-shaped, higher than it is wide.

C3 in UM 111558 (Figs. 47-48; Table 18) has a damaged vertebral body; however the body seems to be flattened craniocaudally and lacks a ventral keel. The neural arch has a knob-like summit. The neural canal is subtriangular. The prezygapophyses are flattened and face ventromedially, and postzygapophyses face dorsolaterally. Transverse processes are wide, flattened, and sloping from the main vertical plane of the vertebral body. The transverse foramen is damaged. The holotype (Fig. 46) preserved only the centrum of C3, and meaningful landmarks are broken away.

Thoracic vertebrae.— Th2 is preserved in UM 111558 (Figs. 47-49). It has a thick, long neural spine that is straight, with a concave anterior edge and bluntly straight apex. Transverse processes are perpendicular to the neural arch and the neural

TABLE 18 — Dimensions of vertebrae *Eotheroides sandersi*, UM 111558. Abbreviations: C, cervical vertebra; Ca, caudal vertebra; CH, centrum height; CL, centrum length; CW, Centrum width; Lr, lumbar vertebra; NCW, neural canal width; NCH, neural canal height; Th, thoracic vertebra; THT, total height; TW, total width; V, vertebra. Measurements are in mm.

V	THT	TW	CL	CW	CH	NCW	NCH
C1	57	106	—	—	—	27	41
C3	65	84	15	36	28	26	24
Th2	113	101	26	33	23	18	23
Th3	—	—	25	—	20	—	20
Th4	103	93	30	34	26	17	21
Th5	—	—	33	33	27	17	21
Th6	103	86	33	36	27	17	23
Th7	103	82	36	40	30	17	21
Th8	99	81	36	38	27	19	23
Th9	—	81	37	42	30	18	21
Th10	101	98	39	43	28	19	12
Th11	109	79	39	45	32	22	22
Th12	108	80	39	47	33	21	20
Th13	110	78	40	50	37	22	20
Th14	105	79	41	54	33	21	19
Th15	—	77	40	56	33	18	19
Th16	108	78	41	53	35	21	22
Th17?	—	—	—	—	—	—	—
Th18	—	—	—	—	—	—	—
Th19	105	118	45	53	33	20	21
Lr1	104	168	44	53	34	22	21
Ca5?	66	144	39	50	35	19	—
Ca6?	—	120	36	51	35	16	12
Ca7?	—	—	35	49	36	17	16
Ca12?	—	—	27	34	32	—	—
Ca13?	—	95	27	29	26	—	—
Ca16	20	40	23	40	20	—	—
Ca19	—	—	18	22	15	—	—

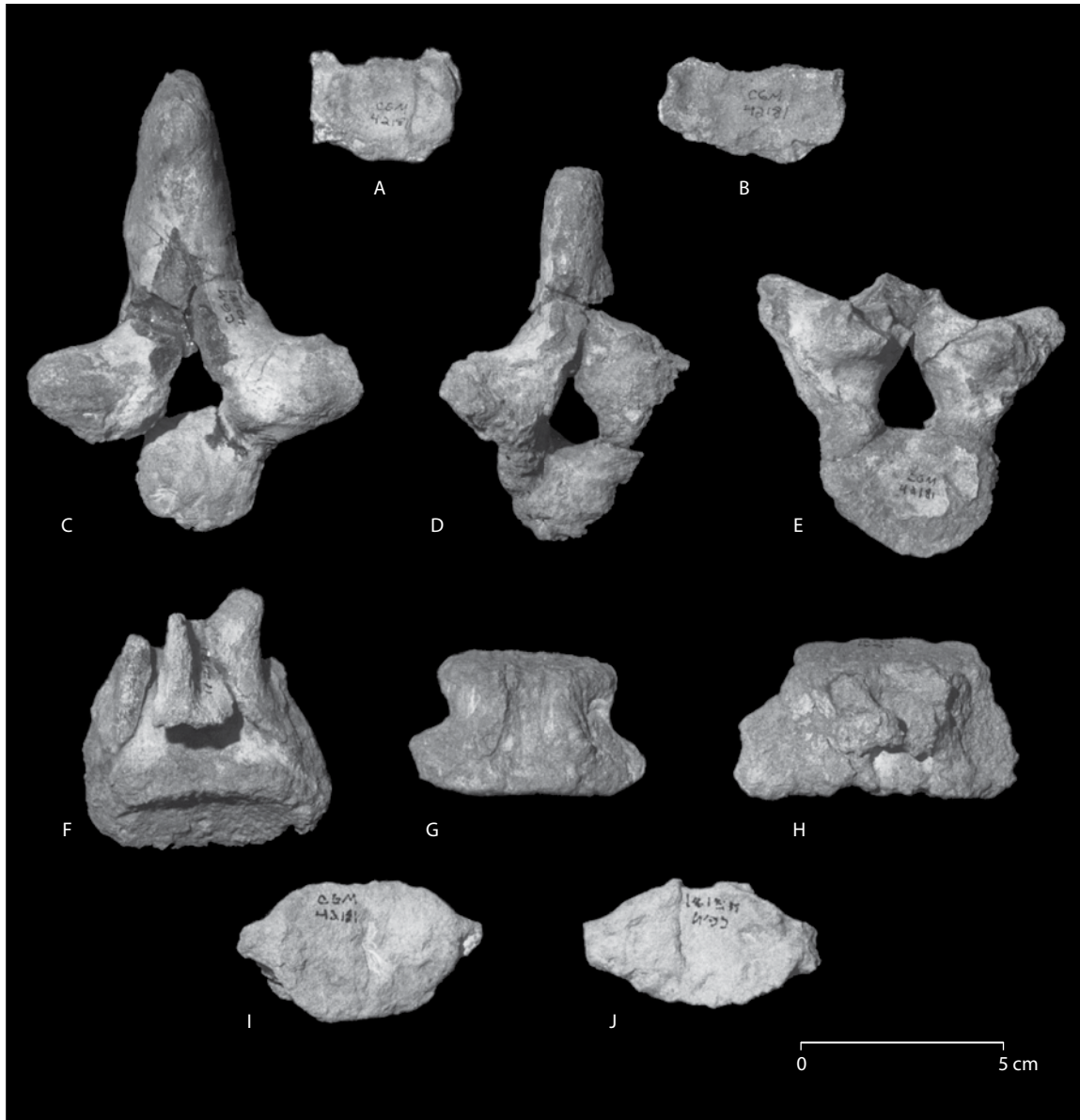


FIGURE 46 — Mid-cervical, thoracic, and caudal vertebrae of the holotype of *Eotheroides sandersi* (CGM 42181) from the Priabonian age Birket Qarun Formation of Wadi Al Hitán. A-B, vertebral bodies (centra) of the third and fourth cervical vertebrae in anterior view. C, second thoracic vertebra bearing a long spine and horizontal transverse processes in anterior view. D, third or fourth thoracic vertebra in anterior view. E, fourth or fifth thoracic vertebra in anterior view. F-H, ninth through the eleventh caudal vertebrae in dorsal view. I-J, more-posterior caudal vertebrae in anterior view.

spine, and extend laterally more than on following thoracics. The vertebral foramen is oval in shape. Prezygapophyses are inclined medially and face anterodorsally, while postzygapophyses are directed posteroventrally. Zygapophyses do not project beyond the most anterior tip of the transverse process nor beyond the most posterior edge of the neural spine.

Th3 is partially preserved in UM 111558 (Figs. 47-49). Its vertebral body is the same length as that of T2, and its ventral

surface is concave anteriorly without a keel. The transverse processes are knoblike, and the preserved prezygapophysis is flat, horizontal, and directed dorsally. The shape of the vertebral canal is ovoid, but smaller than that of T2.

Th4 is preserved in UM 111558 (Figs. 47-49). Its neural spine is shorter than that of Th2 and it is directed backward. The transverse processes make an angle relative to the neural arch and spinous process; the zygapophyses are in the same planes

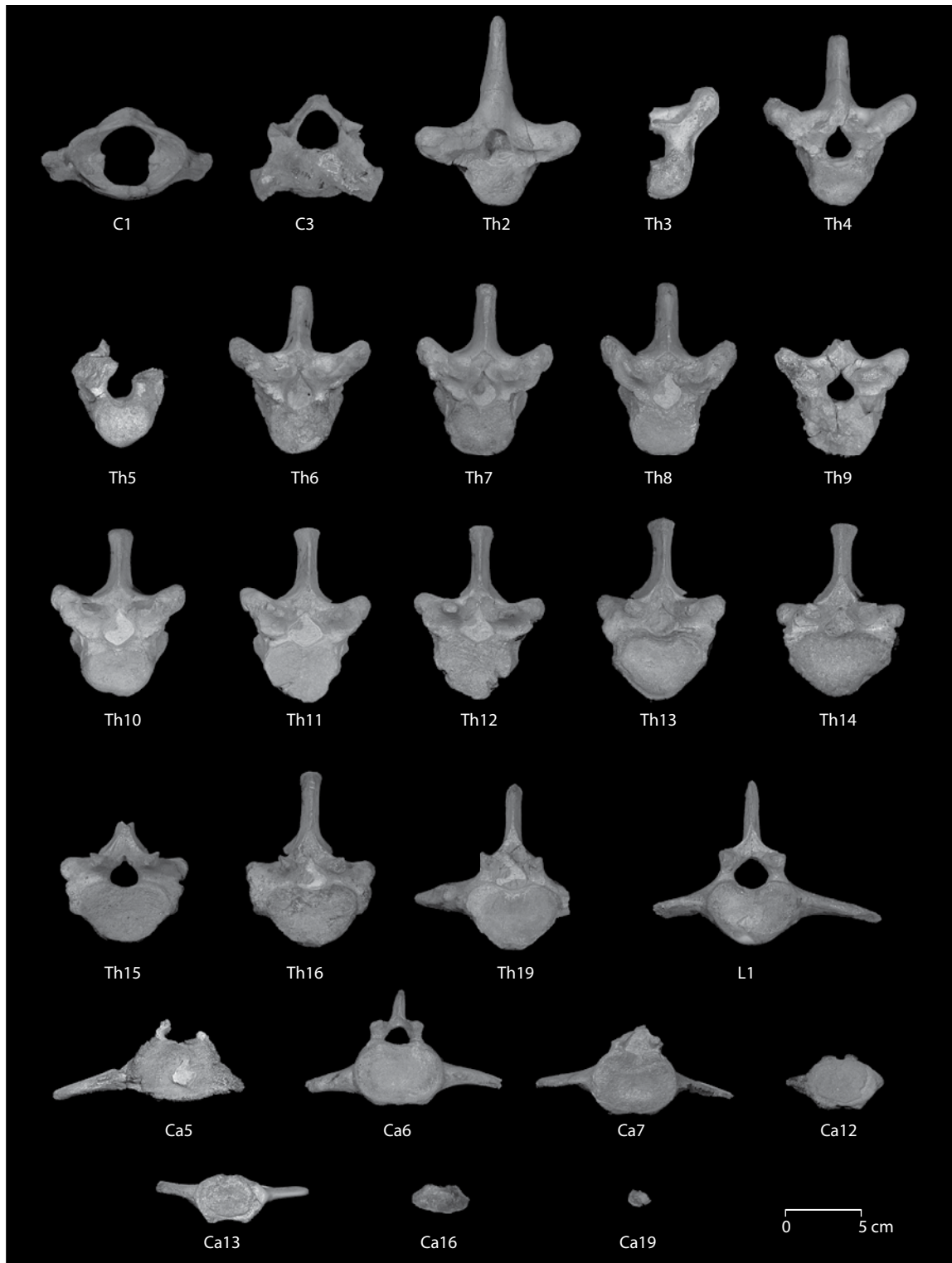


FIGURE 47 — Cervical, thoracic, lumbar, caudal vertebrae of *Eotheroides sandersi* (UM 111558) from the Priabonian age Birket Qarun Formation of Wadi Al Hitan. Vertebrae shown are C1 and C3, Th2 through Th16, Th19 (pre lumbar), L1, Ca5 through Ca7, Ca12 and Ca13, Ca16, and Ca19. All are shown in anterior (cranial) view. The atlas has transverse processes squared in outline. The thoracic vertebrae were arranged according to their centrum length, spinous process height, and transverse process curvature. More anterior thoracics have high spines, almost horizontal transverse processes, and large neural canals. More posterior thoracics have short and rounded transverse processes. Mid and posterior thoracics (Th4-Th18) have neural canals with a narrow groove or slit at the top when seen in anterior view. Abbreviations: *C*, cervical; *Ca*, caudal; *L*, lumbar; *Th*, thoracic; *S*, sacral.

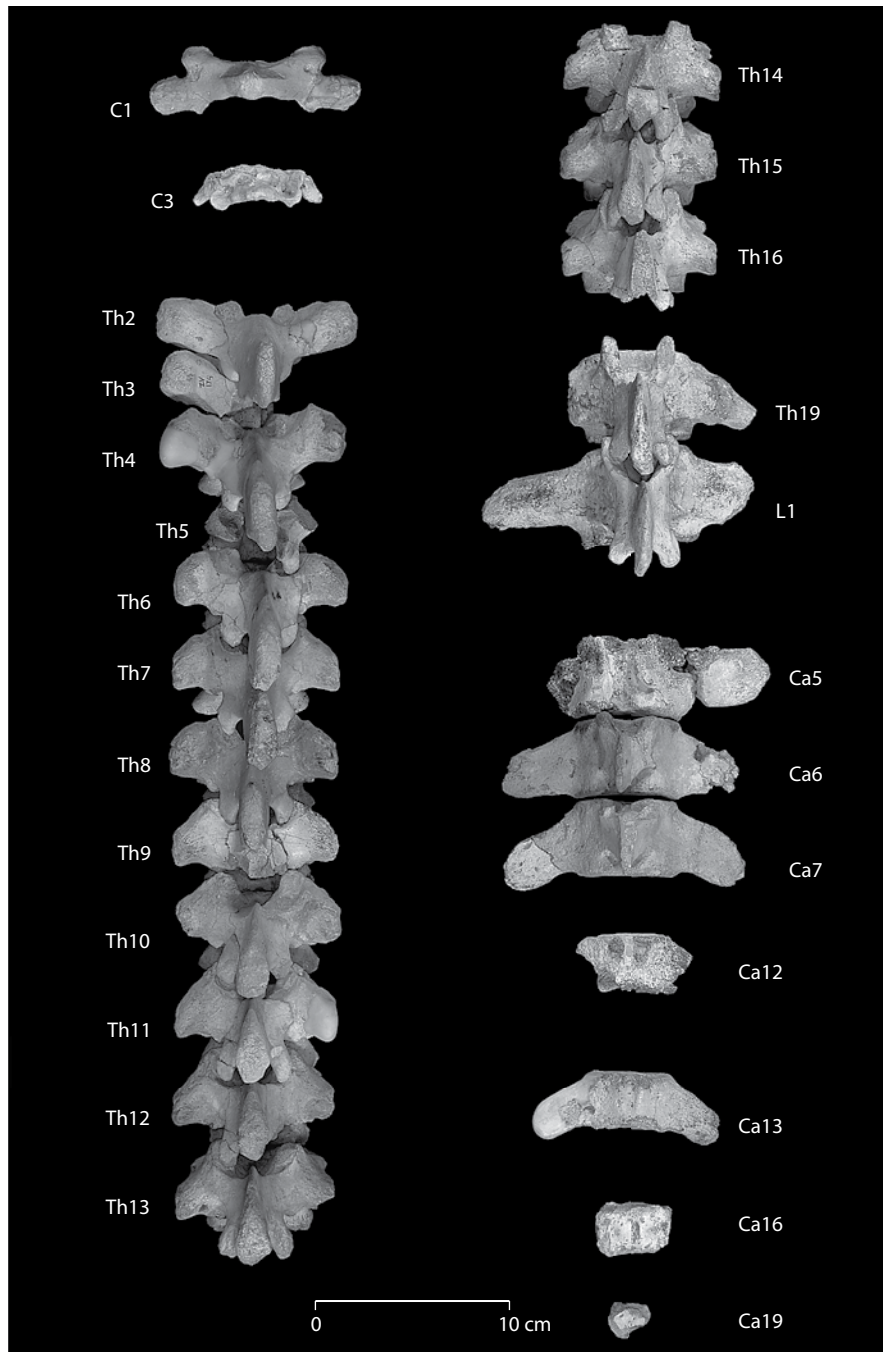


FIGURE 48 — Cervical, thoracic, lumbar, and caudal vertebrae of *Eotheroides sandersi* (UM 111558) from the Priabonian age Birket Qarun Formation of Wadi Al Hitán. Vertebrae are shown in dorsal view. Spacing between regional areas indicates missing vertebrae. Abbreviations: *C*, cervical; *Ca*, caudal; *L*, lumbar; *Th*, thoracic; *S*, sacral.

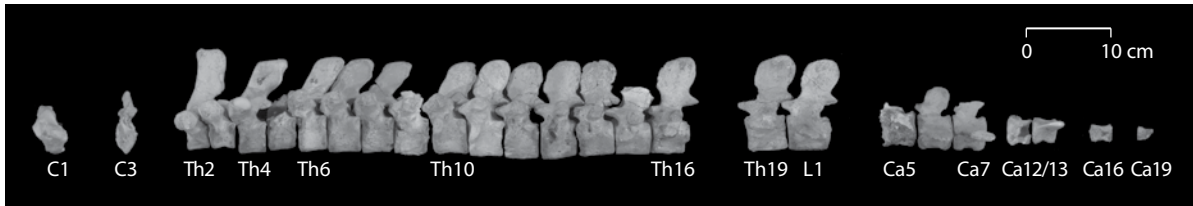


FIGURE 49 — Cervical, thoracic, lumbar, and caudal vertebrae of *Eotheroides sandersi* (UM 111558) from the Priabonian age Birket Qarun Formation of Wadi Al Hitan. Vertebrae are shown in left lateral view. Abbreviations: C, cervical; Ca, caudal; L, lumbar; Th, thoracic; S, sacral.

as those of Th2. The vertebral canal is smaller, subrounded, and notched at the top. The vertebral body is heart-shaped, with its prezygapophyses positioned high on the lateral sides. The postzygapophyses are more elongated than those on more anterior vertebrae.

Th5-11 (Figs. 47-53) bear thick, stout neural spines that are strongly inclined backward, with bluntly rounded apices and concave posterior surfaces. More posteriorly, the latter surfaces develop a median ridge, faint at first but eventually becoming so prominent that the spines have no posterior surface but only a sharp posterior edge. The spines become progressively thinner and more vertical. Transverse processes are angled upward from the neural arches. In dorsal view, they are irregularly rectangular in outline and are perpendicular to the axis of the vertebral body. More posteriorly, they are shorter, appear more horizontal, and their forward edges are swept back, making them more triangular in dorsal view.

The pedicles of the neural arches are very thick and massive, visually dominating the relatively small and constricted neural canal, which on all the thoracics has a sharply peaked apex. A thick, rounded ridge extends from the front edge of the tubercular costal facet down and medially to the forward edge of the prezygapophysis. This ridge separates the ventrolateral surface of the transverse process and pedicle from the more or less broad and flat anterior surface, which is especially distinct on the more anterior thoracics. This feature is common in all Eocene Tethyan genera, including *Protosiren* and *Eotheroides*, and was designated the “*Vorderfeld*: the border of the field” of Sickenberg (1934). Posterior and more or less parallel to this ridge is another irregular and ill-defined crest (*crista subcostalis*) that descends beneath the posterior edge of the tubercular facet. Between the zygapophyses and the base of the neural spine, on both front and back sides, the surfaces of the neural arch are sculpted by ridges into pairs of crescentic concavities to which Sickenberg (1934) applied the term “*Area*.” According to his description, these features are characteristic of all Priabonian *Eotheroides*, in contrast to *Eotheroides aegyptiacum* from the middle Eocene of Gebel Mokattam. The vertebral bodies have dorsal indentations and concave ends, and lack any distinct midventral keel although the undersides of the vertebral bodies are convex. The epiphyseal surfaces of some appear irregularly and asymmetrically flat.

Th12-16 (Figs. 47-53; Tables 18, 19) have long zygapophyses projecting beyond the length of the vertebral bodies; neural spines are shorter, longer anteroposteriorly, and compressed me-

dolaterally. The top of the spinous process is blunt and convex. Neural canals are more or less diamond-shaped due to the degree of narrowing in the apex and the presence of a shallow groove on the dorsal side of the vertebral body. The epiphyses are strongly fused with the vertebral bodies. The lateral sides of the vertebral bodies are notably concave inward, and ventrally the vertebral bodies lack any keel. Zygapophyses progressively move toward the transverse processes, joining the tubercular facet. In the most caudal thoracic vertebrae, but not the last one, only a single rib facet is present on the end of a short process jutting out from the side of the centrum.

Th17 and Th18 were not preserved. Th19 (Figs. 47-49) is the last thoracic, and this is only known from the thoracic series in UM 111558. It is distinct in having a short (about 25 mm long) and rounded transverse processes on the left side, this transverse process was formed from the fusion of the last rib, which is the shortest rib in the ribcage, with the thick root of the transverse process of the centrum. The right transverse process is broken and missing, leaving the thick process empty. The neural spine is shorter than in vertebrae more anterior in the series, wide anteroposteriorly, and thin. Zygapophyses are long, and the neural canal lacks the slit-like apex seen in more anterior thoracics (Fig. 47). The vertebral body is heart-shaped, with a gently convex dorsal surface (the base of the vertebral foramen), laterally biconcave in the middle, and characterized by a flat ventral torus that is too flat to be called a keel. The surfaces lateral to the torus are marked by a pair of vascular foramina. Epiphyses are solidly fused to the vertebral body.

Lumbar vertebrae.— L1 (Figs. 47-49) is preserved in UM 111558. The transverse process of the first lumbar is flat, short, and directed posteriorly. The vertebral body is markedly heart-shaped, with a distinct dorsal indentation and a thick midventral torus. It has shallowly concave epiphyses. The neural spine is similar to that of the last thoracic; the neural canal is almost round in shape, and the zygapophyses are slightly shorter than those in the last thoracic, as well.

L2, L3, and L4 (Figs. 50, 52, 53; Table 19) are preserved in UM 97514. L2 is missing its neural spine and the right transverse process is incomplete. The left transverse process is short, flattened, and posteromedially indented. The midventral pillar on the vertebral body is more pronounced than that on L1 of UM 111558.

L3 and L4 have transverse processes longer and more flattened than those in L1 and L2 (Figs. 50, 52; Table 19). These extend nearly horizontally from the middle of the centrum, and

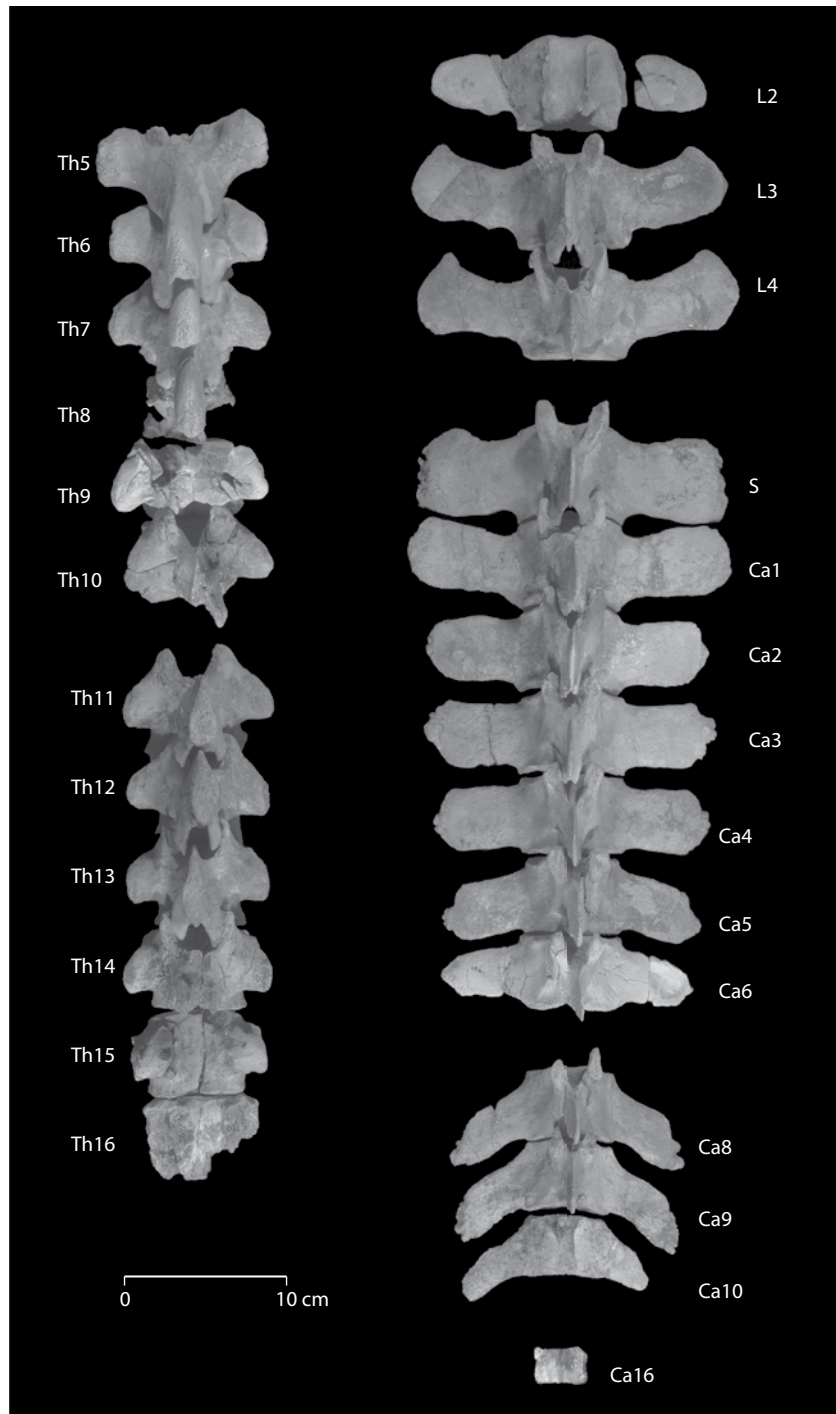


FIGURE 50 — Thoracic vertebrae of *Eotheroides sandersi* (UM 97514) from the Priabonian age Birket Qarun Formation of Wadi Al Hitan. Vertebrae are shown in dorsal view. At least three thoracic should follow thoracic vertebra T16. Abbreviation: *Ca*, caudal; *L*, lumbar; *Th*, thoracic; *S*, sacral.

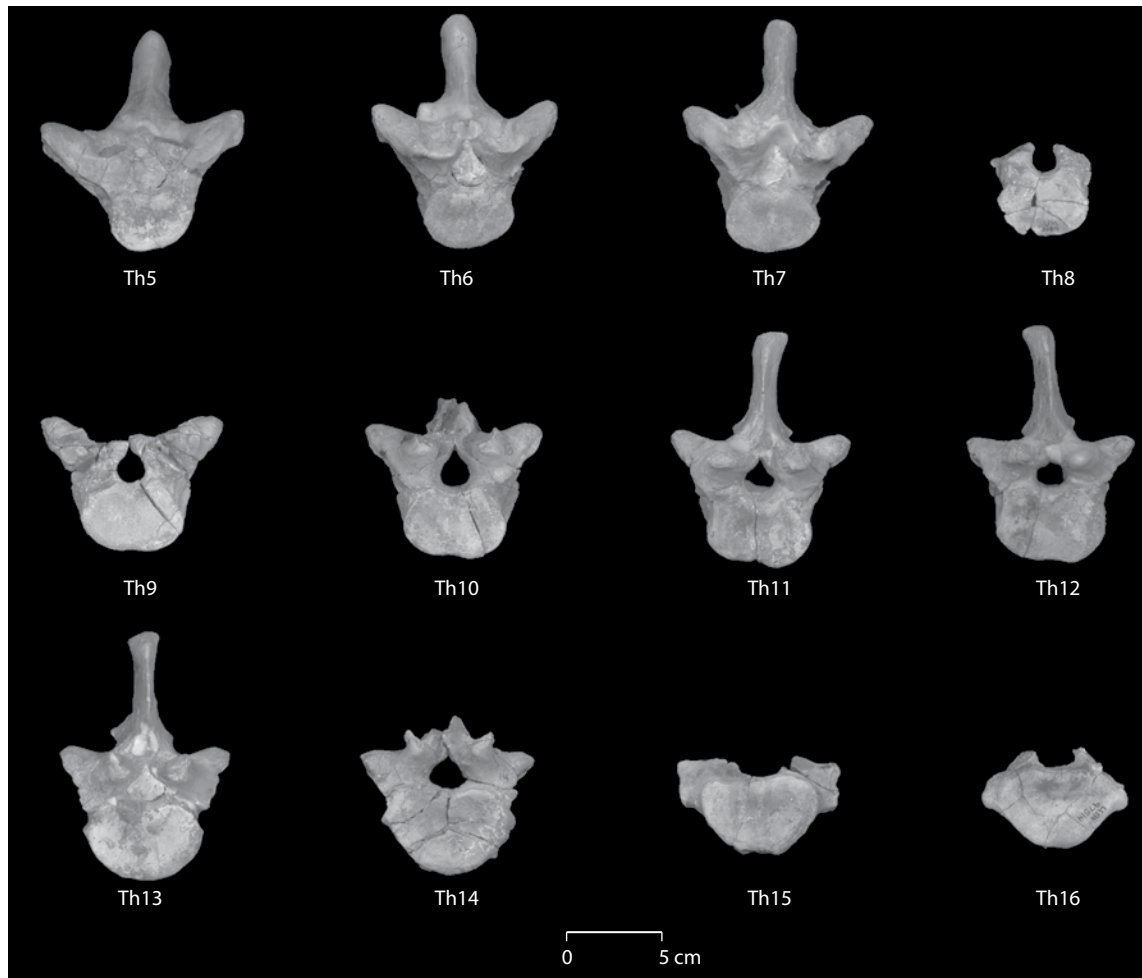


FIGURE 51 — Thoracic vertebrae of *Eotheroides sandersi* (UM 97514) from the Priabonian age Birket Qarun Formation of Wadi Al Hitan. Vertebrae are shown in anterior (cranial) view. Abbreviation: *Th*, thoracic.

are curved forward. Their tips are flattened dorsoventrally, and their most anterolateral corners point forward. The apex of the neural canal is not slit-like. The neural spine is thin and sharp on both edges, and slightly inclined backward. The neural spines progressively become thinner and lower caudally. The zygapophyseal articular surfaces are inclined at about 45° to the horizontal. The midventral torus on L4 is more flattened than the one on L3.

Sacral vertebrae.— The sacrum is represented by a single vertebra (S1; Figs. 50, 52, 53; Table 19), which is only known in UM 97514. It is characterized by thick, downwardly-sloping transverse processes with thickened, rugose auricular processes for attachment to the ilia. The rugose ends measure up to 29 mm thick dorsoventrally, and extend well below the bottom of the centrum. The transverse processes are somewhat expanded anteriorly near their ends in an asymmetrical manner. The neural canal widens posteriorly and does not have a slit-like apex. The neural spine is thin and sharp on both edges, and it

is nearly vertical. Zygapophyseal articular surfaces are inclined about 45° to the horizontal. The ends of the vertebral body are shallowly concave, and the ventral surface of the centrum is flat. The dorsal surface of the vertebral body is indented anteriorly but not posteriorly.

Caudal vertebrae.— Caudal vertebrae are best preserved in UM 97514. The first six caudal vertebrae Ca1–Ca6 (Figs. 50, 52, 53; Table 19) of UM 97514 are well preserved, along with three of the more posterior ones. UM 111558 also has vertebrae from the posterior portion of the tail.

Ca1 (Figs. 50, 52, 53; Table 19) is unusual in that its transverse processes are inclined forward slightly, nearly horizontal, and even appear turned up slightly at the tips (due to thickening of the tips). This contrasts with the preceding sacral and the succeeding caudal vertebrae, whose transverse processes are perpendicular to the body axis and markedly inclined downward. However, in the shape of its vertebral body, degree of separation of its zygapophyses, and overall dimensions, this vertebra fits

TABLE 19 — Measurements of vertebrae of *Eotheroides sandersi*, UM 97514. Abbreviations: *Ca*, caudal vertebra; *CH*, centrum height; *CL*, centrum length; *CW*, Centrum width; *Lr*, lumbar vertebra; *NCW*, neural canal width; *NCH*, neural canal height; *S*, sacral vertebra; *Th*, thoracic vertebra; *THT*, total height; *TW*, total width; *V*, vertebra. Measurements are in mm.

V	THT	TW	CL	CW	CH	NCW	NCH
Th4	120	—	—	—	—	—	—
Th5	116	99	31	40	29	19	23
Th6	109	91	35	44	31	18	23
Th7	111	93	36	47	34	17	20
Th8	—	—	35	46	—	14	—
Th9	—	89	37	53	34	15	18
Th10	—	87	38	54	39	15	21
Th11	111	88	38	50	36	18	18
Th12	116	83	38	52	38	16	15
Th13	119	81	40	57	41	19	17
Th14	—	86	40	57	44	18	16
Th15	—	79	41	57	39	19	—
Th16	—	—	—	—	—	—	—
Th17?	—	70	40	57	39	18	—
Th18	—	—	—	—	—	—	—
Lr1	—	—	—	—	—	—	—
Lr2	—	—	41	60	42	22	—
Lr3	112	190	42	63	39	19	16
Lr4	106	188	43	62	41	31	18
Lr5	—	—	—	—	—	—	—
Lr6	—	—	—	—	—	—	—
S	98	191	42	61	39	30	14
Ca1	94	192	42	60	37	26	12
Ca2	89	175	40	61	39	23	14
Ca3	83	177	40	62	41	19	13
Ca4	81	168	38	63	42	24	10
Ca5?	76	156	38	56	41	14	90
Ca6?	74	—	39	61	47	16	11
Ca7?	—	—	—	—	—	—	—
Ca8	65	143	37	53	41	15	8
Ca9	58	136	35	53	38	10	7
Ca10	43	114	28	48	36	8	—
Ca16?	14	33	17	26	14	—	—

better in the first caudal position than elsewhere in the column. The vertebral body is flat-bottomed like that of the sacrum, and not indented dorsally. Like the other caudals, the ends of the centrum are shallowly concave, and the neural spine is thin with sharp front and back edges. The neural spine is vertical. Small postzygapophyseal articular facets are present.

Ca2 (Figs. 50, 52, 53; Table 19) has very faint chevron attachments on the caudal edge of its ventral surface. It also has downwardly-directed transverse processes that are still more recurved at their tips. The tips are slightly expanded and rugose.

Ca3 (Figs. 50, 52, 53; Table 19) lacks these recurved tips, and bears rather indistinct demifacets for a chevron bone at each end. Ca4 (Figs. 50, 52, 53; Table 19) and subsequent vertebrae have distinct anterior and posterior chevron demifacets and lack postzygapophyses. The prezygapophyseal processes of

following caudal vertebrae remain large, but lack articular facets and serve only as mammillary processes for transversospinal muscle insertion. The spinous process of Ca4 shows a hint of posterior inclination, which becomes distinct on Ca5 and quite marked on Ca6 (Figs. 50, 52, 53; Table 19). Backward inclination of the transverse processes also begins with Ca5 and gradually increases toward the peduncle (Figs. 49, 53).

In UM 97514 (Figs. 50, 53), at least one vertebra is missing immediately subsequent to Ca6. Ca8 through Ca10 continue the trends described above. The latter exhibits the lowest and most inclined neural spine, and the most sharply swept-back transverse processes.

One isolated vertebra from the posterior part of the fluke region probably represents the third or fourth vertebra from the end. It has only a very short transverse process and no trace of a neural arch. In its lack of long transverse processes it has a general resemblance to a posterior caudal of a modern dugong.

The caudal series in UM 111558 (Figs. 48, 49) is missing all of the anterior caudals, estimated to be Ca1 through Ca4, but preserves Ca5 through Ca7, Ca12 and Ca13, ?Ca16, and a very posterior caudal that is close to the measured centrum height of the last vertebra available from UM 97514. The trends of tapering, decreasing size, and dorsoventral flattening of the caudal vertebral bodies are the same in both vertebral columns.

Ribs

Ribs.— The holotype of *Eotheroides sandersi*, CGM 42181 (Fig. 54; Table 20), includes nearly the entire right rib series, missing only the first and second ribs, and it also preserves the second rib on the left side. The second through sixth ribs are swollen (pachyostotic) and massive in construction. The seventh through eleventh ribs are the longest and have the greatest arc widths. All are rounded in cross-section and equally massive and thick. Ribs from the twelfth to the last are cylindrical and more gracile.

The second rib is pachyosteosclerotic. Its neck is straight and diminutive. The head is as small as the capitular facets. The tuberculum is slightly higher than the head, with a small pointed facet. The ligamentous fossa lateral to the tuberculum is very shallow and poorly developed. The shaft of R2 is thick, oval in cross section, with a smooth outline. The shaft maintains a consistent thickness and shape proximally. Just before midshaft it becomes more swollen and increases its thickness, with a rectangular to quadratic cross-section. More distally, the shaft reaches its greatest thickness, measuring 37 mm mediolaterally and 26 mm anteroposteriorly. The distal end of the rib is banana-shaped, tapering to a pointed end. The lower posteromedial area is characterized by an irregular surface for muscle attachment.

Ribs 3-5 are missing their heads. All are pachyosteosclerotic and taper distally, having a banana-like shape. The third rib has the greatest pachyosteosclerosis of all of the ribs, and it has the greatest midshaft diameter and circumference. The fifth rib has the most crescentic shape in the series.

Rib 6 is complete, slightly compressed anteroposteriorly, and the tip of its head is missing. The tuberculum is less pronounced than those of the posterior ribs. The cross-sectional area at midshaft is greater than those of more posterior ribs.

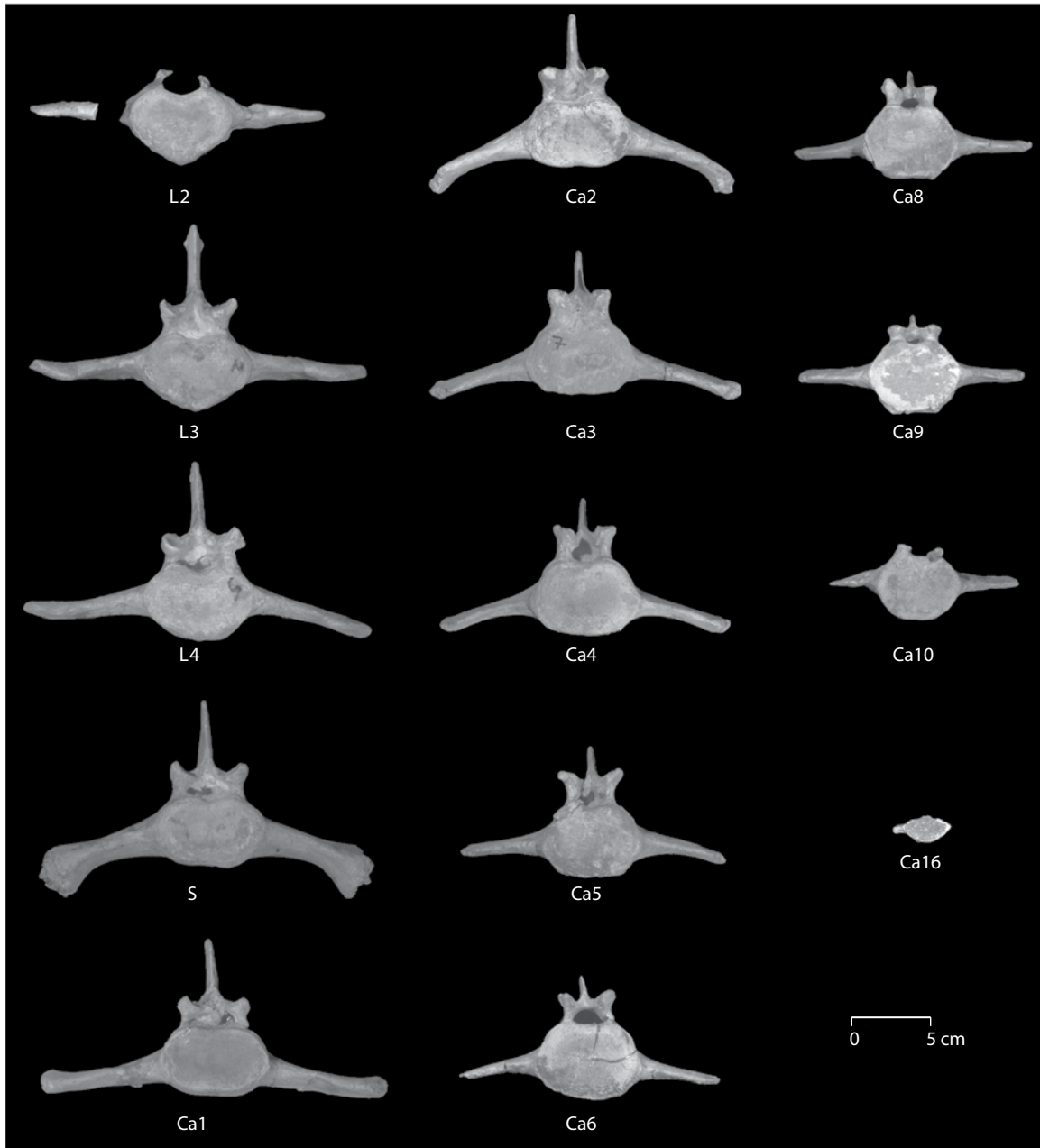


FIGURE 52 — Lumbar, sacral, and caudal vertebrae of *Eotheroides sandersi* (UM 97514) from the Priabonian age Birket Qarun Formation of Wadi Al Hitan. Vertebrae are shown in anterior (cranial) view. Abbreviations: *Ca*, caudal; *L*, lumbar; *Th*, thoracic; *S*, sacral.



FIGURE 53 — Thoracic, lumbar, sacral, and caudal vertebrae of *Eotheroides sandersi* (UM 97514) from the Priabonian age Birket Qarun Formation of Wadi Al Hitan. Vertebrae are shown in left lateral view. Abbreviations: *C*, cervical; *Ca*, caudal; *L*, lumbar; *Th*, thoracic; *S*, sacral.

TABLE 20 — Measurements of preserved ribs of the holotype of *Eotheroides sandersi*, CGM 42181; most of the left side of the ribcage was weathered away and never recovered. Abbreviations: *L*, left rib; *MAWM*, maximum anteroposteriorly width of midshaft; *MLWM*, maximum mediolateral width at midshaft; *R*, right rib; *TL*, total length. Measurements are in mm.

Rib	TL	MLWM	MAWM
L2	145	38	27
R3	—	41	32
R4	—	—	—
R5	—	36	30
R6	230	32	28
R7	260	34	25
R8	265	35	24
R9	260	32	23
R10	—	—	—
R11	—	32	22
R12	—	31	21
R13	—	28	21
R14	—	27	18
R15	—	24	14
R16	242	23	15
R17	—	22	13
R18	225	22	15

TABLE 21 — Measurements of preserved ribs of *Eotheroides sandersi*, UM 111558. Abbreviations: *CM*, circumference around midshaft; *CT*, capitulum to tubercle length; *EAL*, external arc length; *IAL*, internal arc length; *L*, left rib; *MAWM*, maximum anteroposterior width of midshaft; *MLWM*, maximum mediolateral width at midshaft; *ND*, neck diameter; *R*, right rib; *TL*, total length. Measurements are in mm.

Rib	TL	EAL	IAL	CT	ND	CM	MLWM	MAWM
L12	—	—	—	49	21	—	18	29
L13	—	—	—	48	20	—	18	29
R1	109	141	91	32	12	78	27	23
R2	151	212	145	36	13	107	33	29
R3	193	283	173	40	15	119	38	37
R4	212	322	200	43	16	112	38	31
R5	246	340	228	48	18	96	33	26
R6	264	352	245	49	19	92	24	34
R7	—	352	—	50	19	89	22	33
R8	—	—	—	—	—	88	31	23
R9	—	—	—	48	18	80	18	30
R10	312	374	295	47	20	78	20	29
R11	309	372	290	46	20	77	18	30
R15	—	—	—	42	18	70	18	25
R16	—	—	—	—	—	—	—	—
R17	—	—	—	28	12	48	16	12

Ribs 7-10 have oval anterior and posterior capitular facets slightly connected at their summit. In each, the neck is slightly straight, long, flat ventrally, semicircular in cross section, and angled cranially. The tuberculum is elevated, with a rounded ligament fossa medial to it. The cross section of the shaft is more or less constant along the upper two thirds of the rib, and the distal end is slightly angled medially.

Rib 11 has a shorter neck than preceding ribs, and the cross section below the tuberculum is rounded. The twelfth and following ribs are slender, gracile, semicircular in cross-section, and taper very gently distally. The most posterior ribs have their head and tuberculum joined to form a flat, straight articular facet.

UM 111558 preserves the anterior and middle part of a ribcage (Fig. 55; Table 21) including 13 ribs from the right side (R1-R11, ?R15 and R17 or R18) and 8 ribs from left side (R2-R6, R12 and 13, an possibly R14). The arrangement of ribs is based on their overall shape and morphology, knowing that they are ribs of single individual. Arrangement is also constrained by comparison to ribcages of extant dugongs and comparison to an articulated rib cage from the Mokattam Eocene of Egypt (Fig. 54C).

The first rib (R1) in UM 111558 (Fig. 55; Table 21) has a well developed head, neck, and tuberculum. The anterior capitular facet is larger than the posterior one; the neck has a sulcus cranially and a shallow transverse concavity caudally. The tuberculum is lower than the capitulum. The tubercular fossa faces laterally as a vertical notch, not a depression as in the succeeding ribs. The proximal end of the shaft is triangular in cross section and compressed mediolaterally into a slight concavity posteriorly for muscle attachment. The midshaft of the rib is convex anteriorly with a distinct ridge formed posteriorly. The distal end of the shaft is flattened anteroposteriorly, and the end is straight and truncated.

The second rib in UM 111558 (Fig. 55; Table 21) is morphologically like that of CGM 42181. It is a banana-like rib with strong pachyosteosclerosis.

The third rib (Fig. 55; Table 21) is the thickest and widest in diameter of all ribs in the ribcage of this individual. It is convex anteroposteriorly. The capitulum is rounded. The anterior capitular facet is smaller than its posterior counterpart. The neck is straight, cylindrical and thickened. The tuberculum is rounded, flat, and lower than the head, and the tubercular fossa is shallow and small. The proximal end of the shaft is oval in cross section, and the lower two-thirds of the shaft maintain a constant thickness and shape. The shaft tapers rapidly just 20 mm before the distal end.

The fourth rib (Fig. 55; Table 21) is similar to that in CGM 42181, with a rounded capitulum that is lower than the tuberculum. The anterior tubercular surface is oval in shape, and is twice as large as the posterior one. The neck is straight, the tuberculum is slightly higher than the capitulum, and the tubercular fossa is larger than that on R3. On the posterior side just above the midshaft, the second and third ribs retained a 30 mm long scar on each, running mediolaterally. R4 possesses a depression anteriorly just below the angle. The scars and the depression are all aligned at the same level, and it is not clear whether this was a pathology, or a healed injury.

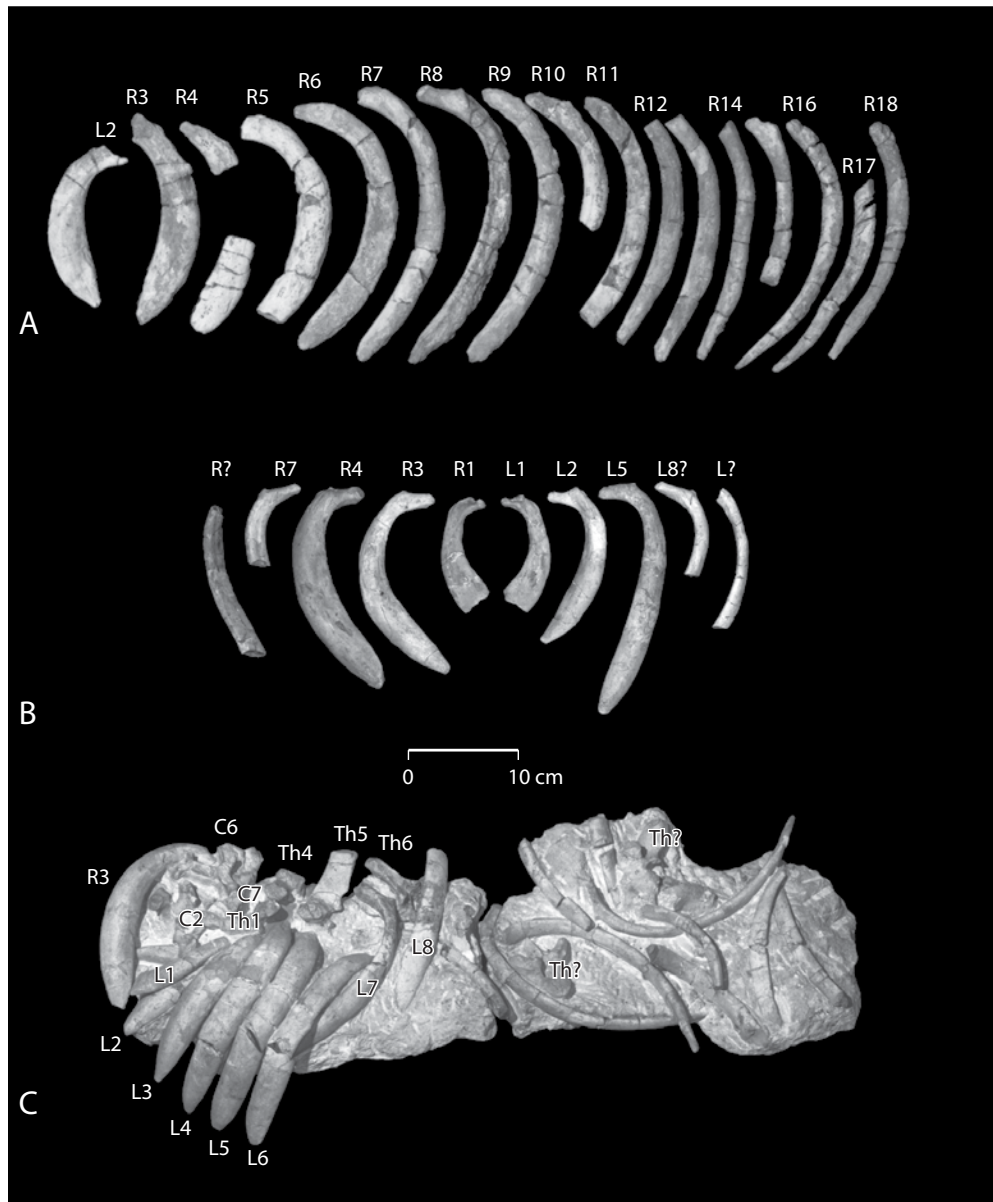


FIGURE 54 — A, cranial view of the ribs of the holotype of *Eotheroides sandersi* (CGM 42181), from the Priabonian age Birket Qarun Formation of Wadi Al Hitan. The right side preserves rib 3 through rib 18; only the second rib from the left series survived natural weathering. Anterior ribs are pachyosteosclerotic and banana-like but posterior ribs are not. B, left and right ribs of *Eotheroides aegyptiacum*, SMNS 43949 or 'St. XV (XIX)', collected from the Lutetian of the Mokattam Hills. The two symmetrical ribs in the middle of the photo are the left and right first rib showing the characteristically distally-flattened and truncated ends. C, Ribs and vertebrae (*Wirbelkomplex*) of *Eotheroides aegyptiacum*, SMNS 3543 or 'St. XVI (XX)' collected near or below Masjid et Tingje from the lowest white bed of the Mokattam Hills; specimen has been prepared as it was preserved in one block. Here too anterior ribs are pachyosteosclerotic and banana-like but posterior ribs are not. The specimen represents a developmentally mature animal notably smaller than *Eotheroides sandersi* and *Eotheroides clavigerum* described here. Abbreviations: C, cervical; L, left rib; R, right rib; Th, thoracic vertebra.

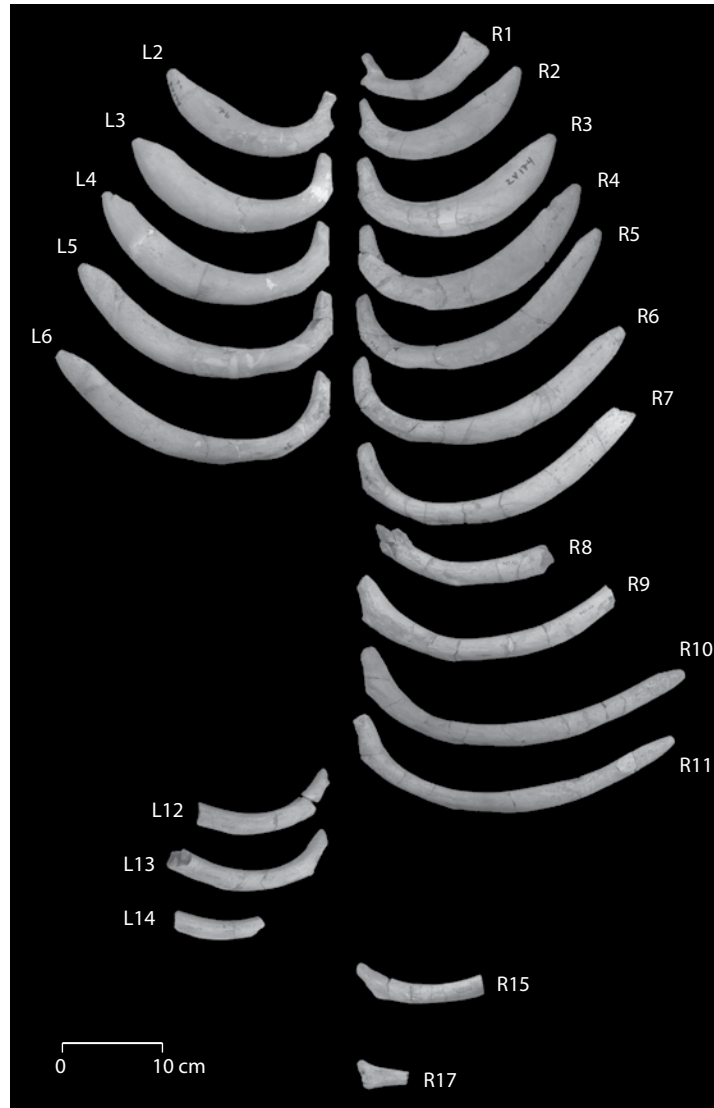


FIGURE 55 — Cranial view of left and right ribs of *Eotheroides sandersi* (UM 111558) from the Priabonian age Birket Qarun Formation of Wadi Al Hitan. Ribs are shown in anterior (cranial) view, arranged by size and morphology. Note the dense and swollen (pachyosteosclerotic) banana-like anterior ribs and thinner posterior ones. R1 has a straight and truncated distal end; the third rib R3 is the most pachyosteosclerotic; and the last rib in the preserved series R17 shows a convoluted head. Abbreviations: *L*, left rib; *R*, right rib.

The fifth rib (Fig. 55; Table 21) is longer, less pachyosteosclerotic, and slightly thinner than the fourth rib. Its neck is widened anteroposteriorly making it more conformable to the body of the rib. The capitular facets are roughly subequal. The mid-shaft of the bone is rectangular to semicircular in cross section. Internal muscle attachments are preserved on the medial surface as downwardly-trending striations. The distal end tapers to a flat attachment area for the costal cartilage.

Ribs 6 and 7 are longer than rib 5 (Fig. 55; Table 21). In these ribs, the ventral surface of the neck is flat, and the posterior surface of the neck is triangular in shape, flat, and pitted. Their tubercular fossae are small and shallow. The distal third of the

shaft in both ribs is twisted posteriorly from the mediolateral position of neck and head.

Rib 8 preserves its proximal half but is missing its capitular facets. The tuberculum is slightly elevated, and the tubercular fossa is narrow, shallow, and triangular in shape. Rib 9 preserves the upper two thirds of the body. It is distinct in having the largest flat attachment area posterior to the head and neck. The shaft is uniformly oval in cross-section. The tuberculum is roughly pyramidal in shape.

Rib 10 is the longest rib in the series (Fig. 55; Table 21), and it is compressed mediolaterally along its shaft. The posterior capitular facet is circular in shape and larger than the anterior

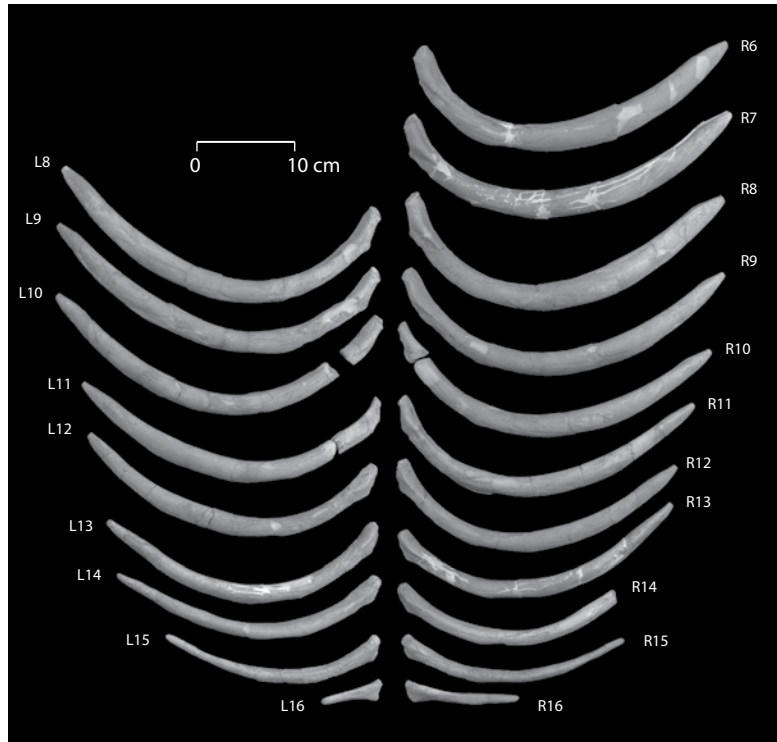


FIGURE 56 — Anterior (cranial) view of left and right posterior ribs of *Eotheroides sandersi* (UM 97514) from the Priabonian age Birket Qarun Formation of Wadi Al Hitan. Ribs are arranged according to their size and morphology. Abbreviations: *L*, left rib; *R*, right rib.

TABLE 22 — Measurements of left and right preserved ribs of *Eotheroides sandersi*, UM 97514. Abbreviations: *CM*, circumference around midshaft; *CT*, capitulum to tubercle length; *EAL*, external arc length; *IAL*, internal arc length; *L*, left rib; *MAWM*, maximum anteroposteriorly width of midshaft; *MLWM*, maximum mediolateral width at midshaft; *ND*, neck diameter; *R*, right rib; *TL*, total length. Measurements are in mm.

Rib	TL	EAL	IAL	CT	ND	CM	MLWM	MAWM
L8	329	416	374	45	24	90	31	23
L9	326	414	367	43	23	87	31	22
L10	310+	396	356	42	22	83	29	20
L11	—	—	—	40	22	84	31	20
L12	294	365	325	35	22	78	28	21
L13	272	330	342	31	22	74	26	19
L14	265	280	315	30	21	63	23	16
L15	215	225	251	27	18	59	21	15
L16	64	58	62	22	13	35	15	9
R6	324	428	368	47	27	102	35	28
R7	320	428	370	49	26	99	33	27
R8	315	421	360	47	24	94	36	30
R9	310	412	300	43	24	89	30	22
R10	—	—	—	42	—	87	29	23
R11	295	375	334	40	23	81	29	21
R12	270	358	318	32	20	76	25	19
R13	268	350	310	31	21	73	25	19
R14	228	288	262	32	18	65	22	15
R15	215	252	235	26	18	53	18	11
R16	118	120	115	22	12	37	13	12

facet. The dorsal surface of the neck shows a mediolateral scar that disappears at the base of the pyramidal tuberculum. The tubercular facet is a shallow, transverse groove. The posterior surface of the neck and the proximal side of the shaft are flat, with two rows of pits. The cross section of the shaft is uniformly oval. The anterior surface of the distal end tapers toward the attachment end for a costal cartilage, while the posterior surface is straight right to the end.

Rib 11 (Fig. 55; Table 21), along with the rest of the more posterior ribs, is shorter and more gracile. The neck is short, the shaft is thinner and less convex than the neck of the more anterior ribs, and the shaft cross-section is oval and smaller than in the shafts of the more anterior ribs.

Ribs 12 and 13 are partially preserved on the left side. Both show reduced shaft diameters and both are more elliptical in cross-section.

Rib 14 preserves a partial shaft from the left side. The distance between the medial end of the capitulum and the tubercular fossa is about 42 mm, which is shorter than the length of any of its antecedents.

The only free rib preserved posterior to rib 15 in UM 111558 (Fig. 55) fits with either thoracic vertebra rib facet 17 or 18, but not with the last thoracic. It is distinct in having a straight proximal end, as the tuberculum and capitulum are joined on the same surface. The proximal end is compressed anteroposteriorly, forming an anterodorsal ridge; the posterior proximal surface exhibits a shallow median groove; the cross-section of the shaft

TABLE 23 — Scapular measurements of *Eotheroides sandersi* sp. nov., CGM 42181 (holotype) and UM 111558 from the Birket Qarun Formation. Measurements are in mm.

Key	Measurement	<i>Eotheroides sandersi</i> CGM 42181 (right scapula)	<i>Eotheroides sandersi</i> UM 111558 (left scapula)
1	Scapular length along the spine	196	192
2	Spine length	103	106
3	Scapular breadth	61	65
4	Infraspinous fossa breadth	43	46
5	Neck breadth	36	34
6	Neck height	17	15
7	Distance from median glenoid cavity to acromion	38	29
8	Glenoid process breadth	47	43
9	Glenoid cavity breadth	36	34
10	Glenoid cavity height	25	26
11	Breadth of the acromion	—	6
12	Spine height from dorsal surface	—	21
13	Spine height from ventral surface	—	39
14	Distance between anterior tip of glenoid process and anterodorsal edge of blade	123	123
15	Distance between posterior tip of the glenoid process and first posterior edge of blade	93	85
16	Circumference of the blade	490	475

is oval. The last rib is distinct in being fused to the last thoracic vertebra (Fig. 55; Table 21).

In UM 97514 (Fig. 56; Table 22), all preserved ribs are from the posterior half of the ribcage, and are arranged in pairs in serial order from rib 6 through 16. The recovered ribs were arranged serially based on the size and morphology of the tuberculum and capitulum, the size and shape of the midshaft, the fit of the capitulum-tuberculum to rib facets on the vertebral bodies, and also comparison to specimens having more complete ribcages, such as UM 111558. The ribs of UM 97514 are equally dense (osteosclerotic), completely lacking any cancellous bone, but the anterior ones (the second third of the ribcage) are much more swollen (pachyostotic) than those of the posterior section of the ribcage, and therefore much heavier. The more anterior ribs in this specimen (R6 through R10) are slightly sigmoid in lateral view, with swept-back distal ends. The articular surfaces are well defined. A pit is present between the capitulum and tuberculum, with another just lateral to the tuberculum. The tuberculum protrudes in pyramidal fashion well above the rib's dorsal surface, as in the ribs of UM 97514. The distal end tapers abruptly in its last 40 mm.

Ribs from the last third of the thorax (R11 through R16) are likewise oval in cross-section and have subcylindrical shafts, but are much more slender. The capitular and tubercular facets are still distinct, but there is no space separating them. The



FIGURE 57 — Xiphisternum of *Eotheroides sandersi* (UM 111558) from the Priabonian age Birket Qarun Formation of Wadi Al Hitan. Specimen is shown in ventral (A) and dorsal (B) views. Notice the asymmetry, and the elliptical foramen near the posterior end of the bone.

anterior surface of the tuberculum slopes more gradually than the vertical posterior surface. The tuberculum continues to rise prominently above each rib's dorsal surface to the end of the ribcage, in contrast with some later dugongids, in which the tuberculum of the posterior ribs is a reduced and circumscribed feature on a broad and dorsoventrally compressed shaft. The last pair of ribs from this series (R16) has unequal lengths. The broken right rib was more than 118 mm long, while the left is only 64 mm long which is its natural length since its distal end shows the remnant of the costal attachment of the cartilage ligament. Both are only slightly curved and have dorsoventrally expanded proximal ends, the summits of which are formed by the tubercula. The capitulum is short, and neither it nor the tuberculum has a well-defined articular surface. Whether this is the last rib in the UM 97514 series is not clear, since the last thoracic vertebra is not preserved.

Sternebra

Xiphisternum.— (Fig. 57) UM 111558 preserves a sternal element that best fits in the xiphisternum position in the sternal series. The bone is asymmetrical. It is elongated craniocaudal, flattened dorsally, and slightly convex ventrally. It is greater than 102 mm in total length, 18 mm wide, 8 mm in dorsoventrally diameter, and it is wider and thicker cranially, while its distal portion is flattened. The proximal end has a central articulation



FIGURE 58 — Scapular and humeral elements of the holotype of *Eotheroides sandersi* (CGM 42181) from the Priabonian age Birket Qarun Formation of Wadi Al Hitan. A, two pieces of a left scapula in lateral view. B, left humerus in posterior view. C, right humerus in posterior view. D, right scapula in lateral view.

for the last mesosternum, and two lateral articulations for rib ends. The distal portion of the xiphisternum is perforated by a large elliptical foramen that measures 15 mm long and 4 mm wide; usually, this foramen is formed as a congenital oval defect in the lower third of the sternal series, either by incomplete fusion of sternal elements or disturbed ossification of cartilage.

The morphology of this sternal bone implies that the cranial sternal elements of this taxon were narrow and thickened. *Eosiren* sternal elements are flattened dorsoventrally, while in *Protosiren* they are more block-like (see below).

Forelimb

Scapula.— Two scapulae are known for this species. The first is the right scapula of the holotype (CGM 42181) (Fig. 58; Table 23), and the second is a well preserved left scapula from UM 111558 (Fig. 59; Table 23).

The right scapula in the holotype (Fig. 58; Table 23) has a total length of 198 mm and a maximum breadth of 61 mm across the spine. The scapular spine is 103 mm long, but missing its acromion process; it is slightly thickened and bears dull edges. The sickle-like scapula has its subscapular fossa laterally flattened with a slightly thickened anterior edge (cranial border) that has a semicircular outline and projects laterally, making the suprascapular fossa more or less convex. The glenoid fossa is ovoid in cross section and deep, wider and broader posteriorly, and smaller than those in *Eotheroides clavigerum*. Both the coracoid and the oval muscle scar on the medial side, which is shallow, are present.

The scapula of UM 111558 (Fig. 59; Table 23) is so far the most complete scapula to be recovered from an Eocene dugongid. It is 4 mm shorter than the scapula of the holotype. The spine is 106 mm thick, bearing a 23 mm long acromion process



FIGURE 59 — Forelimb elements of *Eotheroides sandersi* (UM 111558) from the Priabonian age Birket Qarun Formation of Wadi Al Hitan. A, left scapula, lateral view. B, left humerus, anterior view. C, right ulna, anterior view.

that projects downward and medially. The acromion rises 21 mm above the surface blade. The spine is thickened and widened at its dorsal end, and the middle part of the spine is thin and narrow. The glenoid fossa is similar to that of the holotype. Cranial and dorsal borders of the blade have semicircular and smooth outlines. The caudal and posterodorsal borders have anteriorly concave outlines; and more posterodorsally the blade is marked by a straight 35 mm long ridge (bordering the teres fossa). The infraspinous fossa and the anterior face of the spine are marked by rough striations. The subscapular fossa is concave and marked by a fan-shaped group of striations.

Humerus.— In the holotype (Fig. 58; Table 24), the right humerus is somewhat damaged and missing its greater tubercle. The proximal epiphyses are slightly fused. The left humerus is fragmentary. UM 111558 has a well preserved humerus (Fig. 59;

Table 24), with its proximal epiphyses fused. Both humeri are at least 10% shorter than the humerus of *Eotheroides clavigerum*.

In general, the humerus of this species is long and slender compared to most sirenians; its internal structure is dense and compact. The head has a rounded outline, and it is notched anteriorly at the top of the narrow and deep bicipital groove. The greater tubercle forms a thick and prominent flange, with a narrow surface for muscle attachment on its summit. The lesser tubercle is robust and rounded at the top, forming the medial wall of the bicipital groove. This groove ends in a shallow cul-de-sac, bounded posteriorly by the notched border of the head (cf. Sickenberg, 1934: fig. 4b). The deltoid crest is distinct and prominent, located about 58 mm from the top of greater tubercle. The sagittal diameter of the shaft (about 23 mm) exceeds the transverse diameter (18 mm).

TABLE 24 — Measurements of humeri of *Eotheroides sandersi* sp. nov., CGM 42181 (holotype) and UM 111558. Measurements are in mm.

Key	Measurement	<i>Eotheroides sandersi</i> CGM 42181	<i>Eotheroides sandersi</i> UM 111558
1	Maximum Length (greater tubercle to distal end)	137	155
2	Length from the head to the distal end	137	142
3	Maximum breadth of the proximal end	43	51
4	Head height	17	17
5	Head length	35	36
6	Head width	33	31
7	Width of the bicipital groove	13	9
8	Maximum width of the shaft in the middle	26	23
9	Minimum width of the shaft in the diaphyses	18	19
10	Minimum circumference of the shaft	71	70
11	Maximum breadth of the distal end	46	42
12	Breadth of the trochlea	32	31
13	Height of the trochlea	21	24
14	Height of the trochlea in the middle	15	18
15	Width of the olecranial fossa	20	20
16	Height of the olecranial fossa	16	28
17	Depth of the olecranial fossa	12	8

Ulna.— Only the right ulna is known for this species, from UM 111558 (Fig. 59; Table 25), and it is missing its olecranon and distal epiphysis. There is no sign that it was ever ankylosed to the radius (Fig. 59). It is slender and gracile, with a preserved length of 135 mm. The olecranon is short, rising 20 mm above the crescent notch, and it has an oval articular surface measuring 23 mm anteroposteriorly and 14 mm mediolaterally. The olecranon is tilted backward slightly (18°) from the axis of the shaft.

The lateral surface of the ulna bears no grooves like those found in *Protosiren smithae* below the level of the semilunar notch. The proximal part of the articular surface is distinct and mediolaterally convex, while the distal end of this articular surface is clearly notched and indented. A slightly depressed, nonarticular surface (perhaps for a humero-ulnar ligament) extends medially beyond the midline of the joint surface. Still more distally, the ulna widens abruptly and bears two articular surfaces: a lateral surface facing anteroproximally, and a medial surface facing more proximally. These are nearly separated anteriorly by a median notch, but no laterally-positioned radial notch is present. There are no signs of a rough surface for radius attachment below the front edge of the semilunar notch. The shaft is triangular in cross section, and becomes oval at its distal end (and convex medially). Medial and lateral margins of the distal end of the ulna bear slight rugosities, but not enough to ankylose with the radius.

UM 97515 is a very short ulna (Fig. 60; Table 25), only 95 mm in total length; it lacks its distal epiphysis, was not ankylosed with the radius, and clearly represents an immature animal. Nevertheless it is slightly larger than the specimen referred to *Eotheroides aegyptiacum* by Sickenberg (1934: 30-31, pl. 4, fig. 6; note that this illustration is about two-thirds natural size, not natural size as stated). It also differs from the latter in having a shorter olecranon (possibly due to loss of an epiphysis),

TABLE 25 — Ulna measurements of a fully mature *Eotheroides sandersi*, UM 111558 and a juvenile individual, UM 97515, compared to an incomplete ulna of *Eotheroides aegyptiacum*, SMNS St. XXX from the Lutetian of the Mokattam hills (illustrated in Sickenberg, 1934, page 30; plate 4, Figs. 6 a-b). Measurements are in mm.

Key	Measurement	<i>Eotheroides sandersi</i> UM 111558 (right ulna)	<i>Eotheroides sandersi</i> UM 97515 (left ulna)	<i>Eotheroides aegyptiacum</i> SMNS St. XXX (right ulna)
1	Greatest length	136	98	—
2	Length of olecranon	21	21	22
3	Smallest depth of olecranon	24	24	15
4	Greatest depth at the anconeal process	26	26	13
5	Height of the trochlear notch	22	23	21
6	Mediolateral breadth of proximal articular surface (coronoid process)	30	26	25
7	Height from the coronoid process to the distal epiphysis	98	66	—
8	Mid shaft circumference	50	44	—
9	Width of the distal epiphysis	16	13	—
10	Length of the distal epiphysis	24	20	—



FIGURE 60 — Left ulna of a juvenile individual of *Eotheroides sandersi* (UM 97515) from the Priabonian age Birket Qarun Formation of Wadi Al Hitan. Ulna is missing its distal epiphysis, and it was not co-ossified with the radius. This is the smallest sirenian individual recovered from Wadi Al Hitan. A, medial view. B, anterior view. C, lateral view.

whose anterior edge is less vertical and not as sharp. The articular surface is not divided into lateral and medial portions by a ridge, and the shaft is semicircular rather than triangular in cross-section. The flat, rugose area where the bone was sutured to the radius has an oblique orientation, suggesting a degree of torsion of the radius and ulna similar to that seen in Sickenberg's specimen. Medial to this area is a large and distinct oval pit. The shaft has an oval cross-section; its distal end remains oval, but with slight enlargement of the cross-sectional area.

Manus.— The known hand elements for *Eotheroides sandersi* include a left metacarpal III (Fig. 61; Table 26), and a probable left metacarpal V. Both elements belong to UM 111558.

Metacarpal III is 53 mm long, minus its distal epiphysis. The proximal third of the metacarpal is compressed anteroposteriorly. Its midshaft has a rounded cross-section, and it is hemispherical

distally. The proximal articular surface possesses three small facets connected with sharp edges and grooves; the most anterior of these facets is a 5-mm, rounded, circular surface separated from the posterior facets by a shallow groove. The posterior facets are connected along a sharp edge that runs dorsoventrally.

Metacarpal ?V, also preserved in UM 111558, is missing its distal shaft. The proximal end and shaft are flattened dorsoventrally. The proximal carpal articular facet is partly preserved. It originally had a trapezoidal outline, with a wide ventral surface marked by a groove.

Hind limb

Innominate.— The holotype of *Eotheroides sandersi*, CGM 42181 (Fig. 62; Table 27), includes a partial left and a partial right innominate. The left innominate is missing the pubic portion, and portions of the ventral side of the ischium.



FIGURE 61 — Left metapodials and carpal (?) of *Eotheroides sandersi* (UM 111558) from the Priabonian age Birket Qarun Formation of Wadi Al Hitan. Metacarpal III, *Met. III*, is distinguished by an oblique proximal articulation. Metacarpal V, *Met. V*, is distinguished by having a blunt posterior edge.

Further, the acetabulum is weathered. The right innominate is just a poorly preserved ilium. The pelvis of this individual is small; the proximal end of the ilium is clublike, but it is not as swollen as is the case in UM 97514 (Fig. 63; Table 27). The medial side of the ilium is flat, and bears irregular bumps and pits where it attached to the sacrum. The medial side of the ilium has no large cavity like that in some other specimens. The acetabulum is shallow, the posterior end of the ischium is flat, and the obturator foramen is damaged. The flattened ischium and its lack of rugosity or tuberosity indicate that this is a female innominate (see below).

The pelvic bones of UM 97514 (Fig. 63; Table 27) are well preserved. The ilium is club-shaped, with a convex lateral surface. The proximal half of the medial surface is flat and rugose where it was in direct contact, via cartilage and ligaments, with the rugose lateral surface of the sacral ala. After narrowing slightly distal to the sacroiliac joint, the shaft of the ilium broadens again at the acetabulum, which has a diminutive, deep, smooth-surfaced, ellipsoidal cavity 18 mm in greatest diameter. The dorsal lip of the acetabulum overhangs the socket, and this lies in approximately the same horizontal plane

TABLE 26 — Metacarpal dimensions of *Eotheroides sandersi* sp. nov., UM 111558. Abbreviation: *Met.*, metacarpal. Measurements are in mm.

Measurement	Met. III	Met. V
Total length	>53	—
Proximal width	14	18
Distal width	14	—
Proximal height	15	10
Distal height	10	—
Midshaft width	9	11
Midshaft height	8	6

as the ventromedial limit of the articular surface when the bone is held in its correct anatomical position. There is no distinctly demarcated acetabular notch. The entire ventral third of the acetabulum is roughened, in contrast to the smooth articular upper portion.

Distal to the acetabulum there is a broad, flat ischium, whose dorsal edge continues the gently concave curve of the ilium. The long axis of the ischium forms an angle of about 135° with the ilium. The posterior end of the ischium is thickened, and flares outward abruptly below a line extending from the middle of the ventral edge to the posterodorsal corner. The entire margin of this flared portion is 10-15 mm thick and rugose. It is also roughened somewhat on its posteromedial surface and on the vertical medial surface of the posterodorsal end. The latter two surfaces, both slightly concave, are separated by a broadly convex horizontal ridge.

The degree of lateral flaring of the distal end of the ischium is comparable to or greater than that which today characterizes male *Dugong*, in contrast to females (Domning, 1991). The most notable features of this specimen are the extremely long and narrow pubic ramus, and the small obturator foramen that it partly surrounds. The foramen is oval, measuring 14 mm \times 8 mm, and it lies about 10 mm below the acetabulum (Fig. 63; Table 27). The pubic ramus is about 18 mm wide and 10 mm thick. This extends 53 mm downward, medially, and slightly forward from the obturator foramen. Here it ends in a rugose symphyseal surface 20 mm long and 12 mm wide. This is flat ventrally and convex dorsally (preserved only on the left side).

Femur.— Three femora of *Eotheroides sandersi* are known from two individuals, and all are missing their proximal and distal epiphyses. The holotype, CGM 42181 (Fig. 64; Table 28), preserves both of its femora, while UM 111558 preserves only the left femur.

The proximal end of these bones is broad and flat, lacking a trochanteric fossa. The lesser trochanter is faintly marked. The shaft has a rounded cross-section, and is nearly straight but slightly concave anteriorly. The distal end of the shaft is ovoid to diamond-shaped. The length of the femur in CGM 42181 is 91 mm, which is 10% shorter than that of UM 111558 (Fig. 64; Table 28).



FIGURE 62 — Left and right innominates and femora of the holotype of *Eotheroides sandersi* (CGM 42181) from the Priabonian age Birket Qarun Formation of Wadi Al Hitan. A, left innominate in lateral view. B, left femur in anterior view. C, right femur in anterior view. D, right ilium in lateral view. Note the expanded proximal ends of the ilia, and the relatively small size of the femora.

When compared to femora of *Protosiren* (Fig. 65; Table 28), and based on their morphology and size, the femora of *Eosiren* and *Eotheroides* are grouped together because they represent an advanced stage of hindlimb reduction and adaptation to a fully aquatic mode of life. *Eosiren* has a femur with a rounded shaft.

The head is reduced and oval-shaped. The proximal end is broad and flat. It has no trochanteric fossa, and the lesser trochanter is not preserved. *Eotheroides* has a nearly straight broad shaft that is slightly concave anteriorly. Unfortunately, proximal and distal condyles have not been recovered for this taxon.

TABLE 27 — Measurements of innominate pelvic bones of *Eotheroides sandersi* sp. nov., CGM 42181 (holotype) and UM 97514, from the Birket Qarun Formation. Measurements are in mm.

Key	Measurement	<i>Eotheroides sandersi</i> CGM 42181 (left pelvis)	<i>Eotheroides sandersi</i> UM 97514 (right pelvis)	<i>Eotheroides sandersi</i> UM 97514 (left pelvis)
1	Total length of the pelvis	153	190	186
2	Length of the ilium from the center of the acetabulum to proximal end	107	113	107
3	Dorsoventral diameter of ilium at midshaft	17	21	21
4	Mediolateral diameter of ilium at midshaft	19	21	20
5	Circumference ilium at midshaft	60	67	65
6	Symphysis length	—	18	18
7	Length of the pubic line from the center of the acetabulum	—	66	75
8	Pubic ramus in front of the obturator foramen	7	12	12
9	Pubic ramus behind the obturator foramen	7	22	21
10	Acetabulum diameter	16	18	17
11	External diameter of the acetabulum	18	21	23
12	Acetabulum depth	5	10	10
13	Obturator foramen length	5	9	8
14	Obturator foramen height	5	13	13
15	Length of the ischium from the center of the acetabulum	48	89	91
16	Dorsoventral depth of the ischiac ramus	30	34	34
17	Ramus of Ischium thickness (mediolaterally)	6	13	11
18	Maximum dorsoventral length of the distal end of the ischium	27	53	52
19	Maximum mediolateral thickness of the distal end of the ischium	6	16	16
20	Distance between the inner posterior edge of the obturator foramen and the ischiac tuberosity	47	99	94
21	Length of the sacral articulation surface with the sacrum (anteroposterior length of the oval articulation)	31	52	45
22	Height of the sacral articulation surface with the sacrum (dorsoventral height of the oval articulation)	16	31	33
23	Maximum height of the proximal end of the ilium dorsoventrally	27	31	33
24	Maximum width of the proximal end of the ilium mediolaterally	23	29	28

TABLE 28 — Femur dimensions of Eocene Egyptian sirenians, including those of *Eotheroides sandersi*, *Eosiren libyca*, and *Protosiren smithae* from the Priabonian of the Birket Qarun and Qasr El Sagha formations. *Protosiren smithae* is the largest. Both specimens of *Eotheroides sandersi* are missing their proximal and distal epiphysis. Measurements are in mm.

Key	Measurement	<i>Eotheroides sandersi</i> CGM 42181 (right femur)	<i>Eotheroides sandersi</i> UM 111558 (left femur)	<i>Eosiren libyca</i> UM 101226 (right femur)	<i>Protosiren smithae</i> CGM 42292 (right femur)
1	Greatest length	—	—	108	144
2	Total length from the femoral head	—	—	108	138
3	Head height	—	—	9	13
4	Head length anteroposteriorly	—	—	13	20
5	Head width mediolaterally	—	—	20	27
6	Greatest proximal width	19	20	26	48
7	Length of the femoral body	91	102	98	122
8	Width across the second trochanter	14	15	18	30
9	Minimum width of the diaphysis	9	7	11	19
10	Minimum circumference of diaphysis	28	25	14	52
11	Minimum width of the distal end	12	11	16	21
12	Greatest width of the distal end	12	12	13	35
13	Width between the external ends of the distal condyles	—	—	6	26
14	Internal distance between the distal condyles	—	—	—	5

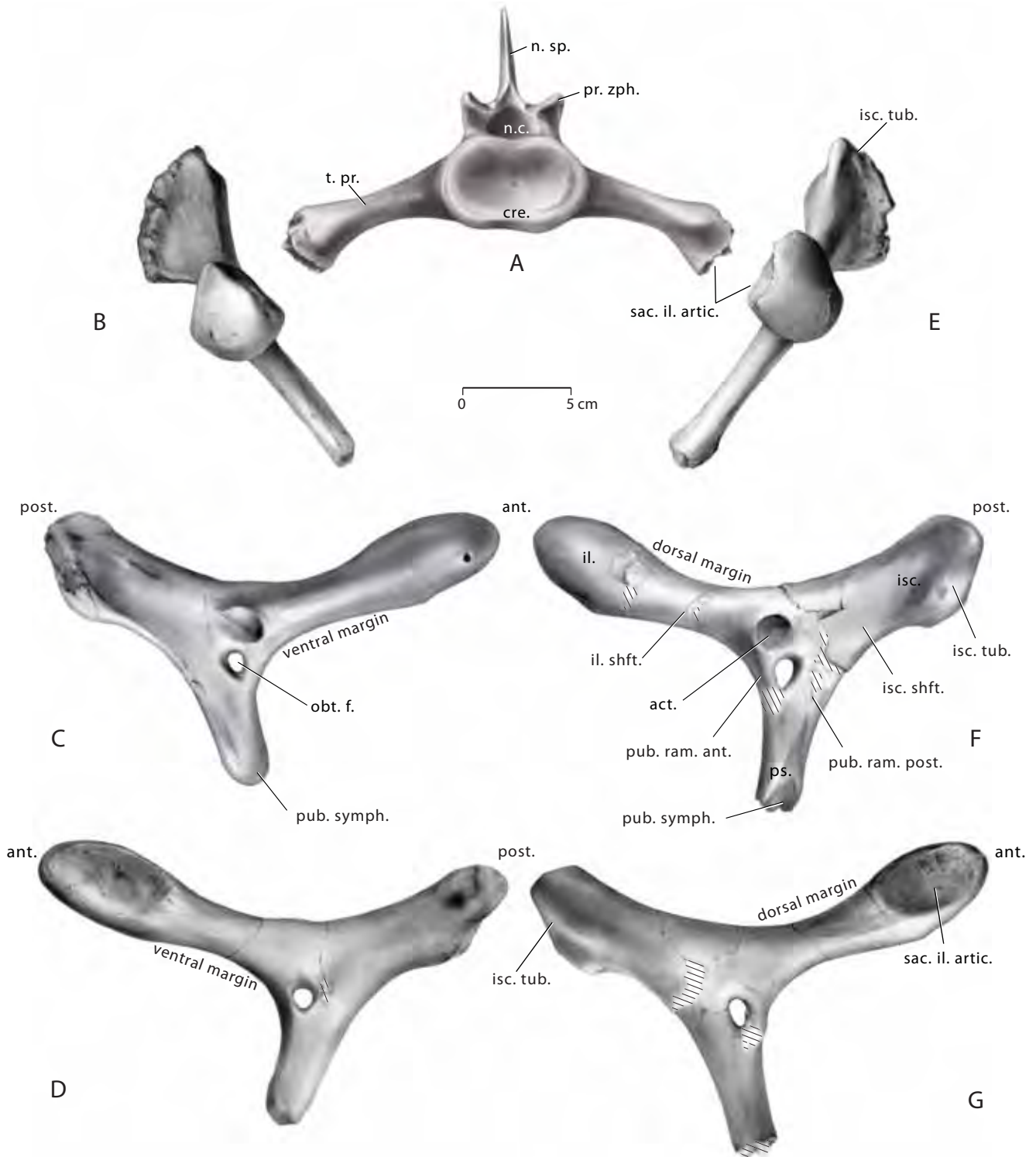


FIGURE 63 — Sacrum and left and right innominates of *Eotheroides sandersi* (UM 97514) from the Priabonian age Birket Qarun Formation of Wadi Al Hitan. A, sacrum in cranial view. B-D, right innominate in anterior (cranial), lateral, and medial views. E-G, left innominate in anterior (cranial), lateral, and medial views. Note the enlarged club-like proximal end of the ilium; the long, narrow, unfused pubis; and the reduced acetabulum and obturator foramen. Abbreviations: *act.*, acetabulum; *act. n.*, acetabular notch; *cre.*, cranial epiphysis; *dor. il. sp.* dorso iliac spine; *il.*, ilium; *isc.*, ischium; *isc. tub.*, ischiac tuberosity; *isc. shft.*, ischiac shaft; *n. c.*, neural canal; *n.sp.*, neural spine; *obt. f.*, obturator foramen; *pr. zph.*, prezygapophysis; *ps.*, pubis; *pub. symph.*, pubic symphysis; *pub. cleft*, pubic cleft; *pub. ram. ant.*, anterior pubic ramus; *pub. ram. post.*, posterior pubic ramus; *sac. il. artic.*, sacroiliac articulation surface; *sac. il.*, sacral pleurapophyses, *t. pr.*, transverse process.



FIGURE 64 — Femora of *Eotheroides sandersi* (A-D) compared to that of *Eosiren* sp. (E-F). A-B, left femur of the holotype of *Eotheroides sandersi* (CGM 42181) from the Priabonian age Birket Qarun Formation of Wadi Al Hitan, in anterior and posterior views. C-D, left femur of *Eotheroides sandersi* (UM 111558) from the Priabonian age Birket Qarun Formation of Wadi Al Hitan, in anterior and posterior views. E-F, anterior and posterior views of the right femur of *Eosiren* sp. (UM 101226) from the Priabonian age Qasr el-Sagha Formation north of Birket Qarun in Fayum. UM 101226 is the only femur of *Eosiren* preserving both the proximal and distal ends. The small size of all of these femora demonstrate that there were no substantial lower limb or foot elements connected to them.

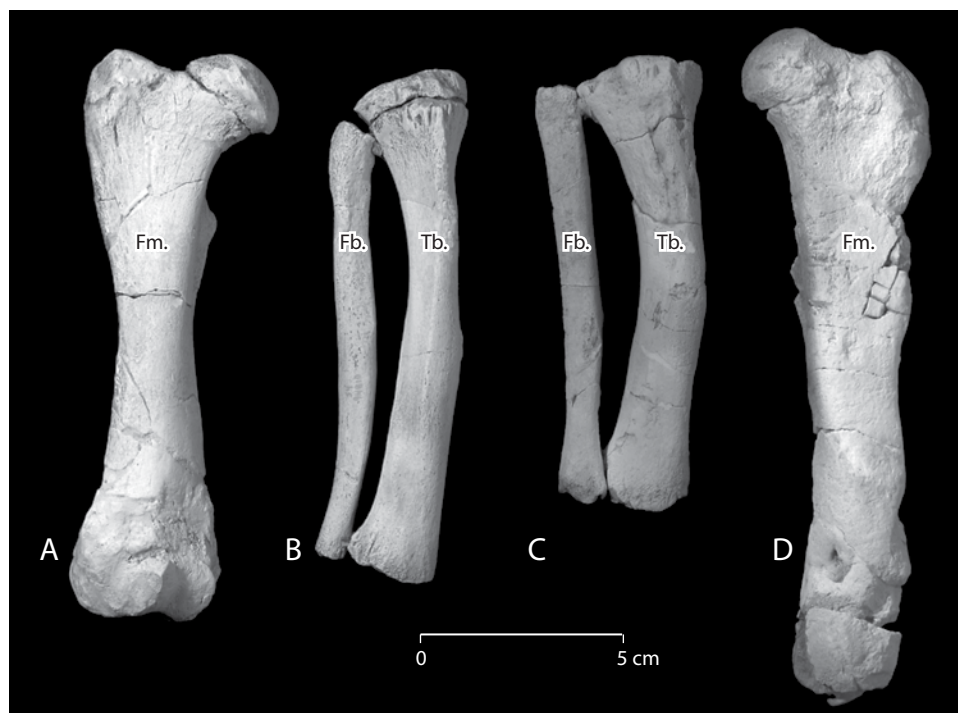


FIGURE 65 — Femora, tibiae, and fibulae of Bartonian and Priabonian *Protosiren* from Egypt and Pakistan. A-B, right femur, tibia, and fibula of the holotype of *Protosiren smithae* (CGM 42292) from the Priabonian age Birket Qarun Formation of Wadi Al Hitan, in anterior view; note the presence of the proximal epiphysis on the tibia. C, right tibia and fibula of *Protosiren smithae* (UM 101224) from the Priabonian age Birket Qarun Formation of Wadi Al Hitan, in anterior view; note the absence of the proximal epiphysis on the tibia. D, left femur of *Protosiren sattaensis* (GSP-UM 3197) from the Bartonian of the Drazinda Formation in the Sulaiman Range of central Pakistan. The size and form of these hindlimb elements suggest that the distal leg was still functional and possibly used in swimming. Abbreviations: *Fb.*, fibula; *Fm.*, femur; *Tb.*, tibia.

IV

COMPARISONS AND RELATIONSHIPS OF WADI AL HITAN *EOTHEROIDES*

The phylogeny and systematics of fossil and living Sirenia have been reviewed by Domning (1994, 1996), who identified many synapomorphies of Dugongidae and its subgroups useful for placing the Fayum Eocene sirenians in a phylogenetic framework. Based on Domning's analysis, *Eotheroides clavigerum* and *Eotheroides sandersi* belong to the family Dugongidae because they have the following derived characters: enlarged premaxillary rostrum; enlarged infraorbital foramen; incised palate; extension of the squamosal to the temporal crest; well developed processus retroversus of the squamosal; dP5 not replaced by a permanent premolar in the upper and lower jaws; innominate with a short, rounded ilium; and femora very reduced compared with femora of Protosirenidae.

Eotheroides clavigerum and *Eotheroides sandersi* from the Priabonian of the Birket Qarun Formation are phylogenetically closest to *Eotheroides aegyptiacum* (Owen, 1875) from the Lutetian nummulitic limestone beds near Cairo. All three species share the following derived characteristics: prominent falx and bony tentorium projecting from the roof of the braincase; nasals long and contacting along the midline; palate broad, with its posterior border lying posterior to the toothrow; and anterior ribs pachyosteosclerotic.

E. sandersi differs from the older species *E. aegyptiacum* in being slightly larger; bearing arched nasals; having frontals contacting the parietals along a deep V-shaped suture marked by a pair of lateral prominences (in *E. aegyptiacum* the contact is W-shaped); and having a longer, wider, and less arched cerebrum compared to the holotype of Owen (1875) and to the braincase published in Abel (1913: plate 4, figs. 3-5). The supraoccipitals of *Eotheroides sandersi* (CGM 42181) are hexagonal in shape, projecting posteriorly from the parietals at an angle of 133°; muscle insertions here form rounded depressions; and the distal lateral sides intersect one another posteriorly to form a V-shaped corner. Conversely, the supraoccipitals of *E. aegyptiacum* illustrated in Abel (1913: plate 2, fig. 1 and plate 4, figs. 3-5; 1928: p. 496) have a straight contact with the exoccipitals; their muscle insertions are not depressions; and they are shifted toward the upper and lateral corners of the supraoccipitals. Also, the supraoccipital and parietals of *E. aegyptiacum* are perpendicular.

The ribcage of the *Eotheroides aegyptiacum* specimen illustrated in Abel (1912: fig. 13; 1919: 836, fig. 663) and discussed in Sickenberg (1937: p. 24-25), illustrated here in Figure 54C, differs from those of the Priabonian species of *Eotheroides* from Wadi Al Hitan in that the fifth rib of *E. aegyptiacum* is the most pachyosteosclerotic, while the third rib is the most pachyosteosclerotic in *E. sandersi* and *E. clavigerum*.

E. clavigerum is at least 30% larger than *E. aegyptiacum* of Owen (1875) in overall skeletal dimensions, and it is at least 70% larger in dental dimensions. The larger species has its unusual nasals convex upward, while the nasals of *E. aegyptiacum* are more or less flattened dorsally and level with the frontals and parietals. Postcranial elements of both species show pachyosteosclerosis in the thoracic vertebrae and ribs; however, *Eotheroides clavigerum* exhibits extreme pachyosteosclerosis in its anterior ribs.

Eotheroides clavigerum is at least 7% larger than *Eotheroides sandersi* in cranial dimensions, and is 25% to 44% larger in dental dimensions (Fig. 66). It is also 7-31% larger in skeletal dimensions. Moreover, its nasals are more convex upward and more arched than in *E. sandersi*. In addition, the innominate of *Eotheroides clavigerum* bears a short, club-like ilium; a flat, broad, and thin ischium; a small obturator foramen; and a short, gracile, unfused, and medially-pointed pubic ramus on each side, lacking a true public symphysis. The pelves of *Eotheroides sandersi* differ from those of the larger, contemporaneous *Eotheroides clavigerum* by their unusually long pubic rami, unlike those in any other sirenian, and by their variability in robustness and thickening of the ischiac tuberosity, interpreted as sexual dimorphism (see Chapter VI).

Domning et al. (1982: 56, fig. 34) described a partial lower jaw of a dentally immature dugong, YPM 24851 (Fig. 67), which was recorded as being from the Qasr El Sagha Formation near 'Zeuglodon Valley' (Wadi Al Hitan). However, the preservation almost certainly indicates derivation from the Birket Qarun Formation (without a specific locality). The preservation and mineralization of this jaw is common in the fine sandstone facies above what is called the University of Michigan Camp White Layer (CWL; Gingerich 1992). The specimen (YPM 24851) is interpreted as *Eotheroides*, probably *E. sandersi*, because it has a laterally compressed mandibular symphysis. It is possible that YPM 24851 is the dentary of UM 97514, which was found on an open plain within easy walking distance of an old Yale camp. Unfortunately the partial mandible of the holotype of *E. sandersi* (CGM 42181) lacks features that would aid comparison with YPM 24851.

Domning et al. (1982) described Smithsonian specimens from the Eocene of North Carolina as *Protosiren* sp. These are in fact the first potential *Eotheroides* representatives from North America. This assessment is based on a well preserved lower jaw with permanent teeth (USNM 214596, Fig. 68; compare with the dentary of *Protosiren* in Fig. 69). This assessment is also based on cervical and thoracic vertebrae, anterior ribs with

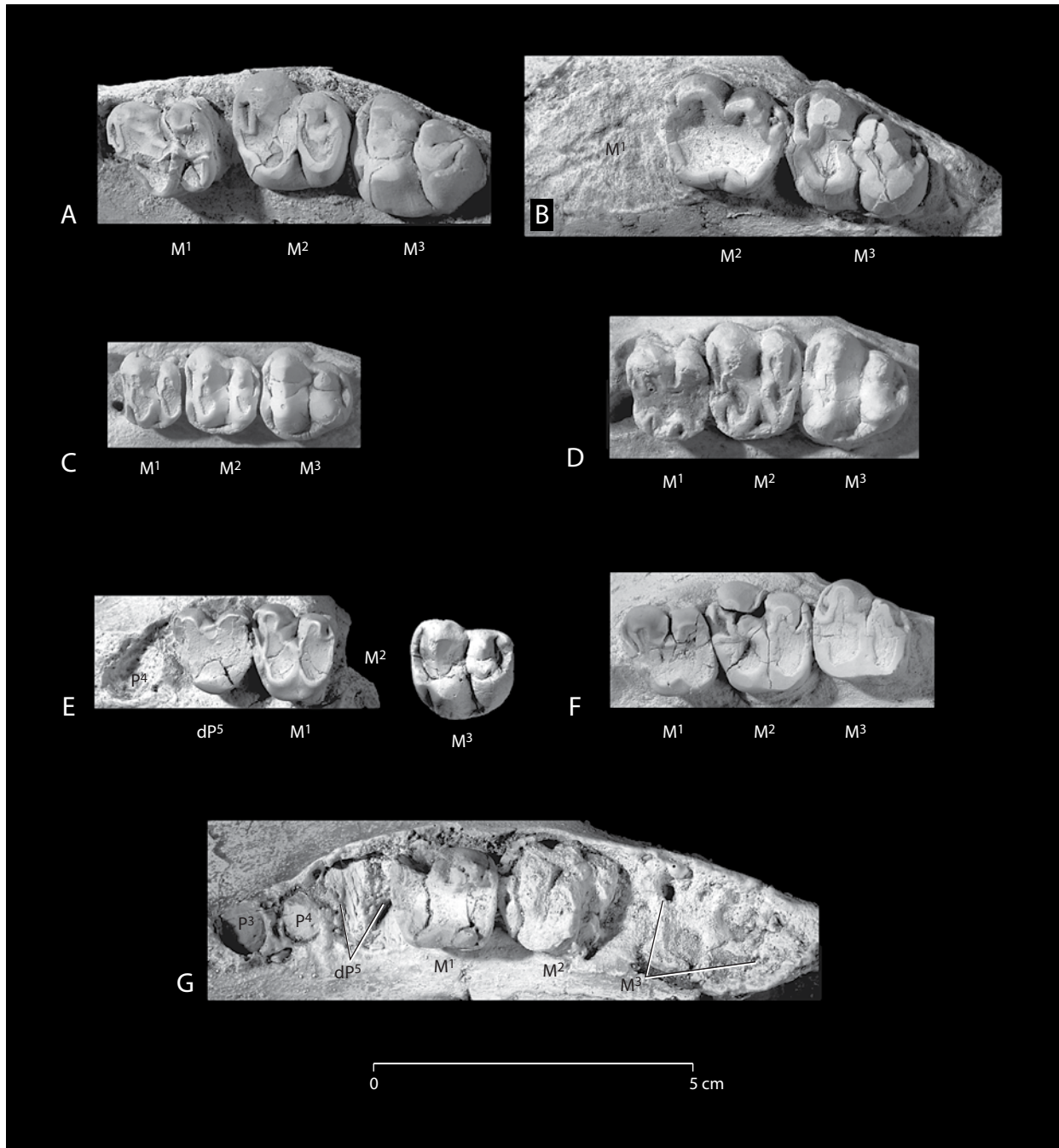


FIGURE 66 — Upper left cheek teeth of Paleogene sirenians from Cairo and Fayum. A, *Protosiren fraasi* from the middle Eocene Mokattam Limestone near Cairo (CGM 10171). B, *Protosiren smithae* from the late Eocene base of the Birket Qarun Formation in Wadi Al Hitán (CGM 42292). C, *Eotheroides sandersi* from the late Eocene middle part of the Birket Qarun Formation in Wadi Al Hitán (UM 111558). D, holotype of *Eotheroides clavigerum* from the late Eocene base of the Birket Qarun Formation in Wadi Al Hitán (CGM 60551). E, *Eosiren* sp. from the late Eocene Qasr El Sagha Formation north of Birket Qarun in Fayum (CGM 42180). F, *Eosiren stromeri* from the late Eocene Qasr El Sagha Formation north of Birket Qarun in Fayum (UM 100137). G, *Eosiren imenti* from the early Oligocene of the Gebel Qatrani Formation (CGM 40210). Note that Protosirenidae have enlarged and robust molars bearing smooth enamel and a strong anterior cingulum, with a large and rounded metaloph on M³. *Eotheroides* has quadrate first and second molars, with strong lingual cingula. *Eosiren stromeri* differs from *Eosiren libyca* in having a second molar significantly larger than M³. *Eosiren imenti* is the largest of all Eocene and Oligocene dugongs seen in Egypt.

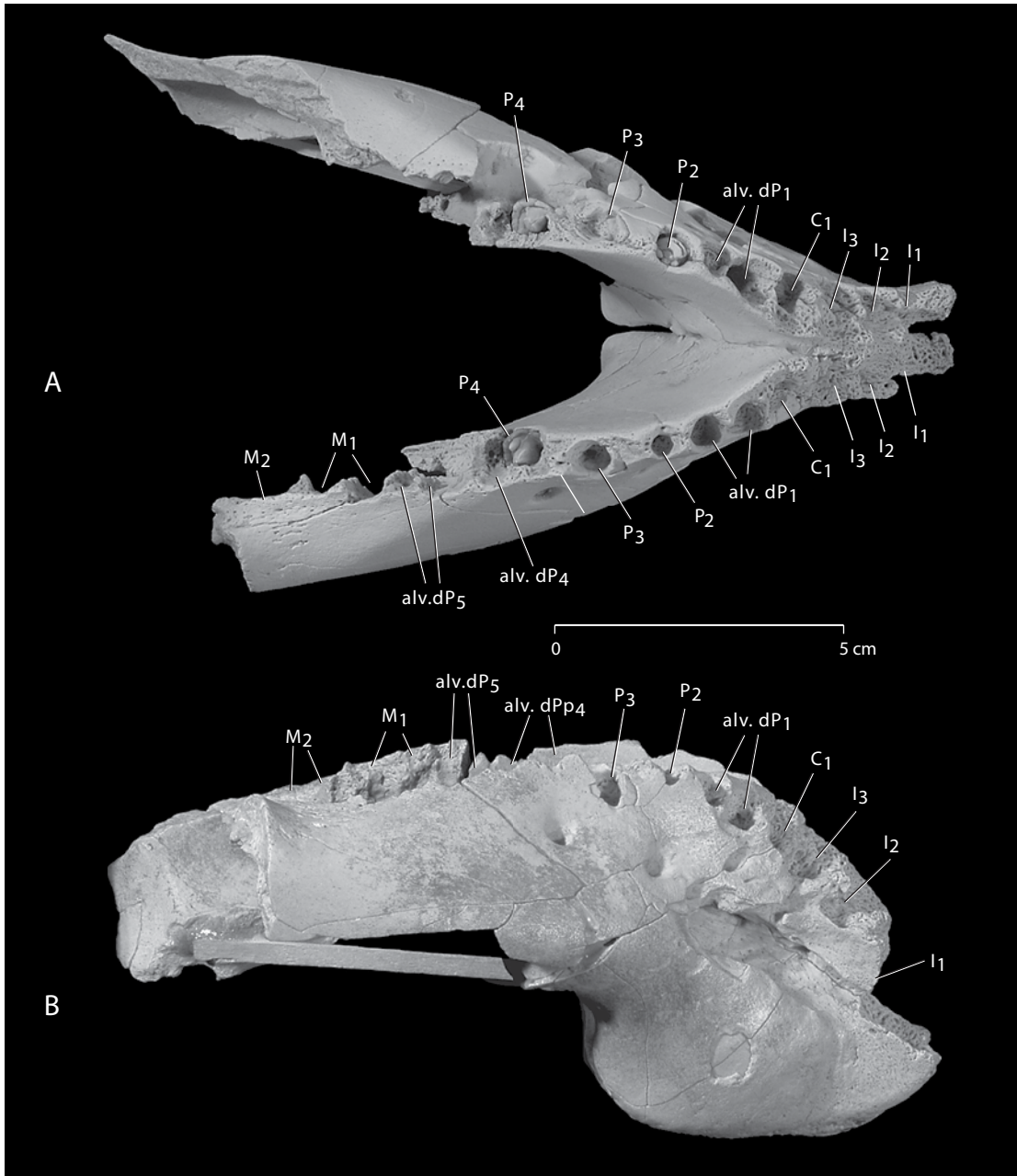


FIGURE 67 — Mandible of a late Eocene dugongid (YPM 24851) collected from Wadi Al Hitan and described by Domning et al. (1982). Mandible is shown in occlusal (A) and right lateral view (B). YPM 24851 is an immature individual as indicated by the erupting permanent teeth and remnants of alveoli for deciduous teeth. The dental formula and tooth count are based on the maximum number of teeth found in the most primitive sirenians (3.1.5.3). Abbreviations: *alv.dp_x*, alveoli of deciduous premolars; *C*, canine; *dP_x*, deciduous premolars; *M_{1-x}*, molars; *P_{1-x}*, premolar.

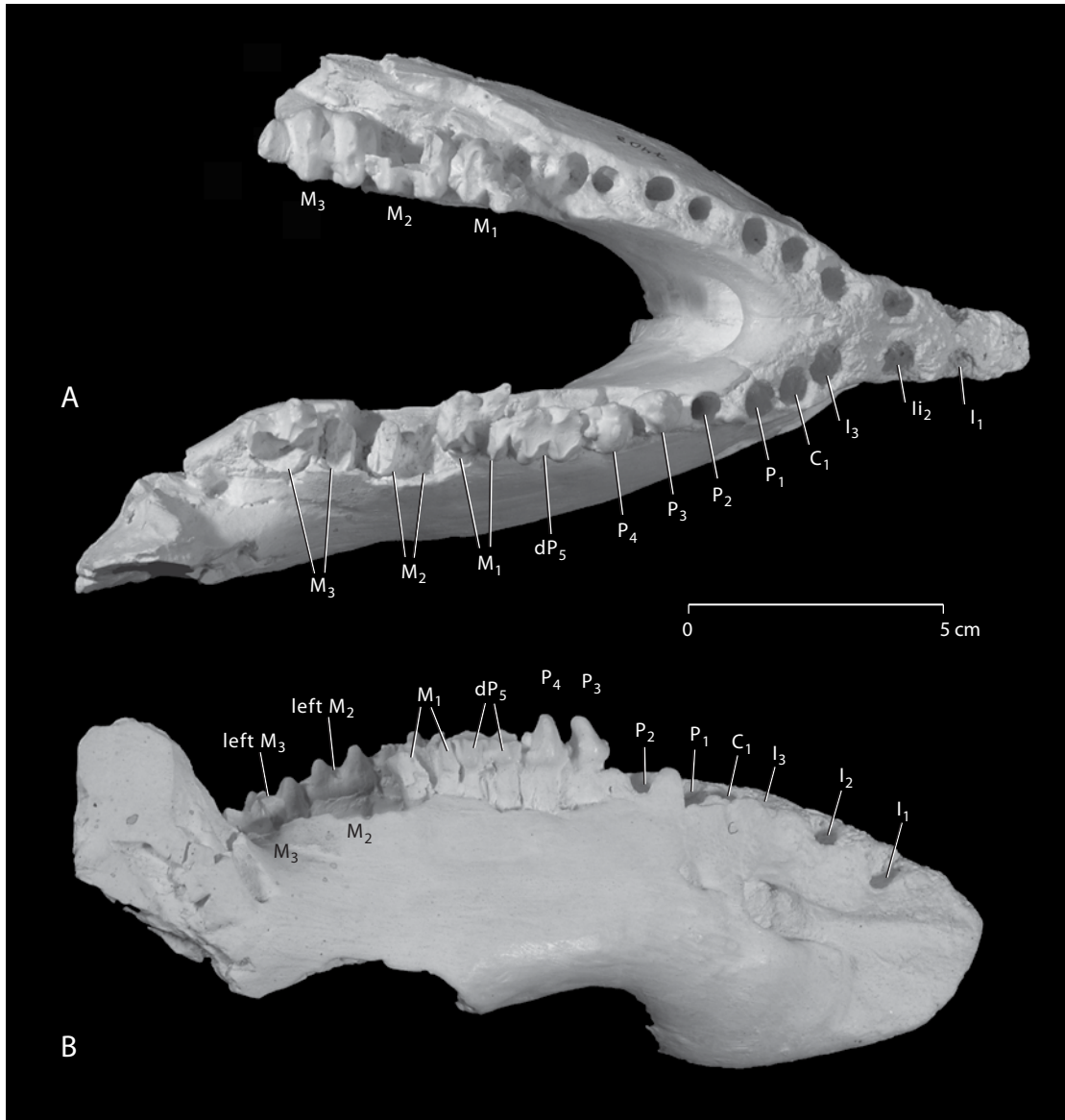


FIGURE 68 — Mandible of late Eocene *Eotheroides* sp. from North Carolina (USNM 214596). Mandible is shown in occlusal (A) and right lateral view (B). The specimen was described as *Protosiren* sp. in Domning et al. (1982). However, associated postcrania show that this is an adult Eocene dugong instead. Dental formula of the lower jaw is 3.1.5.3. Note the narrowing of the tip of the masticating rostrum and the weak arching of the central surface of the mandible. Abbreviations: *C*, canine; *dP_x*, deciduous premolars, *P_{1-x}*, premolar; *M_{1-x}*, molars.

well-developed pachyosteosclerosis and quadric cross-sections, a partial humerus and ulna, and a partial pelvic bone. The ribs and vertebrae are similar to those of *Eotheroides* from Mokattam and Fayum. However, the North Carolina taxon differs from *Eotheroides sandersi* and *Eotheroides clavigerum* in having a gently arched ventral outline of the mandible, and a very small degree of deflection of the mastication surface at the symphysis (which is greater in Egyptian *Eotheroides*). The North Carolina taxon also differs in retaining a very narrow mandibular lip (see Fig. 68).

The dental formula of the lower jaw of USNM 214596 is 3.1.5.3, the same as in *Eotheroides clavigerum* (CGM 60551; Fig. 29) and *E. sandersi* (UM 100138; Fig. 45). The rudimentary innominate associated with the postcranial and cranial elements was described in Domning et al. (1982: fig. 33), who interpreted it to belong to an animal at an advanced stage of aquatic adaptation similar to that of *Eosiren libyca*.

Within Dugongidae, the nearest relatives to *Eotheroides* are: *Eosiren* (Andrews, 1902b), *Prototherium* (de Zigno, 1875), *Sirenavus* (Kretzoi, 1941), and *Halitherium* (Kaup, 1838a,b).

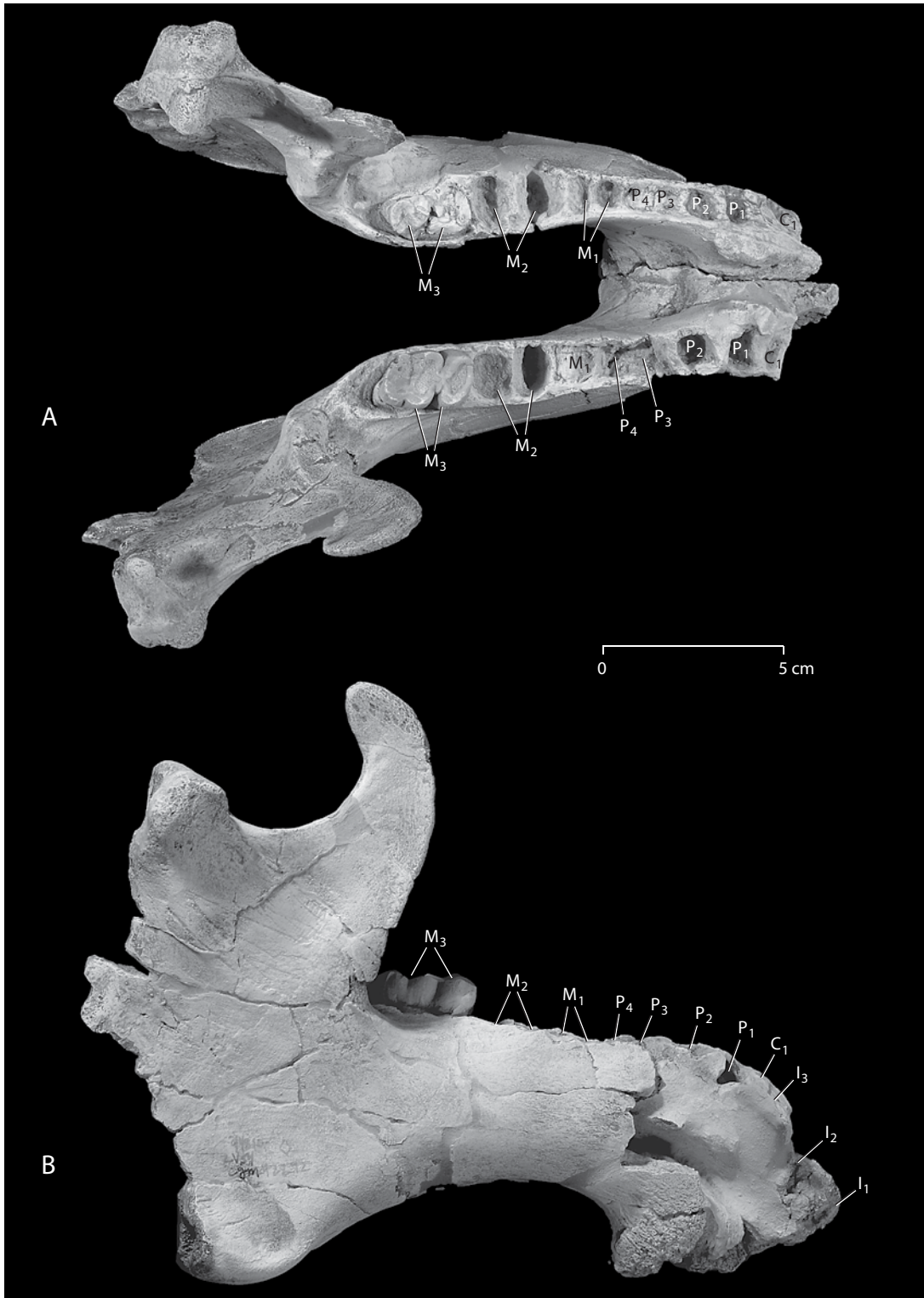


FIGURE 69 — Mandible of late Eocene *Protosiren smithae* (CGM 42292) described by Domning and Gingerich (1994). Mandible is shown in occlusal (A) and right lateral view (B). *Protosiren smithae* has lost its fifth premolar in both upper and lower jaws, and the dental formula for the lower jaw is 3.1.4.3. Abbreviations: C, canine; dP_x , deciduous premolars, P_{1-x} , premolar; M_{1-x} , molars.

Eosiren evidently overlapped with *Eotheroides* to some extent in space and time, as it is reported from the Lutetian (middle Eocene) through the Priabonian (late Eocene) of Egypt. *Prototherium*, *Sirenavus*, and *Halitherium* are spatially separated from *Eotheroides*, as they were evidently restricted to the middle and late Eocene of Europe.

Eosiren, including all species known from the Eocene and Oligocene of Egypt, is distinguished from *Eotheroides* in the following characteristics: larger body size; more robust skull and lower jaws; broader and more flattened skull roof, with laterally flared supraorbital processes (as seen in *Eosiren imenti* from the Oligocene of the Gebel Qatrani Formation; Domning et al., 1994); nasals separated from each other (in *Eosiren imenti*) or in slight contact (in *Eosiren libyca*); presence of a very narrow maxillary-palatal gutter; jugals contributing extensively to the anteromedial margins of the orbit; presence of a true foramen ovalis (the fissura ovalis is closed posteriorly by a bony bridge in *Eosiren abeli*, Abel, 1913: 55, fig. 4 'skull IV', and in *Eosiren stromeri*, UM 100137); enlarged cheek teeth with the dental formula 1-3.1.5.3 / 3.1.5.3; and lower jaws lacking a compressed anterior lip (see UM 100137, Fig. 70).

In addition, vertebrae of *Eosiren* retained large, heart-shaped centra, marked by a ventral keel in the thoracic region (Figs. 71, 72), and long neural spines in the anterior and mid-thoracic region. Vertebrae of *Protosiren* are distinctly different in having higher neural spines and large keyhole-shaped vertebral canals (Figs. 73, 74). Anterior ribs of *Eosiren* are osteosclerotic and a little thickened (Fig. 75), but lack the pachyostosis of *Eotheroides*. Ribs of *Protosiren* are even more gracile and differ in having cartilaginous rather than synovial articular surfaces (Fig. 76). Innominates of *Eosiren* are very reduced (Fig. 77E, F), with ilia that are gracile and an obturator foramen that is either closed or little more than a pin hole.

The xiphisternum of *Eotheroides* (Fig. 78E, F) is long and narrow, while sternbrae of *Protosiren* are more blocky (Fig. 78A-D), and sternbrae of *Eosiren* are broad and relatively flat (Fig. 78K, L).

Prototherium is known from two species based on cranial and postcranial elements from the late Eocene of Italy: *P. veronense* (de Zigno, 1875) and *P. intermedium* Bizzotto (1983 and 2005). Pilleri et al. (1989) erected two new Bartonian species from Spain, *P. solei* and *P. montserratense*, but these seem similar if not identical to the Priabonian *P. intermedium* (Domning, 1994). A distinctive feature of *Prototherium* is the unusual anteroposterior elongation of the skull that makes it look relatively compressed bilaterally. *Prototherium* anterior ribs are pachyosteosclerotic, and the ilium is swollen, as shown in Bizzotto (1983, plate II) and Pilleri et al. (1989: 42, fig. 12).

Sirenavus hungaricus of Kretzoi (1941), which is based on a partial skull (MTM V.60.1712) and dentaries (MTM V.83.42) from the middle Eocene of Hungary, shows some affinities with *Eotheroides clavigerum* and *Eotheroides sandersi* in retaining strongly arched, upwardly-concave nasals; large infraorbital foramina; and enlarged ribs associated with the partial skull. Further examination of *Sirenavus hungaricus* by Kordos (1981) and Domning (1994, 1996) shows that it is more closely related to Dugongidae than it is to Protosirenidae or Prorastomidae. The

innominate (MÁFI V.15366) and femur (MÁFI V.15367) of *Sirenavus hungaricus* mentioned in Kordos (2002) represent a dugongid stage of evolution: the ilium is rod-like, the acetabulum is reduced, the pubic ramus is retracted medially, and the obturator foramen is diminutive. In addition, the femur is morphologically typical of an *Eosiren* femur, and is particularly similar to specimen UM 101226 (Fig. 64F) from the Qasr El Sagha Formation of Fayum.

Halitherium (Kaup, 1838a,b) includes three European Paleogene species: *Halitherium taulannense* from the Priabonian of Haute Province of France (Sagne, 2001); *H. schinzii* (Kaup, 1838a) from the early Oligocene (Rupelian) of Germany, Hungary, Switzerland, Belgium, and France (Lepsius, 1882; Spillmann, 1959; Voss, 2011); and *H. christolii* (Fitzinger, 1842) from the late Oligocene Austria. *Halitherium taulannense* shares several cranial synapomorphies with *Eotheroides*; however, *Halitherium taulannense* is more derived because it possesses the following characters: contact between the lacrimal and premaxilla, and an enlarged first incisor with an alveolus extending about half the length of the rostrum (Sagne, 2001).

The right innominate of *H. taulannense* (NSM PV 20523) is 248 mm in total length. It bears a rod-like ilium (130 mm in total length) that lacks any swelling. The ischium is long, and the obturator foramen (18 × 12 mm) is wider than those in *Eotheroides*. The pubic ramus and symphysis are very reduced. The femur is incomplete, as it is missing the distal end, but it is reduced as well. The head of the femur did still articulate with the acetabulum, and it was round in cross-section.

Beyond Dugongidae, the protosirenid species *Protosiren fraasi* of Abel (1907) from the Lutetian of the Mokattam Hills and the later *Protosiren smithae* from the Priabonian of Fayum differ greatly from contemporary *Eotheroides* species. Cranial and postcranial differences between of *Protosiren* and *Eotheroides* were listed in Sickenberg (1934, p. 192-193) and then recounted in Gingerich et al. (1994:44 and table 1). However, since *Protosiren smithae* is slightly different from the type *P. fraasi*, a slight modification to the list is necessary. *Protosiren* differs from *Eotheroides* in the following characteristics: larger body size; less rostral deflection in the maxilla and premaxilla; a premaxillary-maxillary suture located well behind the premaxillary symphysis; presence of an alisphenoid canal; a squamosal that does not contribute to the back of the skull; a squamosal and supraoccipital completely separated by a process of the parietal; a post-tympanic process of the squamosal absent; a supra-auditory region thickened and outer ear passage somewhat elongated; a lamina orbitalis of the frontal contributing substantially to separation of the orbits and the nasal cavity; a large brain; lack of a bony falx, bony tentorium, and internal occipital protuberance; a relatively small infraorbital foramen compared to cranium size; absence of a pterygoid fossa; elongated cheek teeth (Fig. 66); large incisors; dp5 replaced in the upper jaw and lost in the dentaries (Fig. 69); postcranial elements osteosclerotic but lack pachyostosis; thoracic and lumbar vertebrae have neural spines higher than any other sirenian described (Fig. 73); thoracic vertebrae have a keyhole-shaped vertebral canal (Fig. 74); rib heads display a cartilaginous rather than fully ossified articular surface (Fig. 76); and hind limbs remain better developed. One



FIGURE 70 — Mandible of late Eocene *Eosiren stromeri* (UM 100137) collected from the Qasr El Sagha Formation near Garet El Esh north of Birket Qarun in Fayum. Mandible is shown in occlusal (A) and right lateral view (B). Anterior teeth are missing and their alveolae are broken. Robustness and width of the anterior rostrum, and its expanded masticatory surface are characteristic of *Eosiren* mandibles. Dental formula and number of teeth is based on the maximum number of teeth found in most primitive sirenians (3.1.5.3 or 3.1.4.dp5.3). Abbreviations: dP_X , deciduous premolars; M_{1-X} , molars; P_{1-X} , premolars.

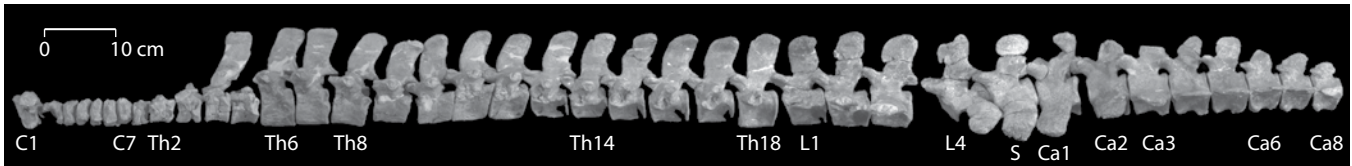


FIGURE 71 — Vertebrae of late Eocene *Eosiren libyca* (UM 101226) from the Qasr El Sagha Formation north of Birket Qarun in Fayum. Vertebral column is shown in left lateral view. Abbreviations: C, cervical; Ca, caudal; L, lumbar; S, sacral; Th, thoracic.

important characteristic of the postcrania unifies *Protosiren* with *Eotheroides* and other dugongs. This is reduction of the sacrum to a single sacral vertebra, with transverse processes connected to the ilia by ligaments and cartilage.

Prorastomidae, the oldest and most primitive of known Sirenia, are known from two Caribbean species: *Prorastomus sirenoides* of Owen (1855) and Savage et al. (1994), and *Pezosiren portelli* of Domning (2001b). Both species are known from sufficient cranial and postcranial elements to support interpretation of an amphibious and quadrupedal lifeway. *Prorastomus sirenoides* is clearly different from *Eotheroides* and other known Eocene dugongs in having a horizontal rostrum and mandibular ramus, double-rooted canine, enlarged first premolar, periotic still connected to the alisphenoid, and alisphenoid canal present. However, it shares some features in common with *Eotheroides* and Eocene dugongs because it has a mediolaterally compressed mandibular symphysis, and the dental capsule is wholly enclosed by the bone of the mandible.

Pezosiren portelli is unique, as it retained a sagittal crest, has an enlarged first premolar, has a single-rooted fifth premolar (dP⁵ was lost and replaced), has multiple sacral vertebrae are fused together, and it retains a large and presumably functional pelvic girdle that articulated with hind limbs capable of supporting the animal's weight on land. *P. portelli* does share some synapomorphies with Eocene dugongs, such as an auditory meatus with the anteroposterior width equal to its height, an unfused periotic and alisphenoid, a ventral border of the mandibular ramus turned down anteriorly, and pachyosteosclerotic anterior thoracic ribs.

DISCUSSION

The new *Eotheroides* species described here increase the number of species that lived during the Paleogene in Egypt to at least nine taxa. These include: *Protosiren fraasi* Abel (1907), *Eotheroides aegyptiacum* Owen (1875), and *Eosiren abeli* (Sickenberg, 1934), which predominate in the Lutetian-aged Mokattam nummulitic limestone; *Protosiren smithae*, which derives from the base of the Birket Qarun Formation (Domning and Gingerich, 1994); *Eotheroides clavigerum* sp. nov. and *Eotheroides sandersi* sp. nov. from the Birket Qarun Formation; *Eosiren libyca* Andrews (1902b), and *Eosiren stromeri* (Sickenberg, 1934) from the Qasr El Sagha Formation, and *Eosiren imenti* Domning et al. (1994) from the Oligocene Gebel Qatrani Formation.

The sirenian fauna represents less than 5% of all the marine mammals found in the Birket Qarun Formation in terms of specimens, far less than the dominant Archaeoceti, which represent 94% of all marine mammals collected or mapped. *Moeritherium* is the least common aquatic or semi-aquatic mammal from the Birket Qarun Formation in Wadi Al Hiton. These percentages are based on a count of 470 skeletons of marine mammals mapped in Wadi Al Hiton (as reported in Gingerich, 1992).

Prorastomidae has been reported from Africa (Hautier et al., 2012), and the possibility of an early radiation of Sirenia beginning in Africa cannot be ruled out. Extant African Sirenia include two species: *Dugong dugon* (Müller, 1776) which inhabits the eastern and southeastern coast of the African continent, and *Trichechus senegalensis* (Link, 1795), the West African manatee from the western side of the continent (Bertram and Bertram, 1973).

The skeletal and cranial material of new *Eotheroides* species from the Priabonian Birket Qarun Formation of Wadi Al Hiton is very important because this provides new information that helps refine identification and phylogeny of the three Eocene genera known from the southern margin of the Tethyan Sea in Egypt. *Eotheroides aegyptiacum* is known from partial skulls and lower jaws, but cranial rostra, caudal vertebrae, and pectoral and pelvic elements are lacking, which complicates attempts to better understand the paleobiology and systematics of this taxon.

Fayum *Eotheroides* were medium to large-sized dugongs: *Eotheroides clavigerum* may have reached 2.2 m in total length, while *Eotheroides sandersi* was approximately 1.5 m long. Both have stout, heavy skulls, and rostra deflected downward between 43° and 50° from the horizontal plane. *E. clavigerum* bears a pair of medium sized tusks, and *E. sandersi* had diminutive ones. The dental formula is 2.1.3.4.dP⁵.3 / 3.1.3.4.dP⁵.3. The vertebral count in *Eotheroides clavigerum* is reconstructed as 7 C, 19 Th, 4 L, 1 S, and 19-22 Ca, with an associated 19 pairs of ribs. In *Eotheroides sandersi* the vertebral count is 7 C, 17-19 Th, 4 L, 1 S, and 19-22 Ca, with an associated 17-19 pairs of ribs. The body was widest between the ninth and eleventh thoracics. The posteriormost vertebrae of the tail seemingly supported a fluke in both species. Hindlimbs are reduced to a short and slender femur attached to a reduced innominate that had a shallow, crescent-shaped acetabulum.

Pelves of Fayum *Eotheroides* make a substantial contribution to generic diagnosis of Eocene Sirenia. The ilia and femora of *Eotheroides clavigerum* and *E. sandersi* are the first definitive posterior limb elements to be assigned to *Eotheroides*, as these were found in association with cranial and other postcranial

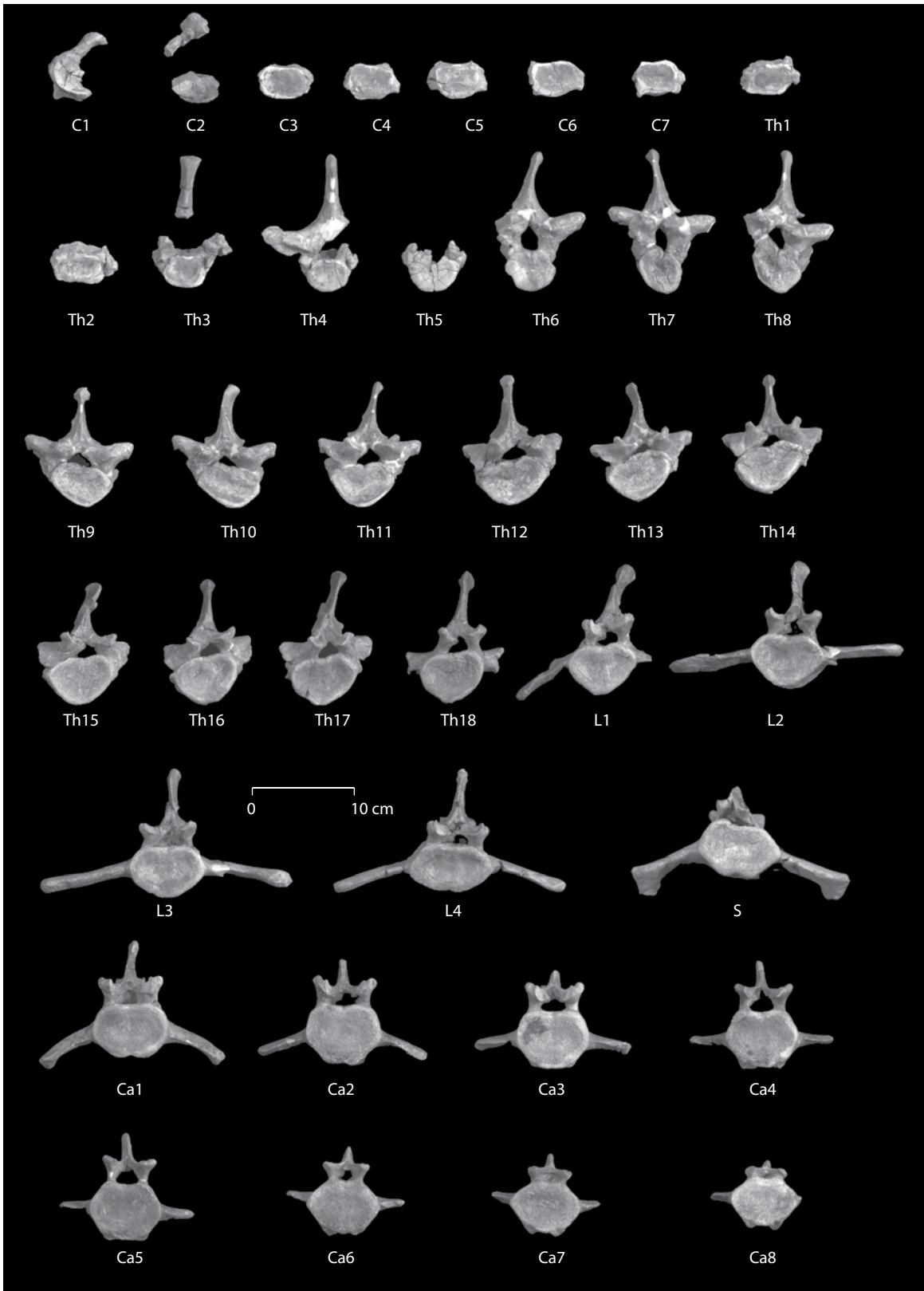


FIGURE 72 — Vertebrae of late Eocene *Eosiren libyca* (UM 101226) from the Qasr El Sagha Formation, in anterior (cranial) view. Note that the thoracic vertebra bodies are close to heart-shape. Abbreviations: *C*, cervical; *Ca*, caudal; *L*, lumbar; *S*, sacral; *Th*, thoracic.

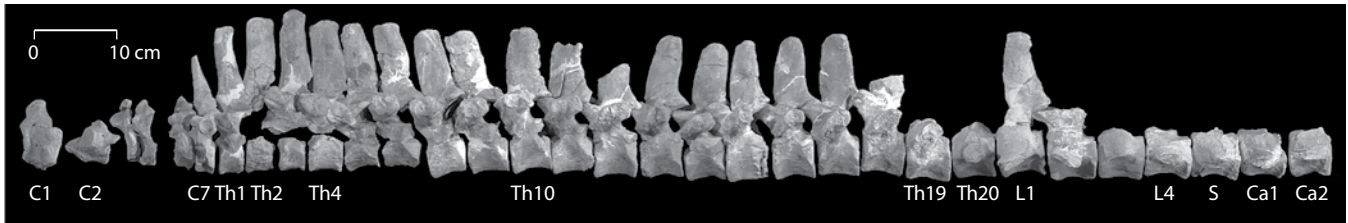


FIGURE 73 — Vertebrae of late Eocene *Protosiren smithae* (UM 101224) from the base of the Birket Qarun Formation in Wadi Al Hitan. Vertebrae are shown in left lateral view. There are 20 thoracic, probably more than 4-6 lumbar, one sacral, and probably 20+ caudal vertebrae in *P. smithae*. Abbreviations: C, cervical; Ca, caudal; L, lumbar; S, sacral; Th, thoracic.

elements. The pelves are unlike any sirenian pelvic bones heretofore described (see Abel, 1907; Domning, 2000, 2001b). They are intermediate between those referred to *Protosiren fraasi* (SMNS 43976A, from Abel, 1904: pl. 7, fig. 1; illustrated in Fig. 77A in the present work) and *Protosiren smithae* (CGM 42292 in Domning and Gingerich, 1994; Fig. 77B here) on one hand, and those of *Eosiren libyca* (UM 101226; Fig. 71E, F) on the other. Both species of *Eotheroides* from Fayum retained a long pubic ramus with a very reduced symphysis. The obturator foramina are much reduced compared to those of *Protosiren*, but have not been totally lost.

The ilium of *Eosiren* is reasonably constant in its diameter and cross-section, as illustrated in Andrews (1906), Stromer (1921), and Siegfried (1967), and here in Figure 77E, F. Extensive swelling of the proximal ilium seen in *Eotheroides* is distinctive among Eocene sirenians. This swelling in the ilium is similar to that which appears on the innominate of the European late Eocene *Protherium intermedium* (See Bizzotto, 1983, 2005). The iliosacral articular area on the dorsolateral surface of the ilium of *Eotheroides* is very shallow, but it is larger than that found in *Eosiren*, implying that there was still a connection between the ilium and the sacrum via ligament and cartilage. Femora of *Eotheroides* are also very reduced in size, with morphology similar to that of *Eosiren* described by Siegfried (1967).

Eotheroides has not been recorded from other places in Africa where sirenians have been extensively documented (see Savage, 1969, 1971, 1977); however, the newly recovered Eocene dugongid *Eotheroides lambdrano* from the western coast of Madagascar (Samonds et al., 2007, 2009) is a dwarf species of *Eotheroides*. Marine mammal remains from the Eocene of Togo (Gingerich et al., 1992) contain some isolated sirenian elements showing dugongid affinities. Outside Africa, the record requires more investigation. *Eotheroides* is reported from the Eocene of the eastern Tethyan deposits of India, along with *Eosiren* and

Protosiren (Bajpai et al., 2006). *Eotheroides babiae*, based on a single mandible (IITR-SB 2775), is similar in part to *Eotheroides* jaws from the Birket Qarun Formation (e.g., YPM 24851 and CGM 42181) in having a slightly arched ventral outline in lateral view, and in having a mediolaterally compressed mandibular lip.

CONCLUSIONS

Eotheroides clavigerum sp. nov. and *Eotheroides sandersi* sp. nov. from the Priabonian Birket Qarun Formation of Fayum Province are closest, phenetically and phylogenetically, to *Eotheroides aegyptiacum* and both are possibly direct descendants of this species. They all have a prominent falx and bony tentorium on the roof of the braincase; long nasals in contact along the midline; a broad palate with the posterior border posterior to the tooth row; and pachyosteosclerotic anterior ribs. The new species described here represent derived forms of dugongid, as they possess large infraorbital foramina, long premaxillary canals, and reduced pelvic girdles.

The most important skeletal elements for diagnosis of the genus *Eotheroides* and its species are the extensively pachyosteosclerotic anterior ribs, and the innominate with club-like ilia. The morphology of the skeletal elements of Lutetian and Priabonian *Eotheroides* are characteristic of fully aquatic marine mammals. These large marine herbivores spent all their life in water, either grazing on sea grass meadows on tidal flats, or consuming planktonic algae floating near the surface. Based on paleontological and geological evidence, *Eotheroides* species lived in shoreface settings in restricted and stable habitats (lagoons and estuaries), although some may have ventured into deltas, keys, and bays.

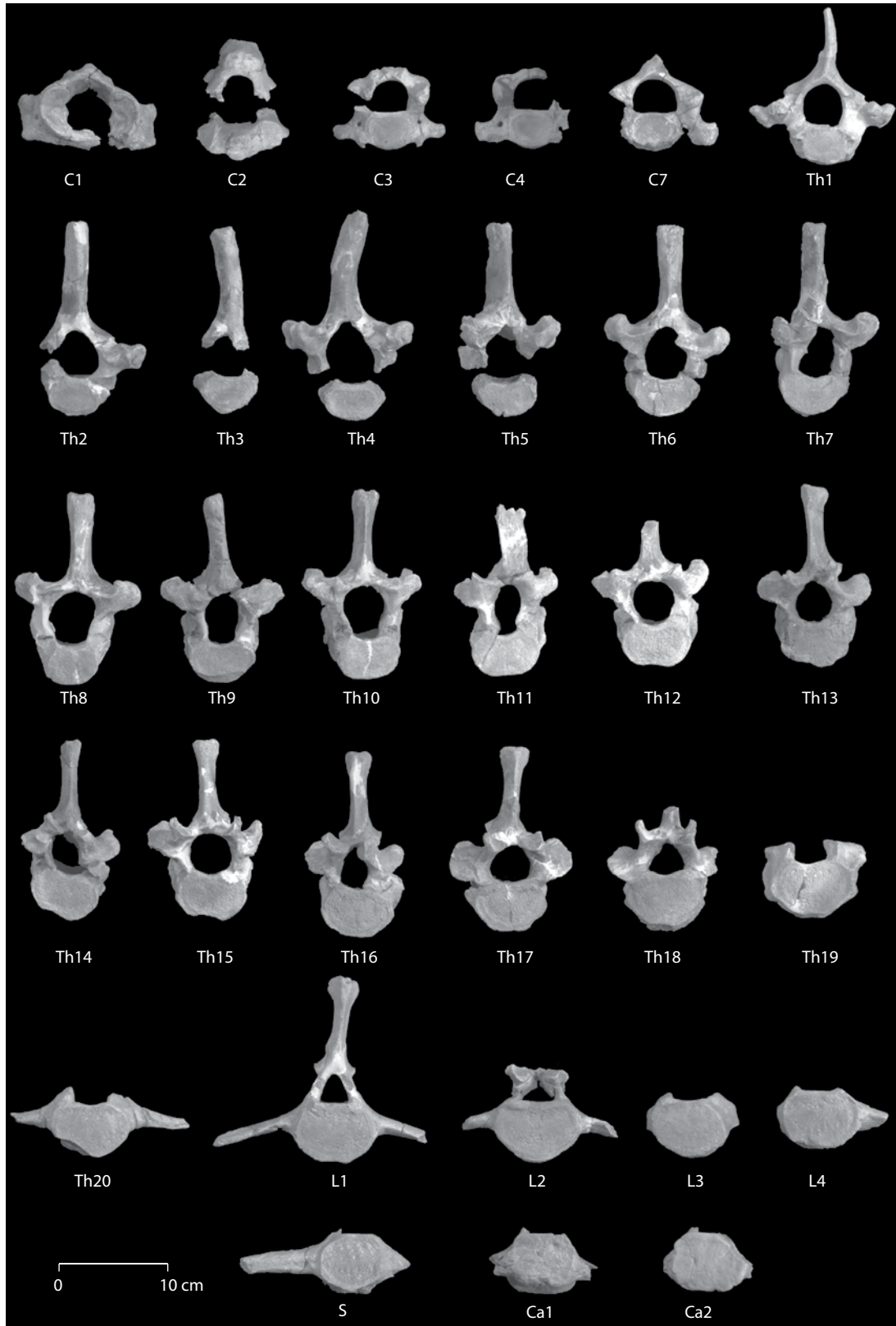


FIGURE 74 — Cervical, thoracic, lumbar, sacral, and caudal vertebrae of late Eocene *Protosiren smithae* (UM 101224) from the base of the Birket Qarun Formation in Wadi Al Hitan. Vertebrae are shown in anterior (cranial) view. Note the keyhole-like neural foramen and long neural spines that distinguish vertebrae of Protosirenidae from those of other Eocene sirenians. Abbreviations: *C*, cervical; *Ca*, caudal; *L*, lumbar; *S*, sacral; *Th*, thoracic.

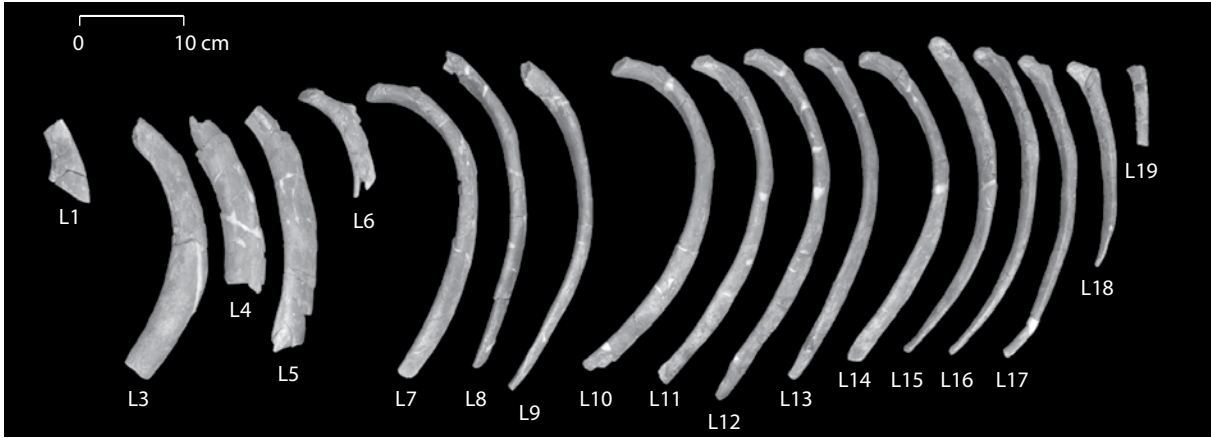


FIGURE 75 — Anterior (cranial) view the left ribs of *Eosiren libyca* (UM 101226) from the Qasr El Saga Formation north of Birket Qarun in Fayum. Note that the last rib is gracile and short. Abbreviations: *L*, left ribs.

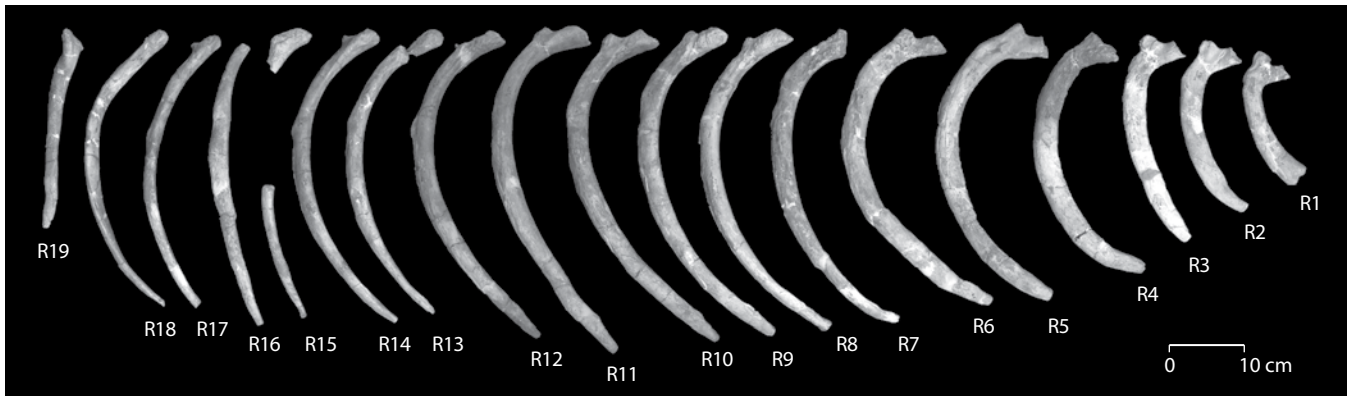


FIGURE 76 — Anterior (cranial) view the right ribs of *Protosiren smithae* (UM 101224) from the base of the Birket Qarun Formation. The last rib on one side is short and fused with the last thoracic vertebra. Abbreviations: *R*, right rib.

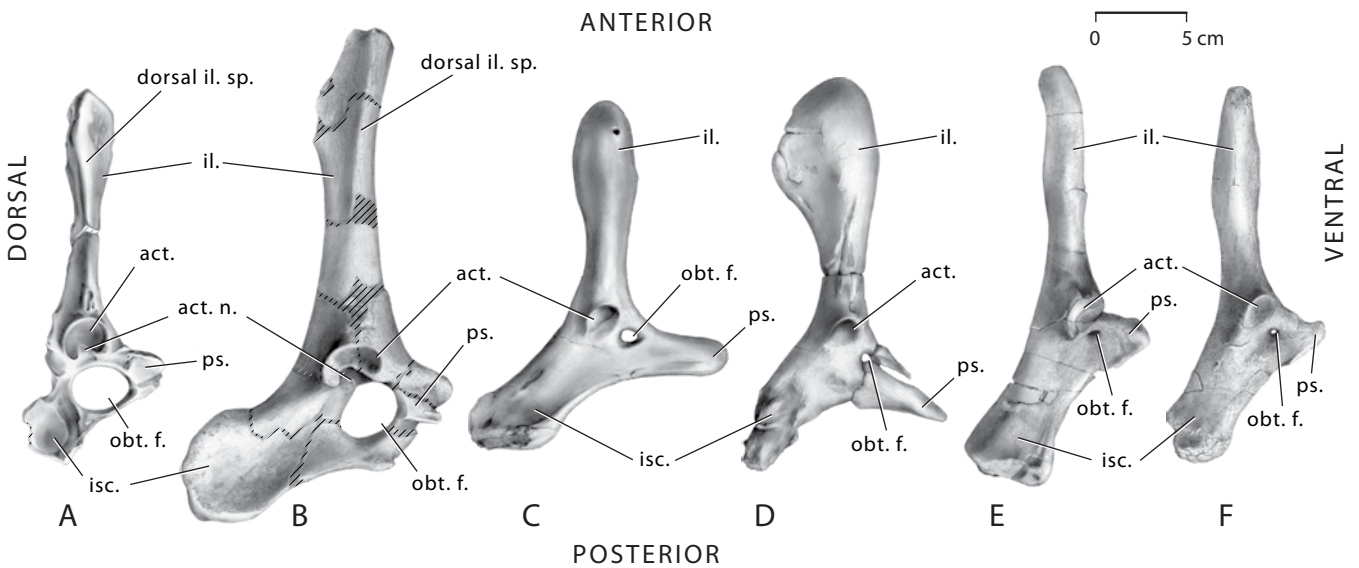


FIGURE 77 — Comparison of right innominate bones of African Paleogene sirenians. All are shown in lateral view. A, *Protosiren fraasi* (SMNS 43976A; from Abel, 1904: pl. 7, fig. 1). B, *Protosiren smithae* (CGM 42292; Domning and Gingerich, 1994). C, *Eotheroides sandersi* (UM 97514). D, *Eotheroides clavigerum* (CGM 60551). E, *Eosiren libyca* (UM 101226). F, *Eosiren libyca* (CGM 29774). Abbreviations: *act.*, acetabulum; *act. n.*, acetabular notch; *dor. il. sp.*, dorsal iliac spine; *il.*, ilium; *isc.*, ischium; *obt. f.*, obturator foramen; *ps.*, pubis; *ps. sym.*, pubic symphysis.

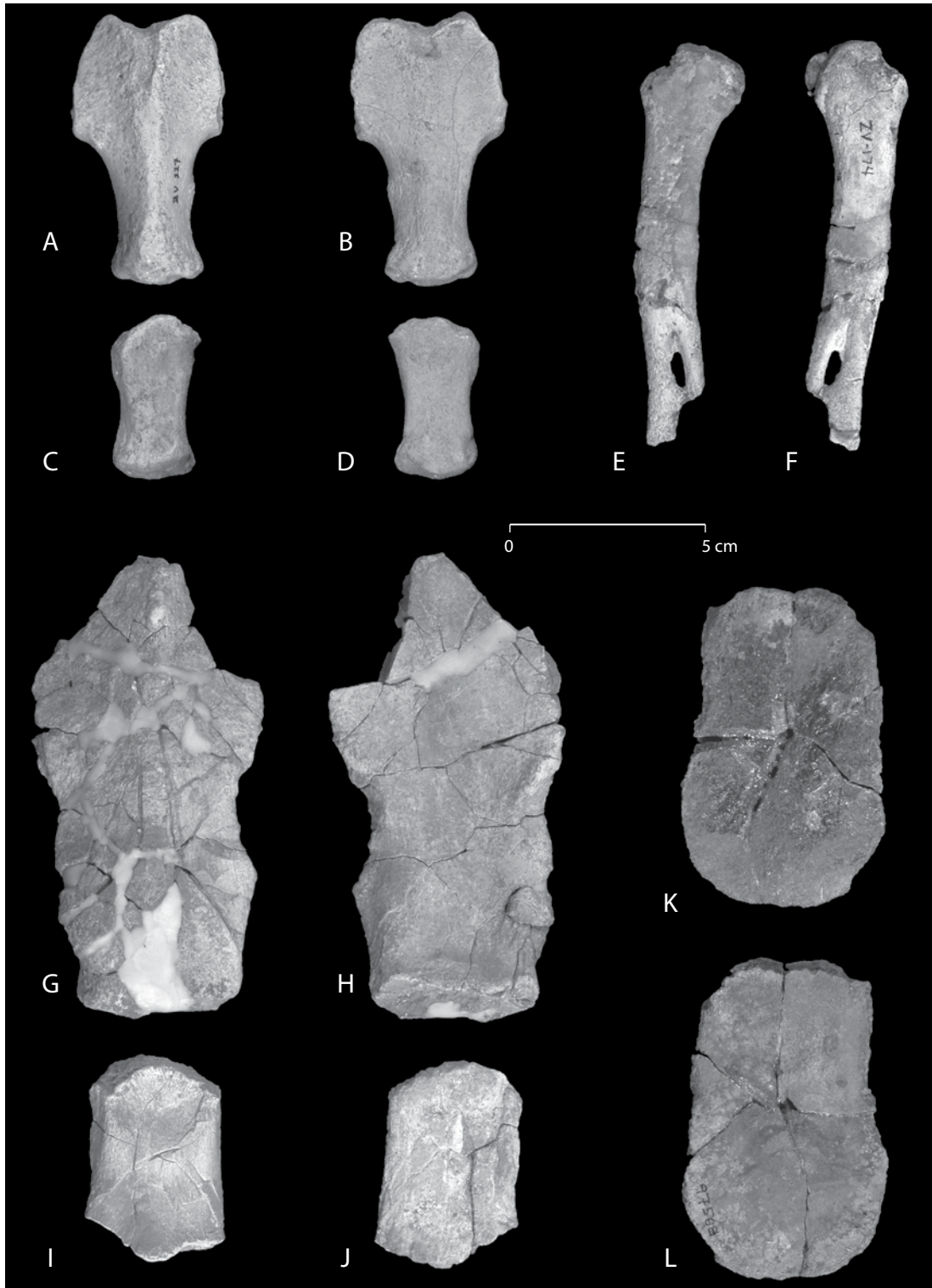


FIGURE 78 — Sternal elements of *Protosiren*, *Eotheroides*, and *Eosiren* from Fayum. A-B, Manubrium of *Protosiren smithae* (UM 101224) in ventral and dorsal view. C-D, sternebrae of *Protosiren smithae* (UM 101224) in ventral and dorsal views; sternal elements of *P. smithae* resemble those of land mammals in being a series of short, blocklike segments corresponding to costal cartilages. E-F, xiphisternum of *Eotheroides sandersi* (UM 111558) in ventral and dorsal views; this is dorsoventrally flattened. G-H, manubrium of *Eosiren libyca* (UM 101226) from the Qasr El Sagha Formation in ventral and dorsal view. I-J, sternebrae of *Eosiren libyca* (UM 101226) in ventral and dorsal view; both elements are dorsoventrally flattened. K-L, xiphisternum of *Eosiren libyca* (UM 97568) in ventral and dorsal views.

V

QUANTITATIVE COMPARISON OF SKELETAL ELEMENTS IN EOCENE SIRENIA FROM EGYPT

It is instructive to compare the Eocene Sirenia now known from Egypt, species of the protosirenid *Protosiren* and dugongids *Eotheroides* and *Eosiren*, to each other quantitatively. Each of these genera includes a pair of species with skulls in the range from 30.5 to 37.8 cm in condylobasal length (*AB* in Table 29), implying body lengths in the range of 2.1 to 2.7 meters and body weights in the range of 160 to 370 kg (Sarko et al., 2010). Within each genus, it appears that there is a species near the lower end of the overall range and a species near the upper end of the overall range, however the body size ranges, genus by genus, overlap very closely.

Each section here comprises one or more tables of raw measurements, and an accompanying chart or charts showing how the measurements compare proportionally on a natural logarithmic (*ln*) scale. The advantage of the *ln* scale is that linear measurements, empirically, within species, have a standard deviation of about 0.05 and an expected ± 2 standard deviation range of about 0.20; area measurements have an expected standard deviation of about 0.10 and an expected ± 2 standard deviation range of about 0.40; and volume measurements have an expected standard deviation of about 0.15 and an expected ± 2 standard deviation range of about 0.60 (Gingerich, 1981, 2000). We have not quantified any expectation for measurements of angles, which may not have the same regularity of empirical variability as measurements of length, area, and volume.

CRANIAL MEASUREMENTS

A standard set of 37 cranial measurements is listed in Table 29, following Domning (1978a). All measurements are linear, in mm, except for deflection of the masticating surface of the rostrum measured in degrees. We report measurements for 12 individual crania. If the matrix were complete, it would be interesting to explore this using a multivariate approach. However, since many measurements are missing we have chosen five of the more complete specimens, representing five species of the three genera, to compare as cranial pattern profiles in Figure 79.

Graphic comparison of successive cranial measurements in Figure 79 shows that all three genera, *Protosiren*, *Eotheroides*, and *Eosiren*, and all five of the species plotted have crania that follow basically the same profile. This is a reflection of inheritance and a common degree of adaptation to a marine environment, sensory specialization, and mode of feeding.

There are differences in size and proportion between the genera and species to be sure, but these are relatively minor.

MANDIBULAR MEASUREMENTS

A standard set of 25 mandibular measurements is listed in Table 30, following Domning (1978a). All measurements are linear, in mm, except for deflection of the symphyseal surface of the dentary measured in degrees. We report measurements for six individual mandibles, and five of these are represented by mandibular pattern profiles in Figure 80.

Graphic comparison of successive mandibular measurements in Figure 80 shows that all three genera, *Protosiren*, *Eotheroides*, and *Eosiren*, and all five of the species plotted have mandibles that follow basically the same profile. This is not surprising given the similarity of profiles in Figure 79 and the functional integration of mandibles and crania. Here similarity reflects inheritance and a common degree of adaptation to a mode of feeding. As before, there are differences in size and proportion between the genera and species, but again these are relatively minor.

VERTEBRAL MEASUREMENTS

In mammals, cranial and mandibular form are indicative of sensory specialization and mode of feeding, while vertebral morphology is more sensitive to locomotion. Vertebral morphology can be quantified in many ways. Here we consider vertebral centrum length; maximum vertebral breadth, including rib facets and transverse processes; and centrum width-to-length shape relationships.

Centrum length.—Centrum lengths of successive vertebrae in the postcranial skeleton of extant male and female dugongids *Dugong dugon* and two species of trichechids *Trichechus manatus* and *T. senegalensis* are listed in Table 31. The table also includes measurements of centrum length for partial skeletons of eight Eocene species, including species of the protosirenid *Protosiren* and the dugongids *Eotheroides* and *Eosiren*.

The pattern profiles of centrum length for the three extant species are shown in Figure 81A. The second cervical vertebra, C2 or the 'axis,' is long in those that have a measured length for the axis. The remaining cervical vertebrae (C3-C7 in Dugongidae or C3-C6 in Trichechidae) are conspicuously short. Thoracic

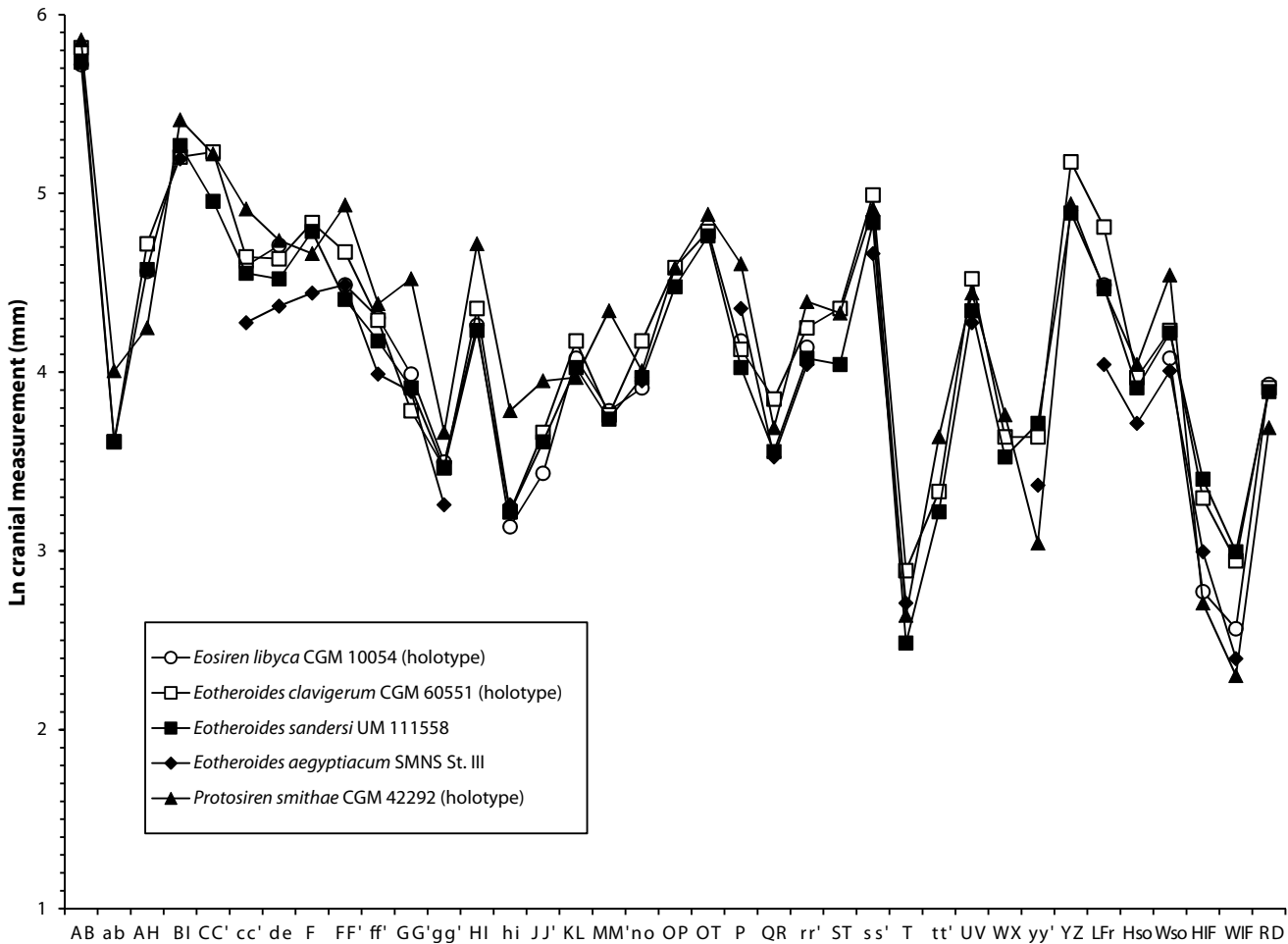


FIGURE 79 — Pattern profiles of cranial measurements for five species of three genera, *Protosiren*, *Eotheroides*, and *Eosiren*, from the Priabonian late Eocene of Egypt. Landmarks and measurements follow Domning (1978a). Descriptions, abbreviations, and measurements are listed in Table 29.

vertebrae increase in length from front to back in *Dugong*, with a maximum length in the lumbar series. Thoracic vertebrae increase in length from front to back in *Manatus* too, but the maximum length is in the posterior part of the thoracic series. There is then a smooth decrease in length through the remainder of the vertebral column.

Pattern profiles of centrum length for the eight Eocene species in Table 31 are shown in Figure 81B. The short cervical series and the progressive elongation through the thoracic series seen in the Eocene taxa is like that of Dugongidae. This isn't surprising considering that *Eotheroides* and *Eosiren* are considered to be dugongids, but progressive elongation through the thoracic series also holds for the protosirenid *Protosiren smithae* (UM 101224).

Maximum vertebral breadth.— Maximum vertebral breadths for successive vertebrae in the postcranial skeleton of extant male and female dugongids, *Dugong dugon*, and two species of trichechids, *Trichechus manatus* and *T. senegalensis*, are listed in Table 32. These include, whenever present, rib facets and

transverse processes. The table also includes measurements of centrum length for partial skeletons of eight Eocene species, including species of the protosirenid *Protosiren* and the dugongids *Eotheroides* and *Eosiren*.

The pattern profiles of vertebral breadth for the three extant species are shown in Figure 82A. The first cervical vertebra, C1 or the 'atlas,' is broad in all that have a measured breadth for the atlas. The following anterior cervical vertebrae tend to be narrow but become broader through the cervical series. Thoracic vertebrae generally decrease in breadth from front to back (but of course the attached ribs make the thorax as a whole much broader than the breadth of the thoracic vertebrae alone). There is then an abrupt change in breadth in the transition from thoracic to lumbar vertebrae. The difference is entirely due to replacement of articulating ribs by fixed transverse processes inherent, by definition, in the distinction of lumbar from thoracic vertebrae. From the lumbar series through the sacrum and caudal series, manatees have a distinctly different breadth profile from that of dugongs. In manatees the vertebrae narrow

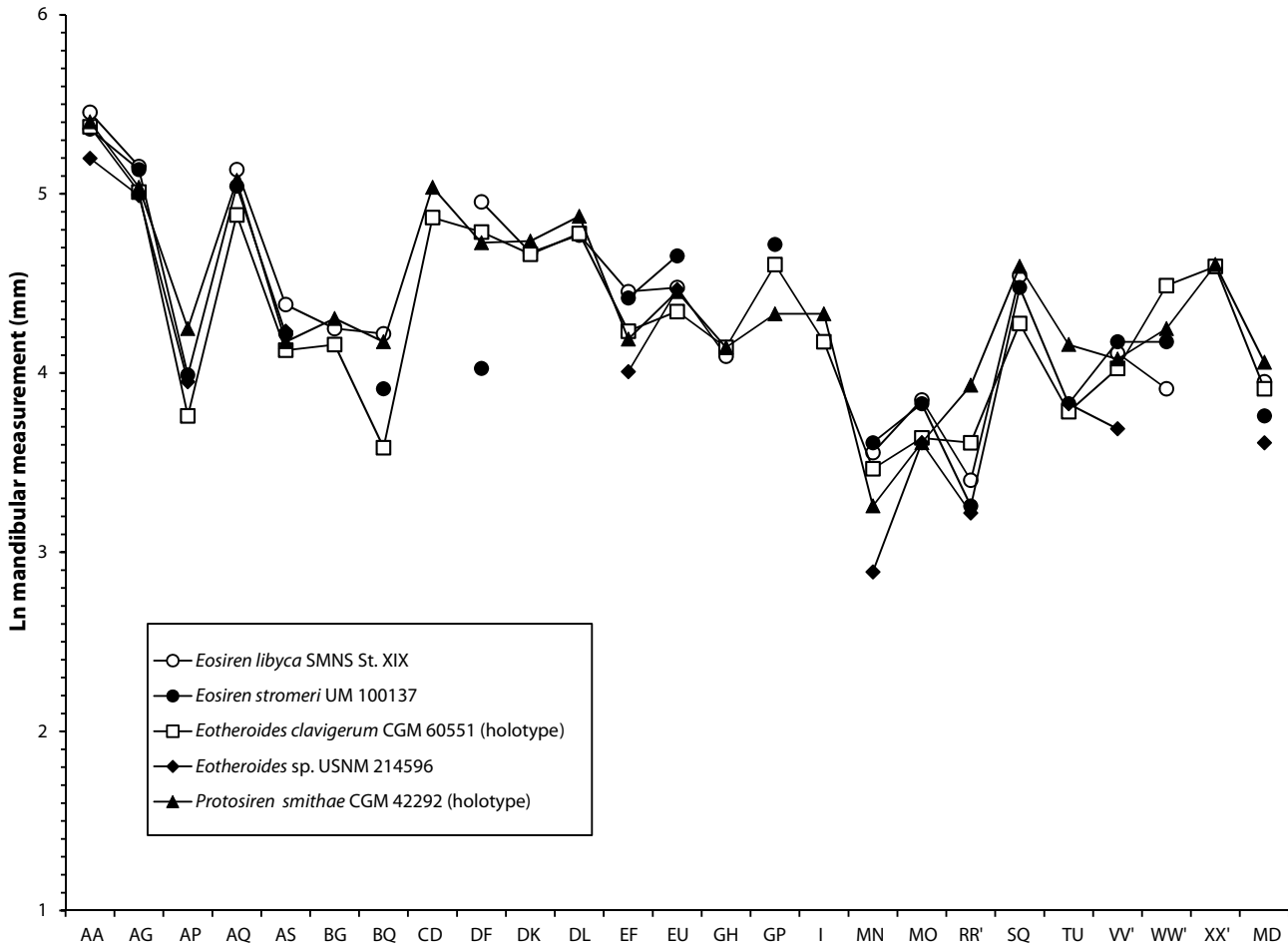


FIGURE 80 — Pattern profiles of mandibular measurements for four species of three genera, *Protosiren*, *Eotheroides*, and *Eosiren*, from the Priabonian late Eocene of Egypt, and one species of *Eotheroides* from the Eocene of North America. Landmarks and measurements follow Domning (1978a). Descriptions, abbreviations, and measurements are listed in Table 30.

posteriorly in a more or less monotonic profile. In dugongs the vertebrae narrow posteriorly, then broaden, and then narrow again in an open sigmoid profile. This is undoubtedly related to the differently-shaped tail flukes and mode of swimming in the two families of Sirenia.

Pattern profiles of vertebral breadth for the eight Eocene species in Table 32 are shown in Figure 82B. The narrow cervical series and the progressive narrowing through the thoracic series seen in the Eocene taxa are like those of both Trichechidae and Dugongidae. Unfortunately the Eocene sirenian skeletons available from Egypt are not complete enough to detect whether they follow a manatee or dugong pattern of narrowing through the lumbar, sacral, and caudal vertebrae.

Centrum shape.— Centrum lengths and widths of successive vertebrae in the postcranial skeleton of extant male and female dugongids, *Dugong dugon*, and two species of trichechids, *Trichechus manatus* and *T. senegalensis*, are listed in Table 33. These enable calculation of natural log values of the ratio of width to length, or the equivalent difference between ln width and ln

length, for each centrum. The table also includes measurements of centrum lengths and widths for partial skeletons of four Eocene species, including species of the protosirenid *Protosiren* and the dugongids *Eotheroides* and *Eosiren*.

The pattern profiles of vertebral breadth for the three extant species are shown in Figure 83A. Here the long centrum length and relatively narrow centrum breadth of the second cervical vertebra, C2 or the ‘axis,’ means that the shape ratio of width to length is small. Succeeding cervicals have shorter and wider centra, and the shape ratio of width to length is consequently much larger. Mid-thoracics have the smallest shape ratios. These climb slightly from mid-thorax to the tail in the pattern profiles for *Dugong*, but fall abruptly in the tail of *Trichechus*. Here again we see a morphological difference in pattern profiles related to the differently-shaped tail flukes and mode of swimming in the two families of Sirenia.

Pattern profiles of vertebral centrum shape for the five specimens representing four Eocene species in Table 33 are shown in Figure 83B. The centrum width-to-length shape ratio

TABLE 29 — Measurements of crania of the Egyptian Eocene sirenians known to date. All measurements are in mm, except for RD, which was measured in degrees. Measurements follow Domning (1978a).

Abb.	Measurements	<i>Eotheroides clavigerum</i> CGM 60551	<i>Eotheroides sandersi</i> UM 111558	<i>Eotheroides aegyptiacum</i> SMNS St. III	<i>Protosiren fraasi</i> CGM 10171
AB	Condylobasal length	335	309	—	378
ab	Height of jugal below orbit	37	37	—	46
AH	Length of premaxillary symphysis	112	97	—	108
BI	Rear of occipital condyles to the anterior end of interfrontal suture	182	194	180	186
CC'	Zygomatic breadth	187	142	—	172
cc'	Breadth across exoccipitals	104	95	72	132
de	Top of supraoccipital to ventral sides of occipital condyles	103	92	79	105
F	Length of frontals, level of tips of supraorbital processes of fronto- parietal suture	126	120	85	104
FF'	Breadth across supraorbital processes	107	82	89	92
ff'	Breadth across occipital condyles	73	65	54	83
GG'	Breadth of cranium at frontoparietal suture	44	50	49	58
gg'	Width of foramen magnum	32	32	26	37
HI	Length of mesorostral fossa	78	69	—	80
hi	Height of foramen magnum	25	25	26	23
JJ'	Width of mesorostral fossa	39	37	—	48
KL	Maximum height of rostrum	65	56	—	45
MM'	Posterior breadth of rostral masticating surface	43	42	—	57
no	Anteroposterior length of zygomatic-orbital bridge of maxilla	65	53	52	60
OP	Length of zygomatic process of squamosal	98	88	—	96
OT	Anterior tip of zygomatic process to rear edge of squamosal below mastoid foramen (length of the squamosal)	120	117	—	126
P	Length of parietals, frontoparietal suture to rear of external oc- cipital protuberance	62	56	78	110
QR	Anteroposterior length of zygomatic process of squamosal	47	35	34	34
rr'	Maximum width between labial edges of left and right alveoli across M ¹	70	59	57	85
ST	Length of cranial portion of squamosal	78	57	—	73
ss'	Breadth across sigmoid ridges of squamosals	147	126	106	136
T	Dorsoventral thickness of zygomatic-orbital bridge	18	12	15	13
tt'	Anterior breadth of rostral masticating surface	28	25	—	37
UV	Height of posterior part of cranial portion of squamosal	92	77	72	81
WX	Dorsoventral breadth of zygomatic process	38	34	—	32
yy'	Maximum width between pterygoid processes	38	41	29	21
YZ	Length of jugal	177	133	—	131
LFr	Length of frontals in midline	123	88	57	72
Hso	Height of supraoccipital	53	50	41	55
Wso	Width of supraoccipital	69	68	55	77
HIF	Height of infraorbital foramen	27	30	20	14
WIF	Width of infraorbital foramen	19	20	11	10
RD	Deflection of masticating surface of rostrum from occlusal plane (degrees)	50	49	—	30

for C2 is again small, while that for succeeding cervicals is again much larger. A narrow cervical series (with a high width-to-length ratio) and the progressive narrowing through the thoracic series (with an increasing width-to-length ratio) seen in the Eocene taxa is like that of both Trichechidae and Dugongidae. Unfortunately the Eocene sirenian skeletons available from Egypt are not complete enough to detect whether they follow

a manatee or dugong pattern of narrowing through the lumbar, sacral, and caudal vertebrae. Here again mid-thoracics have the smallest shape ratios. These climb slightly from mid-thorax to the tail as in the pattern profiles for *Dugong*, suggesting that the tail fluke and mode of swimming in *Eotheroides* at least was like that of *Dugong* rather than *Trichechus*. Again this is not surprising as *Eotheroides* is considered to be a dugongid.

TABLE 29 — (continued).

Abb.	<i>Protosiren fraasi</i> SMNS 10576 St. V	<i>Protosiren smithae</i> CGM 42292	<i>Eosiren stromeri</i> SMNS ST. I	<i>Eosiren stromeri</i> UM 100137	<i>Eosiren libyca</i> CGM 10054	<i>Eosiren libyca</i> ST. XIX	<i>Eosiren libyca</i> MNHN 1913-22	<i>Eosiren libyca</i> BMNH M10910
AB	318	350	—	350	305	—	—	—
ab	47	55	—	40	—	41	50	—
AH	62	70	119	90	96	120	106	118
BI	196	224	217	240	—	—	—	—
CC'	—	185	—	160	—	166	166	164
cc'	108	136	104	104	99	—	—	—
de	89	114	104	101	111	—	—	—
F	105	106	129	100	—	120	97	—
FF'	112	139	124	118	89	—	108	105
ff'	59	80	—	66	74	—	—	—
GG'	58	92	60	53	54	43	55	55
gg'	26	39	35	31	33	—	—	—
HI	85	112	—	—	71	96	75	91
hi	—	44	35	—	23	—	—	—
JJ'	47	52	—	—	31	45	41	42
KL	48	53	68	75	59	74	58	66
MM'	51	77	63	44	44	55	43	42
no	52	55	—	64	50	66	52	65
OP	—	98	110	112	—	100	96	104
OT	—	132	—	138	—	—	130	—
P	86	100	71	96	65	82	96	82
QR	40	40	—	43	—	46	40	—
rr'	75	81	88	58	63	61	—	—
ST	77	76	—	82	—	—	75	—
ss'	—	136	149	123	—	—	—	—
T	13	14	—	12	—	17	11	—
tt'	—	38	35	—	—	31	29	23
UV	68	85	—	87	—	—	86	—
WX	38	43	49	37	—	38	37	45
yy'	—	21	—	24	—	51	—	—
YZ	—	140	—	—	—	—	147	—
LFr	54	87	107	—	89	105	89	95
Hso	42	57	43	51	—	46	55	—
Wso	85	94	82	70	59	67	65	72
HIF	10	15	—	—	16	22	20	21
WIF	7	10	—	—	13	18	18	18
RD	40	40	—	55	51	—	—	44

RIB MEASUREMENTS

Measurements of the cross-sectional area of successive ribs in the thorax of *Trichechus manatus* are listed in Table 34. Specimens representing four species of the three Egyptian Eocene Sirenia, *Protosiren*, *Eotheroides*, and *Eosiren*, are also listed in Table 34. The measurements for each specimen are compared as pattern profiles in Figure 84.

Graphic comparison in Figure 84 shows that ribs of *Trichechus manatus* become larger in cross-sectional area from front to back, with the thickest ribs being R10 and R11. In *Trichechus* only the last two ribs are substantially thinner than the preceding ribs.

Of the Eocene taxa, *Protosiren* has thinner ribs than *Trichechus* throughout, but follows a similar pattern in having ribs thicken posteriorly, with only the last two ribs being notably

TABLE 30 — Measurements of Eocene sirenian mandibles, including those from North America. Measurements are in mm, except for MD, which is in degrees. Measurements follow Domning (1978a).

Abb.	Measured dimension	<i>Eotheroides</i>	<i>Eosiren</i>	<i>Eosiren</i>	<i>Protosiren</i>	<i>Eotheroides</i>
		<i>clavigerum</i> CGM 60551	<i>stromeri</i> UM 100137	<i>libyca</i> ST. XIX	<i>smithae</i> CGM 42292	sp. USNM 214596
AA	Total Length	216	213	234	222	181
AG	Anterior tip to front ascending ramus	150	170	173	154	147
AP	Anterior tip to rear of mental foramen	43	54	—	70	52
AQ	Anterior tip to front of mandibular foramen	132	155	170	160	—
AS	Length of symphysis	62	68	80	65	69
BG	Posterior extremity to front of ascending ramus	64	—	70	74	—
BQ	Posterior extremity to front of mandibular foramen	36	50	68	65	—
CD	Height of coronoid process	130	—	—	154	—
DF	Distance between anterior and posterior ventral extremities	120	56	142	113	—
DK	Height of mandibular notch	106	—	107	114	—
DL	Height of condyle	119	—	118	131	—
EF	Height at deflection point of horizontal ramus	69	83	86	66	55
EU	Deflection point to rear of alveolar row	77	105	88	86	87
GH	Minimum anteroposterior breadth of ascending ramus	63	—	60	63	—
GP	Front of ascending ramus to rear of mental foramen	100	112	—	76	—
IJ	Maximum anteroposterior breadth of dorsal part of ascending ramus	65	—	—	76	—
MN	Top of ventral curvature of horizontal ramus to line connecting ventral extremities	32	37	35	26	18
MO	Minimum dorsoventral breadth of horizontal ramus	38	46	47	37	37
RR'	Maximum breadth of masticating surface	37	26	30	51	25
SQ	Rear of symphysis to front of mandibular foramen	72	88	94	99	—
TU	Length of the alveolar row (M ₁₋₃)	44	46	—	64	46
VV'	Maximum width between labial edges of left and right alveoli across M ₁	56	65	61	59	40
WW'	Minimum width between angles	89	65	50	70	—
XX'	Minimum width between condyles	99	—	—	100	—
MD	Deflection of symphyseal surface from occlusal plane (degrees)	50	43	52	58	37

thinner. *Eotheroides* and *Eosiren* have a very different pattern where the thickest ribs are among the first in the series, generally R3 and R4, and the remaining ribs become progressively thinner through the end of the series. Here the pattern in Dugongidae is distinctly different from that in Protosirenidae and Trichechidae.

FORELIMB MEASUREMENTS

Forelimb elements compared here include the scapula, the humerus, and the ulna. These are known for species of the Eocene genera *Protosiren* and *Eotheroides*, but not for *Eosiren*.

Scapula.— A set of 16 scapular measurements is listed in

Table 35. All measurements are linear and in mm. We report measurements for five scapulae, two each for *Eotheroides clavigerum* and *Eotheroides sandersi*, and one for *Protosiren smithae*. These are compared in the pattern profiles in Figure 85.

Graphic comparison of scapular measurements in Figure 85 shows that the two genera, *Protosiren* and *Eotheroides*, and all three of the species plotted have scapulae that follow basically the same profile. Here similarity reflects inheritance and probably also a common adaptation of forelimb function in feeding and locomotion. There are differences in size of the scapulae but differences in proportion are relatively minor.

Humerus.— A set of 17 humeral measurements is listed in Table 36. All measurements are linear and in mm. We report

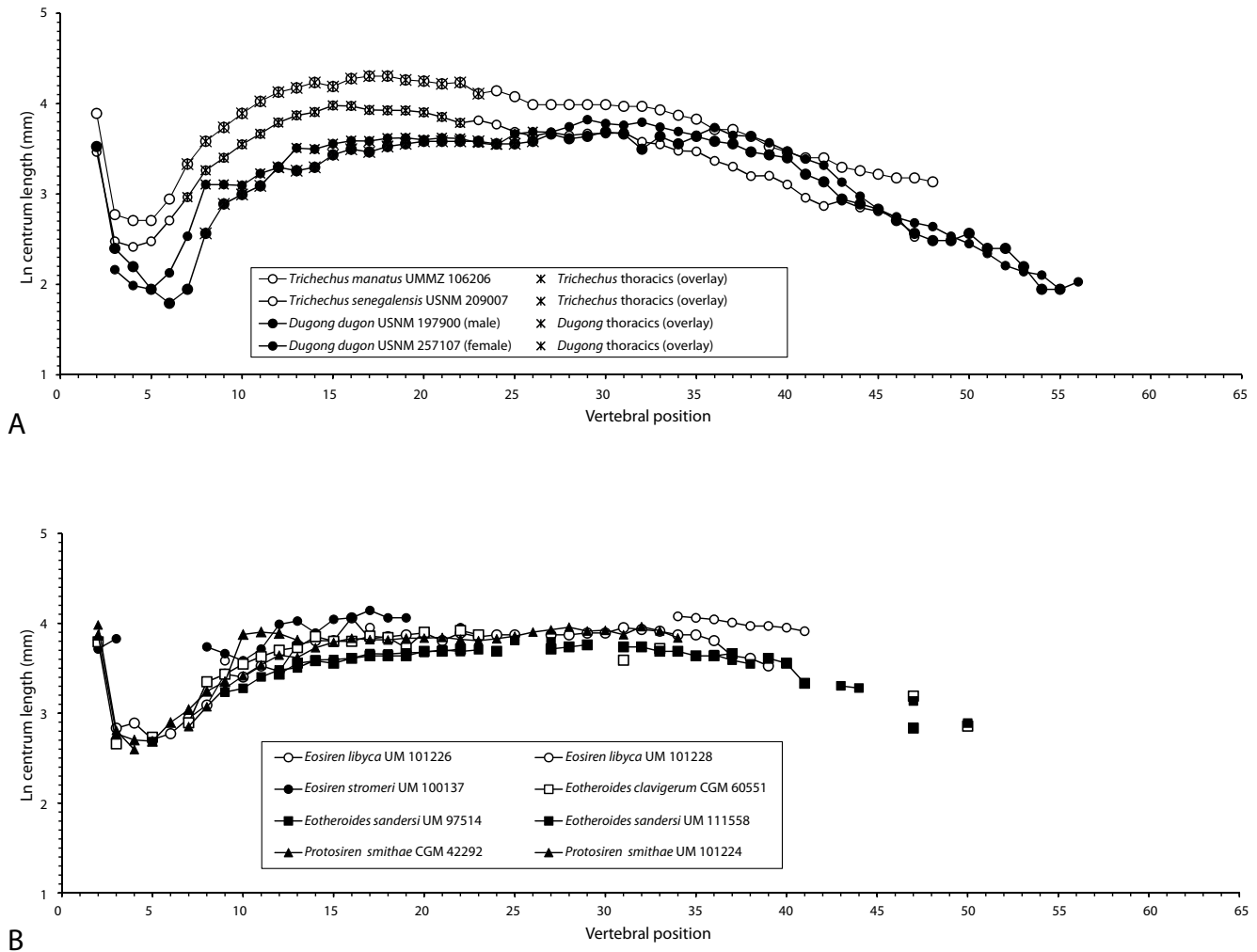


FIGURE 81 — Pattern profiles of vertebral centrum length in Sirenia. A, three species in two genera, *Dugong* and *Manatus*, of extant Sirenia. B, five species in three genera, *Protosiren*, *Eotheroides*, and *Eosiren*, of Priabonian late Eocene Sirenia from Egypt. Symbols for thoracic vertebrae of extant taxa have an ‘X’ overlay. Note the short cervicals characteristic of all sirenians shown here. Note also that the pattern of elongation of centra through the thoracic series is different in *Manatus* and *Dugong*, with elongation continuing into the lumbar series in *Dugong*. Eocene sirenians follow the *Dugong* pattern. Measurements are listed in Table 31.

measurements for five humeri, two each for *Eotheroides clavigerum* and *Eotheroides sandersi*, and one for *Protosiren smithae*. These are compared in the pattern profiles in Figure 86.

Graphic comparison of humeral measurements in Figure 86 shows that the two genera, *Protosiren* and *Eotheroides*, and all three of the species plotted have humeri that follow basically the same profile. As with the scapula, similarity reflects inheritance and probably also a common adaptation of forelimb function in feeding and locomotion. There are differences in size of the humeri but differences in proportion are relatively minor.

Ulna.— A set of 10 ulna measurements is listed in Table 37. All measurements are linear and in mm. We report measurements for four ulni, for three species of the genus *Eotheroides*, and for one species of the genus *Protosiren*. These are compared in the pattern profiles in Figure 87.

Graphic comparison of humeral measurements in Figure 87 shows that the two genera, *Protosiren* and *Eotheroides*, and all four species plotted have ulnae that follow a similar profile. As with the scapula and humerus, similarity reflects inheritance and probably also a common adaptation of forelimb function in feeding and locomotion. There are differences in size of the ulnae but differences in proportion are relatively minor.

HIND LIMB MEASUREMENTS

Hind limb elements compared here include pelvic bones comprising the innominate, the femur, the tibia, and the fibula. The innominate and femur are known for species of all three Eocene genera *Protosiren*, *Eotheroides*, and *Eosiren*, while the tibia and fibula are known only for *Protosiren*.

TABLE 31 — Measurements of sirenian vertebral centrum length. Data for *Dusisiren jordani* are from Domning (1978a). All measurements are in mm. Abbreviations: *f*, female; *m*, male.

<i>Dugong dugon</i>		<i>Dugong dugon</i>		<i>Dusisiren jordani</i>		<i>T. manatus</i>		<i>T. senegalensis</i>	
Vert.	USNM 197900 m	USNM 257107 f	Vert.	UCMP 77037	Vert.	UMMZ 106206	USNM 209007		
C2	34	—	C2	85	C2	49	32		
C3	11	9	C3	23	C3	16	12		
C4	9	7	C4	19	C4	15	11		
C5	7	7	C5	16	C5	15	12		
C6	6	8	C6	20	C6	19	15		
C7	7	13	C7	25	Th1	28	19		
Th1	13	22	Th1	35	Th2	36	26		
Th2	18	22	Th2	41	Th3	42	30		
Th3	20	22	Th3	45	Th4	49	35		
Th4	22	25	Th4	49	Th5	56	39		
Th5	27	27	Th5	53	Th6	62	44		
Th6	26	33	Th6	60	Th7	65	48		
Th7	27	33	Th7	65	Th8	69	50		
Th8	31	35	Th8	67	Th9	66	54		
Th9	33	36	Th9	69	Th10	72	53		
Th10	32	36	Th10	71	Th11	74	51		
Th11	34	37	Th11	74	Th12	74	51		
Th12	35	37	Th12	74	Th13	71	51		
Th13	36	37	Th13	74	Th14	70	60		
Th14	36	37	Th14	79	Th15	68	47		
Th15	36	37	Th15	77	Th16	69	44		
Th16	36	35	Th16	75	Th17	61	45		
Th17	35	35	Th17	76	L1	63	43		
Th18	35	39	Th18	75	L2	59	40		
Th19	36	40	Th19	72	Ca1	54	38		
L1	39	40	Th20	74	Ca2	54	40		
L2	37	42	Th21	77	Ca3	54	38		
L3	38	46	L1	74	Ca4	54	39		
L4	40	44	L2	81	Ca5	54	39		
S	39	43	L3	78	Ca6	53	40		
Ca1	33	45	S	76	Ca7	53	36		
Ca2	38	42	Ca1	73	Ca8	51	35		
Ca3	35	40	Ca2	70	Ca9	48	32		
Ca4	38	39	Ca3	70	Ca10	46	32		
Ca5	36	32	Ca4	70	Ca11	41	29		
Ca6	35	38	Ca5	67	Ca12	41	27		
Ca7	32	38	Ca6	67	Ca13	38	25		
Ca8	31	35	Ca7	69	Ca14	34	25		
Ca9	30	32	Ca8	66	Ca15	32	22		
Ca10	25	30	Ca9	64	Ca16	30	19		
Ca11	23	28	Ca10	59	Ca17	30	18		
Ca12	19	23	Ca11	59	Ca18	27	19		
Ca13	18	20	Ca12	56	Ca19	26	17		
Ca14	17	17	Ca13	50	Ca20	25	17		
Ca15	15	16	Ca14	46	Ca21	24	16		
Ca16	13	15	Ca15	42	Ca22	24	13		
Ca17	12	14	Ca16	40	Ca23	23			
Ca18	12	13	Ca17	39					
Ca19	13	12	Ca18	33					
Ca20	11	10	Ca19	31					
Ca21	11	9	Ca20	29					
Ca22	9	9	Ca21	26					
Ca23	7	7	Ca22	24					
Ca24	7	8	Ca23	21					
			Ca24	19					
			Ca25	17					
			Ca26	17					
			Ca27	16					
			Ca28	15					
			Ca29	15					
			Ca30	14					

TABLE 31 — (continued).

Vert.	<i>Eotheroides sandersi</i> UM 97514	<i>Eotheroides sandersi</i> UM 111558	<i>Eotheroides clavigerum</i> CGM 60551	<i>Eosiren libyca</i> UM 101226	<i>Eosiren stromeri</i> UM 100137	<i>Eosiren libyca</i> UM 101228	<i>Protosiren smithae</i> CGM 42292	<i>Protosiren smithae</i> UM 101224
C2	—	—	44	—	41	—	—	54
C3	—	—	14	17	46	—	48	17
C4	—	—	—	18	—	—	16	13
C5	—	15	15	15	—	—	15	—
C6	—	—	—	16	—	—	15	—
C7	—	—	18	19	—	—	18	17
Th1	—	—	28	22	42	—	21	22
Th2	—	25	31	31	39	36	26	27
Th3	—	26	35	30	36	—	29	30
Th4	—	30	38	34	41	—	48	34
Th5	31	33	40	32	54	—	50	38
Th6	35	33	42	43	56	—	49	37
Th7	36	36	47	45	49	—	45	42
Th8	35	36	45	45	57	—	—	44
Th9	37	37	45	58	58	—	—	46
Th10	38	39	47	46	63	52	—	46
Th11	38	39	47	47	58	—	—	45
Th12	38	39	41	48	58	—	—	46
Th13	40	40	49	49	—	—	—	46
Th14	40	41	—	45	—	—	—	47
Th15	41	40	50	49	52	—	—	46
Th16	—	41	48	47	—	—	—	45
Th17	40	—	—	48	—	—	—	46
Th18	—	45	—	48	—	—	—	47
Th19/20	—	—	—	—	—	—	—	50
L1	41	44	—	48	—	—	—	51
L2	42	—	—	48	—	—	—	52
L3	43	—	—	49	—	—	—	50
L4	—	—	—	49	—	—	—	51
S	42	—	36	52	—	—	—	48
Ca1	42	—	—	51	—	—	—	53
Ca2	40	—	41	50	—	—	—	50
Ca3	40	—	—	48	—	59	—	46
Ca4	38	—	—	48	—	58	—	—
Ca5	38	39	—	45	—	57	—	—
Ca6	39	36	—	38	—	55	—	—
Ca7	—	35	—	37	—	53	—	—
Ca8	37	—	—	34	—	53	—	—
Ca9	35	—	—	—	—	52	—	—
Ca10	28	—	—	—	—	50	—	—
Ca11	—	—	—	—	—	—	—	—
Ca12	—	27	—	—	—	—	—	—
Ca13	—	27	—	—	—	—	—	—
Ca14	—	—	—	—	—	—	—	—
Ca15	—	—	—	—	—	—	—	—
Ca16	17	23	24	—	—	—	—	—
Ca17	—	—	—	—	—	—	—	—
Ca18	—	—	—	—	—	—	—	—
Ca19	—	18	17	—	—	—	—	—

TABLE 32 — (continued).

Vert.	<i>Eosiren libyca</i> UM 101226	<i>Eotheroides clavigerum</i> CGM 60551	<i>Eotheroides sandersi</i> UM 97514	<i>Eotheroides sandersi</i> UM 111558	<i>Eosiren stromeri</i> UM 100137	<i>Eosiren libyca</i> UM 101228	<i>Protosiren smithae</i> CGM 42292	<i>Protosiren smithae</i> UM 101224
C1	105	116	—	106	—	—	126	134
C2	—	70	—	—	—	—	83	93
C3	—	—	—	—	—	—	90	104
C4	—	—	—	—	—	—	90	99
C5	—	107	—	84	—	—	—	—
C6	—	—	—	—	—	—	104	—
C7	—	—	—	—	—	—	110	115
Th1	—	108	—	—	119	—	118	132
Th2	—	100	—	—	126	—	121	123
Th3	—	100	—	101	118	—	—	105
Th4	134	94	—	93	107	—	—	99
Th5	—	90	99	—	—	—	—	89
Th6	108	93	91	86	95	—	—	111
Th7	102	86	93	82	94	—	—	112
Th8	106	87	—	81	—	—	—	112
Th9	104	87	89	81	—	—	—	111
Th10	98	86	87	98	—	81	—	106
Th11	98	85	88	79	—	—	—	90
Th12	99	91	83	80	—	—	—	105
Th13	98	79	81	78	—	—	—	98
Th14	94	—	86	79	—	—	—	96
Th15	88	—	79	77	—	—	—	107
Th16	86	—	—	78	—	—	—	88
Th17	83	82	70	—	—	—	—	105
Th18	92	—	—	—	—	—	—	111
Th19/20	—	—	—	118	—	—	—	—
L1	196	—	—	168	—	—	—	213
L2	229	—	—	—	—	—	—	—
L3	236	—	190	—	—	—	—	—
L4	228	—	188	—	—	—	—	—
S	210	—	191	—	—	—	201	107
Ca1	181	—	192	—	—	—	—	—
Ca2	164	—	175	—	—	—	181	113
Ca3	141	—	177	—	—	—	—	—
Ca4	152	182	168	—	—	—	—	—
Ca5	133	—	156	—	—	153	—	—
Ca6	116	—	—	144	—	119	—	—
Ca7	106	—	—	120	—	106	—	—
Ca8	104	—	143	—	—	97	—	—
Ca9	—	—	136	—	—	93	—	—
Ca10	—	—	114	—	—	90	—	—
Ca11	—	—	—	—	—	88	—	—
Ca12	—	—	—	—	—	87	—	—
Ca13	—	—	—	95	—	—	—	—
Ca14	—	—	—	—	—	—	—	—
Ca15	—	—	—	40	—	—	—	—
Ca16	—	67	33	—	—	—	—	—
Ca17	—	—	—	—	—	—	—	—
Ca18	—	—	—	—	—	—	—	—
Ca19	—	23	—	—	—	—	—	—

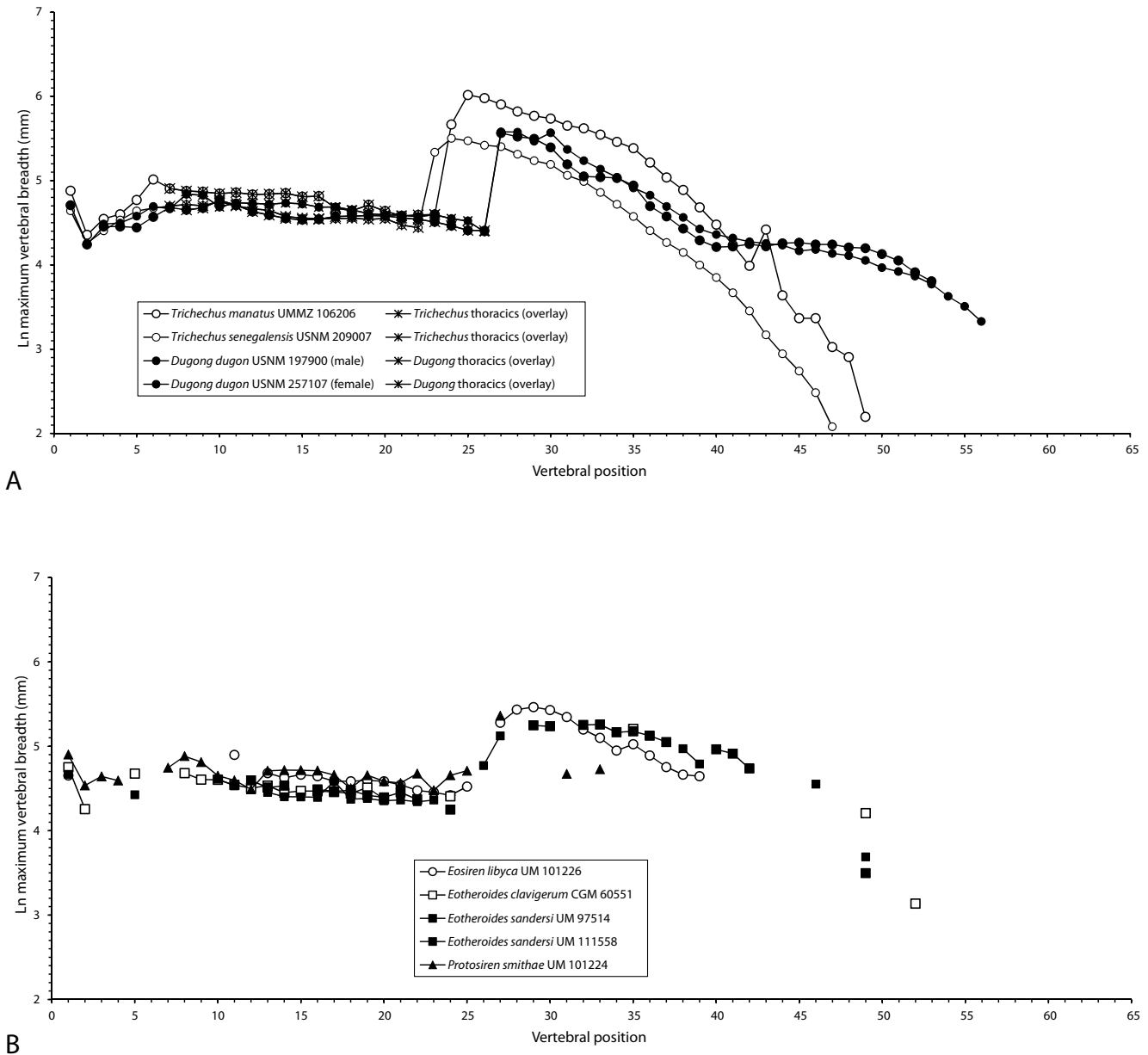


FIGURE 82 — Pattern profiles of maximum vertebral breadth in Sirenia. A, three species in two genera, *Dugong* and *Trichechus*, of extant Sirenia. B, five species in three genera, *Protosiren*, *Eotheroides*, and *Eosiren*, of Priabonian late Eocene Sirenia from Egypt). Symbols for thoracic vertebrae of extant taxa have an 'X' overlay. Note the slightly narrow cervicals characteristic of all sirenians shown here. Note also the pattern of narrowing of vertebrae through the thoracic series, the abrupt increase in breadth in the transition from thoracics to lumbar, and the differing patterns of narrowing through the lumbar, sacral, and caudal series in *Trichechus* and *Dugong*. It is not clear whether tail-narrowing in the Eocene sirenians follows the *Trichechus* pattern, the *Dugong* pattern, or something in between. Measurements are listed in Table 32.

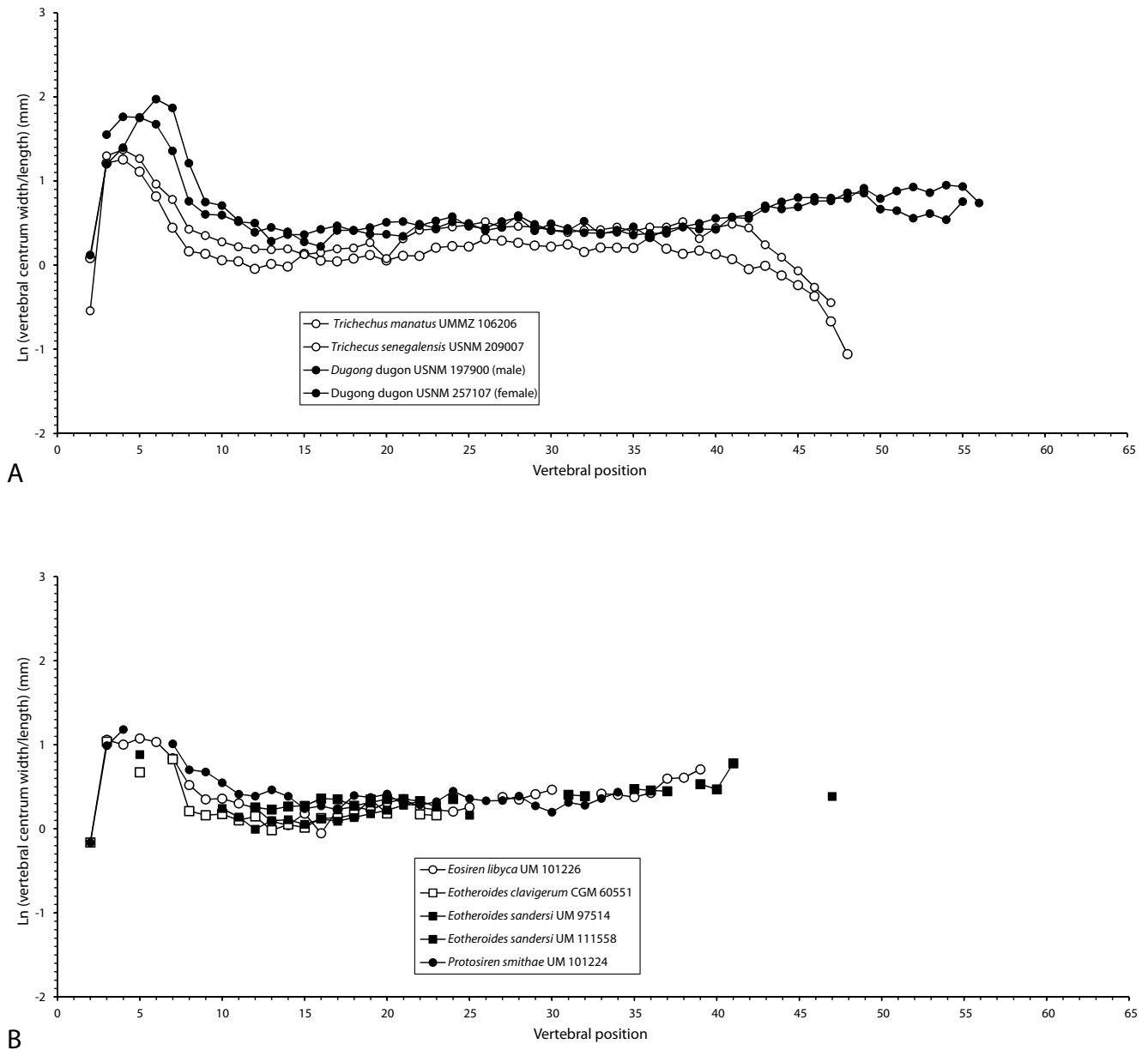


FIGURE 83 — Pattern profiles of vertebral centrum width-to-length shape relationships in Sirenia. A, three species in two genera, *Dugong* and *Trichechus*, of extant Sirenia. B, four species in three genera, *Protosiren*, *Eotheroides*, and *Eosiren*, of Priabonian late Eocene Sirenia from Egypt. Note that the shape ratio for C2 (vertebra 2 in the whole series) is low, while those for remaining cervicals are higher. Anterior thoracic vertebrae have a low shape ratio and this climbs slightly from mid-thorax to the tail in *Dugong* and the fossil specimens, while the shape ratio falls sharply in the tail of *Trichechus*. Measurements enabling calculation of the shape ratios are listed in Table 33.

TABLE 33 — Centrum dimensions and shape quotients for vertebrae of *Sirenia* studied here. Measurements are in mm. Abbreviations: *f*, female; *L*, length; *m*, male; *W*, width.

Vert.	<i>Dugong dugon</i> USNM 197900 m			<i>Dugong dugon</i> USNM 257107 f			Vert.	<i>Trichechus manatus</i> UMMZ 106206			<i>Trichechus senegalensis</i> USNM 209007		
	L	W	W/L	L	W	W/L		L	W	W/L	L	W	W/L
C1	—	—	—	—	—	—	C1	—	—	—	—	—	—
C2	34	38.3	1.13	—	—	—	C2	49	53.3	1.09	32.0	18.6	0.58
C3	11	36.5	3.32	8.7	41.0	4.71	C3	16	53.7	3.36	11.9	43.6	3.66
C4	9	36.3	4.03	7.3	42.5	5.82	C4	15	52.6	3.51	11.2	44.1	3.94
C5	7	40.2	5.74	7.0	40.5	5.79	C5	15	45.5	3.03	11.9	42.2	3.55
C6	6	43.1	7.18	8.4	44.8	5.33	C6	19	43.0	2.26	15.0	39.3	2.62
C7	7	45.3	6.47	12.6	48.9	3.88	C7	28	43.7	1.56	19.4	42.3	2.18
Th1	13	43.6	3.35	22.3	47.6	2.13	Th1	36	42.4	1.18	26.1	40.0	1.53
Th2	18	38.1	2.12	22.3	40.8	1.83	Th2	42	48.0	1.14	30.0	42.6	1.42
Th3	20	40.6	2.03	22.1	40.0	1.81	Th3	49	51.9	1.06	34.8	45.9	1.32
Th4	22	37.4	1.70	25.2	42.2	1.67	Th4	56	58.6	1.05	39.1	48.6	1.24
Th5	27	39.9	1.48	26.9	44.3	1.65	Th5	62	59.3	0.96	44.3	53.6	1.21
Th6	26	40.7	1.57	33.4	44.4	1.33	Th6	65	65.9	1.01	47.9	57.6	1.20
Th7	27	40.1	1.49	33.0	47.4	1.44	Th7	69	67.8	0.98	49.7	60.3	1.21
Th8	31	40.9	1.32	35.0	50.3	1.44	Th8	66	75.5	1.14	53.5	60.6	1.13
Th9	33	41.2	1.25	36.2	55.3	1.53	Th9	72	76.0	1.06	53.2	61.9	1.16
Th10	32	48.3	1.51	36.1	57.6	1.60	Th10	74	77.4	1.05	50.9	61.7	1.21
Th11	34	51.5	1.51	37.2	56.0	1.51	Th11	74	80.0	1.08	50.7	62.2	1.23
Th12	35	50.6	1.45	37.4	58.4	1.56	Th12	71	80.0	1.13	50.6	66.1	1.31
Th13	36	51.9	1.44	36.6	60.9	1.66	Th13	70	74.0	1.06	49.6	64.4	1.30
Th14	36	50.7	1.41	37.4	62.7	1.68	Th14	68	76.0	1.12	47.1	64.4	1.37
Th15	36	58.6	1.63	37.1	59.3	1.60	Th15	69	77.0	1.12	44.1	66.8	1.51
Th16	36	55.9	1.55	35.4	59.8	1.69	Th16	61	75.0	1.23	45.4	69.8	1.54
Th17	35	58.5	1.67	34.6	61.5	1.78	Th17	63	79.0	1.25	43.3	68.2	1.58
Th18	35	57.5	1.64	39.0	61.8	1.58	Th18	59	73.5	1.25	40.0	64.4	1.61
Th19	36	54.3	1.51	40.0	62.0	1.55	Th19	54	73.7	1.36	38.1	63.8	1.67
L1	39	61.1	1.57	39.8	66.8	1.68	L1	54	72.3	1.34	39.7	62.3	1.57
L2	37	66.7	1.80	42.3	74.5	1.76	L2	54	70.4	1.30	38.4	60.9	1.59
L3	38	61.7	1.62	45.7	68.7	1.50	L3	54	68.1	1.26	39.2	61.7	1.57
L4	40	60.3	1.51	43.8	71.6	1.63	L4	54	67.3	1.25	39.2	59.3	1.51
S	39	58.6	1.50	43.0	66.4	1.54	S	53	67.8	1.28	39.7	58.5	1.47
Ca1	33	55.6	1.68	44.5	65.3	1.47	Ca1	53	62.0	1.17	35.8	54.3	1.52
Ca2	38	54.8	1.44	42.1	61.5	1.46	Ca2	51	62.9	1.23	34.8	53.0	1.52
Ca3	35	53.0	1.51	40.1	59.2	1.48	Ca3	48	59.1	1.23	32.4	50.9	1.57
Ca4	38	54.3	1.43	38.5	60.7	1.58	Ca4	46	56.4	1.23	32.2	48.0	1.49
Ca5	36	52.5	1.46	41.9	58.3	1.39	Ca5	41	57.2	1.40	29.0	45.6	1.57
Ca6	35	51.0	1.46	38.4	58.3	1.52	Ca6	41	49.8	1.21	27.2	42.7	1.57
Ca7	32	50.3	1.57	38.1	60.1	1.58	Ca7	38	43.5	1.14	24.5	41.0	1.67
Ca8	31	47.5	1.53	35.4	58.1	1.64	Ca8	34	40.4	1.19	24.6	33.7	1.37
Ca9	30	45.9	1.53	32.3	56.3	1.74	Ca9	32	36.4	1.14	22.3	34.8	1.56
Ca10	25	44.3	1.77	29.6	52.2	1.76	Ca10	30	32.2	1.07	19.3	31.4	1.63
Ca11	23	41.6	1.81	27.6	48.0	1.74	Ca11	30	28.6	0.95	17.6	27.4	1.56
Ca12	19	38.5	2.03	22.9	44.8	1.96	Ca12	27	26.8	0.99	18.7	23.8	1.27
Ca13	18	35.1	1.95	19.6	41.5	2.12	Ca13	26	23.0	0.88	17.3	19.0	1.10
Ca14	17	33.9	1.99	17.0	37.9	2.23	Ca14	25	19.7	0.79	16.6	15.5	0.93
Ca15	15	32.1	2.14	15.5	34.6	2.23	Ca15	24	16.6	0.69	15.6	12.0	0.77
Ca16	13	27.9	2.15	14.6	32.4	2.22	Ca16	24	12.3	0.51	12.5	8.0	0.64
Ca17	12	28.3	2.36	14.0	30.9	2.21	Ca17	23	8.0	0.35	8.0	—	—
Ca18	12	28.2	2.35	12.6	31.4	2.49	Ca18				12.6	31.4	2.49
Ca19	13	25.3	1.95	11.6	25.6	2.21	Ca19				11.6	25.6	2.21
Ca20	11	21.0	1.91	10.4	25.1	2.41	Ca20				10.4	25.1	2.41
Ca21	11	19.2	1.75	9.1	23.0	2.53	Ca21				9.1	23.0	2.53
Ca22	9	16.6	1.84	8.5	20.1	2.36	Ca22				8.5	20.1	2.36
Ca23	7	12.0	1.71	8.2	21.2	2.59	Ca23				8.2	21.2	2.59
Ca24	7	14.9	2.13	7.0	17.8	2.54	Ca24				7.0	17.8	2.54
Ca25				7.6	15.9	2.09	Ca25				7.6	15.9	2.09

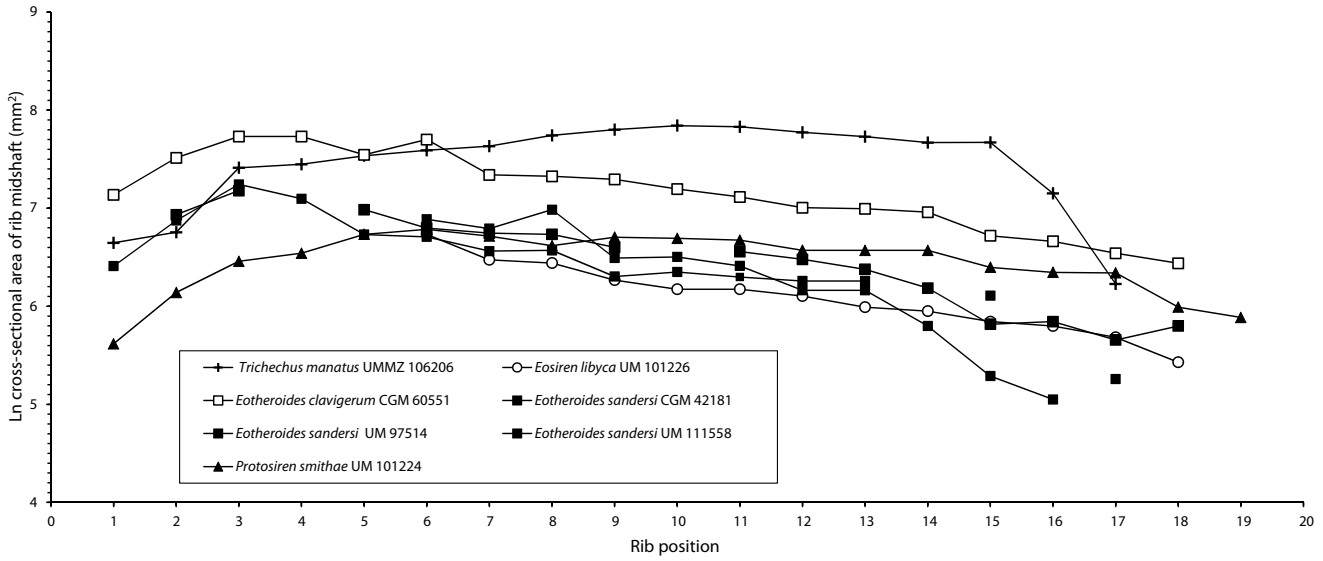


FIGURE 84 — Pattern profiles of rib midshaft cross-sectional area for extant *Trichechus manatus* and for five species in three genera of Sirenia from the Priabonian late Eocene of Egypt. Note the distinctly different patterns of increasing midshaft cross-section through the rib cage in *Manatus* and *Protosiren*, and decreasing midshaft cross-section in *Eosiren* and *Eootheroides*. Measurements are listed in Table 34.

TABLE 34 — Cross-sectional area of sirenian rib midshafts. Measurements are in mm².

Rib	<i>Protosiren smithae</i> UM 101224	<i>Eootheroides sandersi</i> UM 111558	<i>Eootheroides sandersi</i> UM 97514	<i>Eootheroides sandersi</i> CGM 42181	<i>Eootheroides clavigerum</i> CGM 60551	<i>Eosiren libyca</i> UM 101226	<i>Trichechus manatus</i> UMMZ 106206
R1	275	608	—	—	1258	—	770
R2	464	967	—	1026	1833	—	858
R3	638	1398	—	1312	2279	—	1656
R4	693	1208	—	—	2279	—	1716
R5	840	839	—	1080	1890	—	1872
R6	884	819	980	896	2208	840	1980
R7	825	708	891	850	1540	648	2065
R8	748	713	1080	840	1518	627	2304
R9	816	546	660	736	1472	527	2442
R10	806	572	667	—	1333	480	2546
R11	792	544	609	704	1230	480	2516
R12	714	522	475	651	1102	448	2376
R13	713	522	475	588	1090	400	2275
R14	713	—	330	486	1053	384	2142
R15	600	450	198	336	828	345	2145
R16	570	—	156	345	782	330	1276
R17	567	192	—	286	693	294	506
R18	400	—	—	330	625	228	—
R19	360	—	—	—	—	—	—

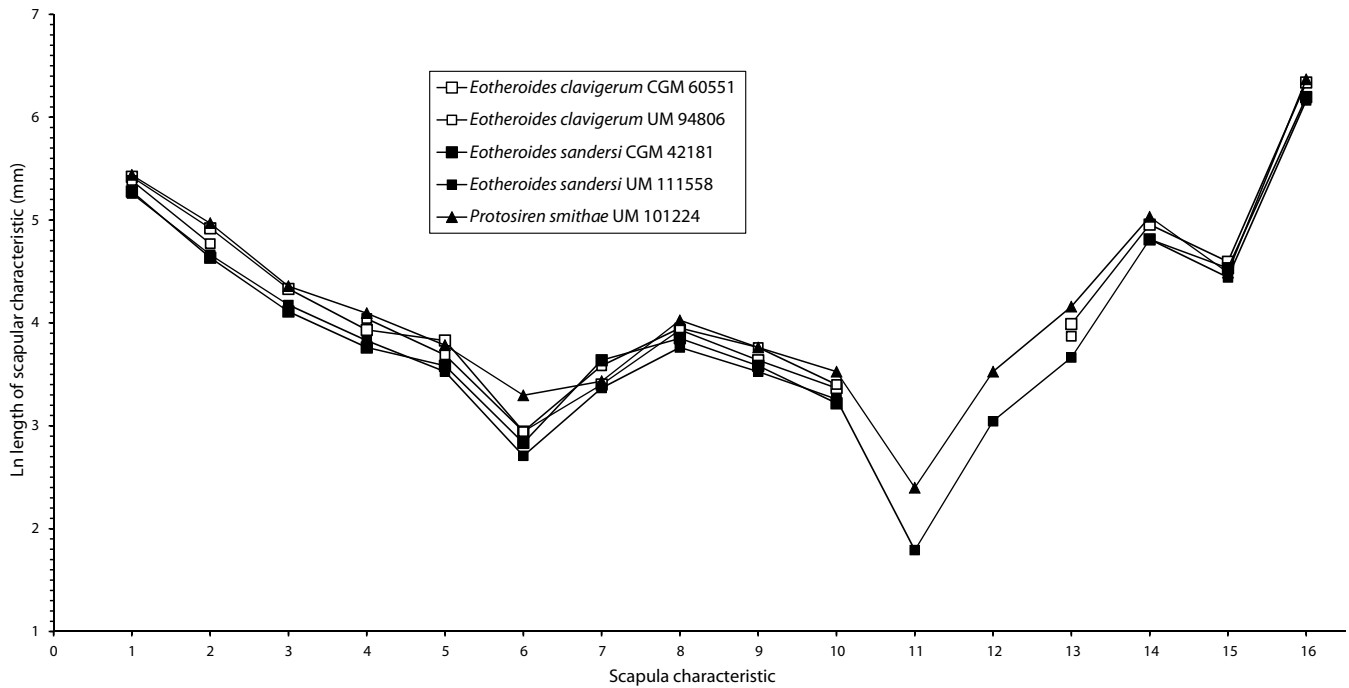


FIGURE 85 — Pattern profiles of scapula measurements for three species in two sirenian genera, *Protosiren* and *Eotheroides*, from the Priabonian late Eocene of Egypt. Note the similarity of all five profiles suggesting similar forelimb adaptation for feeding and locomotion in both genera. Measurements are listed in Table 35.

TABLE 35 — Scapula dimensions of Eocene Sirenia from Egypt. Note that *Eotheroides clavigerum* and *Protosiren smithae* have the longest blades and spines, and widest breadths. Measurements are in mm.

Key	Measurement	<i>Eotheroides clavigerum</i> CGM 60551	<i>Eotheroides clavigerum</i> UM 94806	<i>Eotheroides sandersi</i> UM 111558	<i>Eotheroides sandersi</i> CGM 42181	<i>Protosiren smithae</i> UM 101224
1	Scapular length along the spine	226	218	192	196	230
2	Spine length	137	118	106	103	144
3	Scapular breadth	76	—	65	61	78
4	Infraspinous fossa breadth	51	57	46	43	60
5	Neck breadth	46	40	34	36	44
6	Neck height	19	19	15	17	27
7	Distance from median glenoid cavity to acromion	30	36	29	38	31
8	Glenoid process breadth	51	52	43	47	56
9	Glenoid cavity breadth	38	43	34	36	43
10	Glenoid cavity height	29	30	26	25	34
11	Breadth of the acromion	—	—	6	—	11
12	Spine height from dorsal surface	—	—	21	—	34
13	Spine height from ventral surface	54	48	39	—	64
14	Distance between anterior tip of glenoid process and anterodorsal edge of blade	142	—	123	123	153
15	Distance between posterior tip of the glenoid process and first posterior edge of blade	99	—	85	93	89
16	Circumference of the blade	565	—	475	490	583

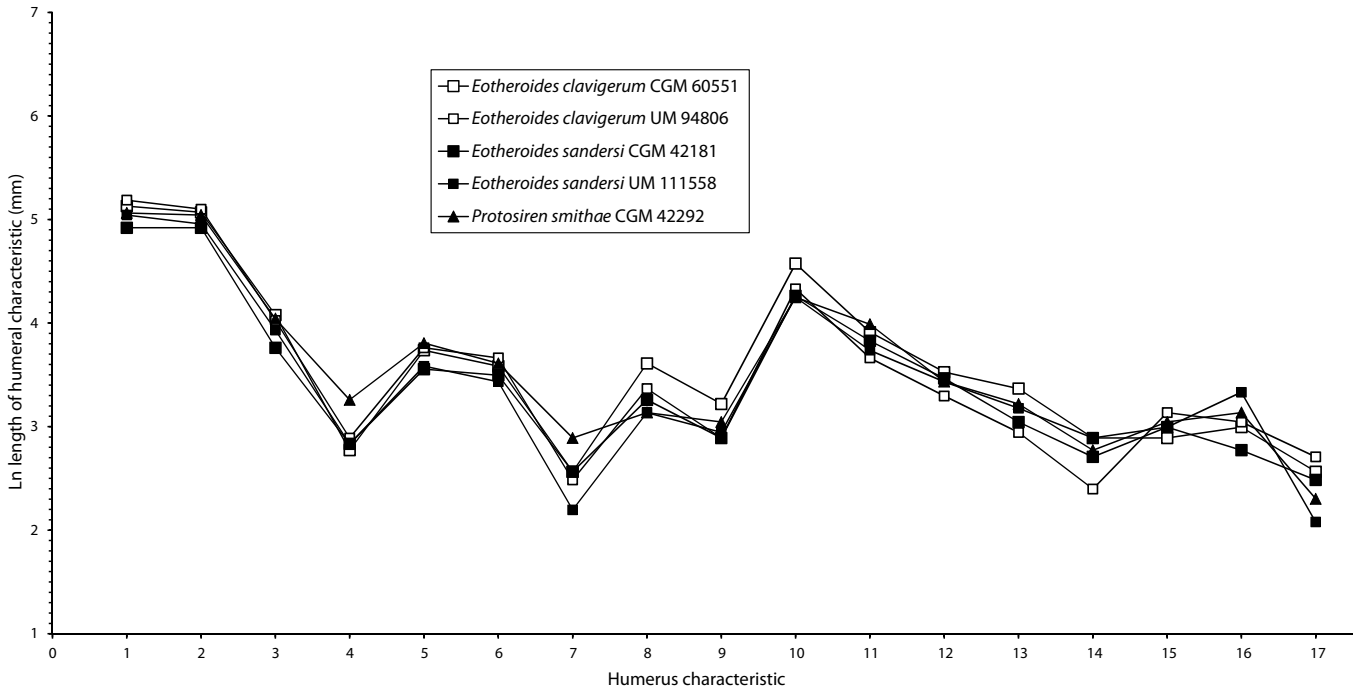


FIGURE 86 — Pattern profiles of humerus measurements for three species in two sirenian genera, *Protosiren* and *Eotheroides*, from the Priabonian late Eocene of Egypt. Note the similarity of all five profiles suggesting similar forelimb adaptation for feeding and locomotion in both genera. Measurements are listed in Table 36.

TABLE 36 — Humerus dimensions of Eocene Sirenia from Egypt. Measurements are in mm.

Key	Measurement	<i>Eotheroides clavigerum</i> CGM 60551	<i>Eotheroides clavigerum</i> UM 94806	<i>Eotheroides sandersi</i> UM 111558	<i>Eotheroides sandersi</i> CGM 42181	<i>Protosiren smithae</i> CGM 42292
1	Length (greater tubercle to distal end)	169	179	155	137	158
2	Length from the head to the distal end	159	164	142	137	155
3	Proximal end maximum breadth	59	56	51	43	57
4	Head height	16	18	17	17	26
5	Head length	42	43	36	35	45
6	Head width	36	39	31	33	37
7	Bicipital groove width	13	12	9	13	18
8	Maximum width of the midshaft	37	29	23	26	23
9	Minimum width of the shaft in the middle	25	18	19	18	21
10	Minimum circumference of the shaft	97	76	70	71	70
11	Distal end maximum breadth	50	39	42	46	54
12	Trochlea breadth	34	27	31	32	31
13	Trochlea height	29	19	24	21	25
14	Trochlea height in the middle	18	11	18	15	16
15	Olecranial fossa width	18	23	20	20	21
16	Olecranial fossa height	20	21	28	16	23
17	Olecranial fossa depth	13	15	8	12	10

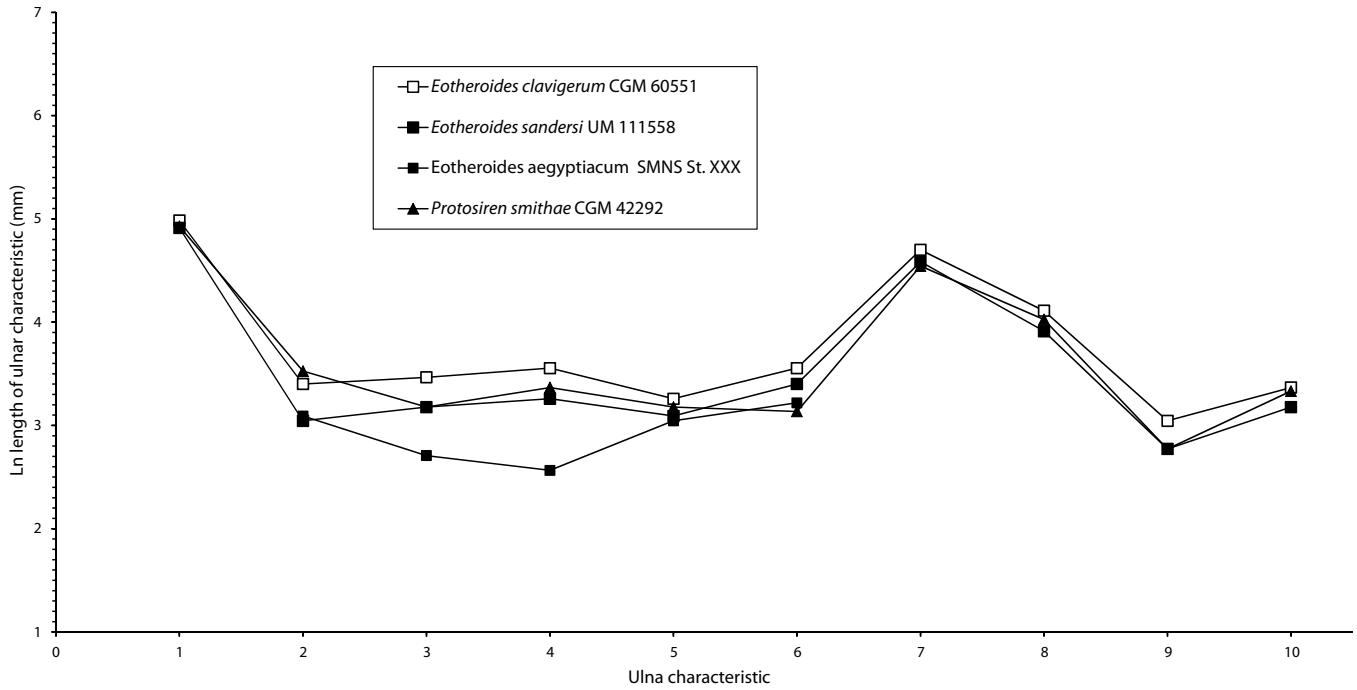


FIGURE 87 — Pattern profiles of ulna measurements for four species in two genera, *Protosiren* and *Eotheroides*, from the Lutetian to Bartonian middle Eocene and from the Priabonian late Eocene of Egypt. Note the similarity of all four profiles suggesting similar forelimb adaptation for feeding and locomotion in both genera. Measurements are listed in Table 37.

TABLE 37 — Ulna dimensions of Eocene Sirenia from Egypt. Measurements are in mm.

Key	Measurements	<i>Eotheroides clavigerum</i> CGM 60551	<i>Eotheroides sandersi</i> UM 111558	<i>Eotheroides aegyptiacum</i> SMNS St.XXX	<i>Protosiren smithae</i> CGM 42292
1	Greatest length	146	136	—	138
2	Length of the olecranon	30	21	22	34
3	Smallest depth of olecranon	32	24	15	24
4	Greatest depth at the anconeal process	35	26	13	29
5	Height of the trochlear notch	26	22	21	24
6	Breadth across the coronoid process	35	30	25	23
7	Height from the coronoid process to the distal epiphysis	110	98	—	94
8	Circumference of midshaft	61	50	—	56
9	Width of the distal epiphysis	21	16	—	16
10	Length of the distal epiphysis	29	24	—	28

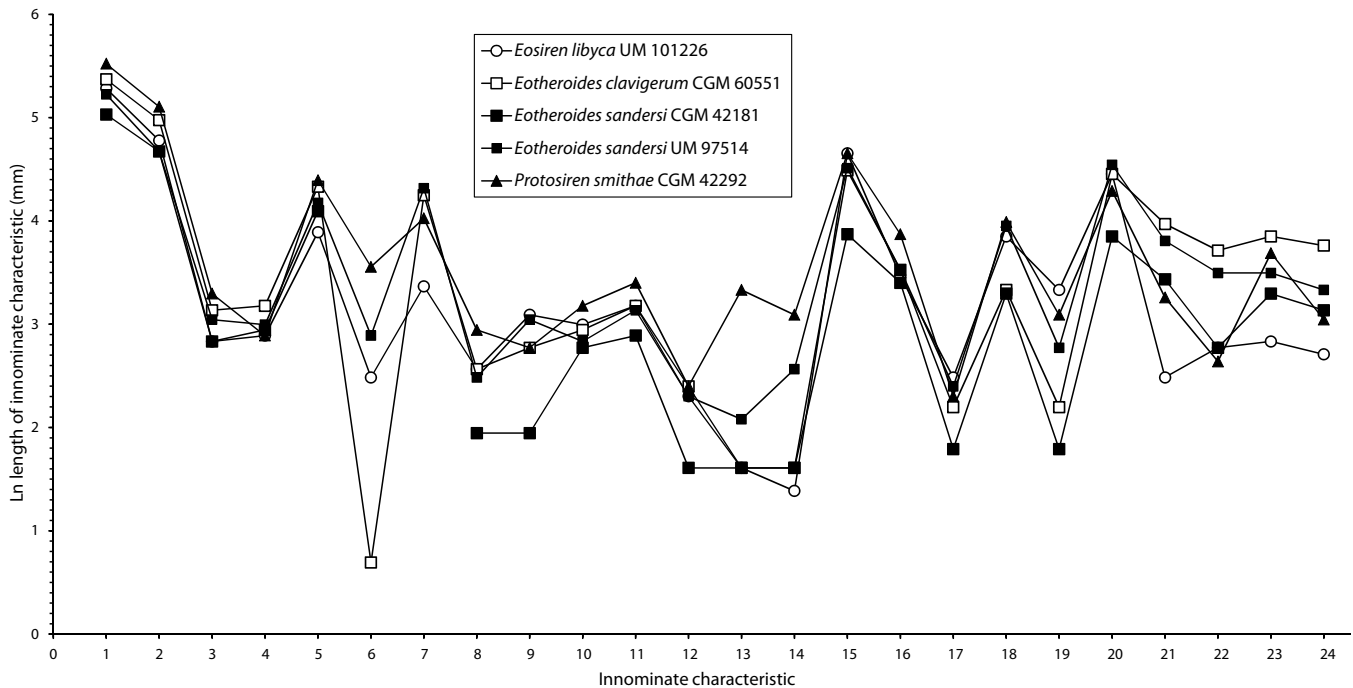


FIGURE 88 — Pattern profiles of innominate measurements for four species in three genera, *Protosiren*, *Eotheroides*, and *Eosiren*, from the Priabonian late Eocene of Egypt. Note the marked differences in pelvic measurements profiled here, making the innominate one of the most distinctive elements in the skeleton of Eocene sirenians. Measurements are listed in Table 38.

Innominate.— A set of 24 innominate measurements is listed in Table 38. All measurements are linear and in mm. We report measurements for five innominates, one for *Protosiren smithae*, one for *Eotheroides clavigerum*, two of *Eotheroides sandersi*, and one for *Eosiren libyca*. These are compared in the pattern profiles in Figure 88.

Graphic comparison of innominate measurements in Figure 88 shows the most scatter of any of the graphic comparisons. Conspicuous differences include pubic symphysis length (characteristic 6), the size of the obturator foramen (characteristics 13 and 14), the size of the surface for articulation with auricular processes of the sacrum (characteristics 21 and 22), and the size of the proximal end of the ilium (characteristics 23 and 24).

Protosiren smithae has the longest pubic symphysis length, while *Eotheroides clavigerum* has the shortest. *Protosiren smithae* has the largest obturator foramen, while *Eotheroides sandersi* and *Eosiren libyca* have the smallest. *Eotheroides clavigerum* and *Eotheroides sandersi* have the largest auricular surfaces while *Protosiren smithae* and *Eosiren libyca* have the smallest. *Eotheroides clavigerum* has the largest proximal ilium while *Eosiren libyca* has the smallest.

Femur.— A set of 14 femur measurements is listed in Table 39. All measurements are linear and in mm. We report measurements for five femora, one for *Protosiren smithae*, two for *Eotheroides sandersi*, one for *Eosiren libyca*, and one for *Pezosiren portelli* from Jamaica (Domning, 2001b). These are compared in the pattern profiles in Figure 89.

Graphic comparison of femur measurements in Figure 89 shows general uniformity, with *Pezosiren* and *Protosiren* having similar but larger femora, and *Eotheroides* and *Eosiren* having similar but smaller femora.

Tibia and fibula.— A set of 16 tibia and fibula measurements is listed in Table 40. All measurements are linear and in mm. We report measurements for three tibiae and two fibulae. These are best known for *Protosiren smithae* from the Priabonian late Eocene of Egypt, and the femur is also known for *Pezosiren portelli* from Jamaica (Domning, 2001b). These are compared in the pattern profiles in Figure 90.

Graphic comparison of tibia measurements in Figure 90 (characteristics 1-7) shows general uniformity, with *Pezosiren* and *Protosiren* having tibiae similar in size and shape.

TABLE 38 — Innominate dimensions of Eocene Sirenia from Egypt. Measurements are in mm.

Key	Measurement	<i>Eotheroides clavigerum</i> CGM 60551	<i>Eotheroides sandersi</i> CGM 42181	<i>Eotheroides sandersi</i> UM 97514	<i>Eosiren libyca</i> UM 101226	<i>Protosiren smithae</i> CGM 42292
1	Total length	215	153	186	197	250
2	Ilium length from center of acetabulum to proximal end	145	107	107	119	165
3	Ilium dorsoventral diameter at midshaft	23	17	21	17	27
4	Ilium mediolateral diameter of at midshaft	24	19	20	18	18
5	Ilium circumference at midshaft	76	60	65	49	81
6	Symphysis length	2	—	18	12	35
7	Pubic line length from center acetabulum to pubic symphysis	70	—	75	29	56
8	Pubic ramus thickness in front of the obturator foramen	13	7	12	13	19
9	Pubic Ramus thickness behind the obturator foramen	16	7	21	22	16
10	Acetabulum diameter	19	16	17	20	24
11	Acetabulum external diameter	24	18	23	24	30
12	Acetabulum depth	11	5	10	10	11
13	Obturator foramen length	5	5	8	5	28
14	Obturator foramen height	5	5	13	4	22
15	Ischium length from center of the acetabulum to distal end	89	48	91	105	105
16	Ischiac ramus thickness dorsoventral	34	30	34	32	48
17	Ischiac ramus thickness mediolaterally	9	6	11	12	10
18	Maximum dorsoventral length of the distal end of the ischium	28	27	52	47	54
19	Maximum mediolateral thickness of the distal end of the ischium	9	6	16	28	22
20	Distance between the inner posterior edge of the obturator foramen and the ischiac tuberosity	86	47	94	86	73
21	Length of the sacral articulation surface with the sacrum (anteroposterior length of the oval articulation)	53	31	45	12	26
22	Height of the sacral articulation surface with the sacrum (dorsoventral height of the oval articulation)	41	16	33	16	14
23	Maximum height of the proximal end of the ilium dorsoventrally	47	27	33	17	40
24	Maximum width of the proximal end of the ilium mediolaterally	43	23	28	15	21

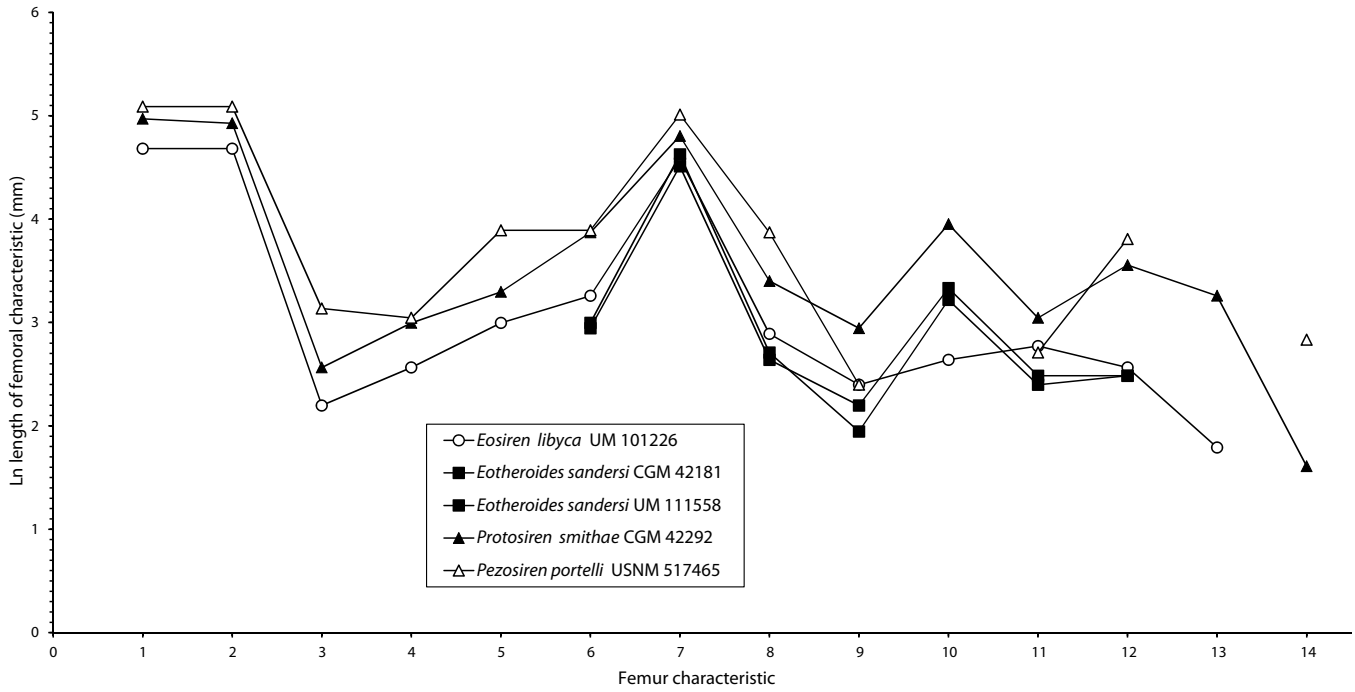


FIGURE 89 — Pattern profiles of femur measurements for four species in three genera, *Protosiren*, *Eotheroides*, and *Eosiren*, from the Priabonian late Eocene of Egypt, and one species, *Pezosiren portelli*, from the middle Eocene of Jamaica. Note the similarity in size and shape of femora of *Pezosiren* and *Protosiren*, and the distinctly smaller size of femora of *Eotheroides* and *Eosiren*. Measurements are listed in Table 39.

TABLE 39 — Femur dimensions of Eocene Sirenian from Egypt and Jamaica (Domning, 2001b). Measurements are in mm.

Key	Measurement	<i>Eotheroides sandersi</i> CGM 42181	<i>Eotheroides sandersi</i> UM 111558	<i>Eosiren libyca</i> UM 101226	<i>Protosiren smithae</i> CGM 42292	<i>Pezosiren portelli</i> USNM 517465
1	Greatest length	—	—	108	144	162
2	Total length from the femoral head	—	—	108	138	162
3	Head height	—	—	9	13	23
4	Head length anteroposteriorly	—	—	13	20	21
5	Head width mediolaterally	—	—	20	27	49
6	Greatest proximal width	19	20	26	48	49
7	Length of the femoral body	91	102	98	122	150
8	Width across the second trochanter	14	15	18	30	48
9	Minimum width of the diaphysis	9	7	11	19	11
10	Minimum circumference of diaphysis	28	25	14	52	—
11	Minimum width of the distal end	12	11	16	21	15
12	Greatest width of the distal end	12	12	13	35	45
13	Width between the external ends of the distal lateral condyles	—	—	6	26	—
14	Internal distance between the lateral condyles	—	—	—	5	17

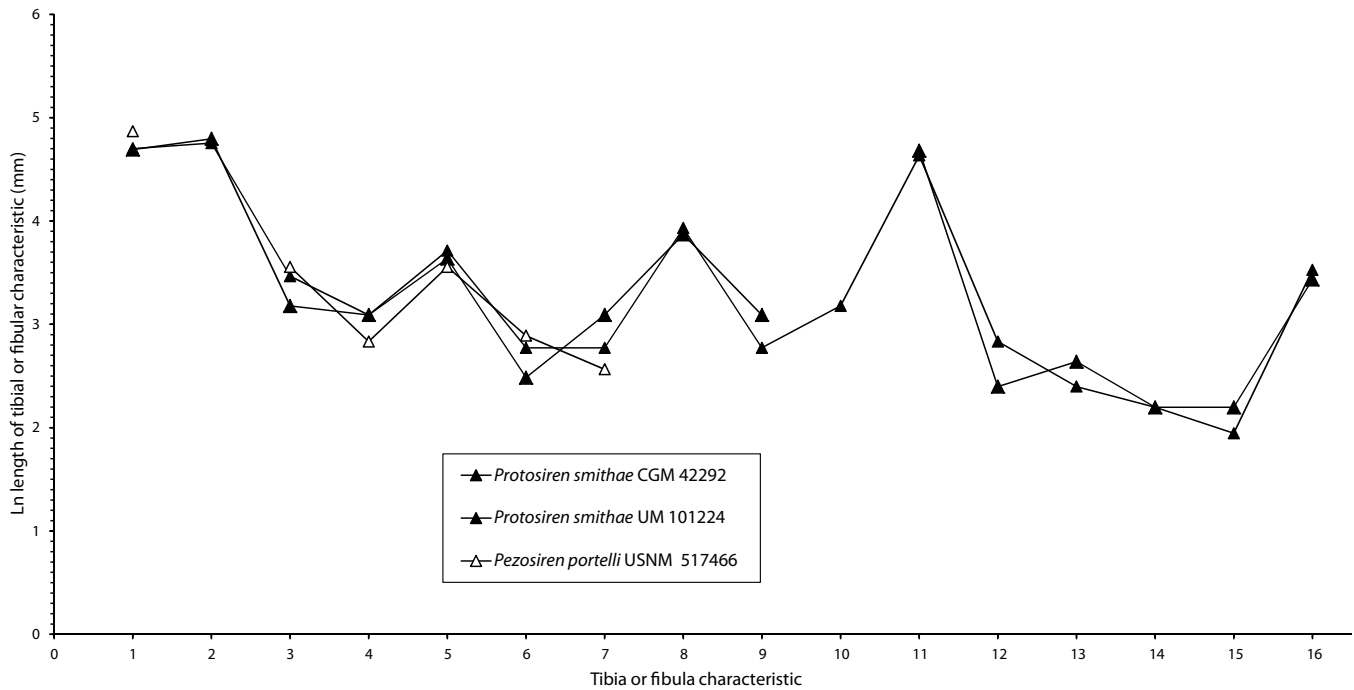


FIGURE 90 — Pattern profiles of tibia measurements (characteristics 1-7) for two genera and species, *Protosiren smithae* from the Priabonian late Eocene of Egypt, and *Pezosiren portelli*, from the middle Eocene of Jamaica (Domning, 2001b). Fibulae (characteristics 8-16) are known only for *Protosiren smithae*. Note the similarity in size and shape of tibiae of *Pezosiren* and *Protosiren*. Measurements are listed in Table 40.

TABLE 40 — Tibia and fibula dimensions of Eocene Sirenian from Egypt and Jamaica (Domning, 2001b). Measurements are in mm.

Key	Measurement	<i>Protosiren smithae</i> CGM 42292	<i>Protosiren smithae</i> UM 101224	<i>Pezosiren portelli</i> USNM 517466
1	Greatest length of the tibia	109	110	130
2	Greatest length of the tibia including the epiphyses	121	116	—
3	Greatest width of the proximal end	24	32	35
4	Greatest length of the proximal end	22	22	17
5	Greatest proximal width including the fibula	38	41	35
6	Median width of the tibial shaft (minimum)	12	16	18
7	Median length of the tibial shaft (minimum)	22	16	13
8	Smallest circumference of the tibial diaphysis	48	51	—
9	Maximum distal tibial end length	22	16	—
10	Maximum distal width	—	24	—
11	Total fibular length	108	103	—
12	Width of the fibular proximal end	11	17	—
13	Length of the proximal fibular end	14	11	—
14	Median shaft length	9	9	—
15	Median fibular width	9	7	—
16	Circumference of the fibular median shaft	31	34	—

VI

SEXUAL DIMORPHISM IN EOCENE SIRENIA

Sexes in mammals often differ in secondary characteristics not related to reproduction directly. Secondary sexual dimorphism can be expressed in many ways in mature males and females of the same species, through differences in overall body size, and difference in the size and form of tusks, horns, and antlers. In extinct animals sexes can often be distinguished based on distinctive size distributions or differences in discrete morphological features.

In mammalian orders, sexual dimorphism ranges from species in which females are larger than males, to those in which males are much larger than females and possess profound secondary sexual characteristics that are absent in females (Bourlière, 1975; Ralls, 1977 and 1976).

Living members of the order Sirenia exhibit little or no sexual dimorphism in body size. Hartman (1971) suggested that female manatees may be larger than males. However, Heinsohn (1972) examined 69 individuals of Australian dugongs, ranging from 1.09 to 3.05 m in body length, and found no significant sexual difference in size.

Sexual dimorphism in dugongs may be inferred from the biometric analyses of cranial elements by Spain and Heinsohn (1974), and then Spain et al. (1976). In the latter study, Spain et al. (1976) analyzed 26 variables in 32 individuals of known sex (16 males and 16 females). Sexual dimorphism was represented in a bivariate scatter of anterior snout width against snout length (Spain et al., 1976: p. 494, fig. 1). In this case, a line separating the two sexes can be given by the expression: snout length = $10.306 + (1.485 \times \text{anterior snout width})$. However, these variables and equation are designed to sex living dugongs and seem not to distinguish males from females in Eocene fossil sirenians.

Another source of sexual dimorphism in the cranium of modern dugongs, not manatees, is in their tusks. Both sexes grow tusks, but they erupt only in males and some older post-reproductive females (Marsh, 1980; Marsh et al., 1984a,b). A study of intraspecific morphological variation in manatee skulls did not detect significant sexual dimorphism in any of the three living manatees (Domning and Hayek, 1986).

The postcranial skeleton is another locus of sexual dimorphism in sirenians. The main form of dimorphism of interest in living and fossil Sirenia is dimorphism of the pelvic bones. Pelvic bones of fossil and living sirenians have some landmarks and structures that are almost certainly related to sexual dimorphism. Krauss (1870: p. 613) suggested that the distal expansion and thickening of *Dugong* ischia might distinguish males

from females (see Lorenz, 1904). Similar morphologies were found in the Miocene hydrodamaline *Dusisiren jordani* (Domning, 1978a), in Miocene *Metaxytherium serresii* (Domning and Thomas, 1987, p. 219), and in Miocene *Metaxytherium krahuletzi* (Domning and Pervesler, 2001, p. 37).

One of the ischium's principal functions is to provide attachment for the crura of the penis or clitoris. Male genitalia require larger surfaces for attachment, so it may be expected that this part of the innominate will be larger in males than in females. Muscle attachments on the distal edge of Recent dugong ischia are highly variable in both sexes (Riha, 1911; Domning, 1977). Males and females have the dorsal distal end of the ischium covered by the ischiococcygeus muscle that connects the ischium to the third chevron bone. In males the posterior edge (medial and lateral) of the ischium is covered partly by the bulbocavernosus muscle but principally by the ischiocavernosus muscle. In females these surfaces are covered by the constrictor vestibuli muscle that supports the lateral walls of the vagina (see Riha, 1911: p. 420, figs. 14 and 15). The ischiocavernosus is the main muscle responsible for expansion and enlargement of erectile tissues in the male penis.

Domning (1991) studied pelvic bones of 70 Australian dugongs of known age and sex, which allowed him to produce a key for interpretation of the variation (Domning, 1991, p. 314). The characters used by Domning (1991) to identify sex in mature Recent dugong innominates include: (1) presence of processes along the ventral border of the ischium; (2) dorsoventral expansion of the posterior (distal) end of the bone; and (3) flaring of the bone's posterior end away from the midline. Moreover, Domning noticed (4) that the ischial distal end of the innominate is thicker (> 0.5 cm) in males than in females (≤ 0.5 cm). All of these characteristics tend to be more pronounced in adults than in immature animals, and more pronounced in males than in females.

The pelvic vestiges of *Trichechus manatus* are sexually dimorphic as well. Krauss (1872) was first to report on sexual and ontogenetic variation in manatee innominates. Female pelvic bones are narrow proximally, with a distinct constriction in the middle of the ischium, while male pelvic bones are broader and thicker than those of females. The same conclusions were reached quantitatively by Fagone et al. (2000) for mature male and female pelvic bones of *Trichechus manatus latirostris*. Fagone et al. (2000) also found that sexual dimorphism in the pelvic bones of manatees is clearly developed and best demonstrated in males and females greater than 225 cm body

TABLE 41 — Dimensions of ischia of Eocene sirenians, showing variation in the thickness of the ischial ramus, ischial tuberosity, and dorsoventral depth of the distal ischium. All measurements are in mm. Symbols: ♂, male; ♀, female. Note that the proportional difference between the thickness of the distal ischium and the thickness of the ischial ramus is much greater in males (bold).

(1) Species	(2) Maximum mediolateral thickness of the distal end of the ischium	(3) Maximum mediolateral thickness of the ischial ramus	(4) Maximum dorsoventral thickness of the distal end of ischium	(5) Ln col. 2	(6) Ln col. 3	(7) Ln col. 4	(8) Difference between columns 5 and 6
<i>Protosiren fraasi</i> SMNS 43976(♀)	8.3	8.1	43	2.116	2.092	3.761	0.024
<i>Protosiren sattaensis</i> GSP-UM 3001(♀)	12.9	10.9	38	2.557	2.389	3.638	0.168
<i>Protosiren sattaensis</i> GSP-UM 3197(♀)	10.8	13.5	50	2.380	2.603	3.912	-0.223
<i>Protosiren smithae</i> CGM 42292(♂)	23.1	11.5	54	3.140	2.442	3.989	0.697
<i>Eotheroides sandersi</i> CGM 42181(♀)	6	7.6	37	1.792	2.028	3.611	-0.236
<i>Eotheroides sandersi</i> UM 97514(♂)	20.6	10.8	53	3.025	2.380	3.970	0.646
<i>Eotheroides clavigerum</i> CGM 60551(♀)	11	11	31	2.398	2.398	3.434	0
<i>Eosiren libyca</i> UM 101228(♀)	11	11.3	28	2.398	2.425	3.332	-0.027
<i>Eosiren libyca</i> CGM 29774(♂)	17	9.5	33	2.833	2.251	3.497	0.582
<i>Eosiren libyca</i> UM 101226(♂)	27.8	12.3	47	3.325	2.510	3.850	0.815

length. In all cases where males and females are longer than 225 cm, the weight of the pelvic bone of the males is always greater, increasing exponentially with age and body length.

Recognition of sexual dimorphism in Eocene Sirenia is likely to be very difficult based on characteristics studied in living dugongs. There are many reasons for this. First, there are relatively few individual skeletons known for any given species. Second, very few skulls preserve tusks, and the sizes of the tusk alveolae are all small in Eocene sirenians compared to those in male *Dugong dugon*. However, the pelvic bones in both living and fossil sirenians (especially dugonids) display other morphological indicators of sex.

DIMORPHISM IN EOCENE SIRENIA

Ten Eocene sirenian specimens from Egypt and Pakistan (representing *Protosiren*, *Eotheroides*, and *Eosiren*) show variation in both form and size that are interpretable as characteristic of males and females (Table 41). Expansion and narrowing, flaring and straightening, robustness and thinning, and smoothness and roughness are all visible on the distal ends of well-preserved Eocene sirenian ischia, including all three Eocene genera represented in Egypt: *Protosiren*, *Eotheroides*, and *Eosiren*. All of the innominates appear to represent subadults to mature individuals, because all three bones of the innominate (ilium, pubis, and ischium) are fused, with no suture line remaining.

The ventral margin of the ischium is preserved in most specimens, including those of *Protosiren fraasi*, *Protosiren smithae*, *Protosiren sattaensis*, *Eotheroides sandersi*, *Eotheroides clavigerum*, and *Eosiren libyca*. Excellent preservation and preparation mean that left and right pelves of the same individual are known in most cases, and these were frequently found in skeletons of dentally mature animals. Having both innominates

of the same individual allowed more comparisons, and detection of distinctive variations and landmarks of interest on both the left and right sides.

Documentation of variation related to sexual dimorphism requires finding features or processes that appear on the ventral or posterior margin of the ischium, like those found in Recent dugongs (Domning, 1991). In all of the Eocene innominates from Egypt, the ventral margins of the ischia are smooth and lack any prominences or processes. Some ischia show narrowing and thinning of the distal ends. Some ischia have their posterior portion expanded and developed into a thick protuberance, expanded dorsoventrally, with or without a rugose surface. In most such cases the distal end is turned posterolaterally. Narrowing and thinning of the distal ends are characteristics of female ischia, and expansion and thickening of the posterior portion of the ischium are male characteristics (Domning, 1991). Dimensions of ischial distal ends in the major Eocene groups are listed in Table 41 to show the variation in size and morphology related to sexual dimorphism.

Pelvic Morphology in Protosirenidae

Protosiren species have pelves with long ilia, wide and deep acetabula, large obturator foramina, and long pubic symphyses. The ischia show more expansion, but not extreme mediolateral thickening at their distal ends. However, there is some intra- and interspecific variation in *Protosiren* ischia.

An innominate of *Protosiren fraasi* (SMNS 43976; Fig. 91A-C) from the Lutetian Mokattam limestone of Cairo (Andrews, 1902; Abel, 1907) has the ventral margin of the ischium broken; the lateral wings of the ischium are slightly deflected and concave laterally to form a shallow basin, and the posterodorsal end is thin with no pronounced tuberosity. This has the appearance of a female innominate.

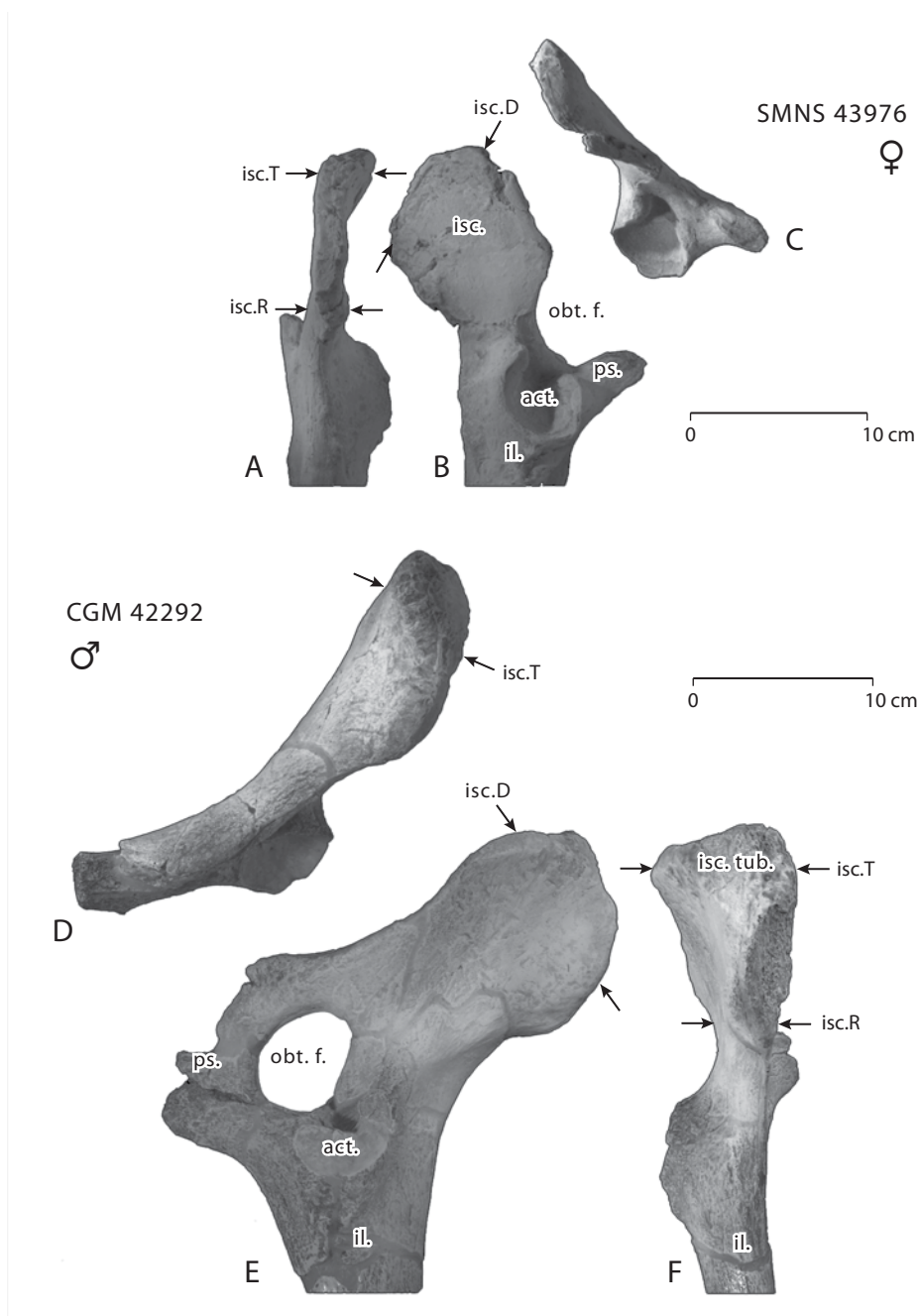


FIGURE 91 — A-C, left innominate of a possible female of *Protosiren fraasi* (SMNS 43976) in dorsal (A), lateral (B), and posterior views (C); the ischium is broad and thin, lacking a pronounced tuberosity, and the mediolateral thickness of the ischium does not change from the ramus to the distal end. D-F, right innominate of a possible male of *Protosiren smithae* (CGM 42292) in posterior (D), lateral (E), and dorsal views (F); extensive mediolateral thickening of the distal end (the tuberosity) is evident in dorsal view. Abbreviations: *act.*, acetabulum; *il.*, ilium; *isc.*, ischium; *isc.D*, ischium tuberosity depth; *isc.T*, ischium tuberosity thickness; *isc.R*, ischium ramus thickness; *isc. tub.*, ischiac tuberosity; *obt. f.*, obturator foramen; *ps.*, pubis; *sac. il. artic.*, sacroiliac articular surface.

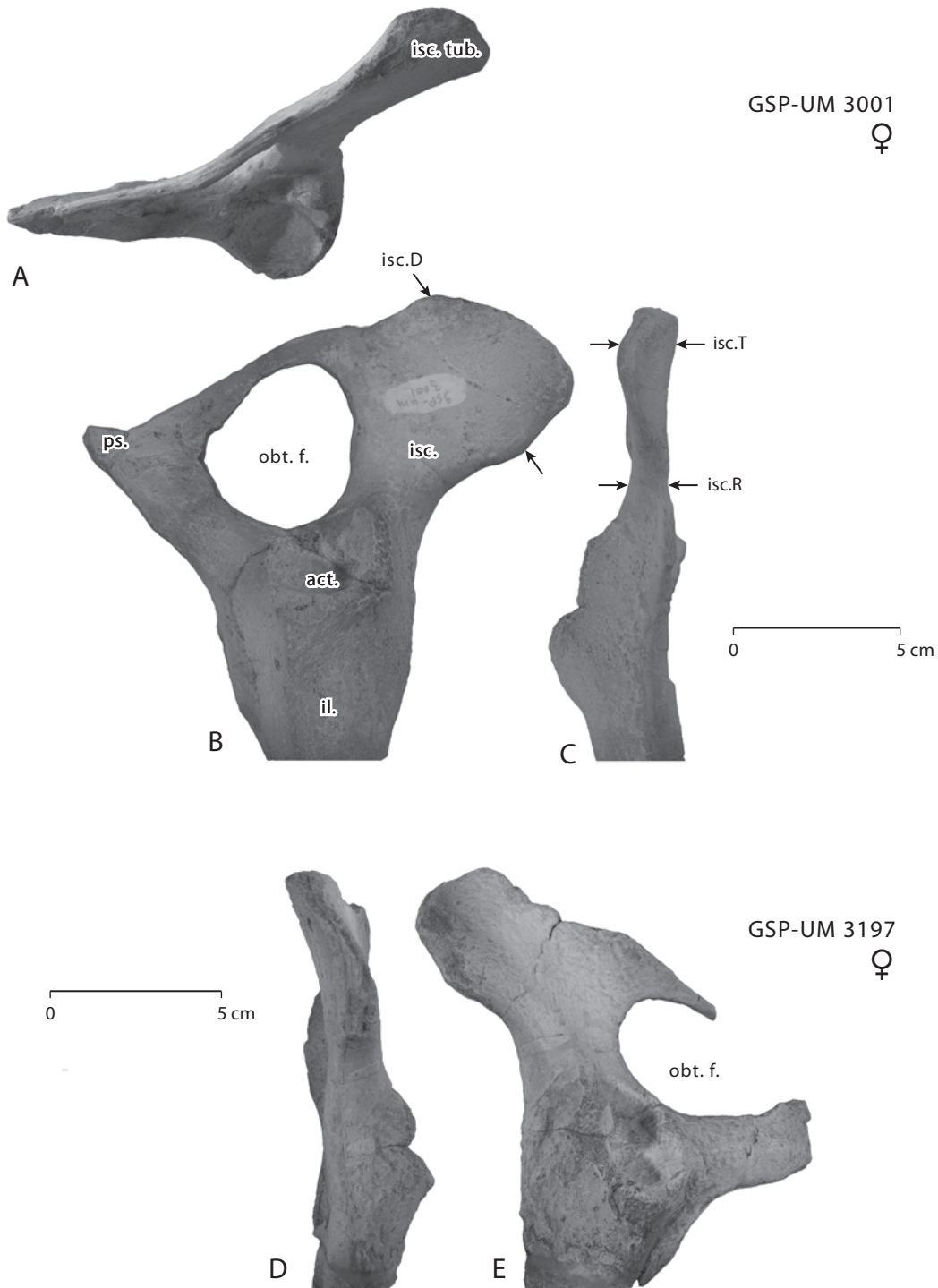


FIGURE 92 — A-C, right innominate of a possible female of *Protosiren sattaensis* (GSP-UM 3001) in posterior (A), lateral (B), and dorsal views (C); the ischium is broad laterally, possessing a small tuberosity at its distal dorsal end, and a slight lateral deflection; however, the mediolateral thickness of the ischium does not change significantly distally, suggesting that this individual was more likely a female (compare to CGM 42292). D-E, left innominate of a possible female of *Protosiren sattaensis* (GSP-UM 3197) in dorsal (D) and lateral (E) views; the mediolateral thicknesses of the ischial distal end and the ramus are almost equal, suggesting that this pelvis is female. Abbreviations: *act.*, acetabulum; *il.*, ilium; *isc.*, ischium; *isc. D*, ischium tuberosity depth; *isc. T*, ischium tuberosity thickness; *isc. R*, ischium ramus thickness; *isc. tub.*, ischiac tuberosity; *obt. f.*, obturator foramen; *ps.*, pubis; *sac. il. artic.*, sacroiliac articular surface.

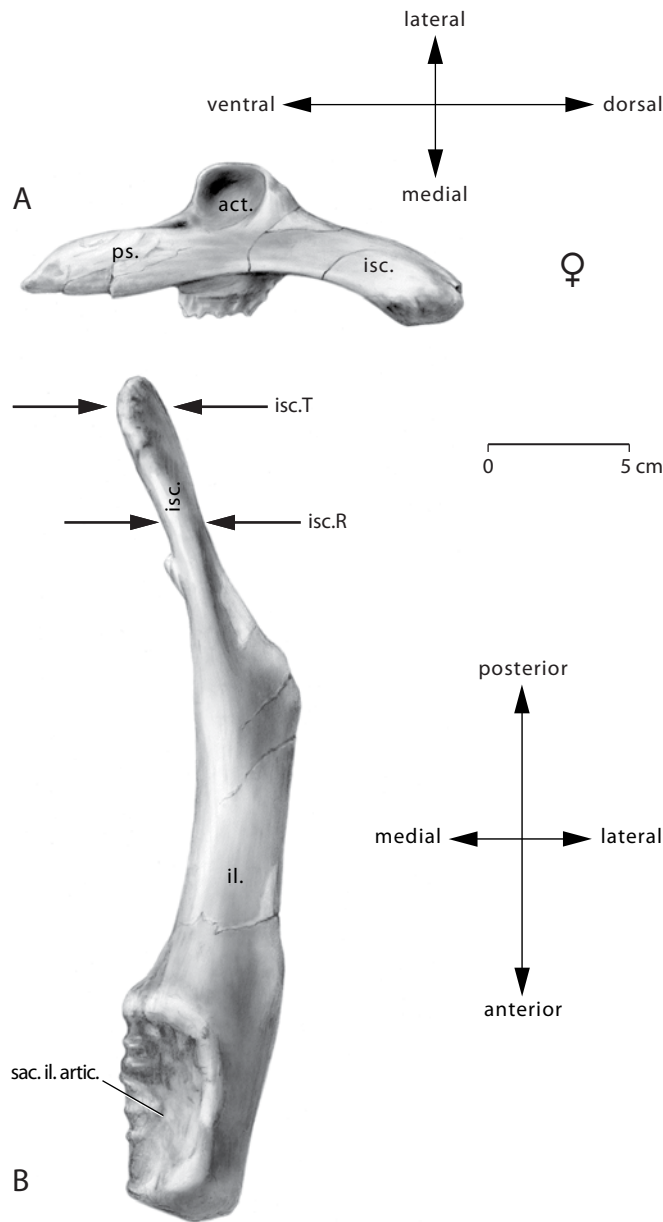


FIGURE 93 — A-B, left innominate of a possible female of *Eotheroides clavigerum* (CGM 60551) in posterior (A) and dorsal view (B); note the thinning and simplicity of the distal end of the ischium in both views and the small variation between the thickness of the ischial ramus and the bone's distal end (black arrows). Abbreviations: *act.*, acetabulum; *il.*, ilium; *isc.*, ischium; *isc.T*, ischium tuberosity thickness; *isc.R*, ischium ramus thickness; *isc.tub.*, ischiatic tuberosity; *ps.*, pubis; *sac. il. artic.*, sacroiliac articulation surface.

The holotype of *Protosiren sattaensis* (GSP-UM 3001, Fig. 92A-C) from the Bartonian-age Drazinda Formation of the Sulaiman Range in Pakistan preserves both innominate bones, but the right side has the ischium better preserved (Gingerich et al., 1995: p. 347, fig. 11). The ischium extends posteriorly from the center of the acetabulum more than 90 mm and flares posteriorly, with a thin tuberosity that is slightly deflected laterally. This is interpreted as a female *Protosiren* as well, since the mediolateral thickness is almost the same as the thickness of the ramus (Table 41).

The other specimen of *Protosiren sattaensis* with a pelvis (and a complete femur) is GSP-UM 3197 (Fig. 92D-E), found close to the locality of the holotype. This pelvis has an incomplete ventral ischial margin but seems to be narrower and thinner than that of the holotype, with a weak tuberosity at its posterior end. This is also interpreted, questionably, as a female pelvis.

The pelvic bone of the type specimen of *Protosiren smithae* (CGM 42292; Fig. 91D-F) has a posterior border that is semicircular in outline, greatly thickened, and somewhat rugose. The dorsal portion of this border bears a broad more or less flat surface facing dorsally; the posterior extremity of the ischium is prolonged into a blunt protuberance whose roughened surface is directed posterolaterally. The ventral part of the posterior border is much less thick but turns markedly outward, helping to form the concavity of the ischium's lateral surface. The overall aspect of this thickened and somewhat laterally curved termination of the ischium resembles that seen typically in males of modern *Dugong* (Domning, 1991), and we interpret CGM 42292 as a male.

Pelvic Morphology of Dugongidae

Eotheroides and *Eosiren* from the Eocene of Egypt have well preserved pelvises that allow close examination and comparison. The ischium in the holotype of *Eotheroides clavigerum* (CGM 60551; Fig. 93) from the Priabonian-age Birket Qarun Formation, best preserved on the left side, is long, thin, and narrow posterodorsally, and curved medially, with a very weak tuberosity on the posteriormost edge and smooth internal and external sides. This probably represents a female. This animal is known from the skull and most of the skeleton of a dentally mature individual showing extensive dental wear, and small erupted tusks.

Eotheroides sandersi innominates are known from the holotype, CGM 42181 (Fig. 94C,D), and from UM 97514 (Fig. 94A,B). The pelvises of CGM 42181 belong to a small or immature individual although the three bones of the pelvis seem to be fused. Here the ischium is flattened, narrow, and lacks any rugosity or tuberosity, which indicates this is a young female. The other individual of *Eotheroides sandersi* (UM 97514) has a broad, flat ischial ramus. The posterior end of the ischium is thickened and flares laterally just below a line extending from the middle of its ventral edge to its posterodorsal corner. The entire margin of this flaring portion is 1-1.5 cm thick and rugose. The posteromedial surface and the vertical medial surface of the bone's posterodorsal end are somewhat roughened. The latter two surfaces, both slightly concave, are separated by a broadly convex horizontal ridge. The degree of lateral flaring at the

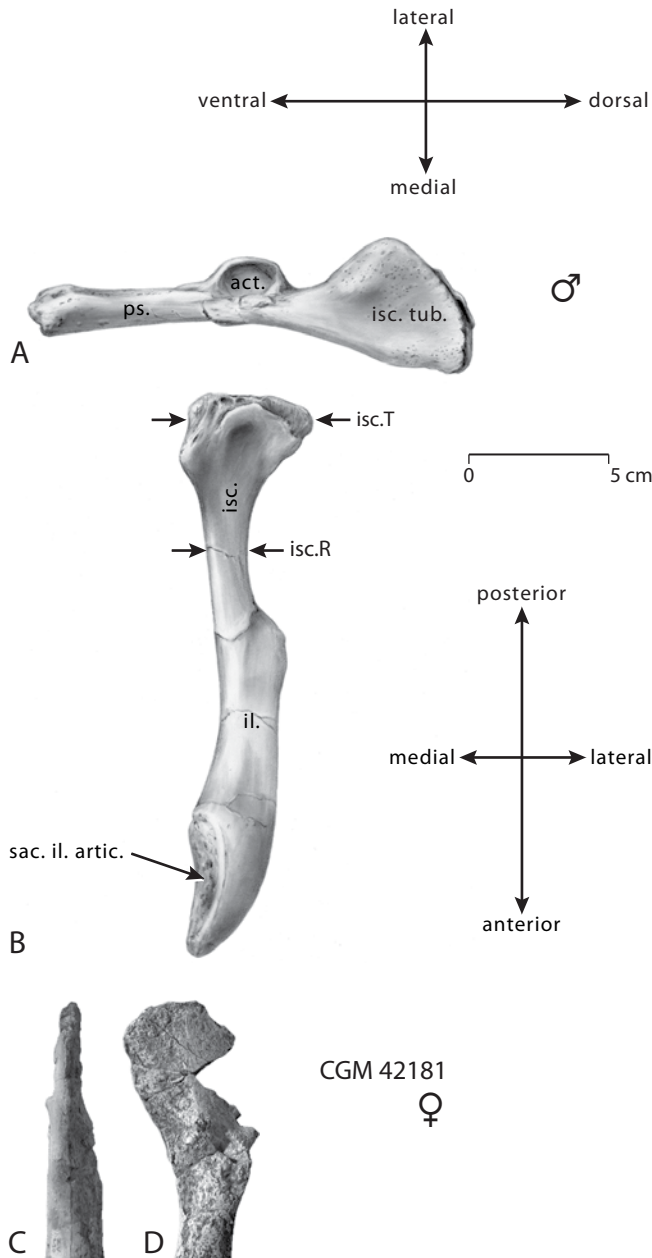


FIGURE 94 — A-B, left innominate of a possible male of *Eotheroides sandersi* (UM 97514) in posterior (A) and dorsal views (B); note expansion and thickening of the distal end. C-D, left pelvis of a possible female of *Eotheroides sandersi* (CGM 42181) in dorsal (C) and lateral views (D); the ischium here is thin and broad, lacking any tuberosity. Abbreviations: **act.**, acetabulum; **il.**, ilium; **isc.**, ischium; **isc.T**, ischium tuberosity thickness; **isc.R**, ischium ramus thickness; **isc. tub.**, ischiac tuberosity; **ps.**, pubis; **sac. il. artic.**, sacroiliac articulation surface.

end of the ischium is comparable to, or greater than, that which today characterizes male *Dugong* (Domning, 1991). Hence we interpret UM 97514 as a male.

Innominate bones of *Eosiren* (Fig. 95) were collected from the Qasr El Sagha Formation, with many individuals and ontogenetic stages and intraspecific variations in the ischium represented. *Eosiren libyca* has a very advanced stage of reduction of the pelvis, in contrast to those of *Eotheroides* and *Protosiren*.

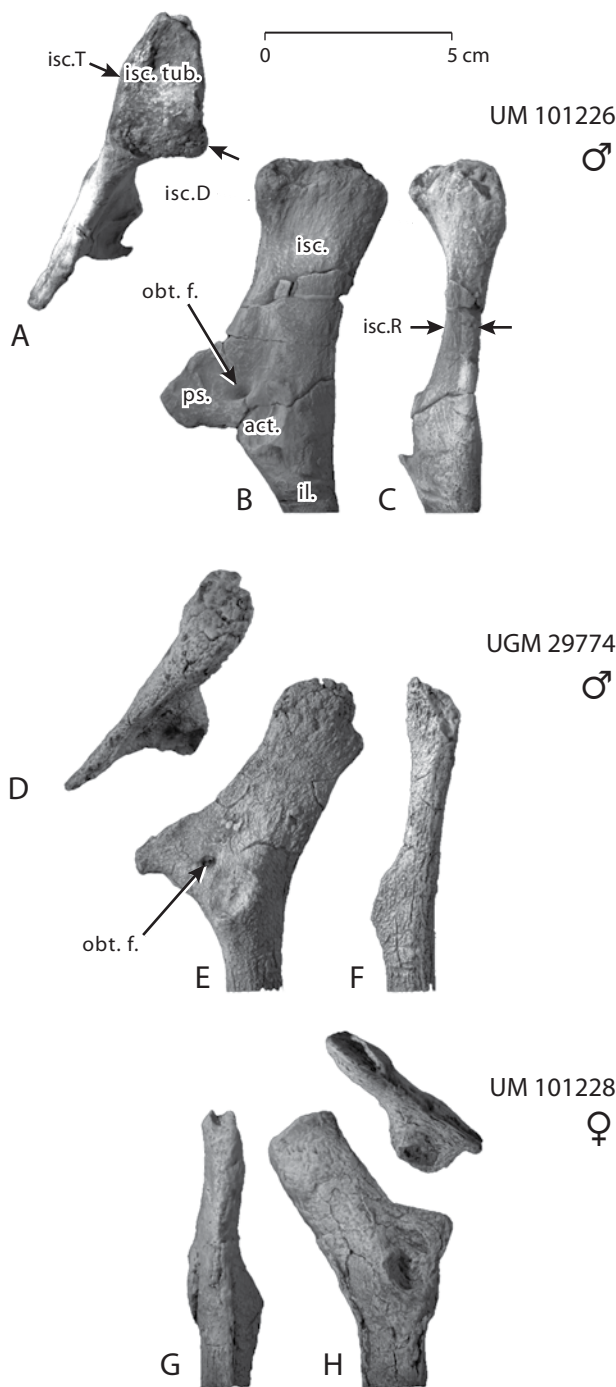
The best preserved pelvis of *Eosiren libyca* include UM 101226, a completely preserved right innominate (Fig. 95A-C) belonging to a skeleton of a large individual. The ilium is slender, straight, long, trihedral in cross section, showing a rugose concavity at the anterior end, and lacking the swelling seen in *Eotheroides*. The acetabulum is shallow and small, but relatively larger than in other described *Eosiren* individuals, including those described by Andrews (1906, p. 214-215). The pubis is triangular with a rough ventromedial end (possibly remains of the symphyseal fibro-cartilage attachment). The obturator foramen is small and opens laterally to form a small basin. The ischium is long and similar to those found in male *Eotheroides sandersi*, but with less distal flaring and expansion. However, it shows considerable thickening and deflection of the end, and its mediolateral side is ornamented with rugosities and scars. The posteriormost end is occupied by two lateral concavities and one large medial depression for ligament attachments. All of these features indicate that UM 101226 was a male.

A cast of another pelvic bone of *Eosiren libyca* (CGM 29774; Fig. 95D-F) is very similar to that described by Andrews (1902). However, it is different from the pelvis of UM 101226 in having the distal end of its ischial ramus thinner and narrower. There is at the same time an enlarged tuberosity with a pitted lenticular basin (8 mm wide) on its dorsal edge. CGM 29774 appears to represent a young male, as the tuberosity is not well developed, yet the end of the tuberosity is already enlarged to twice the width of the ischial ramus.

The last specimen of *Eosiren libyca* to be discussed here, UM 101228 (Fig. 95G-I), has a pair of poorly preserved pelvises whose ischia are 12 mm thick mediolaterally and are conservative in thickness through the distal end. Its sex is ambiguous because of the moderate thickness of the ischium and the presence of a narrow dorsoventral depression on both pelvises at the terminal distal portion. Although lack of expansion and flaring may make it a good candidate for a female *Eosiren*, this specimen is an immature individual, as the caudal centra associated with it are not totally fused to the neural arches.

DISCUSSION AND CONCLUSIONS

Thickening of the distal end of the ischium in Protosirenidae and Dugongidae could be the best criterion to use in sexing Eocene sirenian innominates. Table 41 and Figure 96 summarize what is known of sexual dimorphism in the Eocene pelvic bones described here. Figure 96 displays natural-log (\ln) values for three ischial measurements from Table 41. Two of these display



significant sexual dimorphism in the pelvic bone. The difference between the mediolateral thickness of the ischial ramus (solid squares in Fig. 96) and the mediolateral thickness of the distal ischium (open diamonds) is great in the following specimens: *Protosiren smithae*, CGM 42292; *Eotheroides sandersi*, UM 97514; *Eosiren libyca*, CGM 29774; and *Eosiren libyca*, UM 101226. These are interpreted as males (open arrows in Fig. 96).

The difference between the mediolateral thickness of the ischial ramus (solid squares) and the mediolateral thickness of the distal ischium (open diamonds) was small to negative in the following specimens: *Protosiren fraasi*, SMNS 43976; *Protosiren sattaensis*, GSP-UM 3001; *Protosiren sattaensis*, GSP-UM 3197; *Eotheroides sandersi*, CGM 42181; *Eotheroides clavigerum*, CGM 60551; and *Eosiren libyca*, UM 101228. These are interpreted as females. In the cases interpreted as male, the differences between \ln values for the mediolateral thickness of the ischial ramus and the mediolateral thickness of the distal ischium ranges from 0.58 to 0.82 ($n = 4$), while in cases interpreted as female the difference ranges from -0.24 to 0.17 ($n = 6$). These values are discretely different for the two sexes regardless of taxon (Fig. 97).

The only complete preserved pelvic bone of *Protosiren smithae* from Wadi Al Hitan (CGM 42292; Fig. 92D-F) shows a massive and robust distal end of the ischium, making it distinct from other Protosirenidae from the Lutetian of the Mokattam Hills (*Protosiren fraasi* SMNS 43976) and from the Bartonian of central Pakistan (*Protosiren sattaensis* GSP-UM 3001 and GSP-UM 3197). The pelvic bones of *Eotheroides* and *Eosiren* show extreme sexual dimorphism compared with other Eocene sirenians; this dimorphism is similar in form and degree to those in living dugongs.

Pelvic bones may be the only elements that can be used to sex Eocene Sirenia. It is not clear if these animals were dimorphic in other features such as body size, or tusk size and morphology. Some Eocene sirenians grew a small tusk (35 mm long in *Eotheroides clavigerum* CGM 60551), several times smaller than those of mature Recent dugongs (up to 200 mm long; Domning and Beatty, 2007), so the tusks are seemingly not well developed in early sirenians. Testing for sexual dimorphism in the tusks of Eocene sirenians would require a large sample for quantitative analysis, but no such sample is available.

FIGURE 95 — A-C, right innominate of a possible male of *Eosiren libyca* (UM 101226) in posterior (A), lateral (B), and dorsal views (C); note expansion and thickening of the distal end. D-F, right innominate of a possible young male of *Eosiren libyca* (CGM 29774) in posterior (D), lateral (E), and dorsal views (F); the ischium is narrow dorsoventrally but it is thick mediolaterally. G-I, left innominate of a possible female of *Eosiren libyca* (UM 101228) in dorsal (G), lateral (H), and posterior views (I); the ischium here is straight, rectangular, and conservative in mediolateral thickness from the ramus to its distal end. Abbreviations: **act.**, acetabulum; **il.**, ilium; **isc.**, ischium; **isc.D**, ischium tuberosity depth; **isc.T**, ischium tuberosity thickness; **isc.R**, ischium ramus thickness; **isc. tub.**, ischiac tuberosity; **obt. f.**, obturator foramen; **ps.**, pubis; **sac. il. artic.**, sacroiliac articulation surface.

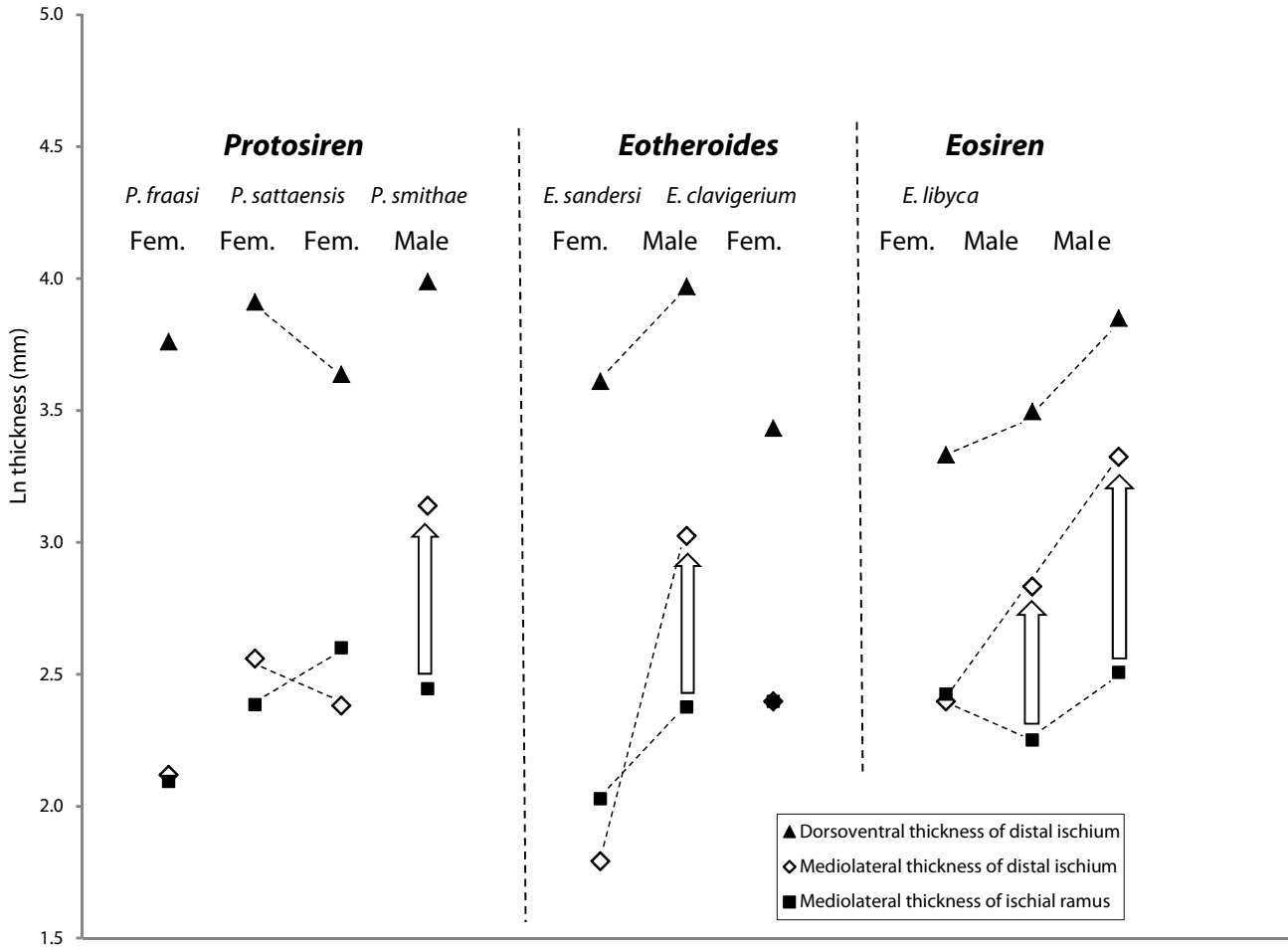


FIGURE 96 — Sexual dimorphism in the pelvic bones of Eocene sirenians (*Protosiren*, *Eotheroides*, and *Eosiren*) interpreted from intra-specific variation in the mediolateral thickness of the ischial ramus (squares) and its distal end (diamonds). The difference between the thickness of the distal end of the ischium and the thickness of its ramus (arrows) is significant in the putative males, while in females the difference is either small or zero. Sexual dimorphism is extreme in *Eotheroides sandersi* and *Eosiren libyca* as both males and females have clearly distinct ischial morphology in all studied pelvises. Measurements plotted here are listed in Table 29.

Gingerich et al. (1994: p. 62, fig. 7) showed that the type cranium of *Protosiren fraasi* (CGM 10171) has unusual features that are symmetrical on both sides of the midline. One of these features was interpreted as a well-developed rostral lacuna or sulcus “most probably for a proboscis” that is only found in the type specimen (CGM 10171), and is totally absent in SMNS 10576; this too could be related to sexual dimorphism. As an analogy, in the Recent southern elephant seal, *Mirounga*, the males have a muscular proboscis that is lacking in females.

Pelvic bones of living and fossil dugongs have a pattern of sexual dimorphism similar to that of advanced whales that

might be expected in Eocene whales as well. An expansion of the ischium and thickening of the ilium seem to be the main sexually dimorphic features found in the pelvises of living whales (Struthers, 1893; Lönnberg, 1908; Kleinenberg et al., 1964; Berzin, 1972; Perrin, 1975; Rommel, 1990; Yoshida et al., 1994).

Living *Dugong dugon* are sexually dimorphic in both tusks and pelvises. Males take advantage of tusks as strategic tools in mating and foraging. Preen (1989) reported that dugong males are more aggressive than manatee males in physical competitions for females. Many dugong scars and injuries appear to have been made by tusks of lunging males when competing for females.

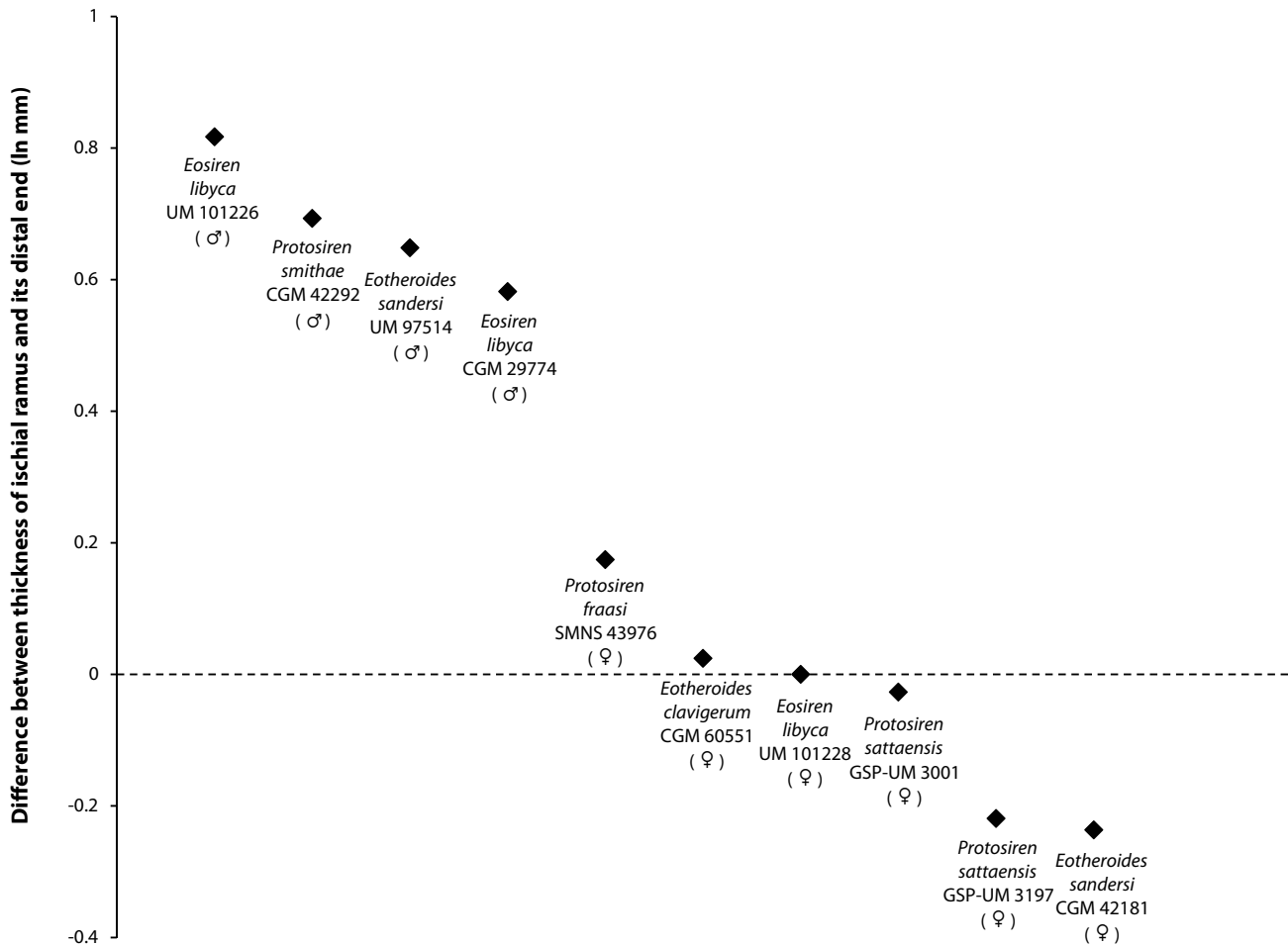


FIGURE 97 — Sexual dimorphism in the pelvic bones of Eocene sirenians represented by the difference between natural logarithms of the mediolateral thickness of the distal end of the ischium (mm) and mediolateral thickness of the ischial ramus (mm). As a general rule, the difference in these numbers is about 0.6 to 0.8 ln units (distal end much thicker) in males, and -0.2 to 0.2 ln units (subequal) in females.

According to Anderson (1997, 2002), Australian dugongs in a cove of Shark Bay use a lekking strategy to secure a successful courtship. Lekking seems to be the main mating strategy in Australian dugongs, where the reproductive males have to establish two major conditions: (1) display territories, smaller than a normal home range, where food resources are limited and there is an opportunity for mate choice by females; (2) strong sexual dimorphism and sexual bimaturism as expressed by males in ritualized display at the center of the mating area (Högland and Alatalo, 1995; Bradbury, 1977; Anderson, 2002).

Compared to modern dugongs, Eocene sirenians from Egypt were smaller in body size, with small and sometimes unerupted tusks. These features make it difficult to draw any conclusions about strategies for successful mating. However, the pattern and amount of sexual dimorphism in the pelves of Eocene sirenians is similar to that in modern dugongs, suggesting that pelvic dimorphism has been present through much of the history of Sirenia.

VII

PALEOBIOLOGY OF WADI AL HITAN SIRENIA

Sirenia represent a distinctive 'evolutionary play' within mammals, and they have long inhabited their own distinctive 'ecological theater.' Here we attempt to characterize the ecological theater of Priabonian late Eocene Sirenia of Wadi Al Hitan, in terms of both paleoenvironment and paleoecology. Then we discuss Priabonian late Eocene Sirenia in Wadi Al Hitan as representatives of an early stage in the sirenian evolutionary play. Where are Wadi Al Hitan Sirenia in terms of secondary adaptation to life in the sea? What can we say about their locomotion and feeding behavior? The chapter ends with a general discussion and conclusions.

PALEOENVIRONMENT

Max Blanckenhorn (1900, 1903) was one of the first to recognize that northern Egypt included both marine and continental environments during the 'middle and late Eocene' (now Eocene and Oligocene). Blanckenhorn envisioned an east-west shoreline passing just north of the present-day Baharia Oasis, south of Fayum, with a river system flowing northward into a delta south and west of Birket Qarun. Blanckenhorn (1903) described upper middle Eocene beds in the vicinity of Qasr el-Sagha as '*obere Mokattam-Stufe*' or '*Carolia-Stufe*,' noting that these were thicker in Fayum than at Gebel Mokattam in Cairo. Greater thickness was attributed to the presence of a river system supplying more sediment, however Blanckenhorn pointed to the presence of marine mammals such as '*Zeuglodon*' and '*Eosiren*' as evidence that the deposits are marine.

Hugh Beadnell (1905) described the stratigraphy of Fayum in terms in a sequence of five geological formations: (1) 'Wadi Rayan Series' or '*Nummulites gizehensis* Beds' (El Gharaq Formation); (2) 'Ravine Beds' (Gehannam Formation); (3) 'Birket el Qarun Series' or '*Operculina*-Nummulite Beds' (Birket Qarun Formation); (4) 'Qasr el-Sagha Series' or '*Carolia* Beds' (Qasr el-Sagha Formation); and (5) 'Fluviomarine Series' or 'Jebel el Qatrani Beds' (Gebel Qatrani Formation). The first four formations were full of marine invertebrates and occasionally archaeocete whales, indicating deposition in a marine environment. Overlying strata had occasional marine invertebrates and vertebrates but also abundant silicified trees and a great diversity of land mammals characteristic of a continental environment.

Building on Blanckenhorn and Beadnell's field observations and fossil collections, Charles Andrews (1906) reiterated that generally speaking, from earlier to later Eocene times, strata of

the Fayum were deposited nearer and nearer to a landmass, and the fauna transitioned from marine to continental.

Carl Vondra (1974) studied the Qasr el-Sagha Formation from a sedimentological point of view and identified four distinct facies: (1) an arenaceous bioclastic carbonate facies deposited on a moderate to high energy, warm, normal salinity marine coast to a more brackish estuarine mouth environment; (2) a gypsiferous-carbonaceous laminated claystone and siltstone facies deposited in open to restricted shallow lagoons on the lee side of barrier islands; (3) an interbedded claystone, siltstone, and quartz sandstone facies deposited on a prograding delta front invading shallow brackish marine waters; and (4) a quartz sandstone facies, incised into facies 3, deposited in distributary channels. These are facies appropriate for a unit transitional from fully marine formations below to a fully continental formation above.

Bown and Kraus (1988: p. 48) were the first to interpret the Birket Qarun Formation in Wadi Al Hitan as offshore subaqueous sand dunes overlain by a coastal mangrove horizon, with the latter being the earliest appearance of a coastline in the Fayum area. Gingerich (1992) interpreted the Gehannam Formation to have been deposited on a shallow but open marine shelf. The Birket Qarun Formation, with an outcrop belt some 60 km long but never more than about 5 km wide was interpreted as a buried barrier bar complex (consistent with Bown and Kraus' idea of offshore subaqueous dunes). The Qasr el-Sagha Formation was interpreted as comprising lagoonal and delta front facies, with the overlying Gebel Qatrani Formation being coastal plain facies. All were seen as a vertically stacked package prograding seaward, interrupted by low sea stands at the beginning and end of Priabonian time (Gingerich, 1992: p. 69).

Geological mapping in Wadi Al Hitan, identification of a lower deltaic sequence in addition to the Dir Abu Lifa deltaic sequence of Bown and Kraus (1988), more critical examination of putative mangrove remains, and further synthesis of the regional literature and global sea level change has clarified the Wadi Al Hitan paleoenvironment (Peters et al., 2009, 2010; Gingerich et al., 2012; Gee et al., in prep.). The environment was not a simple east-west coastline, but rather a mosaic of land masses and intervening seas (Fig. 98). This complexity of surface topography reflects structural effects of the underlying Syrian Arc basement (Dolson et al., 2002). The resulting environment had much more coastline and marine shallow shelf than the simple east-west shoreline that Blanckenhorn and Beadnell envisioned.

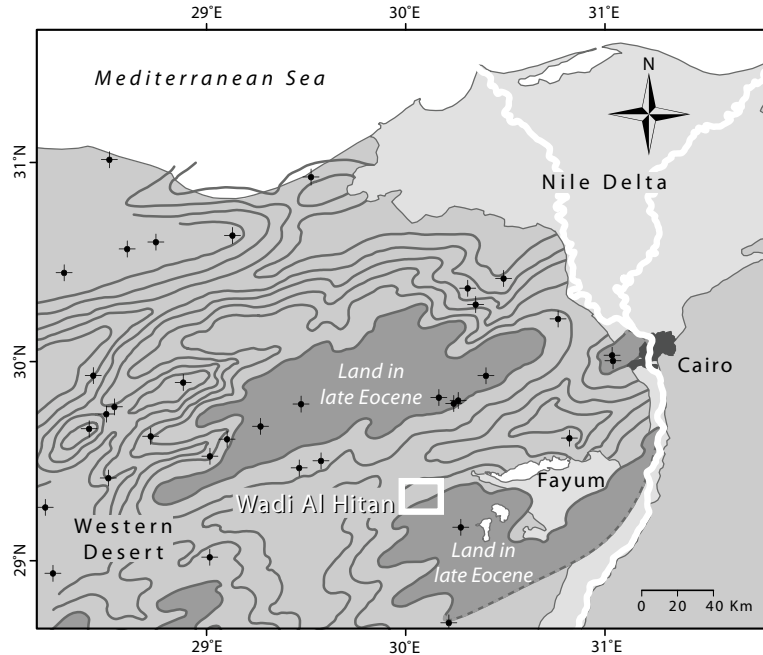


FIGURE 98 — Paleogeography and paleobathymetry of northern Egypt in the late Bartonian–Priabonian (Peters et al., 2009). White rectangle shows the location of the Wadi Al-Hitan World Heritage Site on the southern margin of a marine strait separating two Eocene land masses. Contours are 50-meter isopachs for late Bartonian and Priabonian strata. Well symbols show the locations of cores used by Salem (1976) to reconstruct paleogeography.

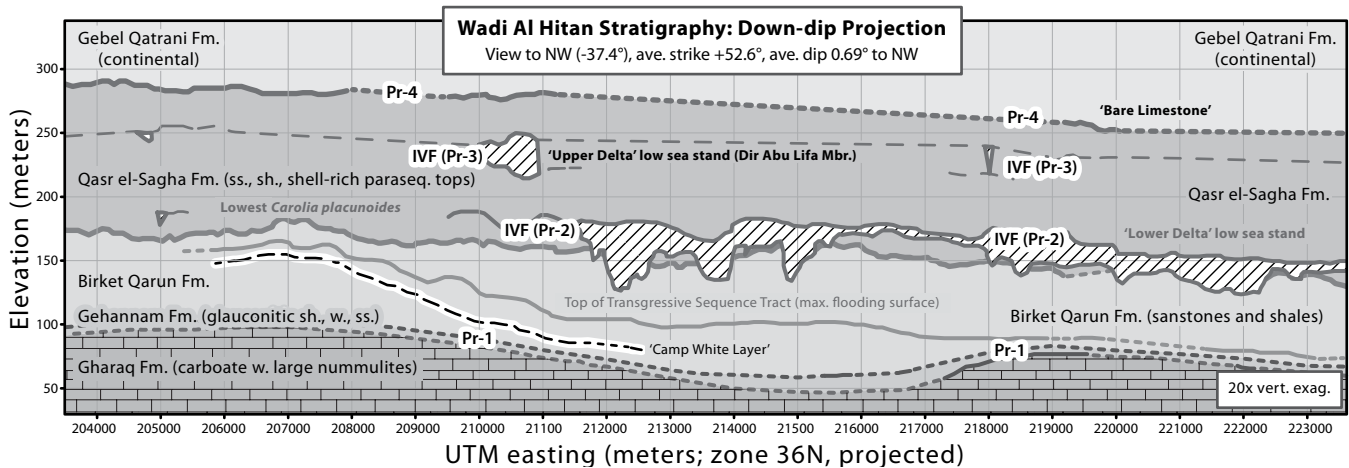


FIGURE 99 — True-scale computed cross-section of Wadi Al-Hitan stratigraphy projected from three-dimensional GPS mapping of bed traces (view down-dip to northwest, vertical exaggeration 20x; Gingerich et al., 2012). Elevation traces are 3-point running averages. Priabonian disconformities Pr-1 through Pr-4 correspond to global low sea stands. Incised valley fill (IVF) deposits are hatched to represent cross-bedding. Pr-2 is documented in Peters et al. (2009, 2010). Abbreviations: Fm., Formation; sh., shale; ss., sandstone.

Further, the environment was dynamic in the sense that three major cycles of late Eocene sea-level rise and fall were superimposed on the topography (Fig. 99). Each of these has clear expression in the sedimentary facies deposited at the time. The Gehannam Formation represents the glauconite-rich initial stage of a transgressive systems tract. The Birket Qarun Formation is partly a continuation of the Gehannam transgressive

sequence tract, partly highstand systems tract, and then partly too a falling-stage systems tract. The Umm Rigl Member of the Qasr el-Sagha Formation has ‘lower delta’ deposits in the lower part, which fill valleys incised through basal beds of the Qasr el-Sagha Formation into the underlying Birket Qarun Formation. These are overlain by transgressive sequence tract and highstand sequence tract deposits of the Harab Member. The Temple

Member is falling-stage deposits, and the lower part of the Dir Abu Lifa Member is incised valley fill again.

Protosiren remains are abundant in the glauconite-rich Gehannam transgressive deposits above the initial Priabonian low sea-stand (Pr-1), partly because sediment accumulation was slow but also because there were probably large areas of seagrass-bearing shallow shelf habitat available. Dugongids are common in the transgressive sequence tract near the base of the Qasr el-Sagha Formation, above the low sea-stand Pr-2 (Peters et al., 2009), presumably for the same reason. Some of the best specimens described here came from sandstones and shales of the intervening Birket Qarun Formation where specimens are not so common but often exceptionally well preserved due to rapid burial.

PALEOECOLOGY

The sirenians described here, Protosirenidae and Dugongidae, are part of a much larger fauna, primarily marine, including shallow benthic and planktonic Foraminifera; Mollusca including diverse bivalves, gastropods, and nautiloids; Cnidaria in the form of solitary corals; Echinodermata, principally echinoids; Arthropoda including crabs (Anderson and Feldmann, 1995), and other marine invertebrates. Vertebrates include a rich and diverse shark and ray fauna (Case and Cappetta, 1990; Underwood et al., 2011; Zalmout et al., 2012); teleost fishes (Fierstine and Gingerich, 2009; Murray et al., 2010); sea snakes (*Pterosphenus*, *Gigantophis*); crocodylians (Brochu and Gingerich, 2000); land mammals (Gingerich, 1992; Holroyd et al., 1996; Seiffert et al., 2008; Peters et al., 2009); sirenians (described here); and cetaceans (Gingerich et al., 1990; Uhen, 2004; Gingerich, 2007, 2008).

Paleobotanical remains are rare but this is surely because they have received little attention. Gingerich (1992) reported tree logs riddled with the trace fossil *Teredolites* produced by shipworms (wood-boring bivalves), and possible mangrove root remains (now questioned) in the Birket Qarun Formation. Engelhardt (1907) described a flora from Blanckenhorn's bed II-5a in what is now the Temple Member of the Qasr el-Sagha Formation. This included *Ficus*, *Litsaea*, *Cinnamomum*, and other genera indicating a continental tropical Indo-Malaysian-like rainforest flora.

The presence of marine seagrass in shallow coastal waters is confirmed by leaf impressions tentatively identified as *Thalassodendron* sp. (Fig. 100). These were found in the Birket Qarun Formation of Wadi Al Hitian, from the excavation producing a complete skeleton of *Basilosaurus isis* (WH-74 or UM 97507). The overlying Qasr El Sagha Formation in Wadi Al Hitian produced leaf impressions tentatively identified as both *Thalassodendron* sp. and *Cymodocea* sp. (Fig. 100), which were collected from siltstones and mudstones entombing the skeleton of *Eosiren libyca* (UM 101226).

Thalassodendron sp. and *Cymodocea* sp. belong to the seagrass family Cymodoceaceae (Phillips and Meñez, 1988; Green and Short, 2001), which appeared in the fossil record as early as the Late Cretaceous and was very common in the

Tethyan Eocene (Ivany et al., 1990). This group of seagrasses is significant as a water-depth indicator because they are limited to depths of less than 10 m, where light and clarity are optimum for longevity and reproduction.

Seagrass remains found in marine mammal excavations in Wadi Al Hitian add information relevant for reconstruction of the Eocene paleoecology of this part of Tethys, and aid in understanding its biogeographic connections to shallow seas of the Caribbean and North America. Domning (1981) reviewed evidence for seagrass-sirenian associations, and Ivany et al. (1990) reported *Thalassodendron* and *Cymodocea* from the Eocene of Florida (Gulf of Mexico) from beds that produced sirenian remains. These seagrasses were colonized or encrusted by epiphytes and invertebrate larvae. Similar relationships of seagrasses and microorganisms occurred too in the Eocene of North Africa as indicated in red siltstone of the Qasr El Sagha Formation (Fig. 100B). Seagrass paleocommunities may have been more successful and widespread during the Eocene than they are today, and their broad distribution may reflect a different pattern of ocean circulation at that time. Fayum sirenians with extremely high $\delta^{13}\text{C}$ values indicate that seagrass was an important component of the diet early in sirenian evolution (Clementz et al., 2006).

Eotheroides sandersi and *Eotheroides clavigerum* were found together with *Protosiren smithae* at the base of the Birket Qarun Formation. The middle and upper part of the Birket Qarun Formation produced *Eotheroides sandersi*. *Eosiren* has not been found in the Birket Qarun Formation. All *Eosiren* species come from either the Qasr el-Sagha or Gebel Qatrani formation in Fayum or from the Mokattam Limestone in Cairo. It is noteworthy too that *Protosiren* has not been found above the lower third of the Birket Qarun Formation nor in the Qasr El Sagha Formation.

The coexistence of three sirenians that are morphologically and dentally different shows the complexity of the biotope and diversity of this group in the early Priabonian of the Fayum Basin. This coexistence is similar to that which occurred in the Lutetian of the Mokattam Limestone where *Protosiren fraasi*, *Eotheroides aegyptiacum*, and possibly *Eosiren abeli* overlapped in the same biotope. Coexistence of three species is probably achieved by partitioning of food resources, although this is not yet well understood.

SECONDARY ADAPTATION TO LIFE IN THE SEA

The fossil record of the earliest sirenian groups shows a gradual transition from more terrestrial ancestors with well developed hind limbs and a multicentrum sacrum to fully aquatic animals with a single sacral vertebra, loss of external hind limbs, and a tail modified as a fluke (Abel, 1907; Domning and Gingerich, 1994; Domning, 2001b). The late Eocene sirenians studied here, Protosirenidae and Dugongidae, have many features of body form comparable to those of living Trichechidae and Dugongidae.

Extant sirenians are fully aquatic, with morphological and hydrostatic characteristics that evolved as secondary adaptations

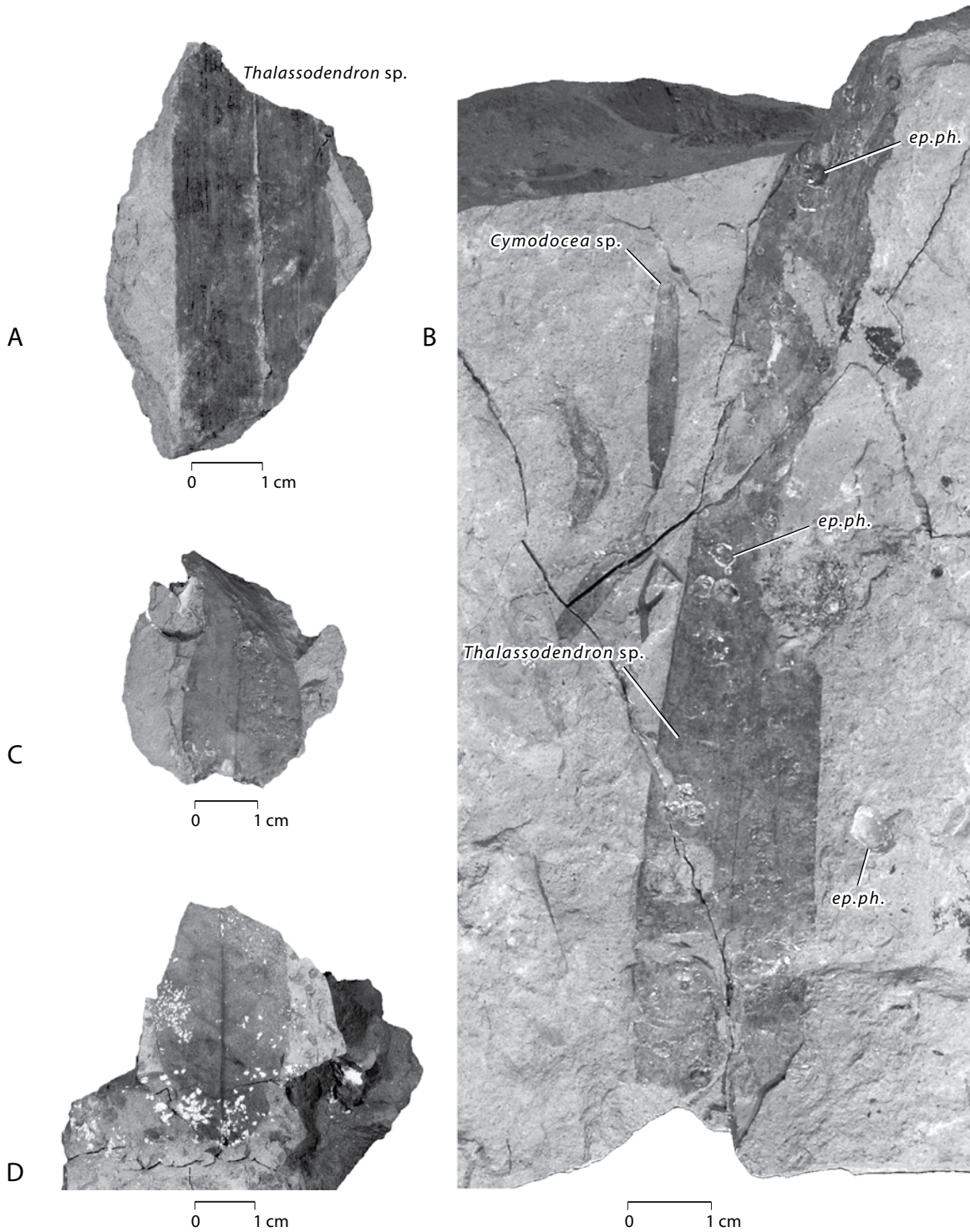


FIGURE 100 — Priabonian age fossil plant remains found with marine mammal skeletons in the Birket Qarun and Qasr El Sagha formations of Fayum. A, Fragment of seagrass from a siltstone where *Basilosaurus isis* (WH-74) was excavated in the lower part of the Birket Qarun Formation. B, Seagrasses with leaves of two different sizes, one wide (possibly *Thalassodendron sp.*) and one narrow (possibly *Cymodocea sp.*); collected from sedimentary matrix associated with the *Eosiren libyca* skeleton (UM 101226) excavated in the Qasr El Sagha Formation. Note that the wide leaf is encrusted by epiphyte invertebrates (ep.ph., *Spirobis?*) and bryozoans. C-D, fossil dicot leaves of terrestrial origin associated with the *Eosiren* skeleton (UM 101226) excavated from the Qasr El Sagha Formation.

to life in water. These morphological and skeletal characteristics include their overall submarine or fusiform body shape; a body stiffened by a subdermal network or sheath of helically wound fibrous connective tissue; thick almost hairless skin; large and mobile lips; short necks (short cervicals); forelimbs modified as flippers; hind limbs reduced to internal vestiges; and a tail modified as a horizontal caudal fluke. Propulsion is by dorsoventral undulation of the spine and tail fluke (Kojeszewski and Fish, 2007).

In the cranium, extant sirenians have deflected rostra, retracted nasal openings with the nostrils well separated, and no paranasal air sinuses. The premaxillae contact the frontals. The nasals are reduced in modern forms and sometimes fused with the frontals or totally absent. The supraorbital processes are prominent and lack a postorbital bar. The skullcap is thick and heavy, with the parietals fused into one mass with the supraoccipital. A sagittal crest is absent in most sirenians, however, a weak sagittal crest is present in *Pezosiren* (Domning, 2001b). The zygomatic processes and the jugals are robust. Most sirenians possess strong deep pterygoids to increase masticatory ability, while early sirenians, *Prorastomus* and *Pezosiren*, have small pterygoids. The infraorbital and mental foramina are large and directed anteriorly.

Sirenia is the only group of marine mammals that feeds extensively on coastal aquatic vegetation (seagrasses). The general dental formula of the most primitive forms of sirenians is 3:1:5:3, which is a synapomorphy for the order. The evolutionary history of the teeth indicates an increase in grinding capacity through heightened crowns (*Dugong*) or continuous replacement during forward migration of their functional teeth (*Trichechus*). Domning (2005: 86) stated that the presence of the large number of premolars, primitively long narrow rostrum, and mandibular symphysis bearing parallel rows of incisors and canines suggest an early mechanism of intraoral food transport. However, in the latest Eocene or early Oligocene most forms (if not all) retained a broad rostrum and symphysis covered by horny pads, followed by loss of most anterior teeth (excluding the first incisor, which evolved into a tusk). Large-bodied Hydrodamalinae appeared in the Miocene, with edentulous jaws and keratinous masticating rostral pads with interlocking ridges and grooves.

Sirenians lack external ear pinnae, and the external auditory canal of the squamosal is very small and opens ventrally. The tympanic is ring-shaped, and the ear ossicles are pachyosteosclerotic (thick and dense): the largest and heaviest of any mammal. The tympanic sac (a membranous enclosure) extends between the basicranium, pterygoid process, petrosal, and the well-ossified and tear-shaped ectotympanic ring. The external auditory meatus is a blind sac that is not connected to the tympanic membrane (Fischer and Tassy, 1993). Sirenians more advanced than *Prorastomus* lack fusion of the petiotic to the skull (Savage et al., 1994; Domning, 2001b).

Postcranial conformation was an important factor in secondary adaptation, determining both hydrostatic and locomotor capabilities of the group in water. Salient features include compression (or fusion) of the cervical vertebrae. Living *Trichechus* has six cervicals, while all other sirenians retain seven like most other mammals. Sirenians have an elongated

thorax and lungs, with a horizontal diaphragm (Domning 1977, 1978b; Rommel and Reynoldas, 2000). There are 14 to 21 thoracic vertebrae, followed by one to five lumbar, one to four sacrals (as in *Dugong* and *Prorastomus*, respectively), and 18 to 35 caudal vertebrae. In quadrupedal forms (*Pezosiren*) there are four lumbar, four fused sacrals, and about 20 caudals.

The living dugong, genus *Dugong*, has 19 thoracic vertebrae, four lumbar, one sacral, and up to 27 caudals (Fig. 81A). The living manatee, *Trichechus*, has the most reduced number of vertebrae, the reduction in the cervicals is followed by a series of reductions in the rest of the trunk: 14 thoracics, two lumbar (the most distal being homologous with the sacrum, and about 23 caudals (Fig. 81A). Homology of the distal lumbar with the sacrum is indicated by the discrete ligament attached to the flat and reduced pelvis, as seen in USNM 217259. Manatees, with their shorter vertebral column and rounded tail, are slower swimmers and divers, while dugongs, the faster swimmers and divers, have a well-developed tail fluke (Home, 1821). The muscle cutaneous trunci or the panniculus carnosus is greatly enlarged and partly inserts on the chevrons of the caudal vertebrae (Domning, 1978b).

Protosiren had 19 thoracic vertebrae, one pre-lumbar, four lumbar, one sacral, and more than 18 caudal vertebrae (Fig. 81B). Our counts of vertebrae in the dugongids *Eotheroides* and *Eosiren* are as complete. Judging from its vertebral centrum length profile (Fig. 81B), *Protosiren* appears to have had a vertebral column more like *Dugong* than like *Trichechus*, and it is reasonable to interpret *Protosiren* and the dugongids *Eotheroides* and *Eosiren* as have been *Dugong*-like swimmers and divers. This comes out clearly too in the width pattern profiles of Figure 82 and the width-to-length pattern profiles of Figure 83.

Sirenian ribs are of great interest because they are among the most recognizable and diagnostic bones of the skeleton. They show either osteosclerotic (dense and compact bone) or pachyosteosclerotic (thickened or swollen compact bone; Kaiser 1966; Domning and De Buffrénil, 1991; and Rommel and Reynolds, 2000). *Dugong*, *Protosiren*, *Pezosiren*, *Prorastomus*, and *Eosiren* have osteosclerotic ribs, while *Trichechus*, *Eotheroides*, and to some degree *Prototherium* have pachyosteosclerotic ribs. In extant *Trichechus* the general pattern of change in the cross-sectional area of successive ribs is an increase from front to back (Fig. 84). We have not quantified this for living *Dugong*, but the Eocene dugongids *Eotheroides* and *Eosiren* show a general decline in rib cross-sectional area from anterior to posterior. *Protosiren* has a flatter profile intermediate between that of extant *Trichechus* and Eocene dugongids. Ventrally the sternum of sirenians is connected to as few as two or as many as five pairs of ribs. No sirenian taxon has a clavicle (Fischer and Tassy, 1993).

Scapulae of extant *Dugong* and *Trichechus* are thin, broad, and fan-shaped. Scapulae of prorastomids are broad, but those of Eocene Protosirenidae and Dugongidae are sickle-shaped. Humeri of all are rounded and robust. The radius and ulna have rounded cross-sections, and are sometimes fused together. Pattern profiles show that forelimb elements of Egyptian Eocene sirenians are all similar to each other (Figs. 85-87). The manus

is paddle-like, with carpals arranged serially, a reduced first digit, and an enlarged and divergent fifth digit (Domning, 1978a, 2001b, 2005).

The pelvic girdle of Prorastomidae and Protosirenidae was functional and connected to either a multi-centrum sacrum (*Pezosiren*) or to a single sacral vertebra (*Protosiren*). Pelvic girdles of Eocene Dugongidae (*Eotheroides*, *Eosiren*, *Prototherium*, and *Halitherium*) are vestigial and connected to a single sacral vertebra. The pelvic girdle of the living *Dugong* is reduced to a slender hip bone attached to the sacral vertebra by a cartilaginous ligament. In manatees the sacrum is a small, triangular, flat bone attached to the lumbosacral region by a long ligament. It floats ventrolaterally in the abdomen. Pattern profiles indicate that the pelvic girdle of Eocene sirenians is highly variable and distinctive in different genera (Fig. 88).

The sirenian femur in post-Eocene forms is very reduced and presumably functionless. Judging from the size and form of the femur, Eocene *Pezosiren* had fully functional hind limbs, able to support the body on land and functional in swimming and paddling (Domning, 2001b). *Protosiren* has a well formed femur, reduced in size by comparison to that of *Pezosiren*, but still substantial. It is doubtful that the femur of *Protosiren* would support an individual's body weight and it is doubtful that the hind limb was important for swimming. The femur in manatees is a small bone fused to the flat pelvis. Hands and feet of most living and fossil sirenians are very similar, with rounded carpals and metacarpals, and tarsals and metatarsals. Domning (2001b) showed that these elements are more flattened in Prorastomidae than in other Eocene relatives.

The Wadi Al Hitan sirenians are grouped into two major families, Protosirenidae and Dugongidae. Morphological and dimensional characteristics of cranial and postcranial elements of both families show that they were fully aquatic mammals, but each was specialized differently for swimming.

Protosirenid adaptations.— Protosirenidae, typified here by *Protosiren smithae*, show the following secondary aquatic adaptations: osteosclerotic cranial and postcranial elements to neutralize buoyancy; slight rostral deflection and reduced nasals for feeding; short cervicals and increased length of the of thoracic part of the vertebral column, for hydrodynamic streamlining and trim; sacrum reduced into a single vertebra, reflecting buoyancy in water replacing the effect of gravity on land; robust proximal tail vertebrae with strong chevrons, reflecting acquisition of tail-powered locomotion; widened (key-hole shaped) neural canals in thoracic and lumbar vertebrae (a specialization of uncertain interpretation); unusually long spinous processes from the seventh cervical (C7) through the second caudal (Ca2), including the sacrum, possibly related to swimming; ribs slender, lacking synovial joints, and connected to the vertebrae by ligaments or cartilage, possibly related to collapse of the thorax during diving.

Protosirenid forelimbs are reduced and form a flipper or hydrofoil, an adaptation for maneuvering while swimming. The pelvic girdle retains long pubes, and long and rod-like ilia, triangular in cross-section, with a large and open obturator foramen. The upper and lower legs retain a femur, tibia, and fibula; these are primitive retentions. The femur has a large head, and a greater and lesser trochanter but no third trochanter. The

distal end of the femur is wide, with well developed functional condyles. The tibia and fibula are robust and rounded, not fused.

Dugongid adaptations.— Dugongidae, typified by *Eotheroides* from Wadi Al Hitan and *Eosiren* from Qasr El Sagha, show variable degrees of osteosclerosis and pachyosteosclerotic cranial and postcranial elements, again to neutralize buoyancy; strong deflection of the cranial rostrum for feeding; nasals reduced but still elongated; short cervicals; 17-19 thoracic vertebrae (compared with up to 20 in Protosirenidae) and up to 4 lumbar (compared with 4-6 lumbar in Protosirenidae); reduction of the sacrum to a single vertebra as in Protosirenidae; robust proximal tail vertebrae with strong chevrons; pachyosteosclerotic anterior ribs (extremely swollen in all *Eotheroides*) connected to vertebrae through synovial joints; forelimbs reduced and flipper-like; pelvis reduced; the ilium varies from a slender rod in *Eosiren libyca* to being club-like in *Eotheroides*; the obturator foramen is diminutive or closed. The tibia, fibula, and pes are unknown.

Comparison.— Protosirenidae, compared to Dugongidae, have the less deflected premaxillary rostrum; narrower infraorbital foramen; lesser width between both pterygoid processes; longer parietals along the midline; wider masticating surface; wider mesorostral fossa; longer frontoparietal suture-contact; wider breadth across the supraorbital processes; higher neural spines; larger vertebral canals; larger and longer infraspinous fossa of the scapula, deeper glenoid cavity; wider bicipital groove on the humerus; shallower olecranon and anconeal processes; pelvis with longer ilia; larger acetabulae; larger obturator foramina; longer ischial processes; longer and wider femora; larger patellar articular surface; and longer and wider fibulae and tibiae.

Egyptian Eocene Dugongidae, compared to Protosirenidae, have greater rostral deflection; wider infraorbital foramina; longer nasal contacts along the midline; longer jugals; an infraspinous fossa lacking deflection; ulnae with deeper olecranon and anconeal processes and wider coronoid processes; pelvis short, with reduced lengths of ilia and ischia, associated with extreme reduction in the pubes and pubic symphysis; acetabulum shallow and small; obturator foramen very reduced; femora shorter, with small heads, proximal trochanters absent, and narrow proximal and distal ends; and tibiae and fibulae very reduced if present at all.

LOCOMOTION

The Eocene sirenians studied here, Protosirenidae and Dugongidae, have many features of body form comparable to those of living Trichechidae and Dugongidae. This means that they were probably basically trichechid or dugongid-like in locomotion. Each genus studied here, *Protosiren*, *Eotheroides*, and *Eosiren*, has distinctive features that give some sense how they may have differed in locomotion.

Protosirenidae.— *Protosiren smithae* is known from complete cervical, thoracic, lumbar, and sacral vertebral series (Figs. 73 and 74). *Protosiren smithae* has profiles of centrum length, width, and width-to-length shape that match *Dugong dugon* more closely than they do *Trichechus manatus* or *T.*

senegalensis (Figs. 81-83). Neural spines are high, especially on anterior thoracic vertebrae. Forelimbs are typically sirenian, but *Protosiren smithae* is distinctive in retaining a robust pelvic girdle with a moderately large femur, tibia, and fibula. Domning and Gingerich (1994) wrote of *Protosiren smithae*:

Protosiren smithae was evidently still an amphibious animal, as shown by its well-developed fore- and hind limbs, and by the high anterior thoracic neural spines that probably served to support the head by way of a nuchal ligament... However, the legs of *P. smithae* were very short relative to its body, and it seems questionable whether the animal could have lifted its body off the ground; it may have merely slid or rested on its belly when out of the water, in a manner analogous to that of modern pinnipeds.

The emerging picture of *Protosiren*, then, is of an animal divergently specialized from other early sirenians, and less fully aquatic than contemporary primitive dugongids. Its ribs were less swollen, and had a unique form of articulation with the vertebrae that led Sickenberg (1934: 88) to conclude that its respiratory mechanics were distinctive.

It seems likely that dorsoventral caudal undulation was the principal swimming mode of *Protosiren*.

Protosiren smithae retained a well formed acetabular surface for articulation with the femur and the femoral head is well developed, but the sacrum had a single-vertebral sacrum and no real auricular surface for articulation with the ilium. Here we suggest that *Protosiren* was not amphibious in the sense that it was able to come out on land, but it was rather a quadruped that may have crawled on the sea bottom while feeding.

The unique articular morphology of the ribs in *Protosiren* and their lack of pachyostosis suggest a mechanism of breathing and buoyancy that was different from the breathing and buoyancy of other sirenians. This too may have been related to feeding by enabling the ribcage to collapse more completely during diving, possibly enabling *Protosiren* to feed in deeper water.

Dugongidae.— The Eocene dugongs *Eotheroides* and *Eosiren* had vertebrae similar to those of living dugongids (Figs. 33-35, 48-53, 72-73), and their centrum length, width, and width-to-length shape profiles match *Dugong dugon* more closely than they do *Trichechus manatus* or *T. senegalensis* (Figs. 81-83). Posterior caudal vertebrae are dorsoventrally compressed suggesting that Eocene dugongs had a fluke at the end of the tail similar to that in recent forms. It seems likely that dorsoventral caudal undulation was the principal swimming mode of *Eotheroides* and *Eosiren*.

Eotheroides and *Eosiren* differ from *Protosiren* in four important ways: (1) they have osteosclerotic and pachyostotic ribs; (2) the ribs are packed more closely together; (3) the ribs have restrictive synovial articulations; and (4) *Eotheroides* and *Eosiren* have much more reduced hind limbs. This probably means that the rib cage was more rigid, with bone density (osteosclerosis) and bone addition (pachyostosis) counterbalancing pneumatic buoyancy (Domning and Buffrénil, 1991). This may also have meant that Eocene dugongids fed in shallower water than protosirenids, where it was easier to come to the surface to breath. Reduced hind limbs in dugongids would preclude quadrupedal crawling on the sea bottom while feeding as postulated above for *Protosiren*.

FEEDING BEHAVIOR

Deflection of the rostrum, dental morphology (Fig. 101), the pattern of dental wear, conformation of the ribs, and the degree of pelvic and hind limb reduction are all different in the Eocene sirenian species from the Birket Qarun and Qasr El Sagha formations studied here. Each trait is related to feeding in some way, providing evidence that each sirenian had a distinctive mode of feeding and a distinct habitat specialization. Domning (2001a) provides a model based on Cenozoic Sirenia of the Caribbean.

Protosiren has rostral deflection averaging 35° in *Protosiren fraasi* and 40° in *Protosiren smithae* (Table 29). Upper molars are large but narrow relative to their length (Fig. 101). Worn teeth have a cupped appearance with large islands of dentine surrounded by thick rims of enamel (Fig. 66). Ribs lack pachyostosis and the entire rib cage appears to have been collapsible to some degree, facilitating deeper diving. The hind limbs were well enough developed to enable quadrupedal locomotion on the sea floor.

Eotheroides has rostral deflection of 50° in *Eotheroides clavigerum* and 49° in *Eotheroides smithae* (Table 29). Upper molars are smaller and more square, with the width approximately the same as the length (Fig. 101). Worn teeth have relatively small islands of dentine surrounded by rims of thinner enamel (Fig. 66). Ribs are pachyostotic and osteosclerotic, and the rib cage as a whole appears to have been relatively rigid. This suggests shallower dives, with buoyancy neutralized by skeletal mass. The hind limbs are too reduced to have been functional in locomotion.

Eosiren has rostral deflection ranging from 44°-51° in *Eosiren libyca* and 55° in *Eosiren stromeri* (Table 29). Upper molars are large, but wide relative to their length (Fig. 101). Worn teeth have relatively large islands of dentine surrounded by rims of thinner enamel (Fig. 66). Ribs are less pachyostotic but still osteosclerotic, with the rib cage as a whole being relatively rigid. This too suggests shallower dives, with buoyancy neutralized by skeletal mass. As in *Eotheroides*, the hind limbs are too reduced to have been functional in locomotion.

Comparing the two common Birket Qarun Formation genera, *Protosiren* and *Eotheroides*, it appears that *Protosiren* with its large tusks probably fed in deeper water on seagrass leaves and rhizomes, while *Eotheroides* fed in shallower water on leaves and rhizomes. The two species *Eotheroides clavigerum* with medium tusks and *Eotheroides sandersi* with diminutive tusks may have differed, respectively, in including a greater and lesser proportion of rhizomes in the diet. The two common Qasr El Sagha species, *Eosiren libyca* and *Eosiren stromeri* replaced *Eotheroides clavigerum* and *Eotheroides sandersi*, and probably filled essentially the same ecological niches.

DISCUSSION AND CONCLUSIONS

The richly fossiliferous marine mammal bone-bearing beds of middle and late Eocene strata in Wadi Al Hitan in the Western

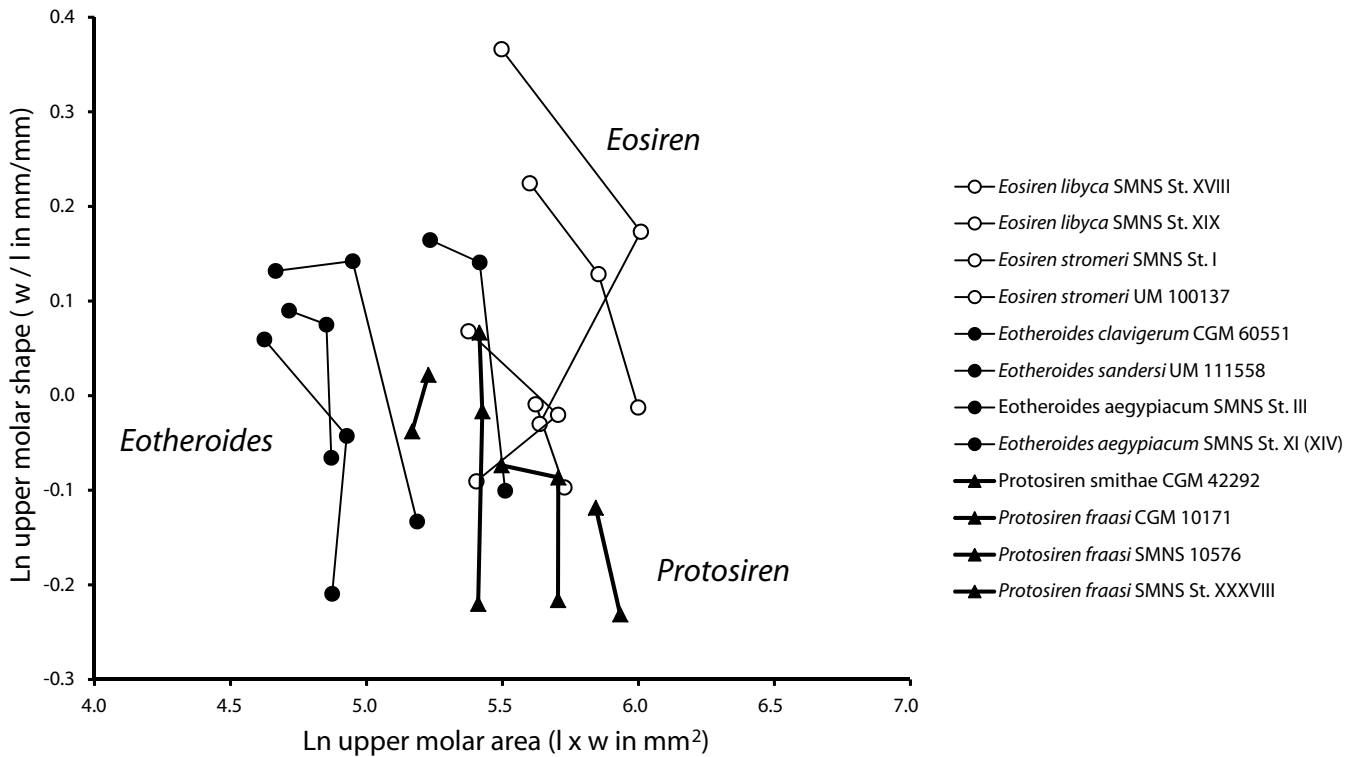


FIGURE 101 — Comparison of upper molars, M^1 , M^2 , and M^3 , of *Protosiren* (solid triangles), *Eotheroides* (solid circles), and *Eosiren* (open circles) in terms of size (abscissa) and shape (ordinate). *Eotheroides* has the smallest upper molars, while those of *Protosiren* and *Eosiren* are larger. *Eosiren* has molars that are wide relative to their length, while molars of *Eotheroides* and *Protosiren* tend to be narrower. Values plotted here are listed in Tables 42–44.

Desert of Egypt are important for understanding the morphology and evolution of Eocene sirenians in Africa. *Protosiren*, *Eotheroides*, and *Eosiren* are all known from Wadi Al Hitán and the Fayum Basin, and all are represented by exceptionally complete skulls and axial skeletons with pectoral and pelvic girdles. Sirenian preservation and taphonomy in Wadi Al Hitán were mostly governed by physical rather than biological factors. The Birket Qarun and Qasr El Sagha formations were deposited in shallow marine environments close to the Eocene shoreline.

Skeletal remains of *Protosiren* and *Eotheroides* of the Birket Qarun Formation are of special interest because they represent intermediate stages of evolution, and intermediate stages of secondary adaptation to life in water.

Protosiren smithae of Domning and Gingerich (1994) is probably a direct descendant of *Protosiren fraasi*, and these species differ from contemporary sirenians (*Eotheroides*) in being larger; having less rostral deflection; having osteosclerotic postcranial elements lacking pachyostosis; having thoracic through lumbar vertebrae with spinous processes higher than those of any other sirenian, having thoracic vertebrae with a keyhole-shaped vertebral canal; and having rib heads with a cartilaginous, rather than fully-ossified, articular surface. *Protosiren* retained larger hind limbs than other contemporaneous sirenians, although these were highly reduced compared to hind

limbs of land mammals and they were incapable of supporting the weight of the body on land.

Eotheroides clavigerum, sp. nov., and *Eotheroides sandersi*, sp. nov., are most similar to *Eotheroides aegyptiacum* (Owen, 1875) from the Lutetian nummulitic limestone beds of Cairo, with which they share the following derived characteristics: prominent falx cerebri and bony tentorium in the roof of the braincase; nasals long and contacting along the midline; palate broad with a posterior border posterior to the toothrow; and anterior ribs pachyosteosclerotic. Wadi Al Hitán *Eotheroides* were medium to large dugongids, ranging in length from 1.5 to 2.5 m; the skull is robust and heavy; the rostrum is deflected and bears medium to diminutive tusks; the trunk is widest between the ninth and eleventh thoracics; the end of the tail was fluked; the pelvis is greatly reduced with a shallow acetabulum, but retains an expanded, club-like ilium, and the femur is short and slender. There cannot have been any substantial lower leg or foot. Of all cranial and postcranial elements, extensively pachyosteosclerotic anterior ribs and club-like ilia are central in diagnosis of the genus and its species. *Eotheroides*, like *Eosiren*, had more reduced hind limbs compared to those of *Protosiren*, and both were fully aquatic.

The most important skeletal elements for the diagnosis of *Eotheroides* species are the anteriorly extensively

TABLE 42 — Dimensions of upper molar teeth in Eocene Sirenia. Measurements are in mm. Abbreviations: *L*, length; *AW*, anterior width; *PW*, posterior width.

Taxon	M ¹			M ²			M ³		
	L	AW	PW	L	AW	PW	L	AW	PW
<i>Eosiren libyca</i> SMNS St. XVIII	14.70	18.60	18.20	17.50	21.00	18.80	20.20	21.70	18.20
<i>Eosiren libyca</i> SMNS St. XIX	—	—	—	16.70	17.80	15.30	18.40	18.60	14.80
<i>Eosiren stromeri</i> SMNS St. I	13.00	19.00	18.50	18.50	23.50	20.50	17.00	18.50	14.50
<i>Eosiren stromeri</i> UM 100137	14.20	15.90	14.50	17.50	18.10	16.20	15.60	15.90	12.60
<i>Eotheroides clavigerum</i> CGM 60551 (holotype)	12.61	15.57	14.16	13.98	17.59	14.60	16.53	17.55	12.35
<i>Eotheroides sandersi</i> UM 111558	9.65	10.74	11.28	11.06	11.75	13.75	14.29	10.51	14.51
<i>Eotheroides aegyptiacum</i> SMNS St. III	10.10	10.90	11.20	10.90	12.60	10.90	11.80	12.40	9.70
<i>Eotheroides aegyptiacum</i> SMNS St. XI (XIV)	9.80	11.20	9.60	12.00	12.30	10.70	12.70	11.90	8.70
<i>Protosiren smithae</i> CGM 42292 (holotype)	—	—	—	19.70	18.00	17.00	21.80	19.00	15.60
<i>Protosiren fraasi</i> CGM 10171 (holotype)	16.20	16.80	13.30	18.10	18.50	14.70	19.30	17.90	13.20
<i>Protosiren fraasi</i> SMNS 10576	14.50	15.50	15.50	15.20	16.10	13.80	16.70	14.90	11.90
<i>Protosiren fraasi</i> SMNS St. XXXVIII	13.50	13.80	12.20	13.50	14.70	12.90	14.90	—	—

TABLE 43 — Upper cheek tooth width and length ratios. These show the shapes of molar teeth of the same species, and enable comparison to other contemporaneous Eocene Sirenian in Egypt. Measurements are in Table 42. Abbreviations: *Ave W*, average width; *L*, length.

Taxon	M ¹ (Ave W/L)	M ² (Ave W/L)	M ³ (Ave W/L)
<i>Eosiren libyca</i> SMNS St. XVIII	1.25	1.14	0.99
<i>Eosiren libyca</i> SMNS St. XIX	—	0.99	0.91
<i>Eosiren stromeri</i> SMNS St. I	1.44	1.19	0.97
<i>Eosiren stromeri</i> UM 100137	1.07	0.98	0.91
<i>Eotheroides clavigerum</i> CGM 60551 (holotype)	1.18	1.15	0.90
<i>Eotheroides sandersi</i> UM 111558	1.14	1.15	0.88
<i>Eotheroides aegyptiacum</i> SMNS St. III	1.09	1.08	0.94
<i>Eotheroides aegyptiacum</i> SMNS St. XI (XIV)	1.06	0.96	0.81
<i>Protosiren smithae</i> CGM 42292 (holotype)	—	0.89	0.79
<i>Protosiren fraasi</i> CGM 10171 (holotype)	0.93	0.92	0.81
<i>Protosiren fraasi</i> SMNS 10576	1.07	0.98	0.80
<i>Protosiren fraasi</i> SMNS St. XXXVIII	0.96	1.02	—

TABLE 44 — Total area of upper cheek teeth in Eocene Sirenian from Egypt. *Eosiren stromeri* is distinctive in having M² larger than M¹ and M³. Measurements are in Table 42. Units here are mm². Abbreviations: *Ave W*, average width; *L*, length.

Taxon	M ¹ (L × Ave W)	M ² (L × Ave W)	M ³ (L × Ave W)
<i>Eosiren libyca</i> SMNS St. XVIII	270.5	348.3	403.0
<i>Eosiren libyca</i> SMNS St. XIX	—	276.4	307.3
<i>Eosiren stromeri</i> SMNS St. I	243.8	407.0	280.5
<i>Eosiren stromeri</i> UM 100137	215.8	300.1	222.3
<i>Eotheroides clavigerum</i> CGM 60551 (holotype)	187.4	225.0	247.1
<i>Eotheroides sandersi</i> UM 111558	106.2	141.0	178.8
<i>Eotheroides aegyptiacum</i> SMNS St. III	111.6	128.1	130.4
<i>Eotheroides aegyptiacum</i> SMNS St. XI (XIV)	101.9	138.0	130.8
<i>Protosiren smithae</i> CGM 42292 (holotype)	—	344.8	377.1
<i>Protosiren fraasi</i> CGM 10171 (holotype)	243.8	300.5	300.1
<i>Protosiren fraasi</i> SMNS 10576	224.8	227.2	223.8
<i>Protosiren fraasi</i> SMNS St. XXXVIII	175.5	186.3	—

pachyosteosclerotic ribs, and the innominates with their club-like ilia. The morphology of the skeletal elements of Lutetian and Priabonian *Eotheroides* are characteristic of fully aquatic marine mammals. These large marine herbivores probably spent their life in water grazing on seagrass.

Distal thickening of the ischium can be used as a sexing criterion in Eocene sirenian innominates. In all supposed males the ratio of the mediolateral thickness of the distal end to the mediolateral thickness of the ischiatic ramus is between 1.8 and 2.3, while in putative females the ratio is between 0.8 and 1.0.

Eosiren libyca Andrews (1902) and *Eosiren stromeri* (Sickenberg, 1934) are limited to the Qasr el Sagha Formation and neither of these species have been found in older units. Both species of *Eosiren* are similar to species of *Eotheroides*. However, in *Eosiren* the ribs are gracile and osteosclerotic but not pachyostotic, and the ilium is narrow and rod-like. In *Eosiren stromeri* the M^2 is always larger than M^3 , a consistent difference from *Eosiren libyca*.

Seagrass preserved as leaf impressions in Priabonian marine mammal beds is a direct indicator of the shallowness of Tethyan waters in the Fayum Basin. This corner of Africa was a special

environment that supported sirenian faunas for more than 13 million years (middle to late Eocene) and sea cows survived here through at least the early Oligocene. The coexistence of *Protosiren smithae*, *Eotheroides clavigerum*, and *Eotheroides sandersi* in the same biotope reflects the diversity of this group in early Priabonian Tethys. The morphological diversity reflects dietary and environmental specialization and niche partitioning. The presence of associated seagrass fossils in both the Birket Qarun and Qasr El Sagha Formations implies that some at least were deposited in settings that are less than 10 meters deep.

Protosirenidae, Dugongidae and Trichechidae (including: *Anomotherium* of Siegfried 1965 and *Miosiren* of Dollo 1889) are the only sirenian families that are known to have lived in the nearshore habitats of the African continent, although it is not unlikely that Prorastomidae were once represented there as well. Dugongidae account for more than 85% of Africa's sirenian fossil record. No trichechid fossils have been found in Africa, and the living West African manatee probably arrived there from the New World in the late Pliocene or Pleistocene (Domning et al., 2010).

LITERATURE CITED

- ABDOU, H. F., and M. R. ABDEL-KIREEM. 1975. Planktonic foraminiferal zonation of the middle and upper Eocene rocks of Fayoum Province, Egypt. *Revista Espanola de Micropaleontologia*, 7: 15-64.
- ABEL, O. 1904. Die Sirenen der mediterranen Tertiärbildungen Österreichs. *Abhandlungen der Kaiserlich-Königlichen Geologischen Reichsanstalt, Wien*, 19 (2): 1-223.
- . 1907. Die Stammesgeschichte der Meeressäugetiery. *Meereskunde*, 1: 1-36.
- . 1912. Grundzüge der Palaeobiologie der Wirbeltiere. E. Schweizerbart'sche Verlagsbuchhandlungen, Stuttgart, 708 pp.
- . 1913. Die eozänen Sirenen der Mittelmeerregion. I Teil: Der Schädel von *Eotherium aegyptiacum*. *Paläontographica*, 59: 289-360 (title page bears date of 1912).
- . 1919. Die Stämme der Wirbeltiere. Walter de Gruyter, Berlin and Leipzig, 914 pp.
- . 1928. Vorgeschichte der Sirenia. In M. Weber. Die Säugetiery: Einführung in die Anatomie und Systematik der Recenten und Fossilen Mammalia. Zweite Auflage, Band II, Systematischer Teil, Gustav Fischer, Jena, pp. 496-504.
- ANDERSON, J. L. and R. M. FELDMANN. 1995. *Lobocarcinus lumacopi* (Decapoda: Cancridae), a new species of cancrid crab from the Eocene of Fayum, Egypt. *Journal of Paleontology*, 69: 922-932.
- ANDERSON, P. K. 1997. Shark Bay dugongs in summer. I: A lek mating system. *Behaviour*, 134: 443-462.
- . 2002. Habitat, niche, and evolution of sirenian mating systems. *Journal of Mammalian Evolution*, 9: 55-98.
- ANDREWS, C. W. 1902a. Dr. C. W. Andrews on fossil vertebrates from Upper Egypt. *Proceedings of the Zoological Society of London*, 1902: 228-230.
- . 1902b. Preliminary note on some recently discovered extinct vertebrates from Egypt, part III. *Geological Magazine, Decade IV*, 9: 291-295.
- . 1904. Further notes on the mammals of the Eocene of Egypt, part III. *Geological Magazine, Decade V*, 1: 211-215.
- . 1906. A Descriptive Catalogue of the Tertiary Vertebrata of the Fayum, Egypt. *British Museum of Natural History, London*, 324 pp.
- ARATA, A. A., and C. G. JACKSON. 1965. Cenozoic vertebrates from the Gulf coastal plain. *Tulane Studies in Geology*, 3: 175-177.
- AS-SARURI, M. L., P. J. WHYBROW, and M. E. COLLINSON. 1999. Geology, fruits, seeds, and vertebrates (?Sirenia) from the Kaninah Formation (middle Eocene), Republic of Yemen. In P. J. WHYBROW and A. HILL (eds.), *Fossil Vertebrates of Arabia: with Emphasis on the Late Miocene Faunas, Geology, and Palaeoenvironments of the Emirate of Abu Dhabi, United Arab Emirates*. Yale University Press, New Haven, pp. 443-453.
- ASTIBIA, H., A. PAYROS, X. P. SUBERBIOLA, J. ELORZA, A. BERRETEAGA, N. ETXEBARRIA, A. BADIOLA, and J. T. OSQUELLA. 2005. Sedimentology and taphonomy of sirenian remains from the middle Eocene of the Pamplona Basin (Navarre, western Pyrenees). *Facies*, 50: 463-475.
- BAJPAI, S., J. G. M. THEWISSEN, V. V. KAPUR, B. N. TIWARI, and A. SAHNI. 2006. Eocene and Oligocene sirenians (Mammalia) from Kachchh, India. *Journal of Vertebrate Paleontology*, 26: 400-410.
- BATALLER, J. R. 1956. Contribución al conocimiento de los Vertebrados terciarios de España. *Cursillos y Conferencias, Instituto Lucas Mallada*, 3: 11-28.
- BATIK, P., and O. FEJFAR. 1990. Les vertébrés du Lutétien, du Miocène et du Pliocène de Tunisie centrale. *Notes Service Géologique de Tunisie*, 56: 69-83.
- BEADNELL, H. J. L. 1901. The Fayum depression: a preliminary notice of the geology of a district in Egypt containing a new Palaeogene vertebrate fauna. *Geological Magazine, Decade IV*, 8: 540-546.
- . 1905. The Topography and Geology of the Fayum Province of Egypt. *Survey Department Egypt, Cairo*, 101 pp.
- BEATTY, B. L. and GEISLER, J. 2010. A stratigraphically precise record of *Protosiren* (Protosirenidae, Sirenia) from North America. *Neues Jahrbuch für Geologie und Paläontologie, Abhandlungen*, 258: 185-194.
- BERTRAM, G. C. L., and C. K. R. BERTRAM. 1973. The modern Sirenia: their distribution and status. *Biological Journal of the Linnean Society of London*, 5: 297-338.
- BERZIN, A. A. 1972. The Sperm Whale (translated from Russian). *Israel Program of Scientific Translations, Jerusalem*, 394 pp.
- BIZZOTTO, B. 1983. *Prototherium intermedium* n. sp. (Sirenia) dell'Eocene Superiore di Possagna e proposta di revisione sistematica del taxon *Eotheroides* Palmer 1899. *Memorie de Scienze Geologiche (Memorie dell' Instituto Geologico della R. Università)*, Padua, 36: 95-116.
- . 2005. La struttura cranica di *Prototherium intermedium* (Mammalia: Sirenia) dell'Eocene superiore Veneto. *Nuovi contributi alla sua anatomia e sistematica. Societa Veneziana di Scienze Naturali Lavori*, 30: 107-125.
- BLAINVILLE, H. M. D. de. 1840. *Ostéographie, Livr. 7, Des Phoques (G. Phoca, L.)*. Arthus Bertrand, Paris.
- . 1844. *Ostéographie, Livr. 15, Des Lamantins (Buffon), (Manatus, Scopoli), ou gravigrades aquatiques*. Arthus Bertrand, Paris.
- BLANCKENHORN, M. 1900. Neues zur Geologie und Paläontologie Aegyptens. II. Das Palaeogen. *Zeitschrift der Deutschen Geologischen Gesellschaft, Stuttgart*, 52: 403-479.
- . 1903. Neue geologisch-stratigraphische Beobachtungen in Aegypten. *Sitzungsberichte der Mathematisch-Physikalischen Classe der Königlichen Bayerischen Akademie der Wissenschaften, München*, 32: 353-433.
- BOUKHARY, M. A., A. I. M. HUSSEIN, and D. KAMAL. 2003. *Nummulites issawii* n. sp., a new species of the *N-laevigatus* group from the Bartonian (middle Eocene) of the southern Fayum area, Egypt. *Neues Jahrbuch für Geologie und Paläontologie, Monatshefte, Stuttgart*, 2003: 351-362.

- BOURLIÈRE, F. 1975. Mammals, small and large: the ecological implications of size. In F. H. Golley and K. Petruszewicz, eds., *Small Mammals: Their Productivity and Population Dynamics*. Cambridge University Press, Cambridge, pp. 1-8.
- BOWEN, B. W., and C. F. VONDRA. 1974. Paleoenvironmental interpretations of the Oligocene Gabal el Qatrani Formation, Fayum Depression. *Annals of the Geological Survey of Egypt*, 4: 115-138.
- BOWN, T. M. 1982. Ichnofossils and rhizoliths of the Nearshore Fluvial Jebel Qatrani Formation (Oligocene) Fayum Province, Egypt. *Palaeogeography, Palaeoclimatology, Palaeoecology*, 40: 255-309.
- , and M. J. KRAUS. 1988. Geology and paleoenvironment of the Oligocene Jebel Qatrani Formation and adjacent rocks, Fayum Depression, Egypt, United States Geological Survey Professional Paper, 1452: 1-60.
- , M. J. KRAUS, S. L. WING, B. H. TIFFNEY, J. G. FLEAGLE, E. L. SIMONS, and C. F. VONDRA. 1982. The Fayum primate forest revisited. *Journal of Human Evolution*, 11: 603-632.
- BRADBURY, J. W. 1977. Lek mating behavior in the hammerheaded bat. *Zeitschrift für Tierpsychologie*, 45: 225-255.
- BROCHU, C. A. and P. D. GINGERICH. 2000. New tomistomine crocodylian from the middle Eocene (Bartonian) of Wadi Hitán, Fayum Province, Egypt. *Contributions from the Museum of Paleontology, University of Michigan*, 30: 251-268.
- CARUS, J. V. 1868. *Handbuch Der Zoologie. Band 1: Wirbelthiere, Mollusken und Molluscoiden*. Wilhelm Engelmann, Leipzig, 894 pp.
- CASE, G. R. and H. CAPPETTA. 1990. The Eocene selachian fauna from the Fayum depression in Egypt. *Palaeontographica, Stuttgart, Abteilung A*, 212: 1-30.
- CLEMENTZ, M. T., A. GOSWAMI, P. D. GINGERICH, and P. L. KOCH. 2006. Isotopic records from early whales and sea cows: contrasting patterns of ecological transition. *Journal of Vertebrate Paleontology*, 26: 355-370.
- DOLLO, L. 1889. Première note sur les siréniens de Boom (résumé). *Bulletin de la Société Belge de Géologie, de Paléontologie, et d'Hydrologie, Procès-Verbaux, Brussels*, 3: 415-421.
- DOLSON, J. C., A. E. BARKOOKY, F. WEHR, P. D. GINGERICH, N. PROCHAZKA, and M. V. SHANN. 2002. The Eocene and Oligocene paleoecology and paleogeography of Whale Valley and the Fayoum Basin: implications for hydrocarbon exploration in the Nile Delta and ecotourism in the greater Fayoum Basin. *AAPG International Conference and Exhibition, Guidebook for Field Trip 7* (http://www.searchanddiscovery.net/documents/cairo/images/cairo_sml.pdf), Cairo, pp. 1-79.
- . 1977. Observations on the myology of *Dugong dugon* (Müller). *Smithsonian Contribution to Zoology*, 226: 1-57.
- . 1978a. Sirenian evolution in the North Pacific Ocean. *University of Californian Publications in Geological Sciences*, 118: 1-179.
- . 1978b. The myology of the Amazonian manatee, *Trichechus inunguis* (Natterer) (Mammalia: Sirenia). *Acta Amazonica*, 8: 1-81.
- . 1981. Sea cows and seagrasses. *Paleobiology*, 7: 417-420.
- . 1991. Sexual and ontogenetic variation in the pelvic bones of *Dugong dugon* (Sirenia). *Marine Mammal Science* 7: 311-316.
- DOMNING, D. P. 1994. A phylogenetic analysis of the Sirenia. *Proceedings of San Diego Society of Natural History*, 29: 177-189.
- . 1996. *Bibliography and Index of the Sirenia and Desmostylia*. *Smithsonian Contributions to Paleobiology*, 80: 1-611.
- . 2000. The readaptation of Eocene sirenians to life in water. In: J.-M. Mazin, V. de Buffrénil, and P. Vignaud (eds.), *Secondary Adaptation of Tetrapods to Life in Water*. *Historical Biology (Special Issue)*, 14: 115-119.
- . 2001a. Sirenians, seagrasses, and Cenozoic ecological change in the Caribbean. In: W. Miller III & S.E. Walker (eds.), *Cenozoic Paleobiology: The Last 65 Million Years of Biotic Stasis and Change*. *Palaeogeography, Palaeoclimatology, Palaeoecology*, 166: 27-50.
- . 2001b. The earliest known fully quadrupedal sirenian. *Nature*, 413: 625-627.
- . 2005. Fossil Sirenia of the west Atlantic and Caribbean region. VII. Pleistocene *Trichechus manatus* Linnaeus, 1758. *Journal of Vertebrate Paleontology*, 25: 685-701.
- and B. BEATTY. 2007. Use of tusks in feeding by dugongid sirenians: observation and tests of hypotheses. *The Anatomical record*, 290: 523-538.
- and V. de BUFFRÉNIL. 1991. Hydrostasis in the Sirenia: quantitative data and functional interpretations. *Marine Mammal Science*, 7: 331-368.
- and P. D. GINGERICH. 1994. *Protosiren smithae*, new species (Mammalia, Sirenia), from the late Middle Eocene of Wadi Hitán, Egypt. *Contributions from the Museum of Paleontology, University of Michigan*, 29: 69-87.
- , P. D. GINGERICH, E. L. SIMONS, and F. A. ANKEL-SIMONS. 1994. A new early Oligocene dugongid (Mammalia, Sirenia) from Fayum Province, Egypt. *Contributions from the Museum of Paleontology, University of Michigan*, 29: 89-108.
- and L. C. HAYEK. 1986. Interspecific and intraspecific morphological variation in manatees (Sirenia: *Trichechus*). *Marine Mammal Science*, 2: 87-144.
- , G. S. MORGAN, and C. E. RAY. 1982. North American Eocene sea cows (Mammalia: Sirenia). *Smithsonian Contribution to Paleobiology* 52: 1-69.
- and P. PERVESLER. 2001. The osteology and relationships of *Metaxytherium krahuletzki* Deperet, 1895 (Mammalia: Sirenia) *Abhandlungen der Senckenbergischen Naturforschenden Gesellschaft*, 553: 1-89.
- and H. THOMAS. 1987. *Metaxytherium serresii* (Mammalia: Sirenia) from the Early Pliocene of Libya and France: a reevaluation of its morphology, phyletic position, and biostratigraphic and paleoecological significance. In N. T. Boaz, A. el-Armaito, A. W. Gaziry, J. DE Heinzelin, and D. D. Boaz (eds.), *Neogene Paleontology and Geology of Sahabi*. Alan R. Liss, New York, pp. 205-232.
- , I. S. ZALMOUT, and P. D. GINGERICH. 2010. Sirenia. In L. Werdelin and W. J. Sanders (eds.), *Cenozoic Mammals of Africa*, University of California Press, Berkeley, pp. 147-160.
- EMMONS, E. 1858. *Agriculture of the eastern counties; together with descriptions of the fossils of the marl beds*. Report of the North Carolina Geological Survey, Raleigh, 314 pp. [Reprinted in part, 1969, *Bulletins of American Paleontology*, 56: 57-230, with a new index].
- ENGELHARDT, H. 1907. *Tertiäre Pflanzenreste aus dem Fajum*. *Beiträge zur Paläontologie und Geologie Österreich-Ungarns und des Orients, Vienna*, 20: 206-216.
- FAGONE, D. M., S. A. ROMMEL, and M. E. BOLEN. 2000. Sexual dimorphism in vestigial pelvic bones of Florida Manatees (*Trichechus manatus latirostris*). *Florida Scientist*, 63: 177-181.
- FIERSTINE, H. L. and P. D. GINGERICH. 2009. A second and more complete rostrum of *Xiphiorhynchus aegyptiacus* Weiler, 1929 (Perciformes: Xiphioidei, Xiphiidae, Xiphiorhynchinae), from the Birket Qarun Formation, late Eocene, Egypt. *Journal of Vertebrate Paleontology*, 29: 589-593.
- FILHOL, H. 1878. Note sur la découverte d'un nouveau Mammifère marin (*Manatus coulombi*) en Afrique dans les carrières de Mokattam près du Caire. *Bulléin de la Société Philomathique de Paris, Série 7*, 2: 124-125.

- FISCHER, M. S. and P. TASSY. 1993. The interrelation between Proboscidea, Sirenia, Hyracoidea, and Mesaxonia: the morphological evidence. In F. S. Szalay, M. J. Novacek, and M. C. McKenna (eds.), *Mammal Phylogeny, Volume 2: Placentals*. Springer Verlag, New York, pp. 217-234.
- FITZINGER, L. J. 1842. Bericht über die in dem Sandlagern von Linz aufgefundenen fossilen Reste eines urweltlichen Säugers, (*Halitherium cristolii*). Bericht über das Museum Francisco-Carolinum, 6: 61-72.
- FLEAGLE, J. G., T. M. BOWN, J. D. OBRADOVICH, and E. L. SIMONS. 1986a. How old are the Fayum primates? In J. G. ELSE and P. C. LEE (eds.), *Primate Evolution*. Cambridge University Press, Cambridge, pp. 3-17.
- _____, _____, and _____. 1986b. Age of the earliest African anthropoids. *Science*, 234: 1247-1249.
- FLOWER, W. H., and J. G. GARSON. 1884. Class Mammalia, other than man. In *Catalogue of the Specimens Illustrating the Osteology and Dentition of Vertebrated Animals, Recent and Extinct, Contained in the Museum of the Royal College of Surgeons of England*, part 2. J. and A. Churchill, London, 779 pp.
- FRAAS, E. 1904. Neue Zeuglodonten aus dem unteren Mitteleocän vom Mokattam bei Cairo. *Geologische und Paläontologische Abhandlungen*, 6: 197-220.
- FREUDENTHAL, M. 1970. Fossiele zeekoeien in het Eoceen van Taulanne. *Experimenteel Geologisch Onderwijs*, 1969/70: 64-65.
- FURUSAWA, H. 1988. A new species of hydrodamaline Sirenia from Hokkaido, Japan. *Takikawa Museum of Art and Natural History, Takikawa*, 1-73 pp.
- GAGNON, M. 1997. Ecological diversity and community ecology in the Fayum sequence (Egypt). *Journal of Human Evolution*, 32: 133-160.
- GILL, T. 1870. On the relations of the orders of mammals. *Proceedings of American Association for the Advancement of Science* 19: 267-270.
- GINGERICH, P. D. 1981. Variation, sexual dimorphism, and social structure in the early Eocene horse *Hyracotherium* (Mammalia, Perissodactyla). *Paleobiology*, 7: 443-455.
- _____. 1992. Marine mammals (Cetacea and Sirenia) from the Eocene of Gebel Mokattam and Fayum, Egypt: stratigraphy, age, and paleoenvironments. *University of Michigan Papers on Paleontology*, 30: 1-84.
- _____. 2000. Arithmetic or geometric normality of biological variation: an empirical test of theory. *Journal of Theoretical Biology*, 204: 201-221.
- _____. 2007. *Stromerius nidensis*, new archaeocete (Mammalia, Cetacea) from the upper Eocene Qasr el-Sagha Formation, Fayum, Egypt. *Contributions from the Museum of Paleontology, University of Michigan*, 31: 363-378.
- _____. 2008. Early evolution of whales: a century of research in Egypt. In J. G. Fleagle and Christopher C. Gilbert (eds.), *Elwyn Simons: A Search for Origins*, Springer, New York, pp. 107-124.
- _____, M. ARIF, M. A. BHATTI, H. A. RAZA, and S. M. RAZA. 1995. *Protosiren* and *Babiacetus* (Mammalia, Sirenia and Cetacea) from the middle Eocene Drazinda Formation, Sulaiman Range, Punjab (Pakistan). *Contributions from the Museum of Paleontology, University of Michigan*, 29: 331-357.
- _____, Y. ATTIA, F. EL-BEDAWI, and S. SAMEEH. 2007. Khasm El-Raqaba: a new locality yielding middle Eocene whales and sea cows from Wadi Tarfa in the Eastern Desert of Egypt. *Journal of Vertebrate Paleontology*, 27: 81A.
- _____, H. CAPPETTA, and M. TRAVERSE. 1992. Marine mammals (Cetacea and Sirenia) from the middle Eocene of Kpogamé-Hahotoé in Togo (abstract). *Journal of Vertebrate Paleontology*, 12 (3, supplement): 29A-30A.
- _____, D.P. DOMNING, C.E. BLANE, and M. UHEN. 1994. Cranial morphology of *Protosiren fraasi* (Mammalia, Sirenia) from the Middle Eocene of Egypt: a new study using computed tomography. *Contributions from the Museum of Paleontology, University of Michigan*, 29: 41-67.
- _____, M. HAQ, I. S. ZALMOUT, I. H. KHAN, and M. S. MAL-KANI. 2001. Origin of whales from early artiodactyls: hands and feet of Eocene Protocetidae from Pakistan. *Science*, 293: 2239-2242.
- _____, B. H. SMITH, and E. L. SIMONS. 1990. Hind limbs of Eocene *Basilosaurus*: evidence of feet in whales. *Science*, 249: 154-157.
- _____, I. S. ZALMOUT, M. S. ANTAR, E. M. WILLIAMS, A. E. CARLSON, D. C. KELLY, and S. E. PETERS. 2012. Large-scale glaciation and deglaciation of Antarctica during the late Eocene: reply. *Geology*, 40: e255.
- GRAY, J. E. 1821. On the natural arrangement of vertebrate animals. *London Medical Repository*, 15: 296-310.
- GREEN, E. P. and F. T. SHORT (eds.). 2003. *World Atlas of Seagrasses*, University of California Press, Berkeley, 310 pp.
- GUIRAUD, R., and W. BOSWORTH. 1999. Phanerozoic geodynamic evolution of northeastern Africa and the northwestern Arabian platform. *Tectonophysics*, 315: 73-108.
- _____, W. BOSWORTH, J. THIERRY, and A. DELPLANQUE. 2005. Phanerozoic geological evolution of northern and central Africa: an overview. *Journal of African Earth Sciences*, 43: 83-143.
- _____, B. ISSAWI, and W. BOSWORTH. 2001. Phanerozoic history of Egypt and surrounding areas. In P. A. Ziegler, W. Cavazza, A. H. F. Robertson, and S. Crasquin-Soleau (eds.), *Peri-Tethys Memoir 6: Peri-Tethyan Rift/Wrench Basins and Passive Margins*, Mémoires du Muséum National d'Histoire Naturelle, Paris, Série D, Sciences de la Terre, 186: 469-509.
- HAGGAG, M. A. Y. 1985. Middle Eocene planktonic foraminifera from Fayum area, Egypt. *Revista Espanola de Micropaleontologia*, 17: 27-40.
- _____. 1990. *Globigerina pseudoamphiapertura* zone, a new late Eocene planktonic foraminiferal zone (Fayoum area, Egypt). *Neues Jahrbuch für Geologie und Paläontologie. Monatshefte*, 5: 295-307.
- HARTMAN, D. S. 1971. Behavior and ecology of the Florida manatee, *Trichechus manatus latirostris* (Harlan), at Crystal River, Citrus County. Ph.D. Thesis, Cornell University, Ithaca, NY, 285 pp.
- _____. 1979. Ecology and behavior of the manatee (*Trichechus manatus*) in Florida, *American Society of Mammalogists, Special Publication* 5: 1-153.
- HAUTIER, L., R. SARR, R. TABUCE R, F. LIHOREAU, S ADNET, D. P. DOMNING, M. SAMB, and M. PHAMEH. 2012. First pro-rastomid sirenian from Senegal (Western Africa) and the Old World origin of sea cows. *Journal of Vertebrate Paleontology*, 32: 1218-1222.
- HEAL, G. J. 1973. Contributions to the study of sirenian evolution. Ph.D. thesis, University of Bristol, 1-245 pp.
- HEIKAL, M. A., M. A. HASSAN, and Y. EL SHESHTAWI. 1983. The Cenozoic basalt of Gebel Qatrani, Western Desert, Egypt; as an example of continental tholeiitic basalt. *Annals of the Geological Survey of Egypt*, 13: 193-209.
- HEINSOHN, G. E. 1972. A study of dugongs (*Dugong dugong*) in northern Queensland, Australia. *Biological Conservation*, 4: 205-213.
- HOLROYD, P. A., E. L. SIMONS, T. M. BOWN, P. D. POLLY, and M. J. KRAUS. 1996. New records of terrestrial mammals from the

- Upper Eocene Qasr El Sagha Formation, Fayum Depression, Egypt. In M. Godinot and P. D. Gingerich (eds.), *Paléobiologie Et Evolution Des Mammifères Paléogènes: Volume Jubilaire En Hommage à Donald E. Russell, Palaeovertebrata*, Montpellier, 25: 175-192.
- HOME, E. 1821. An account of the skeletons of the dugong, two-horned rhinoceros, and tapir of Sumatra, sent to England by Sir Thomas Stamford Raffles, Governor of Bencoolen. *Philosophical Transactions of the Royal Society of London*, 111: 268-275.
- ILLIGER, C. 1811. *Prodromus systematis mammalium et avium additis terminis zoographicis utriusque classis, earumque versione Germanica*, 302 pp.
- ISKANDER, F. 1943. Geological survey of the Gharag el Sultani sheet no. 68/54. Standard Oil Company, Egypt S. A., Reports, 51: 1-29.
- ISMAIL, M. M., and ABDEL-KIREEM, M. R. 1971a. Microfacies of the Fayoum surface sections. Part 1: middle Eocene. *Bulletin of the Faculty of Science, Alexandria University*, 11: 65-84.
- and ———. 1971b. Microfacies of the Fayoum surface sections. Part 2: upper Eocene. *Bulletin of the Faculty of Science, Alexandria University*, 11: 85-105.
- IVANY, L., R. W. PORTELL, and D. S. JONES. 1990. Animal-plant relationships and paleobiogeography of an Eocene seagrass community from Florida. *Palaios*, 5: 244-258.
- KAISER, H. E. 1974. Morphology of the Sirenia: A Macroscopic and X-Ray Atlas of the Osteology of Recent Species. S. Karger, Basel, 75 pp.
- KAUP, J. J. 1838a. Über Zähnen von *Halytherium* und *Pugmeodon* aus Flonheim. *Neues Jahrbuch für Geognosie, Geologie und Petrefactenkunde*, 1838: 318-320.
- . 1838b. Über Zähnen von *Halitherium* und Dugong. *Neues Jahrbuch für Geognosie, Geologie und Petrefactenkunde*, 1838: 356.
- KHASHAB, B. el. 1974. Review of the early Tertiary eutherian faunas of African mammals in Fayum Province, Egypt. *Annals of the Geological Survey of Egypt*, 4: 95-114.
- KLEINENBERG, S. E., A. V. YABLOKOV, B. M. BELKOVICH, and M. N. TARASEVICH. 1964. Beluga (*Delphinapterus leucas*): Investigation of the species. Translated from Russian by Israel Program for Scientific Translations, Jerusalem, 1969. *Akademi Nauk SSSR*, Moscow, 376 pp.
- KOENIGSWALD, G. H. R. von. 1952. Fossil sirenians from Java. *Proceedings of the Section of Sciences, Series B, Koninklijke Nederlandse Akademie van Wetenschappen*, Amsterdam, 55: 610-612.
- KOJESZEWSKI, T., and F. E. FISH. 2007. Swimming kinematics of the Florida manatee (*Trichechus manatus latirostris*): hydrodynamic analysis of an undulatory mammalian swimmer. *Journal of Experimental Biology*, 210: 2411-2418.
- KORDOS, L. 1977. A new upper Eocene Sirenian (*Paralitherium tarkanyense* n.g., n.sp.) from Felsötrárkány, NE Hungary. *Magyar Állami Földtani Intézet Évi Jelentése az 1975 Évről*, 1977: 349-367.
- . 1978. Major finds of scattered fossils in the palaeovertebrate collection of the Hungarian Geological Institute (communication No 3). *Magyar Állami Földtani Intézet Évi jelentése az 1976 Évről*, 1978: 281-290.
- . 1979. Major finds of scattered fossils in the palaeovertebrate collection of the Hungarian Geological Institute (communication No. 4). *Magyar Állami Földtani Intézet Évi jelentése az 1977 Évről*, 1979: 313-326.
- . 1980. Contribution to the knowledge of sirenians from the Hungarian Eocene. *Magyar Állami Földtani Intézet Evi Jelentese*, 1978: 385-397.
- . 1981. Some complements to the knowledge of a middle Eocene Sirenia, *Sirenavus hungaricus* Kretzoi, 1941. *Fragmenta Mineralogica et Palaeontologica*, 10: 75-78.
- . 2002. Eocene sea cows (Sirenia, Mammalia) from Hungary. *Fragmenta Palaeontologica Hungarica*, 20: 43-48.
- KORTLAND, A. 1980. The Fayum forest: did it exist? *Journal of Human Evolution*, 9: 277-297.
- KOSTANDI, B. 1963. Eocene facies maps and tectonic interpretation in the Western Desert, U.A.R. *Revue de l'Institut Français du Pétrole*, 18: 1331-1343.
- KRAUSS, F. 1870. Beiträge zur Osteologie von *Halicore*. *Archiv für Anatomie, Physiologie, und Wissenschaftliche Medecin*, 1870: 525-614.
- . 1872. Die Beckenknochen des surinamischen *Manatus*. *Archiv für Anatomie, Physiologie, und Wissenschaftliche Medecin*, 1872: 257-292.
- KRENKEL, E. 1924. Der syrische Bogen. *Zentralblatt fuer Mineralogie, Geologie und Palaeontologie*, 9: 274-281.
- KRETZOI, M. 1941. *Sirenavus hungaricus* n.g. n. sp., ein neuer Prokastomide aus dem Mitteleozän (Lutetium) von Felsögalla in Ungarn. *Annales Musei Nationalis Hungarici, Pars Mineralogica, Geologica et Palaeontologica*, 34: 146-156.
- . 1953. A legidősebb magyar ősemlős-lelet. *Földtani Közlöny*, 83: 273-277.
- LEPSIUS, G. R. 1882. *Halitherium Schinzi*, die fossile Sirene des Mainzer Beckens. Eine vergleichend-anatomische Studie. *Abhandlungen des Mittelrheinischen Geologischen Vereins*, 1: 1-200.
- LINK, H. F. 1795. Beiträge zur Naturgeschichte. Vol. 1, part 2. K. C. Stiller, Rostock and Leipzig, 126 pp.
- LINNAEUS, C. 1758. *Systema naturae per regna tria naturae, secundum classes, ordines, genera, species, cum characteribus, differentiis, synonymis, locis*. Decima Edition. Laurentius Salvius, Holmiae, 824 pp.
- LÖNNBERG, E. 1910. The pelvic bones of some Cetacea. *Arkiv für Zoologie*, 7: 1-15.
- LORENZ, L. V. 1904. Das Becken der Steller'schen Seekuh. *Abhandlungen der Kaiserlich-Königlichen Geologischen Reichsanstalt*, Wien, 19: 1-11.
- MARSH, H. 1980. Age determination of the dugong (*Dugong dugon* (Müller)) in northern Australia and its biological implications. *Reports of the International Whaling Commission, Special Issue 3*: 18 1-201.
- , G. E. HEINSOHN, and T. D. GLOVER. 1984a. Changes in the ovaries and uterus of the dugong, *Dugong dugon* (Sirenia: Dugongidae) with age and reproductive activity. *Australian Journal of Zoology*, 32: 743-747.
- , G. E. HEINSOHN, and T. D. GLOVER. 1984b. Changes in the male reproductive organs of the dugong, *Dugong dugon* (Sirenia: Dugongidae) with age and reproductive activity. *Australian Journal of Zoology*, 32: 721-742.
- McKENNA, M. C. 1975. Toward a phylogenetic classification of the Mammalia. In W. P. Luckett and F. S. Szalay (eds.), *Phylogeny of the Primates*. Plenum Press, New York, pp. 21-46.
- MÜLLER, P. L. S. 1776. Des Ritters Carl von Linne' ... vollständiges Natursystems Supplements- und Register-Band. Gabriel Nicolaus Raspe, Nuremberg, 384 pp.
- MÜLLERRIED, F. K. G. 1932. Primer hallazgo de un sirénido fósil en la República Mexicana. *Anales del Instituto de Biología Universidad Nacional de México*, 3: 71-73.
- MURRAY, A. M., T. D. COOK, Y. ATTIA, P. CHATRATH, and E. L. SIMONS. 2010. A freshwater ichthyofauna from the late Eocene Birket Qarun Formation, Fayum, Egypt. *Journal of Vertebrate Paleontology*, 30: 665-680.
- OWEN, R. 1855. On the fossil skull of a mammal (*Prorastomus sirenoides* Owen) from the island of Jamaica. *Quarterly Journal of the Geological Society of London*, 11: 541-543.

- . 1875. On fossil evidences of a sirenian mammal (*Eotherium aegyptiacum*, Owen) from the Nummulitic Eocene of the Mokattam Cliffs, near Cairo. *Quarterly Journal of the Geological Society of London*, 31: 100-105.
- PALMER, T. S. 1899. *Catalogus Mammalium tam viventium quam fossilium* [Review of Dr. E. L. Trouessart's *Catalogus Mammalium*]. *Science*, 10: 491-495.
- PERRIN, W. F. 1975. Variation of spotted and spinner porpoise (genus *Stenella*) in the Eastern Pacific and Hawaii. *Bulletin of the Scripps Institution of Oceanography*, 21: 1-206.
- PETERS, S. E., M. S. ANTAR, I. S. ZALMOUT, and P. D. GINGERICH. 2009. Sequence stratigraphic control on preservation of late Eocene whales and other vertebrates at Wadi al-Hitan, Egypt. *Palaios*, 24: 290-302.
- , A. E. CARLSON, D. C. KELLY, and P. D. GINGERICH. 2010. Large-scale glaciation and deglaciation of Antarctica during the late Eocene. *Geology*, 38: 723-726.
- PHILLIPS, R. C., and E. G. MEÑEZ. 1988. Seagrasses. *Smithsonian Contributions to the Marine Sciences*, 34: 1-104.
- PILLERI, G., J. BIOSCA, and L. VIA. 1989. The Tertiary Sirenian of Catalonia. *Brain Anatomy Institute, University of Berne, Ostermündingen*, 1-98 pp.
- PREEN, A. 1989. Observations of mating behavior in dugongs (*Dugong dugon*). *Marine Mammal Science*, 5: 382-387.
- RALLS, K. 1976. Mammals in which females are larger than males. *Quarterly Review of Biology*, 51: 245-276.
- . 1977. Sexual dimorphism in mammals: avian model and unanswered questions. *American Naturalist*, 111: 917-938.
- REINHART, R. H. 1959. A Review of the Sirenian and Desmostylia. *University of California Publications in Geological Sciences*, 36: 1-146.
- . 1976. Fossil sirenians and desmostylids from Florida and elsewhere. *Bulletin of the Florida State Museum of Biological Sciences*, 20: 187-300.
- RICHARD, M. 1946. Les gisements de mammifères tertiaires: contribution à l'étude du Bassin d'Aquitaine. *Mémoires de la Société Géologique de France (nouvelle série)*, 24 (Mémoire 52): 1-380.
- RIHA, A. 1911. Das männliche Urogenitalsystem von *Halicornis dugong* Erxl. *Zeitschrift für Morphologie und Anthropologie*, 13: 395-422.
- ROBINEAU, D. 1969. Morphologie externe du complexe osseux temporal chez les sirenians. *Mémoires du Muséum National d'Histoire Naturelle, Paris, Série A, Zoologie*, 60: 1-32.
- ROMMEL, S. A. 1990. Osteology of the bottlenose dolphin. In R. R. Reeves and S. Leatherwood (eds.), *The Bottlenose Dolphin*. Academic Press, San Diego, pp. 29-49.
- , and J. E. REYNOLDS. 2000. Diaphragm structure and function in the Florida manatee (*Trichechus manatus latirostris*). *Anatomical Record*, 259: 41-51.
- ROSE, K. D., T. SMITH, R. S. RANA, A. SAHNI, H. SINGH, P. MISIAEN, and A. FOLIE. 2006. Early Eocene (Ypresian) continental vertebrate assemblage from India, with description of a new anthracobunid (Mammalia, Tethytheria). *Journal of Vertebrate Paleontology*, 26: 219-225.
- SAGNE, C. 2001. *Halitherium taulannense*, nouveau sirenien (Sirenian, Mammalia) de l'Eocene superieur provenant du domaine Nord-Tethysien (Alpes-de-Haute-Provence, France). *Comptes Rendus de l'Academie des Sciences, Serie II A, Sciences de la Terre et des Planetes*, 333: 471-476.
- SAHNI, A., and V. P. MISHRA. 1975. Lower Tertiary vertebrates from western India. *Monographs of the Palaeontological Society of India*, 3: 1-48.
- SAID, R. 1962. *The Geology of Egypt*. Elsevier, Amsterdam, 377 pp.
- . 1990. Cenozoic. In R. Said (ed.), *The Geology of Egypt*. A. A. Balkema, Rotterdam, pp. 451-486.
- SALEM, R. M. 1976. Evolution of Eocene-Miocene sedimentation patterns in parts of northern Egypt. *American Association of Petroleum Geologists Bulletin*, 60: 34-64.
- SAMONDS, K. E., I. S. ZALMOUT, M. T. IRWIN, and L. L. RAHARIVONY. 2007. Sirenian postcrania from Nosy Mahakamby, northwestern Madagascar (abstract). *Journal of Vertebrate Paleontology*, 27: 139A.
- , I. S. ZALMOUT, M. T. IRWIN, D. W. KRAUSE, R. R. ROGERS, L. L. RAHARIVONY. 2009. *Eotheroides lambondrano*, new middle Eocene seacow (Mammalia, Sirenian) from the Mahajanga Basin, northwestern Madagascar. *Journal of Vertebrate Paleontology*, 29: 1233-1243.
- SANDERS, A. E. 1974. A paleontological survey of the Cooper Marl and Santee Limestone near Harleyville, South Carolina (preliminary report). *South Carolina State Development Board, Division of Geology, Geologic Notes*, 18: 4-12.
- SARKO, D. K., D. P. DOMNING, L. MARINO, and R. L. REEP. 2010. Estimating body size of fossil sirenians. *Marine Mammal Science*, 26: 937-959.
- SAVAGE, R. J. G. 1969. Early Tertiary mammal locality in southern Libya. *Proceedings of the Geological Society of London*, 1657: 167-171.
- . 1971. Review of the fossil mammals of Libya. In C. Gray (ed.), *Symposium on the Geology of Libya*. University of Libya, Tripoli, pp. 215-225.
- . 1977. Review of early Sirenian. *Systematic Zoology*, 25: 344-351.
- , D. P. DOMNING, and J. G. M. THEWISSEN. 1994. Fossil Sirenian of the West Atlantic and Caribbean region. V. The most primitive known sirenian, *Prorastomus sirenoides* Owen, 1855. *Journal of Vertebrate Paleontology*, 14: 427-449.
- SCHAUB, H. 1981. Nummulites et Assilines de la Tethys paléogène. Taxonomy, phylogenèse et biostratigraphie. Text and atlas. *Schweizerische Paläontologische Abhandlungen*, 104-106: 1-236.
- SCHLOSSER, M. 1923. *Grundzüge der Paläontologie (Paläozoologie)* von Karl A. von Zittel, II Abteilung: Vertebrata. Neuarbeitet von F. Broili und M. Schlosser. R. Oldenbourg, Munich and Berlin, 706 pp.
- SCHWEINFURTH, G. A. 1883. Ueber die geologische Schichtengliederung des Mokattam bei Cairo. *Zeitschrift der Deutschen Geologischen Gesellschaft*, 35: 709-737.
- SEIFFERT, E. R., T. M. BOWN, W. C. CLYDE, and E. L. SIMONS. 2008. Geology, paleoenvironment, and age of Birket Qarun locality 2 (BQ-2), Fayum Depression, Egypt. In J. G. Fleagle and C. C. Gilbert (eds.), *Elwyn Simons: a Search for Origins*, Springer, New York, pp. 71-86.
- SHOSHANI, J. 1986. Mammalian phylogeny: comparison of morphological and molecular results. *Molecular Biology and Evolution*, 3: 222-242.
- SICKENBERG O. 1934. Beiträge zur Kenntnis Tertiärer Sirenen. I. Die Eozänen Sirenen des Mittelmeergebietes; II. Die Sirenen des Belgischen Tertiärs. *Mémoires du Musée Royal d'Histoire Naturelle de Belgique*, 63: 1-352.
- SIEGFRIED, P. 1965. *Anomotherium langewieschei* n. g. n. sp. (Sirenian) aus dem Ober-Oligozän des Dobergs bei Bunde, Westfalen. *Palaeontographica*, Stuttgart, 124: 116-150.
- . 1967. Das Femur von *Eotheroides libyca* (Owen) (Sirenian). *Paläontologische Zeitschrift*, 41: 165-172.

- SILER, W. L. 1964. A middle Eocene sirenian in Alabama. *Journal of Paleontology*, 36: 1108-1109.
- SIMONS, E. L. 1968. Early Cenozoic mammalian faunas, Fayum Province, Egypt. Part I. African Oligocene mammals: introduction, history of study and faunal succession. *Bulletin of the Peabody Museum, Yale University*, 28: 1-21.
- and D. T. RASMUSSEN. 1990. Vertebrate paleontology of Fayum; history of research, faunal review and future prospects. In R. SAID (ed.), *The Geology of Egypt*. A.A. Balkema, Rotterdam, pp. 627-638.
- and P. D. GINGERICH. 1974. New carnivorous mammals from the Oligocene of Egypt. *Annals of the Geological Survey of Egypt*, 4: 157-166.
- SIMPSON, G. G. 1945. The principles of classification and a classification of mammals. *Bulletin of the American Museum of Natural History*, 85: 1-350.
- SPAIN, A., and G. HEINSOHN. 1974. A biometric analysis of measurement data from a collection of North Queensland dugong skulls, *Dugong dugon* (Muller). *Australian Journal of Zoology*, 22: 249-257.
- , G. HEINSOHN, H. MARSH, and R. CORRELL. 1976. Sexual dimorphism and other sources of variation in a sample of dugong skulls from north Queensland. *Australian Journal of Zoology*, 24: 491-497.
- SPILLMANN, F. 1959. Die Sirenen aus dem Oligozän des Linzer Beckens (Oberösterreich), mit Ausführungen über "Osteosklerose" und "Pachyostose". *Österreichische Akademie der Wissenschaften, Mathematisch-Naturwissenschaftliche Klasse. Denkschriften*, 110: 1-68.
- STELLER, G. 1751. The beasts of the sea. (translated by W. Miller and J. E. Miller, orig. published in 1751). Pp. 180-201 in D. Jordan, ed. *The fur seals and fur seal islands of the North Pacific Ocean*. Part 3. Washington, D.C.: U.S. Government Printing Office.
- STROMER VON REICHENBACH, E. 1921. Untersuchung der Huftbeine und Huftgelenke von Sirenia und Archaeoceti. *Sitzungsberichte der Königlichen Bayerischen Akademie der Wissenschaften, Mathematisch-physikalischen Classe, München*, 1921: 41-59.
- STROUGO, A. 1985a. Eocene stratigraphy of the eastern greater Cairo (Gebel Mokattam-Helwan) area. *Middle East Research Center, Ain Shams University, Scientific Research Series*, 5: 1-39.
- . 1985b. Eocene stratigraphy of the Giza Pyramids plateau. *Middle East Research Center, Ain Shams University, Scientific Research Series*, 5: 79-99.
- . 1986. Mokattam stratigraphy of eastern Maghgha-El Fashn district. *Middle East Research Center, Ain Shams University, Scientific Research Series*, 6: 33-58.
- . 1992. The middle Eocene/upper Eocene transition in Egypt reconsidered. *Neues Jahrbuch für Geologie und Palaeontologie. Abhandlungen*, 186: 71-89.
- . 2008. The Mokattamian stage: 125 years later. *Middle East Research Center, Ain Shams University, Cairo, Earth Science Series*, 22: 47-108.
- , R. A. ABUL-NASR, and M. A. HAGGAG. 1982. Contribution to the age of the middle Mokattam beds of Egypt. *Neues Jahrbuch für Geologie und Paläontologie, Monatshefte, Stuttgart*, 1982: 240-243.
- and M. A. Y. HAGGAG. 1984. Contribution to the age determination of the Gehannam Formation in the Fayum Province, Egypt. *Neues Jahrbuch für Geologie und Palaeontologie. Monatshefte*, 1984: 46-52.
- STRUTHERS, J. 1893. On the rudimentary hind-limb of a great fin-whale (*Balaenoptera musculus*) in comparison with those of the humpback whale and the Greenland right-whale. *Journal of Anatomy and Physiology*, 27: 291-335.
- UHEN, M. D. 2004. Form, function and anatomy of *Dorudon atrox* (Mammalia, Cetacea): an Archaeocete from the middle to late Eocene of Egypt. *University of Michigan Papers on Paleontology*, 34: 1-222.
- UNDERWOOD, C. J., D. J. WARD, C. KING, M. S. ANTAR, I. S. ZALMOUT, and P. D. GINGERICH. 2011. Shark and ray faunas in the late Eocene of the Fayum area, Egypt. *Proceedings of the Geologists' Association, London*, 122: 47-66.
- VERNON, R. O. 1951. *Geology of Citrus and Levy counties, Florida*. Florida Geological Survey Bulletin, 33: 1-256
- VLIET, H. J. van, and G. ABU EL KHAIR. 2010. A new Eocene marine mammal site in the Qattara depression (Egypt). *Cainozoic Research*, 7: 73-77.
- VONDRA, C. F. 1974. Upper Eocene transitional and near-shore marine Qasr El Sagha Formation, Fayum Depression, Egypt. *Annals of the Geological Survey of Egypt*, 4: 79-94.
- VOSS, M. 2011. A new sea cow record from the lower Oligocene of western Germany: new indications on the skeletal morphology of *Halitherium schinzii* (Mammalia: Sirenia). *Paläontologische Zeitschrift*, 86: 205-217.
- WELLS, N. A., and P. D. GINGERICH. 1983. Review of Eocene Anthracobunidae (Mammalia, Proboscidea) with a new genus and species, *Jozaria palustris*, from the Kuldana Formation of Kohat (Pakistan). *Contributions from the Museum of Paleontology, University of Michigan*, 26: 117-139.
- WING, S. L., and B. H. TIFFNEY. 1982. A paleotropical flora from the Oligocene Jebel Qatrani Formation of northern Egypt: a preliminary report (abstract). *Miscellaneous Series of the Botanical Society of America*, 162: 67.
- , S. T. HASIOTIS, and T. M. BOWN. 1995. First ichnofossils of flank-buttressed trees (late Eocene), Fayum Depression, Egypt. *Ichnos*, 3: 281-286.
- YOSHIDA, H., M. SHIRAKIHARA, A. TAKEMURA, and K. SHIRAKIHARA. 1994. Development, sexual dimorphism, and individual variation in the skeleton of the finless porpoise, *Neophocaena phocaenoides*, in the coastal waters of western Kyushu, Japan. *Marine Mammal Science*, 10: 266-282.
- ZALMOUT, I. S., M. S. M. ANTAR, E. ABD-EL SHAFY, M. H. METWALLY, E. E. HATAB, and P. D. GINGERICH. 2012. Priabonian sharks and rays (late Eocene: Neoselachii) from Minqar Tabaghbagh in the western Qattara Depression, Egypt. *Contributions from the Museum of Paleontology, University of Michigan*, 32: 71-90.
- , M. UL-HAQ, and P. D. GINGERICH. 2003a. New species of *Protosiren* (Mammalia, Sirenia) from the early middle Eocene of Balochistan (Pakistan). *Contributions from the Museum of Paleontology, University of Michigan*, 31: 79-87.
- , P. GINGERICH, H. MUSTAFA, A. SMADI, and A. KHAMMASH. 2003b. Cetacea and Sirenia from the Eocene Wadi Esh-Shallala Formation of Jordan (abstract). *Journal of Vertebrate Paleontology*, 23(3, supplement): 113.
- ZDANSKY, O. 1938. *Eotherium majus* sp.n., eine neue Sirene aus dem Mitteleozän von Aegypten. *Palaeobiologica*, 6: 429-434.
- ZIGNO, A. de. 1875. Sireni fossili trovati nel Veneto. *Memorie dell' Real Istituto Veneto di Scienze Lettere ed Arti*, 18: 427-456.

